

Distribution Agreement

In presenting this thesis or dissertation as a partial fulfillment of the requirements for an advanced degree from Emory University, I hereby grant to Emory University and its agents the non-exclusive license to archive, make accessible, and display my thesis or dissertation in whole or in part in all forms of media, now or hereafter known, including display on the world wide web. I understand that I may select some access restrictions as part of the online submission of this thesis or dissertation. I retain all ownership rights to the copyright of the thesis or dissertation. I also retain the right to use in future works (such as articles or books) all or part of this thesis or dissertation.

Signature:

Zachary Strongin

Date

**Mechanisms of HIV Pathogenesis, Persistence and Control in SIV-infected Rhesus
Macaques**

By

Zachary Strongin
Doctor of Philosophy

Graduate Division of Biological and Biomedical Science
Immunology and Molecular Pathogenesis

Mirko Paiardini, Ph.D.
Advisor

Steven Bosinger, Ph.D.
Committee Member

Haydn Kissick, Ph.D.
Committee Member

Jacob Kohlmeier, Ph.D.
Committee Member

Vincent Marconi, M.D.
Committee Member

Accepted:

Kimberly J. Arriola, Ph.D.
Dean of the James T. Laney School of Graduate Studies

Date

**Mechanisms of HIV Pathogenesis, Persistence and Control in SIV-infected Rhesus
Macaques**

By

Zachary Strongin

B.S., Boston College, 2016

Advisor: Mirko Paiardini, Ph.D.

An abstract of

A dissertation submitted to the Faculty of the

James T. Laney School of Graduate Studies at Emory University

In partial fulfillment of the requirements for the degree of

Doctor of Philosophy

Program in Immunology and Molecular Pathogenesis
Graduate Division of Biological and Biomedical Sciences

2023

Abstract

Mechanisms of HIV Pathogenesis, Persistence and Control in SIV-infected Rhesus Macaques

By Zachary Strongin

With over 37 million people infected, HIV remains one of the largest public health burdens worldwide, with a unique ability to continually evade the immune response and persist in a latent viral reservoir despite effective antiretroviral therapy. The ultimate goal of current HIV research is the development of a therapeutic intervention that induces HIV remission in the absence of antiretroviral therapy. In order to further understand mechanisms of HIV pathogenesis, persistence and viral control, we utilized the non-human primate model of HIV infection to investigate target cell populations contributing to pathogenesis and viral persistence, and mechanisms promoting post-treatment and CD8-mediated control of infection.

We identified 7 SIV-infected rhesus macaques that mirrored the human post-treatment controller phenotype and performed immunologic and virologic analysis of blood, lymph node, and colorectal biopsy samples to further understand the characteristics that distinguish them from non-controllers. Overall, lower plasma viremia, reduced cell-associated SIV-DNA, and preserved Th17 homeostasis, including at pre-ART, are the main features associated with sustained viral control after ATI in SIV-infected RMs.

There is a great interest in identifying surface markers on cells that play a role in pathogenesis and persistence to elucidate potential therapeutic targets. We describe CD101-expressing CD4 T cells as an immunosuppressive population that is preferentially depleted following SIV/HIV infection and find that this loss is associated with higher viral burden and increased inflammatory cytokine levels. Furthermore, during long-term antiretroviral therapy, these cells display a phenotypical and functional profile consistent with cells that may critically contribute to reservoir persistence.

HIV cure efforts are increasingly focused on harnessing CD8 T cell functions and better understanding the profile of CD8 T cells promoting HIV control can critically inform novel therapeutic approaches. We explored dynamics of TOX and TCF1 expression in CD8 T cells after SIV infection in lymphoid tissue. CD8 T cells upregulated TOX and differentiated into distinct subsets, including a novel TCF1+CD39+ subset expressing high levels of TOX and inhibitory receptors, but not expressing cytotoxic molecules despite responsiveness to antigen stimulation. Transcriptional analysis of SIV-specific CD8 revealed TCF1+CD39+ cells as an intermediate effector population retaining stem-like features. TOX+TCF1+CD39+ CD8 T cells express higher levels of CXCR5 than terminally-differentiated cells and were found at higher frequency in follicular micro-environments. Importantly, their levels were strongly associated with viral control and lower reservoir size. Collectively, these data describe a unique population of lymphoid CD8 T cells possessing both stem-like and effector properties that contribute to limiting SIV persistence.

Taken together, these studies highlight potential pathways to target in the design of future therapeutic interventions to achieve an HIV cure.

**Mechanisms of HIV Pathogenesis, Persistence and Control in SIV-infected Rhesus
Macaques**

By

Zachary Strongin

B.S., Boston College, 2016

Advisor: Mirko Paiardini, Ph.D.

A dissertation submitted to the Faculty of the
James T. Laney School of Graduate Studies at Emory University
In partial fulfillment of the requirements for the degree of
Doctor of Philosophy

Program in Immunology and Molecular Pathogenesis
Graduate Division of Biological and Biomedical Sciences

2023

Acknowledgements

Table of Contents

<i>Chapter One: Introduction</i>	1
The HIV Pandemic	1
HIV Infection, Transmission and Life Cycle	1
HIV Pathogenesis	3
Innate Immune Response to HIV	4
Adaptive Immune Response to HIV	5
Antiretroviral Therapy	8
The HIV reservoir	10
Chronic infection and CD8 T cell exhaustion	13
CD8 T cell Exhaustion in HIV infection	16
HIV Cure	18
Animal models of HIV infection	22
Chapter One Summary	25
<i>Chapter Two: Virologic and immunologic features of SIV control post-ART interruption in rhesus macaques</i>	26
Abstract	27
Introduction	28
Results	30
Discussion	37
Materials and Methods	43
Chapter Two Figures	48
<i>Chapter Three: The role of CD101-expressing CD4 T cells in HIV/SIV pathogenesis and persistence</i>	59
Abstract	60
Introduction	62
Results	64
Discussion	72
Materials and Methods	77
Chapter Three Figures	86

Chapter Four: Distinct SIV-specific lymphoid tissue CD8 T cells simultaneously exhibit effector and stem-like profiles and associate with viral control and reduced reservoir size ...104

Abstract	105
Introduction.....	106
Results	108
Discussion.....	117
Materials and Methods.....	124
Chapter Four Figures	130
<i>Chapter Five: Discussion</i>	<i>155</i>
<i>References.....</i>	<i>161</i>

Table Index

Table S.2.1. Animal and infection characteristics.

Table 3.1. Correlations of CD101 dynamics with plasma viral load, immune activation and plasma cytokine levels.

Table 3.S1. Association of CD101 gut depletion and mucosal viral burden.

Table 3.S2. Intestinal epithelial damage biomarker correlations.

Table 3.S3. Animal characteristics.

Table 4.1. Rhesus macaque characteristics.

Figure Index

Figure 2.1. PTCs exhibit strong viral control after ART interruption

Figure 2.2. PTCs have reduced viral burden prior to ART initiation

Figure 2.3. PTCs experience reduced immunopathogenesis prior to ART initiation

Figure 2.4. Reservoir and immune characteristics of PTCs and NCs on ART

Figure 2.5. PTCs maintain viral control and preserve immune homeostasis during ATI

Figure S.2.1. CD4 T cell activation

Figure S.2.2. ROC analysis

Figure 3.1. Phenotype of CD101-expressing CD4 T cells in healthy rhesus macaques

Figure 3.2 Dynamics of CD101-expressing CD4 T cells after SIV infection

Figure 3.3 Phenotypic profile of CD101⁺ CD4 during long-term antiretroviral therapy

Figure 3.4. HIV DNA levels in sorted memory CD4 T cells

Figure 3.S1. CD101 in healthy RM

Figure 3.S2. UMAP with phenograph cluster locations

Figure 3.S3. Representative gating for cytokine expression after stimulation

Figure 3.S4. Frequency of CD4 Tregs in HIV-infected individuals

Figure 3.S5. *In vitro* infection of sorted CD4 T cells and exclusion of CD101 downregulation

Figure 3.S6. Preferential depletion of CD101⁺ CD4 T cells in the gut

Figure 4.1. TOX expression and CD8 phenotype during SIV infection

Figure 4.2. TCF1⁺ CD39⁺ CD8 T cells expand after SIV infection and are a unique phenotypic population

Figure 4.3. scRNA-seq of SIV-specific LN CD8 reveals distinct transcriptional clusters

Figure 4.4. Association between TOX⁺ and TCF1⁺ CD39⁺ LN CD8 frequencies and viral burden

Figure 4.5. TCF1⁺ CD39⁺ CD8 T cells penetrate follicular environment

Figure 4.6. TCF1⁺ CD39⁺ CD8 T cells contract during long-term ART but remain associated with viral burden

Figure 4.S1. Dynamics of TOX-expressing LN CD8 T cells during early chronic SIV infection

Figure 4.S2. Phenotype of TCF1/CD39 LN CD8 subsets during late chronic SIV infection

Figure 4.S3. Sorting of SIV-specific LN CD8 T cells

Figure 4.S4. scRNA-seq of SIV-specific LN CD8 T cells

Figure 4.S5. Association of LN CD8 T cells with cell-associated SIV RNA

Figure 4.S6. CXCR5 within LN CD8 T cells during early chronic SIV infection

Figure 4.S7. Imaging and dynamics of LN CD8 T cells

Figure 4.S8. Phenotype of TCF1/CD39 LN CD8 subsets during ART

Chapter One: Introduction

The HIV Pandemic

In the summer of 1981, acquired immune deficiency syndrome (AIDS) was first described in young, previously healthy men showing symptoms of opportunistic infections and rare cancers ¹. The rapid and widespread reporting of cases across the United States led to a flurry of research, resulting in the initial finding that AIDS was an infectious disease transferred by bodily fluids and exposure to blood and blood products ². Shortly thereafter, the causative agent of AIDS was discovered to be a retrovirus, Human Immunodeficiency Virus (HIV), by Françoise Barre-Sinoussi and Luc Montagnier ³. According to World Health Organization estimates, as of 2021 there were 38.4 million people living with HIV, with 1.5 million new annual infections and 650,000 deaths from HIV-related causes.

HIV Infection, Transmission and Life Cycle

HIV infection and transmission occurs through contact with bodily fluids, including blood, semen, vaginal fluid and breastmilk ⁴. Despite very low risk of transmission following an exposure event (1 transmission per 200-2000 exposures in heterosexual transmission), an estimated 70% of HIV infections occur via heterosexual transmission, with the remainder of infections occurring primarily via male-male sexual transmission, injection drug use and maternal-infant infection ⁴. Clinical presentation of HIV infection in the majority of the patients occurs as acute retroviral syndrome (ARS), which involves symptoms such as fever, headache, malaise, cough and lymphadenopathy ^{5,6}. These initial symptoms are self-limited and will often resolve within a few weeks, despite continued progression of HIV infection.

HIV is a single-stranded, enveloped RNA retrovirus as a part of the lentivirus group. The genome of HIV is 9.2 kilobases (kb) long and encodes nine open reading frames (ORFs). The three major proteins Gag, Pol and Env, are produced as polyproteins and subsequently proteolyzed into individual proteins ⁷. The Gag proteins include MA (matrix), CA (capsid) NC (nucleocapsid) and p6 and cooperate with the two Env proteins (gp120 and gp41) to serve as the structural components of the virion and envelope. The Pol proteins (protease, reverse transcriptase (RT) and integrase) are responsible for carrying out enzymatic activities required for HIV infection replication. The genome also includes 6 accessory or regulatory proteins (Vif, Vpr, Vpu, Tat, Rev and Nef) that serve roles in gene regulation, virion assembly and host immune evasion.

The target cells for HIV infection are cells in the human immune system (primarily CD4 T cells and macrophages) expressing the surface receptor CD4, the main receptor for the HIV envelope ⁸. In order to enter a cell, gp120 initially interacts with CD4 and this induces conformational change of the gp120 protein, exposing the binding site for a second surface molecule, or co-receptor, CCR5 or CXCR4 ^{9, 10}. This engagement allows gp41 to initiate fusion of the viral envelope with the cell's plasma membrane utilizing a six-helix hairpin structure, resulting in viral entry ^{11, 12}. Following viral entry, the viral nucleoprotein complex is exposed via uncoating of the virion core and subsequently transported to the nucleus. Once in the nucleus, RT is responsible for converting the RNA genome into double-stranded DNA followed by the integration of this DNA into the host chromosome by the integrase enzyme ¹³. Integration into the host genome allows for HIV to persist for the lifetime of the infected cell and utilized host machinery to replicate and disseminate to other cells.

HIV Pathogenesis

During the initial stages of HIV infection, the virus replicates rapidly at the site of infection and then spreads quickly to draining lymph nodes and subsequently systemically to distal lymph nodes and tissue sites ¹⁴⁻¹⁶. HIV RNA levels in plasma typically peak at this time of primary, acute infection, and the presenting symptoms during initial diagnosis are strongly associated with the peak viral load ¹⁷. The Fiebig staging system, developed in 2003 using samples from donors across stages of HIV infection, is used to classify the early stages of infection ¹⁸. The “eclipse phase” defines the initial period in which local tissue dissemination is occurring but the virus is not yet detectable in blood. The remaining 6 stages are defined by the varying levels of RNA, protein and immune responsiveness detected. Fiebig I (days 13-28 post-infection) are the stage at which viral RNA is detectable in the blood, while progression to Fiebig II (days 18-34) is defined by the presence in plasma of viral p24 antigen, an HIV capsid protein. Soon thereafter, in Fiebig III (days 22-37), the adaptive immune response becomes detectable and anti-HIV antibodies are measurable by standard enzyme-linked immunosorbent assay (ELISA). Fiebig IV-VI and progression into chronic infection are defined by progressive detectability of HIV antibodies via western blot and specifically the detection of anti-p31 antibodies.

As the primary target cell of HIV infection, CD4 T cells are dramatically depleted during the acute phase of infection ^{19, 20}. While macrophages and myeloid cells are also infected, infection occurs at much higher rates in CD4 T cells due to the preference for CCR5 as a coreceptor and the ability of some myeloid cells to provide stronger resistance to infection ²¹⁻²³. In particular, transmitted virus and virus isolated during acute infection are overwhelmingly specific for the CCR5 co-receptor, rather than CXCR4, and individuals with mutations in the

CCR5 gene are immune to HIV infection ^{4, 24-27}. This preference leads to a depletion of memory CD4 T cells in the mucosal sites, where CD4 T cells express high levels of CCR5 ^{20, 28, 29}. While more pronounced in the mucosa, the loss of memory CD4 T cells occurs systemically, with an estimated 30-60% of memory CD4 T cells infected during viremia, and the majority of these cells dying within days of infection ¹⁹. As target cells die off and the immune system mounts a response, plasma viremia decreases, CD4 T cell counts slightly recover and the disease enters a chronic phase, often initially asymptomatic ^{30, 31}. Over the following years, CD4 T cell counts will slowly decline as infection continues and the immune system fails to control the disease, oftentimes reaching CD4 T cell counts less than 200 cells/uL, the defined level for AIDS, when opportunistic infections and cancers begin to onset more frequently ³⁰.

Innate Immune Response to HIV

While HIV is often considered a disease of the adaptive immune system, the innate immune system is the first to respond and play a role during initial HIV infection. The initial response is triggered by the interaction of the single-stranded RNA virus with pattern recognition receptors, specifically TLR7 and TLR8 which detect this foreign material ³²⁻³⁴. This interaction results in activation of dendritic cells (DCs), including upregulation of MHC molecules and costimulatory molecules, and abundant production of Type 1 interferons (IFNs) and tumor necrosis factor α (TNF α). The triggering of these PRRs and activation of DCs has been shown to induce a systemic cytokine storm, with a flurried release of many pro-inflammatory cytokines including IFN α , IL-15 and IP-10 ³⁵. In particular, the role of IFN α in HIV infection has been extensively examined and IFN α has been shown to play an important protective role, as blocking of the IFN α receptor leads to increased viral loads and treatment with IFN α can lower HIV RNA

levels³⁶⁻⁴⁰. However, due to its pro-inflammatory nature, increased type 1 IFN signaling is also associated with increased activation, recruitment and depletion of CD4 T cells⁴¹⁻⁴³.

The pro-inflammatory signaling induced by HIV infection also leads to the upregulation of host restriction factors aimed at limiting viral replication. The APOBEC family of proteins, particularly APOBEC3G, are transcriptionally induced by type 1 IFNs and target the virus through DNA/RNA cytidine deaminase activity after being packaged into assembling virions^{44, 45}. The hypermutation of ~10% of all HIV genomes results in faulty virus production, but the activity of APOBEC3G is countered by the HIV protein Vif, which serves to bind APOBEC3G and recruit it for ubiquitination and degradation, preventing mutational activity^{46, 47}. Another vital host restriction factor is TRIM5 α , which binds directly to the HIV capsid, disrupting the uncoating process and preventing nuclear import and reverse transcription^{48, 49}. Tetherin, a third restriction factor, was identified in the search for the purpose of HIV accessory protein Vpu. In the absence of Vpu activity, tetherin keeps HIV virions trapped at the surface of infected cell, preventing budding and release from the plasma membrane^{50, 51}. Vpu works to antagonize this activity and allow proper release of the virion into the extracellular space.

Adaptive Immune Response to HIV

In addition to being a primary target, CD4 T cells do respond specifically to HIV infection. HIV-specific CD4 T cells have been shown to develop strong proliferative and cytolytic response to infection and the presence of these cells has been associated with better control of viremia^{52, 53}. On the other hand, due to their activated state, HIV-specific CD4 T cells are preferentially infected and harbor more viral DNA, leading to an eventual loss of the HIV-specific CD4 T cell response⁵⁴. Additionally, during chronic infection, responding CD4 T cells

typically become less functional, or exhausted, a state defined by an upregulation of inhibitory receptors and a loss of the ability to proliferate and produce effector cytokines ^{55, 56}.

Another class of CD4 T cells that play a major role in HIV infection are TH17 cells, a subset of T helper cells that produce IL-17 and are found predominately in the gastrointestinal tract, where are vitally important to mucosal health and against bacterial and fungal antigens ⁵⁷. During chronic HIV infection, Brenchley et al. have shown that TH17 cells are preferentially lost in the GI tract compared to uninfected individuals ⁵⁸. In contrast, using non-human primate models of HIV infection, it was shown that animals that do not experience depletion of these cells after SIV infection experience non-pathogenic effects and remain relatively healthy, while animals that lose their mucosal TH17 populations experience a pathogenic infection ⁵⁸. This may be due to a phenomenon known as microbial translocation, in which damage to the gut mucosa leads to systemic inflammation and progression to AIDS, as this loss of IL-17 and IL-22 producing cells likely leads to the breakdown of the gut mucosa ⁵⁹. This concept is further supported by studies that have demonstrated that restoration of levels of TH17 CD4 T cells using IL-21 therapy can subsequently reduce systemic inflammation in SIV infection ^{60, 61}.

The antibody response to primary HIV infection is first defined by gp41-specific IgM antibodies, that progress to IgG antibodies but do not have a capacity to control HIV replication ⁶². As the infection and B cell response progress, neutralizing antibodies targeting the HIV envelope are eventually generated after significant class switching and affinity maturation processes ⁶³. Given the slow nature of this process and the quickly evolving nature of the virus, neutralizing antibodies that are developed are often quickly evaded by the virus. An additional factor contributing to the difficulty of the immune system to generate an effective antibody response is the infection and impairment of T follicular helper cells (TFH), a class of CD4 T cell

that plays a critical role in the maturation of a B cell response⁶⁴. A rare subset of individuals mount remarkable B cell responses that result in the development of broadly neutralizing antibodies (bnAbs) that are capable of neutralizing the a broad array of HIV envelopes despite its highly diverse nature. These antibodies typically target highly conserved epitopes on the HIV envelope that are difficult for the virus to mutate without significant loss of function, such as the CD4 binding site, the V1/V2 loop, and the membrane proximal external region (MPER) of gp41⁶⁵. While provoking natural generation of these antibodies via vaccination or other methods is extremely difficult, treatment with bnAbs in HIV-infected individuals has shown promise for preventing HIV acquisition and limiting viral load, suggesting potential for bnAbs playing a role in HIV cure efforts⁶⁶. Non-neutralizing antibodies are also generated against HIV and can limit viral load via FC-dependent antiviral functions such as antibody-dependent cellular cytotoxicity (ADCC) and antibody-dependent cellular phagocytosis (ADCP)⁶⁷. Indeed, studies of the RV144 vaccination trial, which resulted in modest efficacy in preventing HIV acquisition, have shown that non-neutralizing antibodies that mediate ADCC activity were shown to be a key correlate of protection⁶⁸.

CD8 T cells play an important role in HIV infection at both the acute and chronic stages. Within 2-4 weeks of infection, cytolytic CD8 T cells directed at the transmitted/founder virus expand and this expansion is strongly associated with the decline of peak viremia towards a viral set point^{31, 69-71}. Additional studies in animal models in which CD8 T cells were depleted during both acute and chronic infection demonstrated a direct link between CD8 T cells and viral control⁷²⁻⁷⁴. Despite this specific and strong response, CD8 T cells are unable to establish complete viral control in most individuals and viral replication persists as the infection moves into a chronic phase. This is primarily driven by two factors: immune exhaustion (discussed in

detail in the CD8 T cell Exhaustion section) and significant immune selection pressure and viral escape from CD8 T cells. Viral escape occurs when the cytolytic CD8 T cell response exerts selective pressure on HIV infected cells, resulting in selection and successful dissemination of viral sequences that have mutated away from the dominant CD8 T cell epitopes^{75, 76}. Studies show that HIV-specific CD8 T cell repertoires broaden in response to this escape, but broader responses do not result in more effective control of viremia⁷⁷⁻⁷⁹. Importantly, most studies on CD8 T cell responses to HIV infection are focused on peripheral blood samples, while the overwhelming majority of HIV target cells, and therefore viral replication, reside in lymphoid tissue^{80, 81}. Recent work has highlighted the importance of specifically investigating lymphoid tissue HIV-specific CD8 T cells, as studies have shown these cells to reside in lymph nodes and be phenotypically and functionally distinct from peripheral CD8 T cells, including an ability to limit viremia via non-traditional cytolytic pathways⁸²⁻⁸⁴.

Antiretroviral Therapy

Within a few years of the discovery of HIV as the retrovirus causing AIDS, azidothymidine (AZT) was approved as the first anti-HIV drug⁸⁵. In the mid-1990s, remarkable advancements in antiretroviral therapy (ART) led to the ability to completely control HIV within most infected individuals⁸⁶⁻⁸⁹. A daily regimen of typical combination ART is able to suppress viremia, prevent new transmission and enable high quality of life with life expectancy similar to that of the general population.

ART is designed to target multiple aspects of the viral lifecycle to ensure complete viral suppression, prevention of spreading infection to other cells, and avoid the rise of drug-resistant mutations. Current ART regimens target the major proteins needed for HIV replication: reverse

transcriptase, integrase and protease. Reverse transcription is typically targeted using nucleoside analogs (nucleoside reverse transcriptase inhibitors, NRTIs) such as Tenofovir disoproxil fumarate (TDF) or emtricitabine (FTC), which interfere with reverse transcription and result in termination of viral DNA synthesis. This same process can also be targeted with non-nucleoside reverse transcriptase inhibitors (NNRTIs), such as efavirenz (EFV), which bind directly to the reverse transcriptase protein and induces conformational changes and reduced polymerase activity, although these drugs are highly susceptible to drug-resistance mutations with low fitness cost for the virus ⁸⁶. The second replication process, viral DNA integration, is targeted using integrase inhibitors, such as Dolutegravir (DTG) and Cabotegravir, which bind the catalytic domain of integrase and block the strand transfer reaction needed for integration ⁹⁰. Protease inhibitors such as darunavir work by preventing the late phase of viral replication through interference with cleavage of precursor polyproteins, precluding the mature virion from forming, but these drugs are generally not used in first-line treatment regimens ⁹¹. All of these drugs are historically taken in combination regimens on a daily basis. However, recent advances in drug delivery and lack of drug resistance have unearthed the potential for long-acting formulations of integrase inhibitors and reverse transcriptase inhibitors given as monthly or bi-monthly injections, some of which have now received FDA approval ⁹².

While antiretroviral therapy is remarkably effective at suppressing viral replication preventing transmission and lengthening the lifespan of HIV-infected individuals, it is unable to eradicate infected cells from the body. This results in infected CD4 T cells remaining latently infected and persisting for the lifetime of the infected individual ⁹³⁻⁹⁵. Therefore, release from ART adherence results in rapid viral rebound in the majority of individuals ⁹⁶. To date, HIV-infected individuals must remain on ART for the duration of their life, a burden for those

infected as well as the public health system. Major financial and cultural barriers exist, particularly in low-income areas, that result in delayed ART initiation and poor adherence. Additionally, despite the effectiveness of ART, residual inflammation and immune activation can persist during therapy and, in combination with long-term side effects of ART, lead to excess risk of cardiovascular, liver, kidney, bone and neurologic diseases ^{97, 98}. These issues provide continued need to work towards an HIV cure.

The HIV reservoir

As mentioned, despite the effectiveness of ART at suppressing viral replication, it is unable to directly eliminate infected CD4 T cells and the interruption of ART results in rapid viral rebound and continued CD4 T cell loss in most individuals ⁹⁹. Work performed shortly after the advent of effective combination ART demonstrated the persistence of a population of latently infected CD4 T cells that harbor replication-competent virus, but do not actively produce replicating virions ⁹³⁻⁹⁵. These cells, termed the latent viral reservoir, have a very long half-life of approximately 3.5 years and therefore natural decay of the reservoir is unlikely to result in eradication of the infected cell population ¹⁰⁰⁻¹⁰². This reservoir can be measured through detection of integrated viral DNA, and progressive advancement of DNA sequencing technology continues to provide new insights into the genetic properties of the reservoir.

The establishment and maintenance of the viral reservoir is an important topic of investigation, with many factors likely contributing to its persistence. Based on studies in animals models of HIV, the reservoir is established within the first few days post-infection and exponentially expands within the first week of infection ¹⁰³. Additionally, extremely early ART initiation in HIV-infected individuals has been shown to be unable to prevent establishment of

the reservoir, although early ART does significantly restrict the overall size of the reservoir¹⁰⁴⁻¹⁰⁶. After establishment, the reservoir likely persists through a variety of mechanisms which are reliant on the long-lived nature of resting CD4 T cells¹⁰⁷⁻¹⁰⁹. Homeostatic proliferation, the process in which memory T cells are maintained over long periods of time, plays an important role in the ability of infected cells to persist. In the absence of virus reactivation or antigenic stimulation, latently infected cells proliferate to maintain normal T cell homeostasis¹¹⁰⁻¹¹². Support for this as a major factor of persistence comes from the presence of large clonal populations of infected CD4 T cells that contain the same integration site¹¹³⁻¹¹⁸. Given the effectiveness of ART, the presence of cells containing the same viral sequence integrated at the same genetic locus provides very strong evidence that the reservoir is being maintained via a clonal process driven by homeostatic proliferation. Chronic antigen stimulation and antigenic proliferation can also contribute to this persistence, as it has been demonstrated that large clonal populations can expand and contract over time, and that persistent low-level viremia on ART is often sourced from a single T cell clone¹¹⁹⁻¹²².

The cellular composition is also an important element of understanding the dynamics of the HIV reservoir. HIV persists on ART in all subsets of CD4 T cells, including the memory subsets (effector memory, central memory, stem cell memory etc.) as well as functional helper subsets (T follicular helper cells, TFh; T regulatory cells, Tregs; Th17 cells). Naïve CD4 T cells have also been shown to contribute to viral persistence, while the contribution of non-CD4 T cells, primarily macrophages, remains controversial, as studies to this point have been largely non-conclusive and are difficult to conduct in HIV-infected individuals¹²³⁻¹²⁷. It is widely hypothesized that cells that maintain self-renewing capacity and are in a more resting state are likely to be the important long-term reservoirs, including central and stem cell memory CD4 T

cells, whereas effector memory CD4 T cells are likely to serve as the most inducible and activated viral reservoirs ^{96, 112, 128-131}. Within lymphoid tissues, higher proportions of the overall CD4 population are infected and additional important contributions from CD4⁺ TFh and Tregs have been demonstrated, highlighting the importance of the lymphoid environment in HIV persistence ¹³²⁻¹³⁷.

Along with the ability to clonally expand, the capacity for continued immune evasion is a major barrier to natural clearance of the viral reservoir. Infected CD4 T cells are able to proliferate and expand without reactivation of virus, giving CD8 T cells no window of opportunity to recognize and target those cells. Additionally, the phenotypic profile of latently infected cells plays a major role in their ability to avoid immune pressure and persist. Great investments have been made in identifying a singular phenotype that marks the reservoir, which would allow for direct targeting and elimination. To date, despite impressive technological advancement and depth of analyses, no such marker has been identified and the phenotype of infected cells has been found to be profoundly heterogeneous ¹³⁸⁻¹⁴¹. However, this work has demonstrated consistent themes of HIV-infected cells. This includes the enrichment of HIV proviruses in cells expressing canonical markers of T cell activation including HLA-DR, CD25 and CD69 ^{139, 142-145}. Importantly, extensive analyses have also shown that latently infected cells are enriched for expression of inhibitory receptors, including PD-1, CTLA-4, LAG-3, TIM-3, CD101 and TIGIT ^{134, 137, 139, 146-148}. These inhibitory receptors act in a twofold manner to prevent immune clearance, acting to prevent the infected cell from becoming activated and expressing virus for detection, while also dampening CD8 T cell activity in these immunosuppressive environments. These cells are also found at high frequency in lymphoid follicular environments, where CD8 T cells have less ability to penetrate and interact with infected cells ^{134, 137}.

Chronic infection and CD8 T cell exhaustion

As mentioned previously, while CD8 T cells mount a robust and specific response to HIV infection, they are most often unable to completely control the virus due to significant viral escape and immune exhaustion. Immune exhaustion occurs when antigen-specific CD8 T cells mount a persistent, but functionally compromised response to a chronic antigen. This phenomenon was first observed in mice with chronic LCMV, where CD8 T cells continued to respond to the infection but were not efficiently exhibiting effector function ^{149, 150}.

In response to a standard acute infection, naïve CD8 T cells will undergo activation, proliferation and expansion upon interacting with their cognate antigen ¹⁵¹. These cells then differentiate into hallmark cytolytic effector CD8 T cells that are capable of killing target cells, driven by a complete reprogramming on the transcriptional and epigenetic levels. Typically, this reprogramming allows for effector CD8 T cells to produce cytokines and cytotoxic molecules such as GzmK, allowing for clearance of infected cells, antigen removal and resolution of inflammation. At this point, self-limiting mechanisms lead to the death of the majority of effector T cells during the ‘contraction’ phase of the response, but a small portion of them survive and differentiate into memory T cells. These memory cells will reduce their effector functions, downregulating cytokine and cytotoxic molecule production, and enact a memory phenotype allowing them to survive long periods of time, undergoing homeostatic proliferation with a dependence on IL-7 and IL-15 ¹⁵². Unlike in acute infection settings, chronic viral infections and cancers do not result in resolution of antigen presence, and therefore the transition from the active effector CD8 T cell population to the quiescent memory CD8 T cell population does not

occur, and responding CD8 T cells progress instead to the exhausted state. CD8 T cell exhaustion is frequently studied using chronic LCMV infection, but it is a ubiquitous phenomenon across chronic disease states, including hepatitis C virus, hepatitis B virus, many different cancer types, and importantly HIV ^{153, 154}.

A major hallmark of CD8 T cell exhaustion is the progressive loss of CD8 T cell effector function. This loss typically occurs in a specific order, first with the loss of IL-2 production, followed by TNF α and overall cytotoxicity ^{155, 156}. Loss of the ability to produce IFN γ occurs at more advanced stages of exhaustion, typically referred to as a state of “terminal exhaustion” ¹⁵⁷⁻¹⁵⁹. These exhausted cells can retain ability to produce various chemokines and less inflammatory cytokines, and are able to continue to degranulate ^{153, 155, 160, 161}. Additionally, exhausted CD8 T cells are no longer responsive to IL-7 and IL-15 and are unable to undergo normal homeostatic proliferation, and instead persist and proliferate in response to continued antigen signal encounter ¹⁶²⁻¹⁶⁶. These functional changes are accompanied by phenotypic changes and sustained expression on a number of inhibitory receptors, allowing for studies to frequently identify exhausted cells by cell surface markers. These receptors typically are upregulated in response to antigen stimulation and serve to dampen sustained T cell activation in a self-limiting manner, but in chronic antigen settings result in deleterious effects on sustained CD8 T cell effectiveness ¹⁶⁷. One such hallmark inhibitory receptor is PD-1, which is widely expressed on antigen-specific T cells across chronic disease settings ¹⁵³. Given its prevalence on exhausted cells, a fundamental study in 2006 demonstrated that utilizing an antibody to block PD-1 during chronic viral infection resulted in dramatic reductions in viral load and reinstatement of the function of previously exhausted CD8 T cells ¹⁶⁸. This study provided a clear indication that exhausted T cells were in a distinct differentiation state and this was a

targetable pathway with therapeutic potential. Other surface markers of CD8 T cells include TIGIT, LAG-3, TIM-3, CD39 and CD101, all of which are highly expressed on terminally exhausted CD8 T cells and likely play a direct role in limiting the function of these cells ¹⁶⁹⁻¹⁷⁵.

As advances were made in the understanding of markers and functional programs defining T cell exhaustion, it became clear that not all exhausted CD8 T cells were the same ^{153, 176}. Recent work has revealed the existence of two distinct subsets of stem-like and terminally exhausted T cells, with a spectrum of intermediate subsets in the middle, that can be defined by their phenotypic, transcriptional, epigenetic and functional programs ^{169, 177, 178}. The stem-like exhausted CD8 T cells are defined by their sustained expression of TCF-1, as well as other markers such as SLAMF6 and CXCR5, decreased expression of TIM3 and other terminal exhaustion markers, and their ability to self-renew, proliferate and differentiate into the intermediate and terminal populations ^{169, 178-183}. Critically, these cells are responsible for providing the proliferative burst and responsiveness to PD-1 blockade ^{169, 178, 181, 182, 184-187}. These stem-like cells go through the intermediate subsets and eventually reach a state of a terminally differentiated exhausted CD8 T cell, defined by the highest expression of PD-1, TIM-3, CD101 and CD39, faulty expression of effector proteins such as IFN γ and GzmB, and an inability to proliferate or self-renew with a lack of TCF1 expression and impaired cell cycling ^{182, 185}.

The programming that drives exhaustion is critical to understand, given its repercussions for therapeutic design in chronic viral infections and cancers. While defining exhausted cells is now widely described and understood, the cellular driver of T cell exhaustion was not well known until 2019. Understanding chronic antigen stimulation as the external driver of T cell exhaustion, studies published in 2019 revealed the transcriptional driver of the CD8 exhaustion program to be the high-mobility group box transcription factor TOX ¹⁸⁸⁻¹⁹². These papers

described TOX as the critical transcription factor for the differentiation and maintenance of the initial TCF1+ PD-1+ stem-like exhausted CD8 T cell population ¹⁸⁸⁻¹⁹². The core mechanism at work was demonstrated to operate via chronic TCR signaling, which results in calcium signaling via NFAT and eventual activation of the *Tox* gene locus ¹⁹³. In turn, TOX is responsible for a wide array of epigenetic and transcriptional changes that drives the exhaustion program described above, including the expression of TCF1, effector molecules and inhibitory receptors such as PD-1 and LAG-3. Importantly, in a chronic antigen setting, the absence of TOX results in the loss of the stem-like TCF1+ CD8 population and development of an extreme effector program similar to acute infection, leading to heavy immunopathology before eventual collapse of the antigen-specific CD8 population ¹⁸⁹⁻¹⁹¹. This demonstrates the importance of TOX in maintaining persistent CD8 responses to chronic antigen, as well as the usefulness of the overall T cell exhaustion program in preventing severe immunopathology and damage in chronic diseases, as TOX was found to drive exhaustion across a plethora of chronic viral infections and cancers ¹⁹⁴⁻²⁰².

CD8 T cell Exhaustion in HIV infection

While the exact kinetics and cellular dynamics vary, similar principles of CD8 T cell exhaustion apply across nearly all chronic viral infections, including HIV. Early investigations into T cell responses to HIV demonstrated that the persistently high antigen levels in chronic infection are accompanied a decreased functional capacity of HIV-specific T cells ^{54, 203}. Despite effective responses in acute infection, during chronic infection HIV-specific T cells have decreased cytolytic potential, reduced proliferative capacity and limited IL-2 and IFN γ production ²⁰⁴⁻²⁰⁸.

During chronic HIV infection, studies demonstrated that PD-1 is expressed on virus-specific CD8 T cells and that this expression correlated with loss of CD8 T cell function, increased viral load and lower CD4 T cell counts^{206, 207, 209}. Similar to chronic LCMV models, it was demonstrated that PD-1 blockade could enhance HIV-specific CD8 T cell survival, proliferation and effector capacity^{206, 209-211}. Additional inhibitory receptors and exhaustion markers including TIGIT, Lag-3 and CD39 expressed on HIV-specific T cells have been linked directly to disease progression in chronic HIV infection^{175, 212-215}. Additional factors contributing to CD8 exhaustion during HIV include the lack of CD4 help due to depletion and impairment of CD4 T cells and the upregulation of immunosuppressive cytokines such as IL-10, which has been shown to increase after HIV infection and has been implicated in exhausted CD8 T cell responses^{154, 216, 217}. The dynamics of exhaustion progression and stem-like exhausted CD8 T cells have not been explored to the same degree in HIV infection as in other LCMV and cancer models. Studies have shown that TCF1 is expressed on HIV-specific CD8 T cells and that this expression is linked to HIV control, but the dynamics of stem-like, intermediate and terminally exhausted populations have not been explored^{218, 219}. Additionally, TOX has been demonstrated to be upregulated on HIV-specific CD8 T cells, although these analyses have been limited to the periphery^{213, 218}. Overall, there is a broad understanding that HIV-specific CD8 T cells progress to an exhausted state and appear similar phenotypically and functionally to those found in other diseases, but additional work on the kinetics and dynamics of this exhaustion can continue to inform therapeutic approaches towards CD8-mediated HIV cure.

HIV Cure

Given the persistence of the viral reservoir, an inability to start ART without viral rebound and the burden of lifelong medication and disease, there is immense interest in developing a cure for HIV. The ideal result of any curative intervention would be a complete eradication of the disease from the body, a sterilizing cure, but this is likely unachievable given the difficulties of eliminating the entire viral reservoir from all organs in the body ²²⁰. There have been multiple documented cases in which the virus was completely undetectable in an individual, but those individuals eventually exhibited viral rebound after months of ART ^{104, 105, 221, 222}. Researchers have shifted their focus to achieving a “functional cure”, a state in which the virus may still be present in an individual, but is maintained at such a low level that it does not cause disease and cannot be transmitted ²²⁰.

There have been three reported cases of individuals completely cured of HIV, with two additional individuals currently exhibiting long term remission ²²³⁻²²⁷. In all of these cases, an HIV infected individual was diagnosed with cancer and required a stem-cell transplant. They each underwent an allogeneic hematopoietic stem cell transplant from a donor homozygous for the CCR5 Δ 32/ Δ 32 mutation. This mutation protects cells from HIV infection by an CCR5-tropic virus, meaning the newly engrafted cells in the HIV infected individuals would not be infected. In each of these cases, these individuals were able to withdraw from ART and remain aviremic ²²³⁻²²⁷. This approach is not foolproof, as cells are still susceptible to infection with CXCR4-tropic HIV variants and individuals receiving CCR5 Δ 32/ Δ 32 transplants are not immune to spread of those viruses that may be present prior to the transplant ²²⁸. Most importantly, despite

its remarkable success for the wellbeing of those individuals, this is not a scalable approach towards HIV cure given its high-risk and resource-heavy nature.

Natural control of HIV, in which individuals undetectable or low levels of viremia in the absence of ART, is a rare but well-documented phenomenon that can provide insight into potential approaches towards concepts of a functional HIV cure. Elite controllers (ECs) are defined by varying criteria, but typically are individuals who have never been treated with ART, exhibit stable CD4 T cell counts, and undetectable viral loads ²²⁹. This natural control has been widely demonstrated to be due to the unique capacities of CD8 T cells in these individuals. One component shown to strongly to be strongly associated with HIV control is the presence of major genetic polymorphisms, primarily within *HLA-B* genetic loci, that likely influence the viral peptides presented to CD8 T cells ²³⁰⁻²³⁴. Additionally, ECs demonstrate highly functional HIV-specific CD8 T cell responses compared to non-controllers, including increased proliferation upon stimulation and greater cytolytic potential ²³⁵⁻²⁴⁰. Interestingly, investigations into CD8 T cells from lymphoid tissue of ECs has demonstrated unique transcriptional and functional characteristics of lymphoid CD8 T cells, including suppression of viral replication in the absence of traditional cytotoxic mechanisms ⁸⁴.

These characteristics demonstrate significant potential for functional CD8 T cells to play a role in HIV cure efforts. Indeed, a number of therapeutic approaches have been developed in an attempt to reinvigorate exhausted HIV-specific CD8 T cells to enable viral control. One such approach is the use of therapeutic vaccination to elicit CD8 responses toward preferred viral epitopes, as control is mediated by targeting of specific epitopes ²⁴¹. The use of dendritic cell-based vaccines (or antigen-pulsed dendritic cells) has shown promise in enhancing immune responses and inducing modest reductions in viral load ²⁴²⁻²⁴⁶. Additional vaccine approaches

dedicating to improving the breadth of T cell responses via “mosaic” vaccines have shown promise²⁴⁷⁻²⁴⁹. The use of combined recombinant adenovirus serotype 26 and modified vaccinia Ankara vaccines have shown promise in animal models to boost CD8 T cell responses, decrease levels of viral DNA and delay viral rebound, but these same effects were not replicated in a clinical trial of ART-treated HIV infected individuals^{250, 251}.

Given the exhausted nature of HIV-specific CD8 T cells, redirection of targeting to preferred viral epitopes is likely insufficient to induce sustained viral control, particularly given the mutability and viral escape capacity of HIV. Given this, ongoing studies are focused on utilizing translating the immunotherapy approaches that have shown remarkable success in cancer to the HIV field. The first study testing PD-1 blockade in chronic infection demonstrated significant expansion of antigen-specific CD8 T cells and reduction in plasma viral load²¹⁰. Additional attempts have been made to treat with PD-1 blockade during long-term ART in animal models and HIV-infected individuals. While these studies have had varying impact on the viral reservoir, they fail to improve CD8 T cell capacity to the same extent and have not demonstrated significant potential for viral control²⁵²⁻²⁵⁶. Continued explorations of immunotherapeutic approaches involving combination inhibitor receptor blockade and the timing of blockade with viremia or ART initiation are required. Another strategy to restore CD8 T cell function is through the use of cytokine therapy, with a particular focus on IL-15²⁵⁷. Administration of IL-15 agonists has been shown to boost the levels of effector CD8 T cells and increase CD8 T cell migration into follicular lymph node environments^{258, 259}.

Additional hints at contributions to HIV cure come from a group of individuals termed post-treatment controllers (PTCs). PTCs are a small subset of HIV-infected individuals that are able to maintain viral suppression and avoid disease progression after interruption of ART. To

date, PTCs have been identified and characterized across a number of cohorts and the observed frequency ranges between 2-15% of individuals undergoing ART interruption²⁶⁰⁻²⁶⁵. Unlike elite controllers, PTCs do not exhibit viral control prior to ART initiation and do not demonstrate evidence of protective HLA alleles or significantly enhanced CD8 T cell responses²⁶⁶. Of note, PTCs demonstrate significantly lower levels of intact HIV DNA compared to non-controllers⁴⁷. Additionally, post-treatment control is more likely to occur in individuals who initiate ART early after HIV infection compared to in the chronic phase of infection²⁶⁰. Studies have demonstrated that earlier initiation of ART limits the size of the reservoir and preserves immune function^{106, 267, 268}. Collectively, these findings suggest that cure strategies targeting reduced reservoir size may be best suited to induce viral control.

Given its complex nature and the potential value of size reduction, the majority of recent HIV cure efforts have been directed at the latent viral reservoir^{220, 257}. Largely, these approaches attempt to reactivate latent cells through use of latency reversing agents (LRAs), leading to expression of the viral reservoir and subsequent clearance by the immune system or another therapeutic compound. Histone deacetylase inhibitors (HDACi's) constitute the one of the earliest LRA's developed, in which the drugs target the chromatin structure to increase histone acetylation of the HIV promoter region, leading to increased viral expression²⁶⁹. Clinical trials of HDAC inhibitors have demonstrated potential to increase HIV RNA levels, but have not shown any reduction in the overall reservoir size and are associated with significant off-target side effects²⁷⁰⁻²⁷². Another strategy involves targeting TLR7, a pattern recognition receptor that induces immune activation. While this approach demonstrated potential in animal models, clinical trial results have indicated that a TLR-7 agonist does not significantly impact HIV RNA levels on ART and does not result in reservoir reduction^{273, 274}. Recent work has elucidated the

potential for CD8 T cell depletion, in combination with IL-15 antagonism, to result in significant viral rebound during ART, although CD8 depletion is not a feasible clinically translational approach and these studies did not result in reduction of the latent reservoir^{275, 276}. Another molecule with demonstrated LRA potential in animal models is SMAC mimetic, which activates the noncanonical NF- κ B pathway and has been shown to induce viremia during ART^{277, 278}. Immunotherapy approaches targeting the inhibitory receptors highly expressed on many reservoir cells have been utilized, with varying degrees of success at inducing latency reversal and a consistent inability to result in delayed viral rebound or viral control^{253, 254, 279-281}. Summarily, approaches to targeting the latent reservoir have shown incremental improvement, but the development of a therapeutic intervention that successfully reduces the viral reservoir and prevents viral rebound following ART interruption will likely require a combinatorial approach that has not yet been identified.

Animal models of HIV infection

The use of animal models to study disease is a consistent theme across all immunology disciplines and have allowed for critical discoveries in the field of HIV research, with the ability to control infection dynamics, perform experiments and access tissues that would not be possible in human subjects. While initial studies focused on chimpanzees as an animal model, these animals are natural hosts (SIVcpz was the origin virus of HIV-1) and therefore these animals did not develop disease at a high rate, while ethical concerns also limited the potential for chimpanzees to serve as a sustainable model system²⁸²⁻²⁸⁴. In order to establish a strong model to study pathogenesis and persistence of HIV and AIDS, researchers turned to non-natural host Asian macaque species including rhesus (*Macaca mulatta*; RMs), pig-tailed (*Macaca nemestrina*; PMs) and cynomolgus (*Macaca fascicularis*; CMs) macaques^{285, 286}.

Rhesus macaques are the most widely used animal model in current HIV research. They are easily infected with SIV via multiple clinically relevant routes, experience significant CD4 T cell loss similar to humans, and eventually progress to AIDS. The most common virus, SIVmac239, replicates with viral dynamics similar to those seen in HIV-infected individuals and is well suppressed using modern ART to allow for investigations of viral reservoirs during long-term ART^{60, 103, 253, 276, 287}. Other experimental strains of SIV have been developed, including viruses with various envelope tropisms, genetic diversity and engineered barcodes, to allow for specific investigations into specific cell targets, neurological disease outcomes and viral clonality and rebound^{288, 289}. Additionally, SIV/HIV hybrid strains, termed SHIVs, are chimeric constructs utilizing an HIV-1 enveloped genetically engineered into an SIV backbone to allow for replication in non-human primate hosts with human envelopes to enable testing of HIV-based vaccines or antibodies targeting the HIV envelope^{285, 290, 291}.

Comparison of non-natural hosts such as macaques with natural host species such as sooty mangabeys (SMs) has given significant insights into mechanisms of SIV pathogenesis, which can be extrapolated to target mechanisms by which HIV causes disease. SMs infected with SIV exhibit high levels of plasma viremia similar to RMs, but do not experience a progressive depletion of peripheral CD4 T cells or destruction of lymphoid tissues. Some of the major findings in non-pathogenic hosts include: the maintenance of healthy frequencies of Th17 in SIV-infected SMs, revealing the importance of the breakdown of the mucosal barrier in HIV infection; a strong but limited interferon response in SIV-infected SMs and African green

monkeys, demonstrating a mechanism of limiting persistent inflammation; and an increased migration of NK cell activities into follicular environments of SIV-infected African green monkeys, suggesting potential for NK cell-mediated viral control mechanisms ^{58, 292-294}.

Use of these non-human primate (NHP) models provides significant experimental advantages to further our understanding of HIV. The route, dose and timing of infection can all be tightly controlled and altered given the question of interest. Animals can be compared across multiple studies and institutions used well characterized SIV strains and consistent inoculating strategies. The initiation of ART can be specifically timed and adherence to the regimen is of no doubt to the researcher, while ART can also be stopped at any necessary time within a specific study with none of the health concerns that come with human analytical treatment interruption trials. NHP studies allow researchers to administer novel therapeutic interventions and simultaneously evaluate the safety and efficacy of that treatment while benefitting from access to frequent blood and tissue collections not possible in human clinical trials. However, NHP studies do require trained veterinary staff, significant institutional oversight, long time periods and significant expense to operate. The development of humanized mouse models of HIV has provided an additional animal model to experiment in a pre-clinical setting, although these systems also have significant limitations ²⁹⁵. Overall, animal models of HIV infection continue to be an invaluable resource to further our understanding of the disease and make progress in therapeutic development.

Chapter One Summary

Since its emergence in the 1980's, HIV has continually been one of the largest threats to public health worldwide. The virus's capacity for immune evasion and chronic disease has led to the death of approximately 40 million individuals ²⁹⁶. Antiretroviral therapy (ART) has been extremely effective at reducing viral transmission, preventing new infections and reducing HIV-related morbidity and mortality. However, the inability of ART to clear the viral reservoir leaves individuals burdened with lifelong HIV infection. Ultimately, a greater understanding of the mechanisms of viral pathogenesis, persistence and control are needed to better design future therapeutics aimed at achieving an HIV cure.

Herein, we evaluate multiple mechanisms of HIV pathogenesis, persistence and control utilizing SIV-infected rhesus macaques as a model for HIV infection. We explore the virologic and immunologic parameters associated with post-treatment control in SIV-infected macaques, a phenomenon mirroring PTC occurrence in HIV-infected individuals. We evaluated key cellular targets of HIV infection and persistence, discovering a role for CD101-expressing CD4 T cells in HIV infection. Finally, we explore the dynamics of a unique subset of lymphoid tissue CD8 T cells that are strongly associated with viral control and reduced reservoir size. In all, these findings continue to further our understandings of the most valuable mechanisms and pathways to target in future therapeutic design.

Chapter Two: Virologic and immunologic features of SIV control post-ART interruption in rhesus macaques

Zachary Strongin¹, Luca Micci¹, Rémi Fromentin^{2,3}, Justin Harper¹, Julia McBrien¹, Emily Ryan¹, Neeta Shenvi⁴, Kirk Easley⁴, Nicolas Chomont^{2,3}, Guido Silvestri^{1,5}, Mirko Paiardini^{1,5,#}

¹Division of Microbiology and Immunology, Yerkes National Primate Research Center, Emory University, Atlanta, GA, 30329, USA.

²Centre de recherche du CHUM, Montreal, QC, H2X 0A9, Canada

³Department of microbiology, infectiology and immunology, Université de Montréal, QC, H3T 1J4, Canada

⁴Rollins School of Public Health, Emory University, Atlanta, GA, 30329, USA.

⁵Department of Pathology and Laboratory Medicine, Emory University School of Medicine, Atlanta, GA, 30322, USA.

Published in *Journal of Virology* Volume 94, Number 14, July 1, 2020, PMID 32350073

Abstract

Antiretroviral therapy (ART) cannot eradicate HIV and a rapid rebound of virus replication follows analytical treatment interruption (ATI) in the vast majority of HIV-infected individuals. Sustained control of HIV replication without ART has been documented in a subset of individuals, defined as post-treatment controllers (PTCs). The key determinants of post-ART viral control remain largely unclear. Here, we identified seven SIV_{mac239}-infected rhesus macaques (RMs), defined as PTCs, who started ART 8 weeks post-infection, continued ART for >7 months, and controlled plasma viremia at <10⁴ copies/mL for up to 8 months after ATI and <200 copies/mL at the latest timepoint. We characterized immunologic and virologic features associated with post-ART SIV control in blood, lymph node (LN), and colorectal (RB) biopsies as compared to 15 non-controllers (NCs) RMs. Before ART initiation, PTCs had higher CD4 T-cell counts, lower plasma viremia and SIV-DNA content in blood and LN compared to NCs, but had similar CD8 T-cell function. While levels of intestinal CD4 T-cells were similar, PTCs had higher frequencies of Th17 cells. On-ART, PTCs had significantly lower levels of residual plasma viremia and SIV-DNA content in blood and tissues. After ATI, SIV-DNA content rapidly increased in NCs while it remained stable, or even decreased in PTCs. Finally, PTCs showed immunologic benefits of viral control after ATI, including higher CD4 T-cell levels and reduced immune activation. Overall, lower plasma viremia, reduced cell-associated SIV-DNA, and preserved Th17 homeostasis, including at pre-ART, are main features associated with sustained viral control after ATI in SIV-infected RMs.

Importance

While effective, antiretroviral therapy is not a cure of HIV infection. Therefore, there is great interest in achieving viral remission in the absence of antiretroviral therapy. Post-treatment controllers represent a small subset of individuals who are able to control HIV after cessation of antiretroviral therapy, but characteristics associated with these individuals have been largely limited to peripheral blood analysis. Here, we identified 7 SIV-infected rhesus macaques who mirrored the human post-treatment controller phenotype and performed immunologic and virologic analysis of blood, lymph node and colorectal biopsies to further understand the characteristics that distinguish them from non-controllers. Lower viral burden and preservation of immune homeostasis, including intestinal Th17 cells, both before and after ART, were shown to be two major factors associated with the ability to achieve post-treatment control. Overall, these results move the field further in the understanding of important characteristics of viral control in the absence of antiretroviral therapy.

Introduction

The advent of modern antiretroviral therapy (ART) has allowed for suppression of HIV-1 replication in HIV-1 infected individuals and has dramatically reduced HIV morbidity and mortality^{297, 298}. Unfortunately, due to the establishment of a pool of quiescent, infected CD4 T cells that harbor replication-competent virus, discontinuation of daily ART leads to rapid viral rebound and continued disease progression in most individuals^{93, 94}. Therefore, there is great interest in understanding the mechanisms regulating HIV persistence, the virologic and immunologic correlates of viral rebound, and the approaches that may lead to maintenance of viremic control after treatment interruption.

One model of such control is seen in a subset of patients referred to as Post-Treatment Controllers (PTCs). These individuals, best characterized by the VISCONTI and CHAMP studies, display an ability to maintain viral suppression after undergoing analytic treatment interruption (ATI) ^{260, 264}. While definitions vary by study, PTCs are typically characterized as maintaining plasma viral loads less than 400 copies/mL for at least 6 months following ATI ^{260, 262-264, 299-302}. Importantly, they seem to represent a distinct group from the more widely characterized Elite Controller (ECs) population. While ECs have been shown to have an overrepresentation of protective HLA alleles (B*27 and B*57), PTCs do not appear to be enriched in these alleles and so far have been shown to have inferior CD8 activity as compared to traditional ECs ^{264, 303}. In fact, these individuals may be more likely to carry HLA alleles previously characterized as “risk” alleles ²⁶⁴. Furthermore, post-treatment control is more widely observed than spontaneous control, with the occurrence estimated to range between 5-15% of individuals undergoing ATI, compared to the estimated EC frequency <0.5% ^{265, 304}. As most approaches targeted at achieving a functional HIV cure utilize HIV control after ATI as a primary readout, it is important to understand the dynamics of HIV control in order to target interventions toward this outcome, as well as be able to distinguish intervention-based control from naturally occurring post-treatment control.

Current studies have been unable to identify the driving mechanisms of PTCs, but control has been associated with earlier initiation of ART, lower prevalence of infected long-lived CD4 T cells (central memory), and an overall smaller reservoir size prior to cessation of treatment ^{47, 260, 264, 265, 305}. Importantly, early initiation of ART may function to both limit the size of the reservoir as well as preserve immune function, allowing for robust immune control of the virus after treatment. Unfortunately, as with many HIV studies, characterization of PTCs has been largely limited to analyses of peripheral blood samples and limited analyses have been performed in early infection,

before initiation of ART. Further challenging to broadly understanding the dynamics of post-treatment control are the limitations of differing infection kinetics and demographics within and across cohorts of human PTCs.

The established SIV model of HIV infection using rhesus macaques (RMs) allows for longitudinal investigations into dynamics of immunologic and virologic parameters of HIV infection, including in tissues. In this study, we identified 7 SIV-infected RMs that exhibit post-treatment control, allowing us to characterize features of virologic control that further the understanding of the PTC phenomenon. Despite identical viral infection and treatment timelines as non-controller RMs, these animals showed robust control of viremia post-ATI, with viral loads less than 10^4 copies/mL for the entire post ATI follow up and less than 200 copies/mL at the latest experimental point, similar to previously described human PTCs. We have identified important factors that seem to be associated with this control, including reduced SIV “exposure” prior to ART-initiation, better preservation of blood and LN CD4 T cells as well as of intestinal Th17 cells, lower levels of immune activation, and smaller reservoir size. Although limited in its size, this study enhances and expands to tissues the understanding of post-treatment control and suggests that non-human primate models of HIV can serve as an important tool in understanding and targeting critical mechanisms of viral control in absence of ART.

Results

Identification of post-treatment controllers among SIV-infected rhesus macaques.

Among different studies performed at the Yerkes National Primate Research Center in which rhesus macaques (RMs) were experimentally infected with SIV, initiated on ART and underwent analytic treatment interruption (ATI), we identified 7 RMs with superior ability to control viral

rebound after ATI as compared to what is normally seen in SIVmac₂₃₉-infected RMs. Specifically, these 7 RMs, defined as post-treatment controllers (PTCs), maintained plasma viremia $<10^4$ copies/mL up to 8 months post-interruption and all had viral loads <200 copies/mL at the final experimental time point (**Figure 1A**). To investigate the main features associated with post-treatment control, multiple virologic and immunologic parameters were assessed and compared with those of 15 RMs (non controllers, NCs) that did not control viral rebound after ATI, with plasma viremia $>10^4$ copies/mL for the majority of post-treatment follow up (**Figure 1B**). Among the very large number of SIVmac₂₃₉-infected RMs that do not control viral rebound after ATI, these 15 animals were selected because they match the experimental conditions used for the 7 PTCs, including (i) being infected with the same route and virus (intravenously; SIVmac₂₃₉); (ii) started ART 8 weeks post-infection (p.i.); (iii) being on ART for a period between 7 to 14 months; and (iv) having multiple viral load measures following ATI, with many of those overlapping in term of time post ATI with the PTC. Characteristics of each animal are described in **Supplementary Table 1**. All 22 animals were negative for B*08 and B*17, MHC class I alleles associated with the control of SIV replication^{306, 307}. Five out of 7 PTCs were MamuA01+, as compared to 4 out of 15 NCs. As indicated in Supplementary Table 1, two different ART regimens were used, with a similar PTC and NC distribution among the two regimens: tenofovir (PMPA), emtricitabine (FTC), raltegravir, and ritonavir-boosted darunavir (5 PTC and 9 NC) or tenofovir (TDF), FTC, and dolutegravir (DTG) (2 PTC and 6 NC). Furthermore, at ATI, all PTCs and NCs reached plasma viremia below the limit of detection (<60 copies/mL) of our standard assay, confirming a comparable efficacy of the two treatments. Control of plasma viremia after ATI in PTCs was partial, with detectable plasma viremia (>60 copies/mL) in 6 out of 7 RMs (**Figure 1A**). However, viral control was clearly superior as compared to NC, with more than a 3-log difference

in the average plasma viremia among the two groups of RMs up to 8 months post-ATI (mean: 2.1 vs. 5.9 log₁₀ copies/mL; **Figure 1C**).

RM PTCs had reduced SIV loads, but similar CD8 T cell responses, prior to ART initiation.

Taking advantage of the availability of specimens collected at multiple phases of infection, we first investigated if animals that became PTCs had a reduced pathogenic SIV infection before initiation of ART as compared to NCs. The levels of plasma viremia were significantly lower in PTC than NC both at peak (mean: 6.4 vs. 7.0 log₁₀ copies/mL, P=0.02) and at chronic phase (mean: 5.1 vs. 6.6 log₁₀ copies/mL, P=0.0008) of infection (**Figure 2A**). Due to sample availability and timing of analyses, only 5 of the 7 identified PTCs and 9 of 15 NCs (PTC 1-5 and NC 1-9) were included in subsequent analysis. Prior to ART initiation at week 8 post-infection, levels of total SIV DNA in peripheral blood CD4 T cells (mean: 10,991 vs. 41,405 SIV DNA copies per 10⁶ CD4 T cells, P=0.007; **Figure 2B**) and cell-associated SIV RNA in the colorectal tissue (mean: 38,445 vs. 168,556 SIV RNA copies per 10⁶ total cells, P=0.04; **Figure 2C**) were lower in PTCs as compared to NCs, while levels of SIV DNA in colorectal tissue only showed a non-significant trend towards lower levels in PTCs (mean: 1,036 vs. 2,171 SIV DNA copies per 10⁶ CD4 T cells, P=0.09; **Figure 2C**). To further investigate if the PTC status is associated with reduced infection of a specific CD4 T cell subset, we then purified naïve (CD28⁺ CD95⁻ CCR7⁺), central memory (T_{cm}; CD95⁺ CCR7⁺), effector memory (T_{EM}; CD95⁺ CCR7⁻) and T follicular helper (T_{FH}; PD-1⁺ CD200^{hi}) CD4 T cell subsets from blood and LN. A representative staining with the detailed gating strategy for LN is shown in **Figure 2D**. Of note, we previously showed that PD-1⁺ CD200^{hi} and PD-1⁺ CXCR5⁺ identify the same frequency of Tfh cells in the LN of SIV-infected RMs³⁰⁸. In both peripheral blood (**Figure 2E**) and LN (**Figure 2F**), levels of total SIV DNA were significantly

lower in PTCs as compared to NCs for all measured CD4 T cell subsets ($P < 0.05$ for all comparisons). Thus, reduced levels of SIV replication and lower frequencies of infected cells in all CD4 T cell subsets prior to ART is a general feature distinguishing RM PTCs from NCs.

To address potential differences in CD8 responses between NCs and PTCs, we assessed cytolytic capacity and proliferation of total CD8 T cells prior to ART initiation in both peripheral blood and LN. Specifically, we analyzed ex-vivo (without stimulation) levels of granzyme B, perforin, T-bet and Ki-67 by flow cytometry on total CD8 T cells. Our analysis revealed no biologically important differences between NCs and PTCs in expression of these markers, indicating similar CD8 cytolytic potential and proliferative response within these animals despite different viral burdens pre-ART ($P > 0.05$ for all comparisons; **Figure 2G,H**).

RM PTCs had reduced SIV-induced immunopathogenesis prior to ART initiation.

We then investigated the main immunologic differences between RM PTCs and NCs before ART initiation. Consistent with reduced levels of SIV infection, and despite similar baseline (pre-infection) levels, PTCs displayed significantly higher CD4 T cell counts (mean: 684 vs. 451 CD4 T cells per μ L blood, $P = 0.02$; **Figure 3A**) and lower frequency of activated (HLA-DR⁺CD38⁺) memory CD4 T cells (mean: 4.6% vs. 8.4%, $P = 0.03$; **Figure 3B**; **Supplemental Figure 1A**) than NCs in blood prior to starting ART. Consistently, the pre-infection to pre-ART change for blood CD4 T cell counts (mean change = -42 for PTC, $P = 0.55$; and mean change = -253 for NC, $P < 0.001$) and %HLA-DR⁺CD38⁺ of memory CD4 T cells (mean change = -0.9% for PTC, $P = 0.56$; and mean change = 4.2% for NC, $P = 0.004$) followed different patterns between the PTC and NC

groups. A trend towards better maintenance of CD4 T cells, as assessed by frequency of CD4⁺ cells in total CD3⁺ cells, was also observed in LN (mean: 56% vs. 44%, P=0.15; **Figure 3C**).

Recently, multiple studies highlighted the loss of intestinal CD4 T cells, particularly those belonging to the Th17 subset, as a main cause of compromised mucosal integrity and systemic immune activation during HIV and SIV infection^{58, 61, 309-312}. Interestingly, our comparative analyses showed that the frequency of bulk intestinal CD4 T cells at pre-infection and at initiation of ART were very similar between NCs and PTCs (**Figure 3D**). We also found equivalent levels of memory CD4 T cell activation in mucosal tissue (**Supplemental Figure 1B**). Th17 cells, defined as intestinal memory CD4 T cells expressing IL-17 after brief *in vitro* stimulation, were also present at comparable frequencies pre-infection (**Figure 3E**). However, after SIV infection, NCs experienced a considerably larger loss of Th17 cells than PTCs (P=0.007; **Figure 3E**), with reduction to 74% and 25% of their baseline level, respectively (P=0.001; **Figure 3F**). Representative staining before infection and before ART initiation is shown in **Figure 3G**. Significantly higher maintenance of Th17 cells despite equivalent loss of total CD4 T cells in the gut is remarkably similar to the phenomenon observed when comparing non-pathogenic SIV infection of sooty mangabeys with pathogenic models of SIV infection in RMs⁵⁸. Of note, although limited to 5 PTCs and 9 NCs, receiver operating characteristic curve (ROC) analysis suggests that total SIV DNA content in peripheral blood CD4 T cells and frequency of Th17 cells in the gut were the two pre-ART markers most strongly associated with increased likelihood of developing a PTC status (**Supplementary Figure 2a**), with an area under the curve (AUC) of 0.93 for both predictors. The estimated AUC indicates a 93% probability that a PTC animal had a higher

(or lower) predicted probability of PTC status than a NC animal for a random pair of animals with and without the outcome.

Viral reservoir and immune dynamics of PTCs differ from NCs during ART

We then assessed the viral and immunological status of NCs and PTCs during ART, prior to ATI. First, we assessed the presence of residual viremia by using an ultrasensitive viral load assay with a limit of detection of 3 copies of SIVmac₂₃₉/mL of plasma³¹³. Consistent with their lower viral loads before ART, PTCs were significantly faster to suppress residual viremia while on ART as compared to NCs, with 4 out of 5 animals (80%) at 75 days and 5 out of 5 (100%) at 200 days after ART initiation achieving plasma viral load <3 copies/mL, as compared to 0 out of 9 (0%) and 3 out of 9 (33%) for NC, respectively (day 75: P=0.002, day 200: P=0.04; **Figure 4A**). While SIV DNA content declined in both PTCs and NCs during ART, PTCs continued to harbor lower levels of SIV DNA in CD4 T cells from peripheral blood both at a mid (mean: 2,608 vs 7,402 SIV DNA copies per 10⁶ CD4 T cells, P = 0.04) and late ART (mean: 367 vs 1,596 SIV DNA copies per 10⁶ CD4 T cells, P = 0.004) time point (**Figure 4B**). The total SIV DNA content in peripheral blood CD4 T cells before ART interruption was the parameter with the strongest association with the development of a PTC status (AUC of 0.96; **Supplementary Figure 2B**). We further assessed levels of replication competent, inducible SIV in LN CD4 T cells during ART using quantitative viral outgrowth assay. PTCs harbored a significantly lower frequency of latently infected CD4 T cells compared to NCs (mean: 0.16 vs 4.46 infectious units per million; **Figure 4C**). Since LN CD4 T cells expressing high level of PD-1 have been identified as one of the main cellular targets for HIV/SIV infection and persistence, we then measured their frequency among our animals¹³⁷. Consistent with the lower level of replication competent reservoir in LN, and despite similar levels

at pre-ART, PTCs showed a trend toward lower levels of PD-1⁺ CD4⁺ T cells in LN throughout ART (**Figure 4D**), providing further support for distinct reservoir environments within NCs and PTCs. However, as seen prior to ART, there was no difference in cytolytic capacity or proliferation of CD8 T cells between PTCs and NCs on ART in both peripheral blood and LN (**Figure 4E, F**).

RM PTCs show preservation of immunological homeostasis during 8 months of ATI

Along with marked differences in viral rebound, we assessed immunological characteristics that distinguished the PTCs and NCs after ATI. After treatment interruption, RM PTCs maintained stable CD4 T cell levels in peripheral blood, while NCs experienced significant loss of CD4 T cells as expected during normal disease progression (**Figure 5a**). Notably, this immune preservation extended to mucosal tissues. Despite similar levels of total mucosal CD4 T cells prior to and throughout the duration of ART, PTCs had a significantly higher frequency of CD4 T cells after treatment interruption (mean: 27.5% vs. 14.7% CD4⁺ of CD3⁺, P=0.03; **Figure 5B**). Furthermore, similar to the environment observed prior to ART, there was a continued maintenance of Th17 cells in PTCs but not NCs (mean: 11.2% vs. 5.1% IL-17⁺ of CD4⁺, P=0.03; **Figure 5C**). Finally, we observed significantly lower levels of intestinal CD4 T cell proliferation in PTCs as compared to NCs when using Ki-67, a marker for which expression has been associated with loss of function of mucosal T cells in SIV infection (mean: 3.4% vs 10.5% Ki-67⁺ of CD4⁺, P=0.004; **Figure 5D**) (24)

To follow up on the lower viral burden observed prior to and on ART, we assessed levels of cell-associated virus in peripheral blood CD4 T cells and in colorectal biopsies also following ATI. We found significantly lower levels of total SIV DNA in blood CD4 T cells in PTCs as compared to

NCs at multiple timepoints during the ATI (mid: 213 vs. 29,976 copies SIV DNA per 10^6 CD4 T cells, $P=0.002$; late: 95 vs. 26,706 copies SIV DNA per 10^6 CD4 T cells, $P=0.001$; **Figure 5E**). Similarly, in colorectal tissue samples, despite having equivalent levels of SIV DNA at the time of ART interruption, PTCs had lower levels of total SIV DNA at a late ATI timepoint (mean: 52 vs 499 copies SIV DNA per 10^6 total cells, $P=0.002$; **Figure 5F**). Remarkably, in both PBMC and mucosal tissue, despite the absence of ART for more than 6 months and persistent plasma viremia in the majority of animals, PTCs experience stable or even decreasing levels of SIV DNA. All together, these data highlight the ability of PTCs to maintain both immune homeostasis and viral control in the absence of ART, while NCs experience continued disease progression.

Discussion

Achieving sustained control of HIV replication in the absence of ART is a critical goal for people living with HIV and the most important readout for currently tested HIV cure strategies. Unfortunately, no interventions have shown efficacy in achieving HIV remission after treatment interruption in humans. The identification of human PTCs, generally characterized by their ability to maintain plasma viral loads at less than 400 copies/mL for at least 6 months following ATI (5–12), offers an important opportunity to identify key mechanisms contributing to HIV remission and provide targets for future interventions. This study identifies 7 SIV-infected RM PTCs that exhibit robust control of viremia for an extended period after ATI and adds to the growing knowledge of the immunologic and virologic characteristics of individuals who maintain low viral load in the absence of ART.

The RM PTCs described in this study mirror much of what has been seen in cohorts of HIV-infected human PTCs. For up to 8 months post-ATI, at which point the study was terminated, RM PTCs maintained viral loads remarkably lower than the NCs and experienced decreased pathogenesis, with significantly higher CD4 counts and lower immune activation in blood. Thus, virologic control did result in clinically relevant immunologic benefits for the RM PTCs. This is important, since a functional cure needs not only to control viral replication but also to reconstitute and maintain a functional immune system. In addition, RM PTCs harbor lower levels of SIV DNA than NCs at all timepoints of infection. In particular, as observed in multiple human PTC cohorts, total SIV DNA content at the time of ART interruption is lower in RM PTCs than NCs ^{47, 262, 300, 314}. While this assay largely measures defective viral DNA, it has been shown that human PTCs do not harbor a significantly different ratio of defective to intact HIV genomes compared to NCs ⁴⁷. The lower levels of total SIV DNA pre-ATI in RM PTCs fits with what was seen in the SPARTAC study of acutely treated HIV-infected individuals, in which it was found that HIV DNA levels at ART cessation predicted time to viral rebound ³¹⁵. Importantly, taking advantage of the RM model, we were able to extend our analysis to lymphoid tissue. In addition to the periphery, using a quantitative viral outgrowth assay we found lower levels of replication competent virus in CD4 T cells of lymph nodes from RM PTCs compared to NCs, in agreement with our measures of total DNA content. Furthermore, in both LN and PBMC, we found lower levels of SIV DNA in naïve, central memory, effector memory and T follicular helper subsets of CD4 T cells, suggesting that RM PTCs have an overall lower viral burden that is not limited to a particular anatomic location or differentiation subset. In lymphoid tissues, PD-1⁺ CD4 T cells have been previously described as a main contributor to HIV/SIV persistence due to their enrichment for HIV content and the ability of PD-1, once engaged, to inhibit HIV production and limit HIV reactivation ¹³⁷,

^{147, 280}. RM PTCs showed lower levels of PD-1⁺ CD4 T cells in LN throughout ART, which may be indicative of an environment less favorable to viral persistence. Interestingly, during ATI, the low levels of SIV DNA remained stable in both peripheral blood and colorectal tissues, with some animals showing a decrease after ART interruption, despite the presence of detectable viremia in most animals. This suggests that, after ART withdrawal, PTCs are capable of clearing virally infected cells at a rate at least equivalent to the rate of new cell infection in the presence of viremia.

Identification of a PTC population within an SIV model allowed for tissue access and assessment of populations previously undescribed in human PTCs. Importantly, we found that the continued maintenance of CD4 T cells during ATI described in peripheral blood of human PTCs extends to both lymphoid and mucosal sites in RM PTCs. Furthermore, we were able to assess mucosal Th17 cells throughout primary infection, ART suppression, and treatment interruption. Th17 cells are among the first cells to be infected after HIV transmission, harbor high levels of HIV DNA (34–36), and are preferentially depleted following HIV and SIV infection, and this loss is known to be a main driver of mucosal barrier breakdown, systemic immune activation, and disease progression ^{58, 61, 309-312, 316-320}. Before initiation of ART, mucosal CD4 T cells were similarly depleted in RM PTCs and NCs; however, PTCs selectively maintained higher frequencies of Th17 cells than NCs. This phenotype is remarkably similar to what is observed in the non-pathogenic SIV infection in the natural host sooty mangabey (SM), which following SIV infection have a significant depletion of CD4⁺ T cells from mucosal sites but maintain normal levels of Th17 cells and do not experience systemic immune activation equivalent to the pathogenic infection of RMs ³²¹. Our findings in RM PTCs, which experienced significantly less Th17 loss and peripheral immune activation as compared to NCs, continue to support these described relationships between Th17 preservation,

chronic immune activation, and disease outcome. Early ART initiation in HIV-infected individuals has also been shown to preserve Th17 cells and mucosal integrity, and is also associated with higher occurrence of post-treatment control ^{265, 322, 323}. Synthesis of these findings in humans in conjunction with our findings in RMs suggests a model in which the early initiation of ART limits viral exposure and preserves mucosal immune integrity, both of which are likely contributors to the development of post-treatment control in a subset of individuals. Furthermore, the demonstrated maintenance of CD4 T cell populations in both lymph node and mucosal tissue in RM PTCs in absence of ART strongly suggests that even partial control of viremia can prevent immune dysfunction.

There are several caveats associated with this study. First, analyses were performed post-hoc on RMs selected from studies not directly intended to assess post-treatment control. Animals in those studies initiated ART 8 weeks after SIV infection thus, although very unlikely based on many studies of SIVmac₂₃₉ infection in RMs, we cannot fully rule out the possibility that these PTCs may have progressed to spontaneous control of plasma viremia in the absence of ART ²⁶². Furthermore, since some animals received immune-based interventions in addition to ART, for those we cannot discriminate between the relative contribution of ART or immune-based intervention in inducing the PTC phenotype. However, it is important to note that those interventions were shown to have no significant impact on viral rebound, that PTC incidence was not increased in treated animals, and that our NCs also include animals receiving the same immune-based interventions (**Supplementary Table 1**) ^{60, 324}. While RM PTCs did have a lower viral burden at ART initiation compared to controls, this alone is not enough to indicate future control without ART. Cases of spontaneous controller RM infected with SIVmac₂₃₉ have been

reported, but are typically associated with favorable MHC class I alleles Mamu-B*08 and B*17, similar to human elite controllers with HLA-B*57 and HLA-B*27 alleles ^{306, 307}. In analyses of Mamu-B*08 and B*17 negative RMs infected with the same SIVmac₂₃₉ virus and who never initiate ART, natural control is rarely observed by our group or others, even in animals with low set point viral loads (Data not shown). We did observe a higher frequency of Mamu-A*01 in the PTC group compared to NC, raising the possibility that Mamu-A*01 may predispose a subset of RMs to post-treatment control but may not be strong enough to induce spontaneous control. Importantly, while we were unable to assess SIV-specific CD8 T cells, we did not find differences between RM PTCs and NCs with regards to cytolytic capacity or proliferative response of total CD8 T cells, neither prior to nor after ART. This is in agreement with reports that HIV-specific CD8 responses are generally weak in human PTCs compared to spontaneous controllers and viremic individuals ^{264, 325}. It is likely, however, that the decreased systemic presence of SIV in the PTC animals prior to starting ART critically contributed to their capacity to control viremia at ATI. Data in human PTCs varies by cohort, with most showing equivalent set point viral loads to NCs but some showing decreased viral load at ART initiation in PTCs ^{260, 262, 264}. It has also been demonstrated in humans that HIV DNA content at the time of starting ART is lower in PTCs than NCs ²⁶². Our data in RM PTCs supports the notion that lower HIV levels in both tissue and blood contributes to control of viremia after ATI. Unfortunately, the retroactive nature of our analysis prevents any further mechanistic characterization of the PTC phenomenon described here. Further studies in RM could be designed to specifically address outstanding mechanistic questions of post-treatment control, particularly with regards to the importance of the timing of ART initiation and the role of CD8 T cells in this control.

In summary, our data identifies 7 SIV-infected RMs characterized as PTCs due to their ability to maintain viral control after cessation of ART. Our RM PTCs exhibit virologic and immunologic characteristics largely similar to those previously reported in cohorts of HIV-infected PTCs, and we extend this analysis into previously unexplored periods of infection and anatomical sites. Importantly, our data highlights the benefits of limiting immune activation, immune damage, and the size of the reservoir early in HIV/SIV infection, all most achievable by early ART initiation, to promote potential viral control. It may be valuable to tailor early stages of intervention trials towards individuals who initiated ART early or who harbor small reservoirs, as they are likely best positioned to experience a positive outcome. Lastly, this report highlights the importance of including non-intervention control arms in all studies in both the SIV and HIV fields, to allow for best analysis of intervention-specific impact on viral control in the absence of ART.

Materials and Methods

Animals, SIV-infection and antiretroviral therapy

22 Indian rhesus macaques (RMs) all housed at the Yerkes National Primate Research Center (YNPRC) in Atlanta, GA, were selected for this study. All RMs were *Mamu-B*08*⁻ and *Mamu-B*17*⁻; *A*01* status for all animals is listed in **Supplementary Table 1**. All RMs were infected intravenously with SIVmac₂₃₉ (provided by Koen Van Rompay, U.C. Davis) at the dose designated in **Supplementary Table 1**. Approximately 8 weeks post-infection, all RMs initiated daily antiretroviral therapy. 14 animals were on a regimen composed of tenofovir (PMPA; 20–25 mg/kg/d, s.c.), emtricitabine (FTC; 30–50 mg/kg/d, s.c.), raltegravir (100–150 mg/bid, oral), darunavir (400–700 mg/bid, oral), and ritonavir (50 mg/bid, oral). 8 animals were on a regimen composed of dolutegravir (DTG; 2.5 mg/kg/d, subcutaneous; s.c.), tenofovir disoproxil fumarate (TDF; 5.1 mg/kg/d, s.c.), and emtricitabine (FTC; 40 mg/kg/d, s.c.). Animals received daily ART for up to 60 weeks. All animals reached viral loads below the limit of detection (60 copies/mL) for multiple timepoints before undergoing analytic treatment interruption (ATI), at which point animals were followed for up to 8 months until necropsy.

In addition to ART, RM designated as “IL-21 Treated” in **Supplemental Table 1** were treated with recombinant IL-21–IgFc at the beginning and at the end of ART and at the beginning of ATI⁶⁰. Animals designated as “aCTLA-4/aPD-1 Treated” in **Supplemental Table 1** received bi-specific α CTLA-4/ α PD-1 IgG1 over 4 weeks starting 6 weeks prior to ATI²⁵³.

Study Approval

All animal experimentation was conducted following guidelines set forth by the Animal Welfare Act and by the NIH's Guide for the Care and Use of Laboratory Animals, 8th edition. All studies were reviewed and approved by Emory's Institutional Animal Care and Use Committee (IACUC; permit numbers 3000065, 2003297, 2003470, 201700665, 2001973) and animal care facilities at YNPRC are accredited by the U.S. Department of Agriculture (USDA) and the Association for Assessment and Accreditation of Laboratory Animal Care (AAALAC) International. Proper steps were taken to minimize animal suffering and all procedures were conducted under anesthesia with follow up pain management as needed.

Experimental timepoints

For consistency across groups, timepoints were defined as the following: Pre-infection (15-21 days pre-infection); peak infection (D14 p.i.); early infection (D28-42 p.i.); Pre-ART/ART initiation (D56-60 p.i.); Early ART (D84-102 p.i.); Mid ART (D110-140 p.i.); Late ART (D197-256 p.i.); Pre-ATI (13-15 days pre-ATI); Early ATI (D27-28 post-ATI); Mid ATI (D59-60 post-ATI) and Late ATI (D180-240 post-ATI).

Sample collection and processing

Peripheral blood, lymph node and rectal biopsy collections were conducted throughout the study and were processed as previously described ¹³⁴.

Flow Cytometry

Fourteen parameter flow cytometry was performed on collected tissues according to previously optimized standard procedures using anti-human antibodies that have been shown to be cross-

reactive with RMs. The following antibodies were used: (from BD Biosciences) anti-CD3–APC–Cy7 (clone SP34-2), anti-CD95–PE–Cy5 (clone DX2), anti-CD28–PE–594 (clone CD28.2), anti–Ki-67–Alexa Fluor 700 (clone B56), anti-CD8–PE–CF–594 (clone RPA-T8), anti-CCR7–PE–Cy7 (clone 3D12), anti-HLA–DR–PerCp–Cy5.5 (clone G46-6) (all from BD Pharmingen); anti–IL-17–Alexa Fluor 488 (clone eBio64DEC17, eBioscience); (from Biolegend) anti-CD4–BV421 (clone OKT4), anti-CD4–BV605 (clone OKT4), anti-PD1–PE (clone EH12.2H7), anti-PD1–BV421 (clone EH12.2H7), anti-T-Bet-PE (clone eBio4B10), anti-CD200-PE (clone OX104) ; (From Invitrogen) anti-CD8–Qdot705 (clone 3B5), anti-GzmB-PE-TR (clone GB11), Aqua LIVE/DEAD amine dye AmCyan; anti-CD38–FITC (clone AT-1; STEMCELL Technologies); and anti-Perforin-FITC (clone-Pf344; MABTECH). Flow cytometric acquisition was performed on at least 100,000 CD3⁺ T cells on a BD LSR II Flow Cytometer driven by BD FACSDiva software and analysis of the acquired data was performed using FlowJo software.

Th17 analysis

Th17 cells in rectal biopsy samples were determined as previously described ⁶¹. Briefly, isolated cells were stimulated for 4 hours with PMA and A23187 in the presence of BD GolgiStop, stained for surface markers, permeabilized and stained intracellularly for cytokines. Th17 levels were determined as the percent of memory CD4 T cells that produced IL-17.

Plasma viral load

Levels of SIV RNA copies in plasma were determined by qRT-PCR as previously described with a limit of detection (LOD) of 60 copies/mL, with values below the LOD imputed as half of the

LOD³²⁶. Ultrasensitive measurements were performed by ultracentrifugation at the described timepoints on ART as previously described³¹³.

Cell-associated SIV DNA and RNA measurements

SIV DNA and RNA in rectal biopsy samples as well as SIV DNA in peripheral CD4 T cells were assessed quantitatively by qRT-PCR assays as previously described⁶⁰. For analysis of SIV DNA content in CD4 T cell subsets, isolated cells from peripheral blood and lymph node were sorted on a FACS AriaII (BD Biosciences) into the following CD4 T cell subsets: naïve (CD28⁺ CD95⁻ CCR7⁺), central memory (T_{cm}; CD95⁺ CCR7⁺), effector memory (T_{EM}; CD95⁺CCR7⁻) and T follicular helper (T_{FH}; PD-1⁺ CD200^{hi}) cells. Sorting strategy is shown in **Figure 2D**. SIV DNA levels were then assessed on sorted populations as previously described⁶⁰.

Quantification of replication-competent virus in CD4 T cells from lymph node

CD4 T cells were purified from cryopreserved lymph node samples and assessed for levels of replication-competent SIV as previously described⁶⁰. Briefly, cells were cocultured with CEMx174 cells (NIH AIDS Reagent Program) in serial dilutions for 25 days, with analysis at days 9, 16 and 25. Positive wells were determined based on flow cytometric analysis of SIV-Gag p27 expression and SIV-GAG viral RNA detection by qPCR and frequencies of infected cells were determined by maximum likelihood method and expressed as infectious units per million CD4 T cells³²⁷.

Statistical Analysis

Statistical tests were all two-sided and p-values ≤ 0.05 were considered to be statistically significant for each comparison. Data plotted as longitudinal grouped analysis are displayed as mean \pm SEM unless otherwise indicated. Comparisons of parameters between non-controllers and post-treatment controllers were calculated using Mann-Whitney U tests. Analyses were conducted using GraphPad Prism 8.3. Analysis of mean change for CD4 T cell count and %HLA-DR+ CD38+ of blood memory CD4 was done by repeated-measures analyses using a mixed-effects model via the SAS MIXED Procedure (version 9.4; SAS Institute, Cary, NC), providing separate estimates of the means by time on study and study group. Two approaches were used to evaluate PB SIV DNA and Th17 frequency as potential markers or predictors of PTC status. First the risk of PTC status was modeled as a function of PB SIV DNA (and separately using Th17 frequency) by using logistic regression (outcome = PTC or NC). Second, marker performance was summarized with classification performance measures, such as sensitivity, specificity, the receiver operating characteristic curves (ROC) and the area under the curve (AUC). The AUC for each marker can be interpreted as the probability that a PTC animal had a higher (or lower) predicted probability of PTC status than a NC animal, for random pairs with and without the outcome.

Acknowledgments

We would like to thank Sherrie Jean, Stephanie Ehnert, Christopher Souder and all veterinary and animal care staff at Yerkes. We also would like to acknowledge the Emory Flow Cytometry Core (Barbara Cervasi and Kiran Gill) and the Emory CFAR Virology core (Thomas Vanderford) for their assistance with flow cytometry and viral load measurements. Ultrasensitive viral load assays were performed by Jeffrey Lifson, AIDS and Cancer Virus Program, Leidos

Biomedical Research Inc., Frederick National Laboratory for Cancer Research. This work was supported by the NIAID, NIH under award numbers R01AI116379 and R01AI11034 to M. Paiardini, and ORIP/OD award P51OD011132 to Yerkes National Primate Research Center. The content of this publication does not necessarily reflect the views or policies of the Department of Health and Human services, nor does mention of trade names, commercial products or organizations imply endorsement by the U.S. Government.

Chapter Two Figures

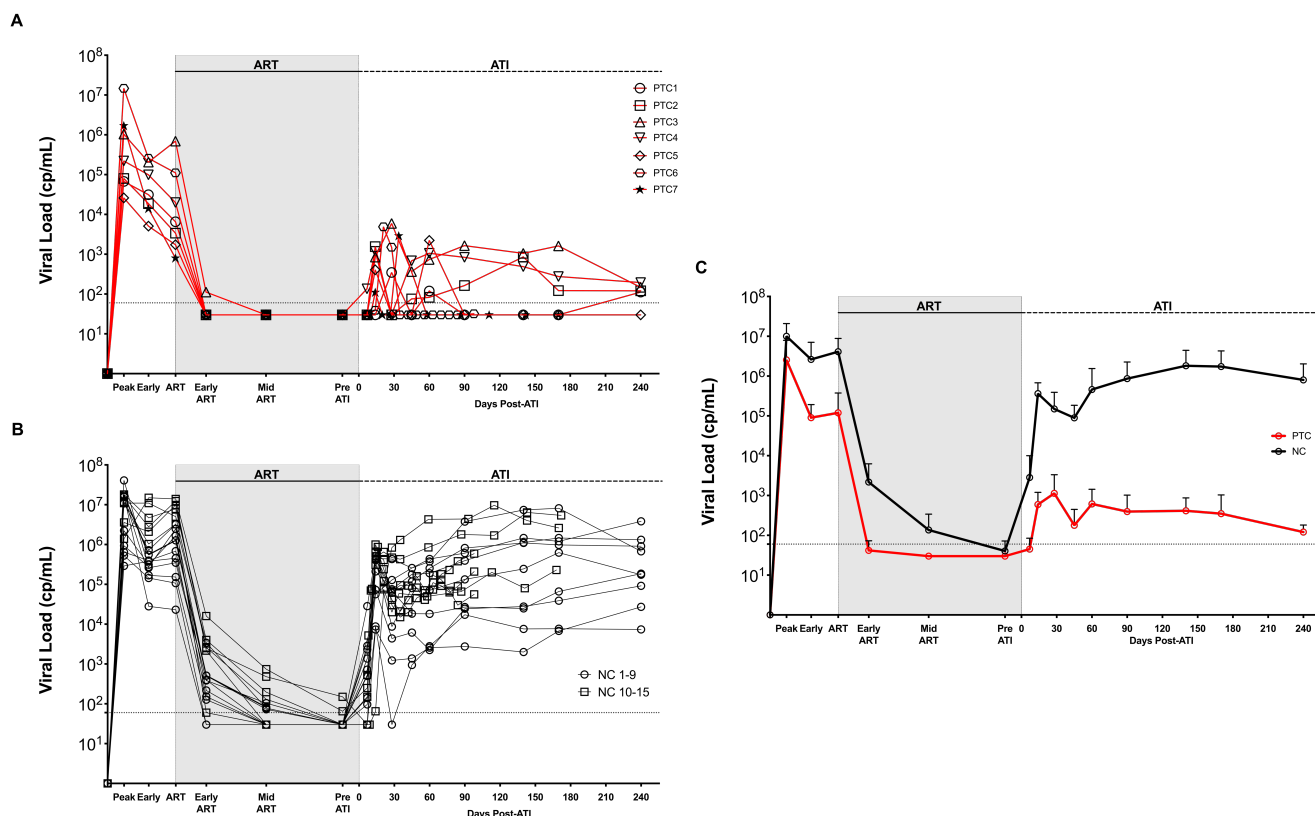


Figure 2.1. PTCs exhibit strong viral control after ART interruption

A-B) Plasma viral load for PTCs (**A**) (n=7) and NCs (**B**) (n=15) at multiple timepoints

throughout infection (see methods for definition). NC1-9 are those included in all subsequent

analyses. **C)** Average viral load for PTCs and NCs displayed as mean \pm std. dev. Shaded area designates period for which animals were on ART. Dotted line designates limit of detection (60 copies/mL).

A) Plasma viral load levels at peak infection and pre-ART timepoints. **B)** Total SIV DNA levels in purified blood CD4 T cells pre-ART. **C)** Cell associated SIV DNA and RNA levels in total rectal biopsy samples pre-ART. **D)** Gating strategy for CD4 T cell subsets from LN. **E)** SIV DNA levels in sorted CD4 T cell subsets from peripheral blood (**E**) and lymph node (**F**) at a pre-ART timepoint. **G-H)** Expression of CD8 T cell functional markers (GzmB: Granzyme B, Perf: Perforin) on total CD8 T cells in peripheral blood (**G**) and LN (**H**). Lines designate mean value.

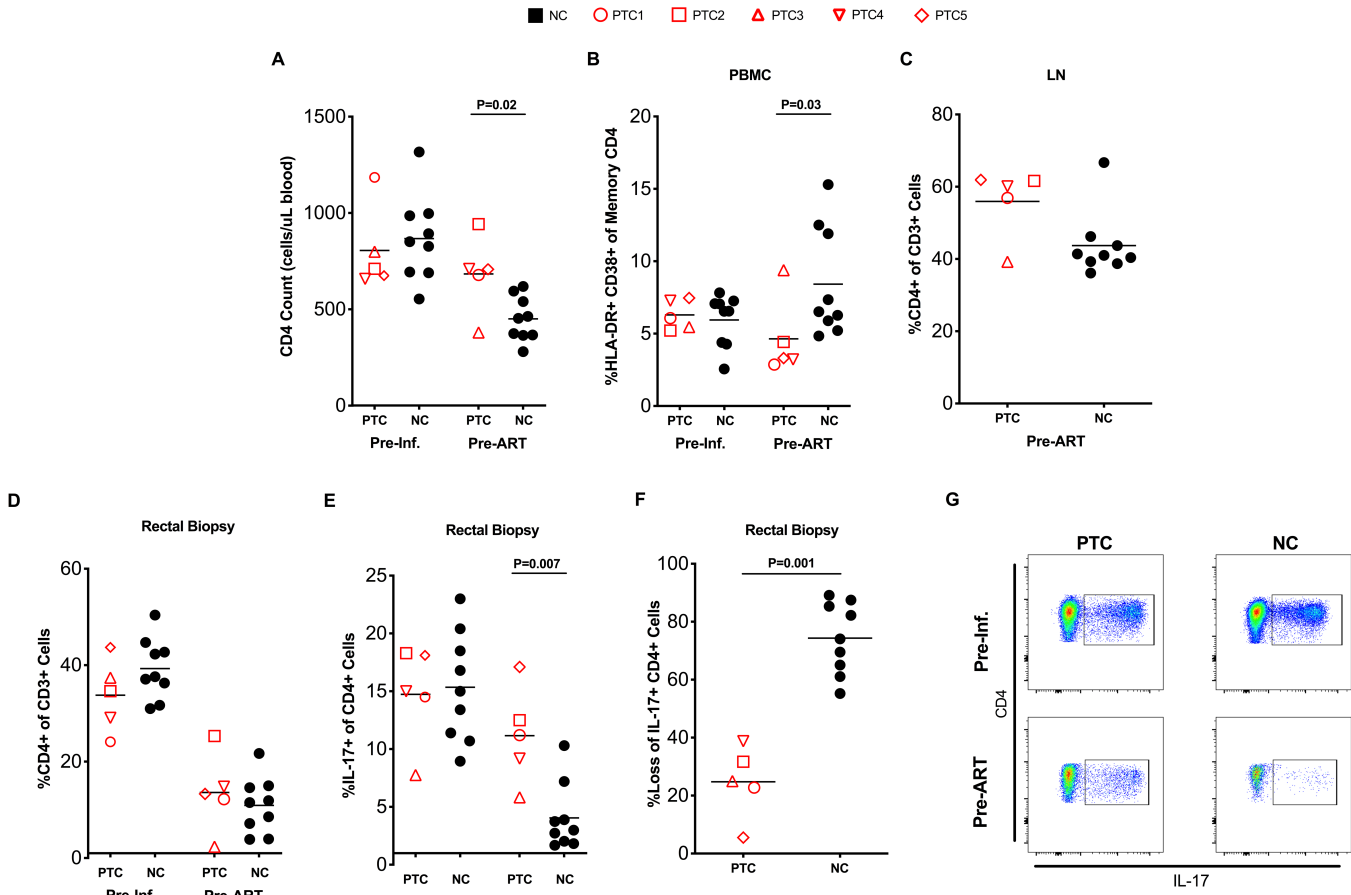


Figure 2.3. PTCs experience reduced immunopathogenesis prior to ART initiation

A) CD4 counts in peripheral blood at pre-infection and pre-ART timepoints. **B)** CD4 T cell activation in peripheral blood pre-infection and pre-ART as assessed by flow cytometry as HLA-DR+ CD38+ memory CD4 T cells. **C)** CD4 frequency in lymph node pre-ART. **D)** CD4 frequency in rectal biopsy pre-infection and pre-ART. **E)** Th17 frequency in rectal biopsy samples as assessed by flow cytometry as frequency of memory CD4 T cells expressing IL-17 after a brief *in vitro* stimulation. **F)** Levels of Th17 cells shown as the percentage of Th17 cells lost from pre-infection to pre-ART timepoint. Lines represent mean values. **G)** Representative staining showing the identification of Th17 cells at pre-infection and pre-ART timepoints.

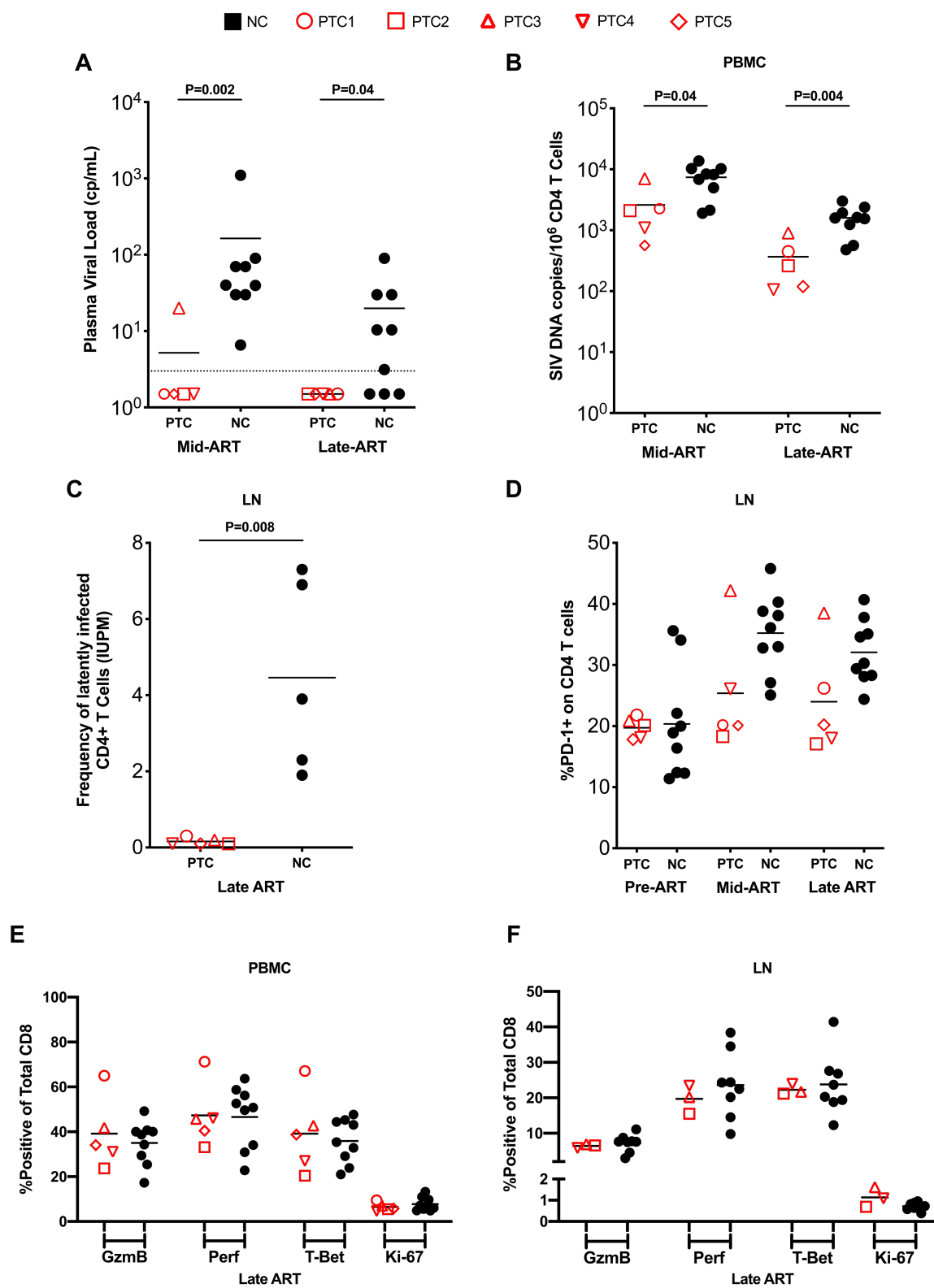


Figure 2.4. Reservoir and immune characteristics of PTCs and NCs on ART

A) Viral load as determined by ultrasensitive assay (LOD=3 copies/mL, dotted line) at mid-ART and late-ART. **B)** SIV DNA levels in purified CD4 T cells from peripheral blood at mid-ART and late-ART. **C)** Frequency of latently infected LN cells at late-ART, expressed as infectious units per million CD4 T cells, assessed by quantitative viral outgrowth assay. **D)** Levels of PD-1 expression on CD4 T cells in LN at pre-ART, mid-ART and late-ART. **E-F)** Expression of CD8 T cell functional markers on total CD8 T cells in peripheral blood (**E**) and LN (**F**). Lines designate mean value.

○ PTC ○ NC

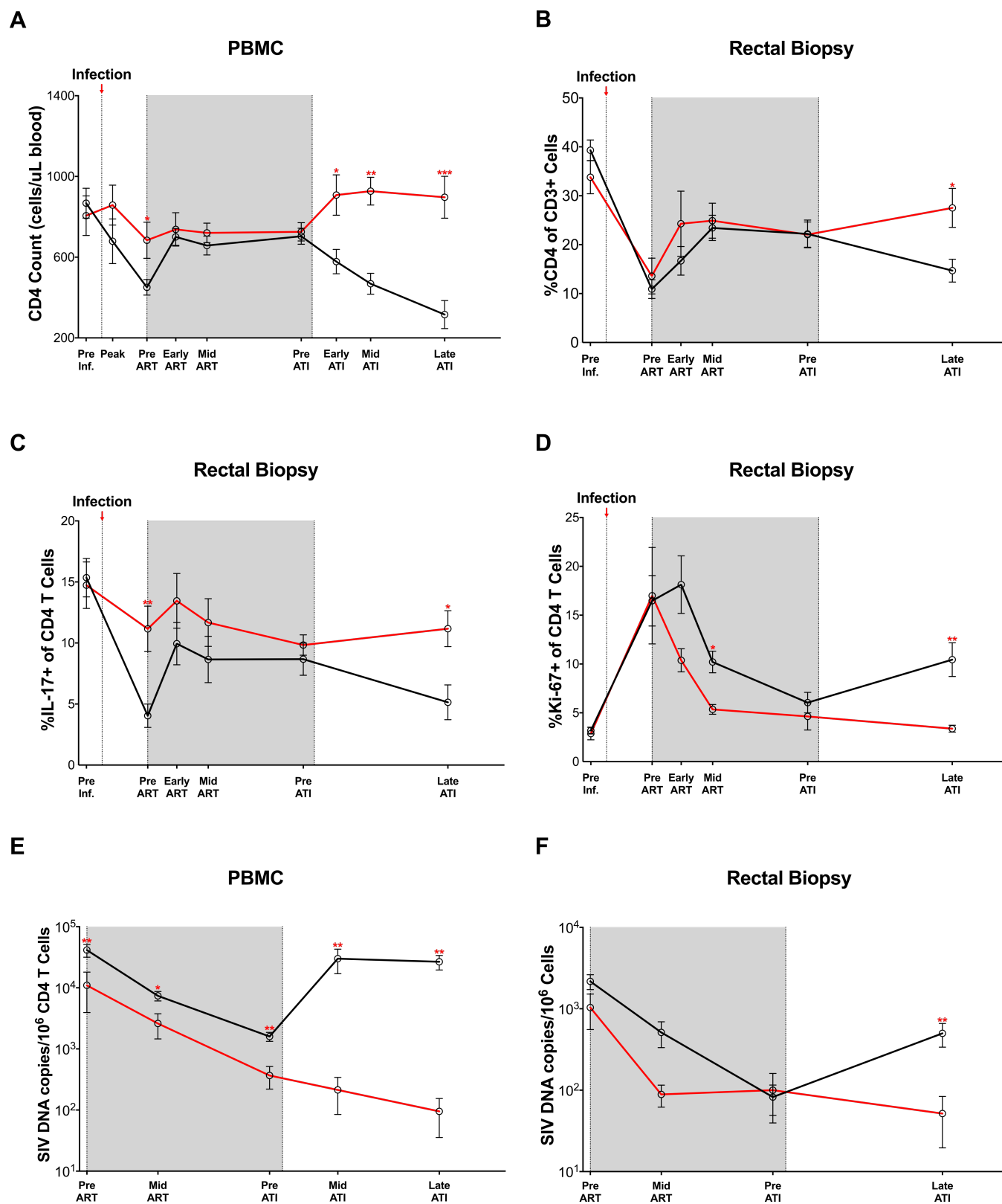


Figure 2.5. PTCs maintain viral control and preserve immune homeostasis during ATI

A) Longitudinal CD4 counts in peripheral blood. **B-D)** Longitudinal frequency of total CD4 T cells (**B**), Th17 cells (**C**) and proliferating CD4 T cells (**D**) in rectal biopsy. **E-F)** Longitudinal SIV DNA levels in PBMC (**E**) and rectal biopsy (**F**). Data shown as mean \pm S.E.M. PTC 1-5 and NC 1-9 were included in this analysis. See methods for timepoint definitions. Shaded area designates period for which animals were on ART. * $p < 0.05$, ** $p < 0.005$, *** $p < 0.0005$.








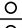
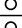
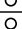
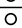


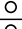
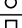
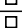





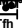
Animal Identity	Mamu A*01 (B*08, B*17)	Virus	Infection Dose (TCID ₅₀)	ART Regimen	ART Initiation (Days post- infection)	Time on ART (Weeks)	Followed after ATI (Weeks)	Immunological Intervention Received
PTCs								
PTC1 	-	SIVmac239	300	PMPA/FTC/Raltegravir/Darunivir	60	30	34	IL-21 Treated
PTC2 	-	SIVmac239	300	PMPA/FTC/Raltegravir/Darunivir	60	30	34	IL-21 Treated
PTC3 	+	SIVmac239	300	PMPA/FTC/Raltegravir/Darunivir	60	30	34	None
PTC4 	+	SIVmac239	300	PMPA/FTC/Raltegravir/Darunivir	60	30	34	IL-21 Treated
PTC5 	+	SIVmac239	300	PMPA/FTC/Raltegravir/Darunivir	60	30	34	None
PTC6 	+	SIVmac239	3000	FTC/TDF/DTG	56	52	14	None
PTC7 	+	SIVmac239	300	FTC/TDF/DTG	60	44	25	aCTLA-4/aPD-1 Treated
NCs								
NC1 	+	SIVmac239	300	PMPA/FTC/Raltegravir/Darunivir	60	30	34	IL-21 Treated
NC2 	-	SIVmac239	300	PMPA/FTC/Raltegravir/Darunivir	60	30	34	None
NC3 	-	SIVmac239	300	PMPA/FTC/Raltegravir/Darunivir	60	30	34	None
NC4 	+	SIVmac239	300	PMPA/FTC/Raltegravir/Darunivir	60	30	34	IL-21 Treated
NC5 	-	SIVmac239	300	PMPA/FTC/Raltegravir/Darunivir	60	30	34	IL-21 Treated
NC6 	-	SIVmac239	300	PMPA/FTC/Raltegravir/Darunivir	60	30	34	None
NC7 	-	SIVmac239	300	PMPA/FTC/Raltegravir/Darunivir	60	30	34	None
NC8 	+	SIVmac239	300	PMPA/FTC/Raltegravir/Darunivir	60	30	34	None
NC9 	-	SIVmac239	300	PMPA/FTC/Raltegravir/Darunivir	60	30	34	IL-21 Treated
NC10 	-	SIVmac239	3000	FTC/TDF/DTG	56	52	14	None
NC11 	-	SIVmac239	3000	FTC/TDF/DTG	56	52	14	None
NC12 	+	SIVmac239	3000	FTC/TDF/DTG	56	52	14	None
NC13 	-	SIVmac239	300	FTC/TDF/DTG	60	46	25	aCTLA-4/aPD-1 Treated
NC14 	-	SIVmac239	300	FTC/TDF/DTG	60	51	25	aCTLA-4/aPD-1 Treated
NC15 	-	SIVmac239	300	FTC/TDF/DTG	60	60	25	aCTLA-4/aPD-1 Treated

Table S.2.1. Animal and infection characteristics.

A) Gating strategy for CD4 T cell activation on memory CD4 T cells as determined by HLA-DR⁺ CD38⁺ cells. **B)** CD4 T cell activation in rectal biopsy samples pre-infection and pre-ART.

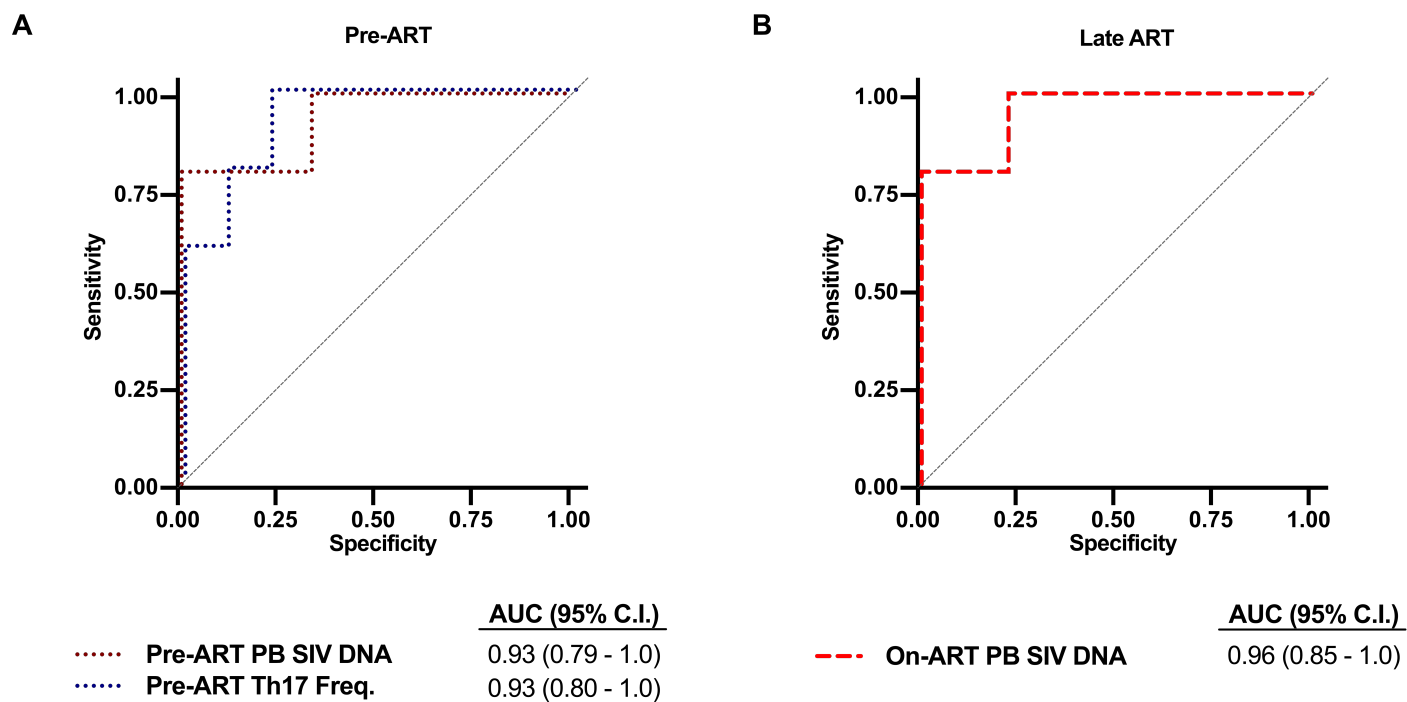


Figure S.2.2. ROC analysis

A-B) ROC curves for the most predictive parameters pre-ART initiation (**A**) and at a late ART (**B**) timepoint.

Chapter Three: The role of CD101-expressing CD4 T cells in HIV/SIV pathogenesis and persistence

Zachary Strongin^{¶1}, Timothy N. Hoang^{¶1}, Gregory K. Tharp¹, Andrew R. Rahmberg², Justin L. Harper¹, Kevin Nguyen¹, Lavinia Franchitti¹, Barbara Cervasi³, Max Lee⁴, Zhan Zhang¹, Eli A. Boritz⁴, Guido Silvestri^{1,5,6}, Vincent C. Marconi^{6,7,8,9}, Steven E. Bosinger^{1,5}, Jason M. Brenchley², Deanna A. Kulpa^{1,5}, Mirko Paiardini^{1,5, *}

¹Division of Microbiology and Immunology, Yerkes National Primate Research Center, Emory University; Atlanta, Georgia, USA.

²Barrier Immunity Section, Laboratory of Viral Diseases, NIAID, NIH; Bethesda, Maryland, USA.

³Flow Cytometry Core, Emory Vaccine Center, Emory University; Atlanta, Georgia, USA.

⁴Vaccine Research Center, National Institutes of Health; Bethesda, Maryland, USA.

⁵Department of Pathology and Laboratory Medicine, Emory University School of Medicine; Atlanta, Georgia, USA.

⁶Division of Infectious Diseases, Emory University School of Medicine; Atlanta, Georgia, USA.

⁷Division of Infectious Diseases Research, Atlanta Veterans Affairs Medical Center; Atlanta, Georgia, USA.

⁸Rollins School of Public Health, Emory University; Atlanta, Georgia, USA.

⁹Emory Vaccine Center, Atlanta, Georgia, USA

[¶]These authors contributed equally

Published in *Plos Pathogens* 18(7) : e1010723, July 22nd, 2022, PMID: 35867722

Abstract

Despite the advent of effective antiretroviral therapy (ART), human immunodeficiency virus (HIV) continues to pose major challenges, with extensive pathogenesis during acute and chronic infection prior to ART initiation and continued persistence in a reservoir of infected CD4 T cells during long-term ART. CD101 has recently been characterized to play an important role in CD4 Treg potency. Using the simian immunodeficiency virus (SIV) model of HIV infection in rhesus macaques, we characterized the role and kinetics of CD101⁺ CD4 T cells in longitudinal SIV infection. Phenotypic analyses and single-cell RNAseq profiling revealed that CD101 marked CD4 Tregs with high immunosuppressive potential, distinct from CD101⁻ Tregs, and these cells also were ideal target cells for HIV/SIV infection, with higher expression of CCR5 and $\alpha 4\beta 7$ in the gut mucosa. Notably, during acute SIV infection, CD101⁺ CD4 T cells were preferentially depleted across all CD4 subsets when compared with their CD101⁻ counterpart, with a pronounced reduction within the Treg compartment, as well as significant depletion in mucosal tissue. Depletion of CD101⁺ CD4 was associated with increased viral burden in plasma and gut and elevated levels of inflammatory cytokines. While restored during long-term ART, the reconstituted CD101⁺ CD4 T cells display a phenotypic profile with high expression of inhibitory receptors (including PD-1 and CTLA-4), immunosuppressive cytokine production, and high levels of Ki-67, consistent with potential for homeostatic proliferation. Both the depletion of CD101⁺ cells and phenotypic profile of these cells found in the SIV model were confirmed in people with HIV on ART. Overall, these data suggest an important role for CD101-expressing CD4 T cells at all stages of HIV/SIV infection and a potential rationale for targeting CD101 to limit HIV pathogenesis and persistence, particularly at mucosal sites.

Author Summary

While much progress has been made in the field of HIV persistence, there remain a number of outstanding mechanistic questions about cells that critically contribute to HIV pathogenesis and the maintenance of the viral reservoir during antiretroviral therapy. In particular, there is a great interest in identifying surface markers on cells that play a role in pathogenesis and persistence to elucidate potential therapeutic targets. In this manuscript, we describe CD101-expressing CD4 T cells as an immunosuppressive population that is preferentially depleted following SIV/HIV infection and find that this loss is associated with higher viral burden and increased inflammatory cytokine levels. Furthermore, during long-term antiretroviral therapy, these cells display a phenotypical and functional profile consistent with cells that may critically contribute to reservoir persistence, including high inhibitory receptor expression and production of immunosuppressive cytokines. Future studies of therapies modulating CD101 expression could uncover additional strategies for HIV therapeutics aimed at limiting residual inflammation and viral persistence.

Introduction

Modern antiretroviral therapy (ART) is a critical tool for managing HIV infection, with high effectiveness at suppressing HIV replication and remarkable reduction of HIV morbidity and mortality^{298, 328}. However, due to the early establishment of a latent viral reservoir, HIV persists and, with very few exceptions, cessation of ART in people with HIV (PWH) results in rapid viral rebound and continued disease progression within weeks^{93, 95}. Therefore, defining key cellular contributors to HIV persistence remains critical to help define strategies to target and eliminate the reservoir in hopes for a functional cure.

With a recent focus in the field on the HIV reservoir, the characteristics of cells that contribute to this latent population have been well defined to this point. The reservoir has been shown to persist in a variety of CD4 T cell subsets, with critical contributions from central and effector memory cells, T follicular helper cells (TFh), Th17 cells and T regulatory cells (Tregs)^{112, 134, 136, 137, 143, 317, 318, 329-333}. Furthermore, the persistence of cells harboring HIV DNA has been linked to expression of a number of inhibitory receptors, including PD-1, TIGIT, LAG-3 and CTLA-4^{134, 137, 147, 148}. Cells that critically contribute to long-term HIV persistence after ART initiation are also known to be preferentially infected during active HIV replication^{136, 310, 317, 330, 334, 335}. Furthermore, recent investigations have confirmed that the reservoir is primarily established at the time of ART initiation^{336, 337}. Finally, early ART initiation can reduce the chronic inflammation associated with increased morbidity/mortality risk during treated HIV infection, indicative of the importance of limiting acute HIV pathogenesis for long term health³³⁸. As a whole, these findings suggest that better understanding of target cell populations during early,

active HIV infection, as well as continued description of characteristic markers of HIV persistence on ART, will inform the design of targeted therapeutic interventions aiming to reduce residual inflammation and the size of the viral reservoir.

The cellular features described above suggest an important role for negative regulators of T cell activation in favoring the persistence of HIV DNA in CD4⁺ T cells. Based on those findings, we investigated the potential role of CD101 in HIV pathogenesis and persistence. CD101 is a cell surface glycoprotein with an unknown ligand that is upregulated upon cell activation, inhibits T cell activation and proliferation, and critically regulates CD4 Tregs functions³³⁹⁻³⁴³. CD101⁺ Tregs are more suppressive than CD101⁻ Tregs *in vitro* and *in vivo*, and CD101 can be used to discriminate the functional potency of Tregs in mice^{342, 344}. Furthermore, CD101 has been described as a marker of resident-memory T cells and has been shown to be anti-inflammatory in gut mucosa³⁴⁴⁻³⁴⁶. In addition to its suppressive role on CD4 T cells, CD101 is specifically induced on terminally differentiated and highly dysfunctional CD8 T cells during chronic viral infection^{347, 348}. Overall, the association of CD101 expression with Tregs, gut mucosa, and inhibitory receptor expression, together with its anti-inflammatory role in gut mucosa, suggests a potential key role for CD101⁺ CD4 T cells in HIV pathogenesis and persistence.

In this study, we take advantage of the established SIV model of HIV infection in rhesus macaques (RMs), which allows for longitudinal analyses and tissue access, to investigate dynamics of CD101-expressing CD4 T cells in healthy, acutely-infected, and ART-suppressed RMs. We confirm high expression of CD101 on CD4 Tregs in healthy RMs, with distinguishing phenotypic and transcriptional signatures of higher suppressive capability compared with

CD101⁻ Tregs. During acute SIV infection, CD101⁺ CD4 T cells are preferentially depleted as compared to their CD101⁻ counterpart, with depletion more pronounced for CD101⁺ Tregs and CD101⁺ CD4 T cells in the gut mucosa. This depletion is associated with higher viral burden in the gut, as well as higher plasma viral load and levels of inflammatory cytokines. After long-term ART, CD101⁺ CD4 T cells are restored to pre-infection levels, harbor intact SIV DNA at levels comparable to those found in the other memory CD4 T cells, and are enriched in inhibitory markers suggestive of a potential for long-term maintenance of the latent viral reservoir. These findings in RMs were extended and confirmed in a cohort of viremic and ART-suppressed PWH. Overall, while CD101⁺ cells were not directly enriched for HIV DNA, these findings reveal a preferential depletion of anti-inflammatory CD101⁺ CD4 T cells and suggest a critical role for CD101⁺ cells in HIV/SIV inflammation and in long-term viral persistence.

Results

CD101 is expressed on memory CD4 T cells and highly upregulated on regulatory CD4 T cells

While CD101 has been investigated in chronic viral infection on CD8 T cell populations using the LCMV mouse model, its role on CD4 T cells has not been investigated in the rhesus macaque model and there have been no studies of CD101⁺ CD4 T cells in acute and chronic viral infection³⁴⁸. To understand the role of CD101 across CD4 T cell subsets in healthy animals, we performed flow cytometric analyses of cryopreserved peripheral blood mononuclear cells (PBMC), lymph node mononuclear cells (LN) and rectal mucosa biopsies (RB). While CD101 was not expressed on naïve CD4 T cells (CD28⁺ CD95⁻), it was moderately expressed on memory CD4 T cells (CD95⁺) and significantly enriched on memory CD4 Tregs (CD95⁺ CD25⁺ CD127⁻ FoxP3⁺), with more than 60% of Tregs expressing CD101 in both blood and LN (Fig 1a, b, c) (S1 Fig).

Despite the significant levels of CD101 expression on CD4 Tregs, they make up only a small fraction of the total CD101-expressing CD4 pool, as the overall contribution of CD101⁺ CD4 T cells largely comes from central and effector memory cells, due to their higher frequency of the total pool of CD4 T cells (Fig 1C). To further investigate the phenotype of CD101-expressing cells, we utilized Uniform Manifold Approximation and Projection (UMAP) of our flow cytometry analysis and focused on memory CD4 T cells. In combination with Phenograph analysis, this revealed distinct clusters of CD101⁺ memory CD4 T cells (Fig 1d, e) (S2 Fig). In particular, CD101 was found highly expressed in clusters (2, 6, 17) also expressing markers of T regulatory cells, including CD25, FoxP3, CD39 and CTLA-4 (Fig 1d, e). An additional group of clusters (8, 10, 15, 23) confirmed the expression of CD101 in the central memory compartment, with co-expression of CCR7 and CD127 (Fig 1d, e).

Given the high expression of CD101 on CD4 Tregs, we performed single-cell RNA-seq (scRNA-seq) analysis on CD4 Tregs (CD95⁺ CD25⁺ CD127⁻) that were sorted into CD101⁻ and CD101⁺ populations. scRNA-seq analysis revealed clearly distinct transcriptional profiles of CD101⁺ Tregs as compared to CD101⁻ Tregs (Fig 1f, S1 File). Specifically, we found an expression profile suggesting CD101⁺ Tregs were more differentiated, with lower levels of *TCF7*, and showed higher potential for suppressive activity with lower levels of *SATB1* (a chromatin modulator that represses FoxP3 expression) and higher levels of *TNFRSF18* (which encodes for GITR), both of which have been strongly linked to the ability of Tregs to exert suppressive activity *in vivo*³⁴⁹⁻³⁵¹. Additionally, CD101⁺ Tregs were highly enriched in expression of *LGALS3* (which encodes for Galectin-3), which has been shown to increase N-glycan branching on CD8 T cells, increasing the antigenic threshold for activation of these cells and contributing to

long-term viral persistence in chronic LCMV model by limiting CD8 T cell antiviral functions

352.

To confirm that CD101⁺ cells represent a functionally distinct population, we performed PMA/ionomycin stimulation of PBMC from healthy individuals. After a 3hr stimulation, CD101⁺ CD4 T cells produced similar levels of traditional effector cytokines IL-2, IFN γ , IL-17a and TNF α as compared to CD101⁻ cells (Fig 1H, S3 Fig). However, CD101⁺ CD4 T cells produced significantly more LAP (Latency Associated Peptide; mean 11.7 fold-difference) than CD101⁻ cells in response to stimulation. LAP is part of the latent TGF- β complex and is produced by Tregs that release TGF- β , suggesting that cells producing LAP are likely to be immunosuppressive³⁵³⁻³⁵⁵. Collectively, these observations suggest CD101-expressing cells represent a functionally distinct population of CD4 T cells that can play a key role in regulating inflammatory environments, such as those after a viral infection.

CD101⁺ CD4 T cells are selectively depleted during SIV infection

To determine the role of CD101-expressing CD4 T cells in SIV infection, we assessed the dynamics of CD101⁺ CD4 T cell populations in SIV_{mac239}-infected RMs. CD101⁺ CD4 T cells are severely depleted during acute SIV infection (14 days post-infection), with a mean 2.6-fold reduction in the frequency of blood memory CD4 T cells expressing CD101 (Fig 2a, b). Absolute counts of CD101⁺ and CD101⁻ CD4 subsets in the periphery were evaluated to determine and compare the absolute loss of these populations during acute infection. CD101⁺ populations were significantly more depleted across all CD4 subsets as compared to CD101⁻ cells (Fig 2c). This preferential depletion was most severe for Tregs, as 80% of CD101⁺ Tregs

were lost compared to only 44% of CD101⁻ Tregs, and for CM, with 84% of CD101⁺ cells lost compared to 64% of CD101⁻ (Fig 2c). Notably, CD4 Tregs shift from being a primarily CD101⁺ population (accounting for 66% of total Treg) to being majority CD101⁻ after SIV infection (only 32% of total Treg being CD101⁺), representing a shift during acute infection toward a population of Tregs with a reduced suppressive potential (Fig 2d, e). While depletion of CD101⁺ memory CD4⁺ T cells, or CD101⁺ Tregs, was not associated with viral load (copies HIV RNA/mL of plasma) or T cell activation at D14 p.i., there was a significant association between the loss of CD101⁺ cells and higher plasma viral load at D42 p.i. (Table 1). Additionally, lower levels of CD101⁺ cells at D42 p.i. was associated with increased plasma levels of the inflammatory cytokines IP-10 and MIP-1a (Table 1). These findings suggest a direct relationship between the depletion of CD101⁺ cells, an increased inflammatory environment and higher viral burden. Interestingly, increased CD8 T cell activation as assessed by levels of HLA-DR/CD38 was associated with better preservation of CD101⁺ CD4 T cell, suggestive of a potential for CD8 antiviral responses to limit the depletion of this population (Table 1). To expand this observation from SIV-infected RMs to humans, we assessed these populations in PBMCs from PWH and confirmed that CD101 expression on CD4 Tregs is significantly lower in individuals with active viremia compared to ART-suppressed individuals, despite equivalent overall frequencies of CD4 Tregs (Fig 2F, S4 Fig). To examine whether this depletion represented preferential susceptibility of CD101⁺ cells to HIV infection, we sorted CD101⁻ and CD101⁺ memory CD4 T cells from healthy human PBMC and performed an *in vitro* HIV infection. After 7 days in culture with ART, we harvested the cells and measured integrated HIV DNA, and found comparable levels of integrated HIV DNA between CD101⁻ and CD101⁺ cell cultures (S5a Fig).

To understand if the preferential depletion of CD101⁺ cells was limited to peripheral blood or represented a migration of CD101⁺ CD4 to tissues, we evaluated these populations in rectal biopsy samples (RB) before and following SIV infection. Similar to PBMC, there was a marked, rapid (already present at d14 p.i.), depletion of CD101-expressing CD4 T cells in the gut after SIV infection (Fig 2g, h). This depletion was preferential, with 97% loss of CD101⁺ CD4 T cells compared to only 83% loss of CD101⁻ CD4 T cells (calculated from baseline to acute infection as % of live lymphocytes) (S6a Fig). Gut depletion of CD4 T cells is well described to be one of the main drivers of systemic inflammation and disease progression in viremic individuals during SIV/HIV infection, and the loss of highly suppressive CD101⁺ CD4 T cells could strongly contribute to this inflammation^{322, 356, 357}. To investigate potential mechanisms for preferential depletion of CD101⁺ cells in the gut, we assessed levels of $\alpha 4\beta 7$ and CCR5 on CD101⁺ and CD101⁻ memory CD4 T cells. These well-described surface receptors are known to drive T cell migration to the gut and to favor SIV/HIV cell entry. In uninfected macaques, CD101⁺ CD4 T cells in the gut express significantly more $\alpha 4\beta 7$ and CCR5 than CD101⁻ cells (Fig 2i). This finding suggests CD101⁺ CD4 T cells have a high potential to migrate and reside in the gut tissues and is consistent with their propensity to be more depleted in the gut during acute SIV infection, especially given the role of $\alpha 4\beta 7$ -high cells as early targets for HIV/SIV infection and of CCR5 as a co-receptor for direct HIV/SIV infection³⁵⁸. To understand potential links between this depletion and viral burden in gut mucosa, we assessed SIV DNA and RNA levels in rectal biopsy samples from day 14 post-infection. We found a significant association between loss of CD101⁺ CD4 T cells (calculated from baseline to acute infection as % of live lymphocytes) and higher SIV DNA levels during acute infection (Fig 2J), while there was no association of SIV DNA/RNA levels with depletion of CD101⁻ CD4 T cells (S1 Table). This finding establishes a

specific link between depletion of CD101⁺ cells in the mucosa and disease progression. Finally, we evaluated levels of circulating biomarkers of microbial translocation and mucosal barrier breakdown (sCD14, IFABp, zonulin) pre- and post-SIV infection. Notably, we found that lower levels of CD101⁺ cells in RB 14 days post-infection was significantly associated with a higher fold-change of zonulin from pre-infection to day 42 post-infection (S6B Fig) (S2 Table). Zonulin is a key regulator of intestinal permeability, with higher circulating levels of zonulin being indicative of intestinal epithelial damage, and has been previously shown to be predictive of HIV-related mortality ³⁵⁹.

To assess whether CD101 is being downregulated on CD4 T cells after infection rather than these cells being directly depleted, we evaluated CD101 surface levels after *in vitro* HIV infection of sorted CD101⁻ and CD101⁺ CD4 T cell cultures. Sorted CD101⁺ cells remained almost entirely CD101⁺ (median 92% CD101⁺) after 7 days in culture and remained clearly distinct from the CD101⁻ cultures, which remained CD101⁻ (S5B,C Fig). To confirm CD101 is not downregulated by T cell activation, we performed aCD3/CD28 stimulation of PBMC from healthy individuals. After 5 days of stimulation, CD101 levels on the total CD4 population had significantly increased (mean 2.5-fold increase) (S5D Fig).

Considering the potential inflammatory implications of a rapid and permanent depletion of highly suppressive Tregs, it is important to understand whether the depleted populations of CD101⁺ memory CD4 and Tregs are restored during antiretroviral therapy. To this aim, we quantified the frequency of blood CD4 T cell subsets expressing CD101 at an early (6 weeks), mid (24 weeks), and late (33-60 weeks) on ART time points. Within PBMC, the proportion of

cells expressing CD101 within each CD4 subset was restored starting from early ART, and fully to pre-infection levels after long-term ART in RMs that initiated ART during the early chronic phase of infection (Fig 2k), thus suggesting direct viral infection or inflammation, both reduced by ART, as mechanisms for the loss of CD101-expressing cells. This restoration occurred very rapidly in the Treg compartment, suggesting the administration of ART prevents further depletion of CD101⁺ cells and allows a restoration of this suppressive population in response to the highly inflammatory environment. In fact, CD101⁺ cells begin to slowly recover prior to the initiation of ART, which is likely reflective of the tendency of Tregs to expand during the chronic phase of HIV/SIV infection and the emergence of SIV-specific CD8 T cells that are able to partially limit viremia during early chronic infection. The contribution of CD101⁺ cells within each subset to the overall pool of CD4 T cells was also fully restored to pre-infection levels (Fig 2l).

During long-term ART, CD101⁺ cells display a phenotype consistent with quiescence and potential for reservoir persistence

We then investigated whether CD101⁺ cells may contribute to viral persistence during long-term ART following reconstitution. Expression of numerous inhibitory receptors on CD4 T cells have previously been described to potentially delineate subsets enriched for HIV/SIV provirus and contribute significantly to the persistent, latent reservoir^{134, 137, 147, 148, 280}. Given the more differentiated state of CD101⁺ Tregs and associations of CD101 with inhibitory receptor expression on CD8 T cells during chronic LCMV infection, we hypothesized that CD101⁺ cells may be enriched for these markers during long-term ART³⁴⁸. We evaluated expression of PD-1 and CTLA-4 within the CD101⁻ and CD101⁺ memory CD4 populations in LN samples from

SIV-infected RMs after >1 year of ART. While CD101⁻ cells primarily lie in the PD-1⁻ CTLA-4⁻ quadrant, CD101⁺ cells are significantly enriched in the PD-1⁻ CTLA-4⁺ and PD-1⁺ CTLA-4⁺ compartments (Fig 3a, b). Of note, we and others have previously reported that these populations of PD-1⁻ CTLA-4⁺ and PD-1⁺ CTLA-4⁺ cells harbor high levels of replication competent SIV DNA and include a high frequency of Tregs and Tfh, respectively^{134, 137, 147}. Directly probing the expression of CD101 on the PD-1 and CTLA-4 quadrants of LN CD4 T cells revealed significantly elevated expression of CD101 in cells expressing any combination of PD-1 and CTLA-4 (Fig 3c, d). We confirmed similar results of CD101 expression on these cell populations in PBMC from PWH on ART (Fig 3e). We further investigated additional immunosuppressive receptors CD39 and TIGIT that are known to be expressed on functional Tregs and have been associated with the HIV reservoir^{147, 360-362}. CD101⁺ cells express significantly more CD39 and TIGIT as compared to CD101⁻ cells and Boolean gating on the 4 receptors of interest reveals a clear enrichment of immunosuppressive receptors on CD101⁺ cells, with 84% of CD101⁺ cells expressing at least one of these receptors compared to only 49% of CD101⁻ cells, and 63% of CD101⁺ cells expressing two or more receptors as compared to only 23% of CD101⁻ (Fig 3f, g, h). Additionally, we found that CD101⁺ cells express significantly higher levels of Ki-67 in both ART-suppressed SIV and HIV infection, suggestive of recent cell cycling of CD101⁺ cells (Fig 3i, j). This is notable considering the potential for cycling CD4 T cells to maintain the reservoir via clonal expansion^{112, 363}. Finally, to assess the functional capacity of CD101⁺ CD4 T cells to contribute to reservoir persistence, we performed PMA/ionomycin stimulation of PBMC from ART-suppressed PWH. Similar to the profile observed in cells from healthy individuals, CD101⁺ CD4 T cells expressed significantly more LAP (TGF- β) as compared to CD101⁻ cells, while producing similar levels of other effector cytokines (Fig 3K). This is particularly interesting, as

TGF- β levels are known to be significantly elevated after HIV infection and remain elevated during suppressive ART and TGF- β has been demonstrated to play a role in potentiating T cell latency^{129, 364-367}.

To assess the potential contribution of CD101⁺ CD4 T cells to the latent HIV reservoir, we measured HIV DNA levels in sorted CD101⁻ and CD101⁺ memory CD4 T cells derived from PBMC from PWH on suppressive ART (Fig 4a). CD101⁺ CD4 harbored similar levels of total proviruses, defective HIV DNA, and intact HIV DNA as compared to CD101⁻ cells when assessed by the intact proviral DNA assay, suggesting that CD101⁺ cells are contributing to the overall pool of latently infected cells during long-term ART at levels comparable to the CD101⁻ counterpart (Fig 4b, c, d)³⁶⁸. Due to their high levels of intact DNA and a phenotype consistent with cell quiescence and survival, CD101⁺ CD4 cells have the potential to critically contribute to the long-term maintenance of the SIV/HIV reservoir.

Discussion

Development of a functional cure for HIV continues to be the ultimate goal in HIV research, but these efforts are hampered by the difficult nature of HIV persistence. Many recent interventions have been aimed at reducing the size of the HIV reservoir, but the limited success to date suggests a need for further investigation into mechanisms maintaining the reservoir to help design targeted therapeutics. In this study, we characterize, for the first time, the phenotype and transcriptional profile of CD101⁺ CD4 T cells in NHPs, as well as their role in HIV/SIV pathogenesis and persistence. Our investigations reveal that CD101⁺ CD4 T cells are preferentially depleted during HIV/SIV infection in both blood and tissues, and this depletion is

associated with increased viral burden in blood and gut and with elevated levels of inflammatory cytokines. While these cells are restored during long-term ART, they exhibit an immunosuppressive profile consistent with cells that critically contribute to the persistence of the latent viral reservoir.

In healthy RMs, we found that CD4 T cells expressing CD101 display a phenotypic and transcriptional profile suggestive of their role as highly functional Tregs, consistent with investigations of CD101⁺ CD4 T cells in other model systems and diseases. CD101⁺ Tregs express a transcriptional signature clearly differentiating them from CD101⁻ Tregs, with lower levels of *TCF7* and *SATB1*, indicative a more terminally differentiated Treg state, and higher levels of *TNFRSF18* and *LGALS3*, both of which have been shown to mark highly suppressive Treg populations³⁴⁹⁻³⁵². Additionally, CD101⁺ CD4 T cells are more functionally suppressive, producing more LAP (TGF- β) in response to stimulation. Given the important role a highly suppressive CD4 population could play in both HIV pathogenesis during acute infection and HIV persistence during long-term ART, we performed the first longitudinal characterization of CD101⁺ CD4 T cells in both SIV and HIV infection. We found CD101⁺ CD4 T cells are preferentially depleted during acute SIV infection, with significantly larger reduction of CD101⁺ cells as compared to CD101⁻ cells across all CD4 subsets. Importantly, this depletion was associated with higher viral load and increased levels of inflammatory cytokines, suggesting that depletion of CD101⁺ cells is directly linked to a more inflammatory environment. The depletion of CD101⁺ CD4 T cells was most pronounced within the Treg compartment. While the frequency of Tregs has been shown to increase during chronic HIV infection, few studies have been able to address the role and dynamics of CD4 Tregs during acute infection, and conclusions

from these studies vary on whether Tregs are increased or decreased during acute infection³⁶⁹⁻³⁷⁵. Our findings that CD101⁺ immunosuppressive Tregs are depleted during acute infection suggest an additional mechanism for increased immune activation during primary HIV infection. Additionally, the confirmation of persistently lower levels of CD101 on Tregs, despite equivalent frequencies of Tregs, in viremic PWH as compared to ART-suppressed individuals implies the persistent inflammatory environment in this setting may be partially due to the lack of highly functional Tregs. The depletion of immunosuppressive CD101⁺ cells may be most impactful in the gut mucosa, where loss of CD4 T cells is known to drive systemic mucosal barrier breakdown and systemic inflammation^{20, 59, 357, 376-378}. We show that CD101⁺ cells express higher levels of CCR5 and $\alpha 4\beta 7$ than CD101⁻ cells, providing rationale for their homing and selective depletion in gut tissue, as both are known to mark cells preferentially infected with HIV/SIV^{358, 379, 380}. Furthermore, depletion of $\alpha 4\beta 7$ ⁺ CD4 T cells during acute HIV/SIV infection is associated with increases in microbial translocation, a key mechanism for SIV/HIV pathogenesis, suggestive of more extensive gut damage³⁵⁸. Indeed, we found that decreased levels of CD101⁺ cells in the gut during acute infection was associated with higher fold-change of zonulin, a marker of intestinal epithelial integrity, during early chronic infection. Additionally, depletion of these cells was associated with increased viral burden (SIV DNA) in the mucosa during acute infection, suggesting that loss of CD101⁺ CD4 T cells in the gut mucosa may play an important role in increased activation, infection and mucosal breakdown as HIV/SIV infection progresses.

While the preferential loss of highly immunosuppressive CD101⁺ CD4 T cells is likely contributing to pathogenesis during primary HIV/SIV infection, cells of this nature also likely

contribute to reservoir persistence during long-term ART. Investigations over recent years have yielded strong evidence that expression of inhibitory receptors, including PD-1, CTLA-4 and TIGIT, contribute to HIV persistence^{134, 137, 147, 148}. As suggested by the differentiation state of these cells and previous reports of CD101 expression on CD8 in viral infection, we demonstrate that CD101⁺ CD4 T cells are highly enriched for expression of immunosuppressive receptors in lymphoid tissue during ART. Interestingly, there is a significant enrichment for CD101⁺ CD4 T cells within CTLA-4⁺ PD-1⁻ cells, which our group has previously shown to be an important contributor to viral persistence within the lymphoid tissue¹³⁴. Additionally, CD101⁺ cells express higher levels of Ki-67, indicative of their ability to proliferate and persist over time on ART and potentially maintain the reservoir through clonal expansion. While CD101⁺ cells did not show enrichment for HIV DNA as compared to CD101⁻ cells in blood, they harbor significant levels of intact HIV DNA and we believe their contribution to viral persistence may still be critical. First, expression of inhibitory receptors is one way in which HIV-infected CD4 T cells maintain latency, and blockade of these receptors can potentiate latency reversal^{253, 280, 381}. Second, CD101⁺ CD4 T cells, due to their highly functional regulatory potential, likely create an immunosuppressive environment that prevents HIV expression and CD8-mediated clearance of infected cells. The enriched production of LAP (TGFβ) by CD101⁺ CD4 T cells compared to CD101⁻ cells in samples from PWH is likely to promote latency of these cells, as recent work has highlighted the important role of TGFβ in promoting reservoir persistence^{129, 365-367, 382, 383}. Additionally, the observation that CD101⁺ Tregs have higher expression of *LGALS3* is particularly interesting in the context of previous findings that galectin-3 participates in N-glycan branching on CD8 T cells during chronic infection that increases the antigenic threshold for CD8 T cell activation and function³⁵². This suggests that CD101⁺ CD4 T cells during long-term ART

could inhibit CD8-mediated clearance of HIV-infected cells in reservoir clearance attempts utilizing a shock and kill strategy.

It is difficult to assess direct cell death *in vivo*, and therefore we cannot say for certain that CD101 cells are preferentially depleted due to increased infection and cell death. However, it is unlikely that the loss of CD101⁺ cells is due to a redistribution of these cells throughout tissues, as we assessed these populations in both blood and mucosal tissue and found depletion in both. Furthermore, it seems unlikely CD101 is downregulated on cells given the terminally differentiated status of these cells, the upregulation of CD101 on TCR-stimulated CD4 T cells, and the lack of downregulation observed in sorted CD101⁺ cells after 7 days in our *in vitro* HIV infection system. Additionally, although our *in vitro* infection model does not show increased infection levels of CD101⁺ CD4 T cells, this model may not fully replicate the phenotypic environment of these cells during *in vivo* infection, particularly given the role of CD101⁺ cells in the gut. Unfortunately, given the very low levels of CD101⁺ CD4 T cells after infection, we are unable to sort these cells and directly assess whether they harbor more virus at this time. The idea that CD101 expression is associated with preferential infection and depletion is additionally supported by two independent studies in which genetic variants in the *CD101* locus are associated with altered immune activation and increased risk of sexually acquired HIV infection^{384, 385}. While we did not find significant enrichment of HIV DNA in CD101⁺ cells from PBMC, we were unable to assess either LN and rectal biopsy samples for these measures, where we believe the impact of both preferential depletion of CD101⁺ CD4 T cells and the immunosuppressive environment created by them on ART may be most significant.

Continued exploration of markers and mechanisms of cells contributing to HIV pathogenesis and persistence is vital to designing more effective interventions focused on HIV cure. Herein, we report the first comprehensive assessment of the role of CD101⁺ CD4 T cells in HIV/SIV infection, in which we define CD101⁺ cells as a marker of highly suppressive CD4 Tregs, a population that is preferentially and severely depleted during acute infection and restored during long-term ART, with the potential to contribute to and promote the persistence of the HIV reservoir. Additional studies assessing how modulation of CD101 expression on CD4 T cells can impact viral pathogenesis and reservoir persistence may reveal additional strategies for HIV therapeutics.

Materials and Methods

Ethics Statement

All animal experimentation was conducted following guidelines set forth by the Animal Welfare Act and by the NIH's Guide for the Care and Use of Laboratory Animals, 8th edition. All studies were reviewed and approved by Emory's Institutional Animal Care and Use Committee (IACUC; permit numbers 201700655, 201800047, 201700665) and animal care facilities at Yerkes National Primate Research Center are accredited by the U.S. Department of Agriculture (USDA) and the Association for Assessment and Accreditation of Laboratory Animal Care (AAALAC) International. Proper steps were taken to minimize animal suffering and all procedures were conducted under anesthesia with follow-up pain management as needed. Individuals with HIV infection were consented for a study approved by the Emory University Institutional Review Board and written consent for research was obtained from the individuals.

Animals, SIV infection, antiretroviral therapy and sample collection

53 Indian rhesus macaques (RMs), housed at the Yerkes National Primate Research Center, were included in this study. All RMs were screened to ensure Mamu-B*08- and Mamu-B*17- status. Animals were infected intravenously with 300 TCID₅₀ SIVmac239. Animals initiated a daily subcutaneous antiretroviral therapy regimen of FTC (40 mg/kg), TDF (5.1 mg/kg) and DTG (2.5 mg/kg) during the early chronic phase of infection (week 6-8 post-infection) and were maintained on ART up to 66 weeks post-infection (S3 Table). Peripheral blood, lymph node and rectal biopsy sample collections were conducted at critical timepoints during the study and processed as previously described ¹³⁴. Infection timepoints were defined as follows: acute (days 14-18 post-infection), early chronic (days 42-56 post-infection), early ART (6 weeks post-ART initiation), mid ART (24 weeks post-ART initiation), late ART (33-60 weeks post-ART initiation).

Samples from participants with HIV infection

For analysis of depletion of CD101-expressing CD4 T cells during viremia, PBMC were obtained prior to initiation of antiretroviral therapy in individuals with a confirmed HIV diagnosis. For analysis of CD101 expression during long-term antiretroviral therapy, PBMC were obtained from individuals with undetectable viremia for at least 1 year prior to sample collection. Individuals were on a variety of combination ART regimens containing a protease inhibitor, integrase inhibitor and/or nucleoside reverse-transcriptase inhibitors. Cryopreserved cells were used for all analyses.

Plasma viral load

Levels of SIV RNA in plasma were measured by RT-qPCR as previously described (limit of detection 60 copies/mL) ³⁸⁶.

scRNA-seq analysis

Single cells were sorted directly into 96 well plates with lysis buffer. Single cell lysates were then converted to cDNA following capture with Agencourt RNA Clean beads using the SmartSeq2 protocol as previously described ³⁸⁷. The cDNA was amplified using 20–24 PCR enrichment cycles prior to quantification and dual-index barcoding with the Illumina Nextera XT kit. The libraries were enriched with 12 cycles of PCR, then combined in equal volumes prior to final bead cleanup and sequencing. All libraries were sequenced on an Illumina HiSeq 3500 by either single-end 150 bp reads or short paired-end reads. Alignment was performed using STAR version 2.5.2b and transcripts were annotated using MacaM Rhesus genome assembly and annotation (v7.8.2: <https://www.unmc.edu/rhesusgenechip/index.htm#NewRhesusGenome>) ³⁸⁸. Transcript abundance estimates were calculated internal to the STAR aligner using the algorithm of htseq-count ³⁸⁹.

Flow Cytometry

Flow cytometric analyses for this study were performed on peripheral blood, LN and gut-derived cells according to previously optimized and standardized procedures with anti-human antibodies with confirmed cross-reactivity with RMs. For T cell phenotyping analyses, the following antibodies were used at pre-optimized staining concentrations: anti-Ki-67-Alexa700 (clone B56), anti-CD3-BUV395 (clone SP34-2), anti-CD8-BUV496 (clone RPA-T8), anti-CD45-BUV563

(clone D058-1283), anti-CD28-BUV737 (clone CD28.2), anti-CD45RA-BUV737 (clone HI100), anti-CTLA-4-BV421 (clone BNI3), anti-Ki-67-BV480 (clone B56), anti-CD27-BV605 (clone L128), anti-CCR5-APC (clone 3A9), anti-CCR7-BB700 (clone 3D12), Fixable Viability Stain 700 (all from BD Biosciences); anti-FoxP3-AF647 (clone 150D), anti-CD4-APC/Cy7 (clone OKT4), anti-CD95-BV605 (clone DX2), anti-HLA-DR-BV650 (clone L243), anti-CD25-BV711 (clone BC96), anti-CD39-BV711 (clone A1), anti-PD-1-BV786 (clone EH12.2H7), anti-CD39-PE/Dazzle594 (clone A1), anti-CD4-PE/Cy5 (clone OKT4), anti-CD101-PE/Cy7 (clone BB27) (all from Biolegend); anti-CXCR5-PE (clone MU5UBEE), anti-CD127-Pe/Cy5 (clone ebioRDR5), anti-TIGIT-PerCP-eF710 (clone MBSA43), LIVE/DEAD fixable aqua (all from ThermoFisher); anti-CD38-FITC (clone AT-1) (StemCell); anti- $\alpha 4\beta 7$ -PE (clone A4B7R1) (NHP reagent resource). To detect intracellular expression of FoxP3, cells were fixed and permeabilized with FoxP3 Fix/Perm solution (Tonbo) and subsequently stained for intracellular markers of interest. Acquisition of stained cells was performed on a minimum of 100,000 live CD3⁺ T cells for LN and PBMC samples on an LSRFortessa or FACSymphony (BD biosciences) driven by FACSDiva software and analyzed using FlowJo software (version 10.8, Treestar). FCS files were imported into FlowJo, compensated electronically, gated on memory CD4 T cells (CD3⁺ CD4⁺ CD8⁻ CD95⁺) and equivalent numbers of cells were input into UMAP analysis (Uniform Manifold Approximation and Projection for Dimension Reduction) was for unbiased evaluation of the distribution of the key markers. Projection of the density of cells expressing markers of interest were visualized/plotted on a 2-dimensional UMAP (<https://arxiv.org/abs/1802.03426>, <https://github.com/lmcinnes/umap>). We used the Phenograph clustering approach (<https://github.com/jacoblevine/PhenoGraph>).

Flow Cytometry cell sorting

In order to perform scRNA-seq on sorted CD101⁺ and CD101⁻ Tregs, cryopreserved PBMC were thawed and stained with the following antibodies: anti-CD95-BV421 (clone DX2), anti-CD28-PE/CF594 (clone 28.2) (from BD Biosciences); anti-CD4-BV650 (clone OKT4), anti-CD101-PE/Cy7 (clone BB27) (from Biolegend); anti-CD8-FITC (clone MHCD08014), anti-CXCR5-PE (clone MU5UBEE), anti-CD127-PE/Cy5 (clone ebioRDR5), LIVE/DEAD fixable aqua (from ThermoFisher). Cells were gated as live, CD3⁺, CD4⁺, CD8⁻ and were then sorted as Naïve (CD28⁺ CD95⁻), CD101⁻ Tregs (CD95⁺, CXCR5⁻, CD127⁻, CD25⁺, CD101⁻) and CD101⁺ Tregs (CD95⁺, CXCR5⁻, CD127⁻, CD25⁺, CD101⁺).

For HIV DNA measurements in CD101⁺ and CD101⁻ CD4 T cells, cryopreserved PBMC were thawed and stained with the following antibodies: anti-CCR7-BB700 (clone 3D12), anti-CD45RA-APC (clone HI100), anti-CD3-APC-Cy7 (clone SP34-2), anti-CD8-FITC (clone RPA-T8) (from BD biosciences); anti-CD4-APC/Cy7 (clone OKT4), anti-CD101-PE/Cy7 (clone BB27) (from Biolegend). Cells were sorted as memory CD101⁺ or CD101⁻ CD4 (gating strategy shown in Fig 4a) and DNA was extracted using a QIAmp DNA minikit (Qiagen) and intact proviral DNA was measured as previously published, with sample processing and IPDA analysis performed by Accelevir Diagnostics in a blinded fashion ³⁶⁸.

In vitro infection

In vitro infection of PBMC was performed as previously described ¹²⁹. Briefly, PBMC were isolated from buffy coats from HIV-negative healthy donors and enriched for memory CD4 T cells by negative selection using the EasySep human CD4 memory T cell enrichment kit

(StemCell). Cells were rested overnight and then sorted as CD101⁺ or CD101⁻ using a FACS Aria II system (BD Biosciences). After another overnight rest, cells were spinoculated with 89.6, a clinical isolate of HIV, at 100ng/mL p24/million cells. Viral supernatant was removed and infected cells were cultured in RPMI supplemented with 30 U/mL IL-2 (R&D Systems) and 5uM saquinavir (NIH AIDS Reagent Program) to prevent viral spread and preintegration latency. On day 4, cells were directed into latency with addition of 40ng/mL recombinant human IL-7 (R&D Systems), 20 ng/mL recombinant human TGF-B1 (PeproTech) and an ART cocktail of 5uM saquinavir, 100nM efavirenz and 200nM raltegravir (NIH AIDS Reagent Program). Cells were harvested on day 7 for flow cytometric analysis and measurements of integrated HIV DNA levels. The following antibodies were used for analysis: anti-CD3-BUV395 (clone SP34-2), anti-CD8-BUV496 (clone RPA-T8), anti-CD45RA-BUV737 (clone HI100), anti-CD27-BV605 (clone L128), anti-CCR7-BB700 (clone 3D12), anti-CD45RA-APC (clone HI100), anti-CD3-BV421 (clone SP34-2), anti-CD8-PE/CF594 (clone RPA-T8), (from BD biosciences); anti-CD4-APC/Cy7 (clone OKT4), anti-CD101-PE/Cy7 (clone BB27) (from Biolegend). Acquisition of stained cells was performed on an LSRFortessa or FACSymphony (BD biosciences) driven by FACSDiva software and analyzed using FlowJo software (version 10.8, Treestar). Measurements of integrated HIV DNA on cells from day 7 was performed as previously described ³⁹⁰.

Measurement of intestinal epithelial damage biomarkers

Levels of circulating biomarkers of mucosal damage in plasma were measured by enzyme-linked immunosorbent assay (ELISA) using a commercially available kit as per the manufacturer's instructions (sCD14: R&D Systems, Cat #DC140l; IFABP: My Biosource, Cat#MBS740424; zonulin: Alpco, Cat #30-ZONSHU-E01).

In vitro stimulations

In vitro stimulations were performed on total PBMC from both healthy donors and ART-suppressed PLWH. For PMA/ionomycin stimulations, cells were stimulated at 37°C with 80 ng/mL PMA and 500 ng/mL ionomycin in the presence of 10ug/mL of BFA and 0.7uL of GolgiStop (BD biosciences). Cells were harvested and stained at 0hr and 3hr post-stimulation, with the 0hr timepoint serving as a negative control. For aCD3/aCD28 stimulations, cells were cultured in RPMI supplemented with 10% heat-inactivated FBS, 100U/mL penicillin, 100ug/mL streptomycin and 20U/mL recombinant human IL-2 (Gemini Bio-products), 5ug/mL anti-CD28-BUV737 (clone CD28.2, BD biosciences), 5ug/mL anti-CD2-purified (clone RPA-2.10, Biolegend), and 5ug/mL anti-CD3-purified (clone SP34-2, BD Biosciences). Fresh IL-2 at 20U/mL was supplemented every 2 days and cells were harvested and stained at days 0, 3 and 5 post-stimulation. For downstream flow cytometry analysis, the following antibodies were used: anti-CD4-APC/Cy7 (clone OKT4), anti-PD-1-BV786 (clone EH12.2H7), anti-CD101-PE/Cy7 (clone BB27), anti-IFN γ -PE/Dazzle594 (clone B27), anti-TNF α -APC (clone MAb11), anti-IL-2-BV650 (clone MQ1-17H12), anti-LAP-BV421 (clone TW4-2F8) (From Biolegend); anti-Ki-67-Alexa700 (clone B56), anti-CD3-BUV395 (clone SP34-2), anti-CD8-BUV496 (clone RPA-T8), anti-CD45RA-BUV737 (clone HI100),), anti-CD27-BV605 (clone L128), anti-CCR7-BB700 (clone 3D12) (from BD biosciences); anti-IL-17a-AF488 (clone eBio64DEC17) from eBioscience; LIVE/DEAD fixable aqua from ThermoFisher.

Plasma Cytokine Levels

Plasma cytokines were measured using the MSD platform as per manufacturer's instruction with NHP-specific U-PLEX for IL-6 (K156TXK), IP-10 (K156U FK), MIP-1a (K156UJK), TNF- α (K156UCK) from plasma samples from day 42 post-infection. Values below limit of detection were imputed at half of the limit of detection.

SIV DNA/RNA measurements

Levels of SIV DNA and RNA in rectal mucosa were measured as previously described^{19, 391}. Briefly, rectal biopsy tissue was homogenized, RNA and DNA were extracted and SIV DNA and RNA levels were measured by qRT-PCR and normalized to cell counts using concurrent rhesus albumin measurements.

Statistical Analyses

Analyses were performed using R studio or GraphPad Prism 9. P values ≤ 0.05 were considered statistically significant with the following definitions: $*P < 0.05$, $**P < 0.01$, $***P < 0.001$, $****P < 0.0001$. Differences in unmatched data were evaluated using Mann-Whitney U test and matched data were evaluated using Wilcoxon matched-pairs signed rank test. For samples with multiple comparisons, values were adjusted for multiple comparisons using Dunn's test, false-discovery rate or Sidak correction. Longitudinal analyses were evaluated using mixed-effects model with Tukey correction. Correlations were calculated using nonparametric Spearman analysis.

Acknowledgements

This manuscript is dedicated in loving memory of our colleague and friend Dr. Timothy Hoang. We would like to thank Sherrie Jean, Stephanie Ehnert and all veterinary and animal care staff at the Emory National Primate Center and all participants who generously provided samples for this study, as well as the Emory Hope clinic and Emory CFAR for sample management. We also thank the Emory Flow Cytometry core (Kiran Gill) for flow cytometry support, the Emory CFAR Virology Core (Thomas Vanderford) for viral load measurements, the Emory Multiplexed Immunoassay Core (Jianjun Chang) for plasma cytokine measurements and Accelevir Diagnostics for intact proviral DNA measurements. We thank Viiv Healthcare and GSK for kindly providing antiretroviral therapy to support this study.

Chapter Three Figures

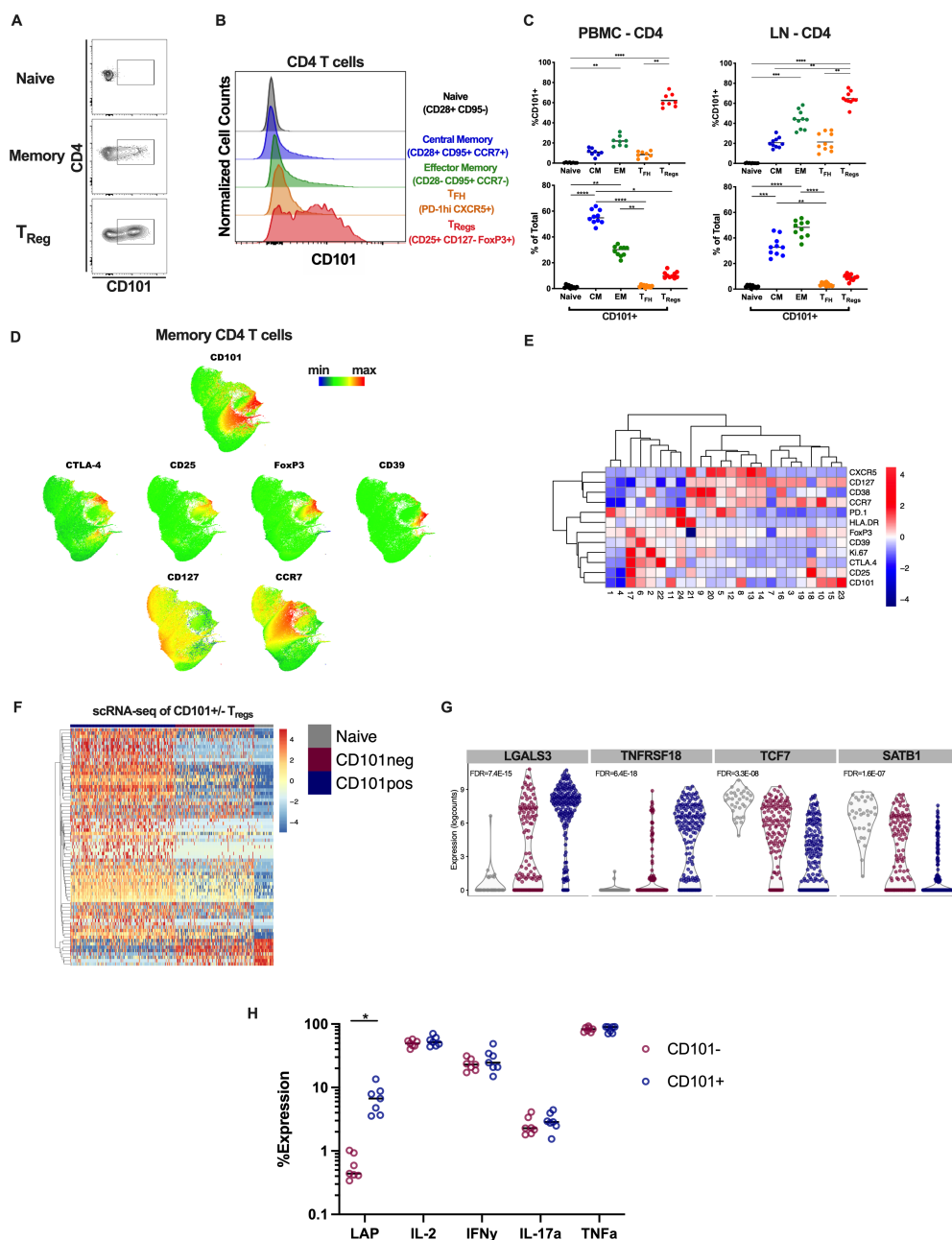


Figure 3.1. Phenotype of CD101-expressing CD4 T cells in healthy rhesus macaques A)

Representative staining of CD101 on CD4 subsets in healthy RM PBMC. B) Representative histograms of CD101 on detailed CD4 subsets in healthy RM PBMC. C) Expression of CD101 within detailed CD4 subsets in PBMC and LN from healthy RM (top); total contribution of

CD101⁺ cells to the overall CD4 pool from each CD4 subset in PBMC and LN. D) UMAP plot of flow cytometry data showing overall Phenograph cluster location and expression intensity of markers of interest. E) Hierarchical clustering of expression (z-score) for selected markers from flow cytometry data in each Phenograph cluster. F) Heatmap of the top 50 differentially expressed genes between CD101⁺ and CD101⁻ Tregs (CD95⁺ CD25⁺ CD127⁻) by scRNA-seq analysis of healthy RM PBMC. G) Violin plots showing RNA expression levels of 4 genes of interest. H) Cytokine expression levels in CD101⁻ and CD101⁺ memory CD4 after 3hr PMA/ionomycin stimulation of total PBMC from healthy individuals.

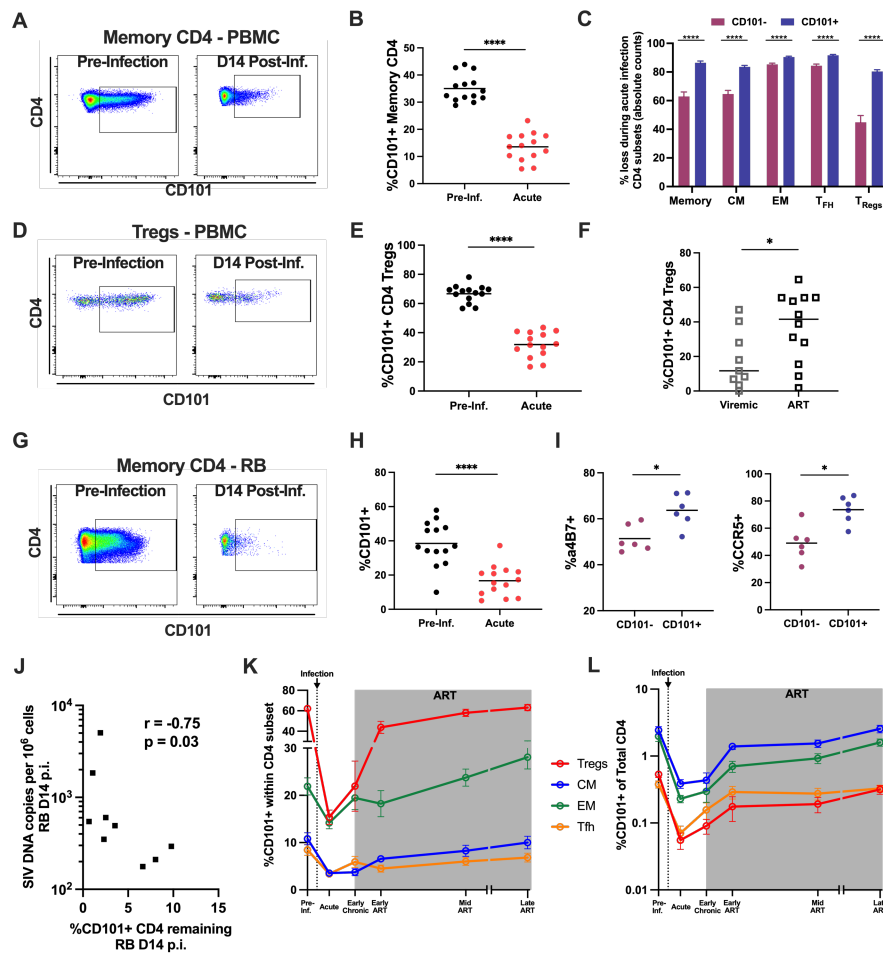


Figure 3.2 Dynamics of CD101-expressing CD4 T cells after SIV infection A)

Representative staining of CD101 on PBMC memory CD4 pre- and post-SIV infection. B)

Expression levels of CD101 on PBMC memory CD4 pre- and post-SIV infection. C) Total loss of CD101⁺ and CD101⁻ cells within CD4 subsets calculated based on absolute counts in blood pre- and post-SIV infection (mean+SEM). D) Representative staining of CD101 on PBMC CD4

Tregs pre- and post-SIV infection. E) Expression levels of CD101 on PBMC CD4 Tregs pre- and post-SIV infection. F) Expression levels of CD101 on PBMC CD4 Tregs from HIV-infected individuals during active viremia and during suppressive antiretroviral therapy (ART). G)

Representative staining of CD101 on rectal biopsy (RB) memory CD4 pre- and post-SIV

infection. H) Expression levels of CD101 on RB memory CD4 pre- and post-SIV infection. I) Expression levels of $\alpha 4\beta 7$ and CCR5 on RB memory CD4 CD101⁻ and CD101⁺ cells from healthy RM. J) Association between depletion of CD101⁺ CD4 T cells in rectal biopsies at day 14 p.i. (calculated from baseline to acute infection as % of live lymphocytes) and SIV DNA levels in rectal biopsies at day 14 p.i. (spearman correlation, n=9). K) CD101 expression within PBMC CD4 subsets during longitudinal SIV infection (mean \pm SEM). L) Overall contribution of CD101⁺ cells to the overall CD4 pool from each PBMC CD4 subset during longitudinal SIV infection (mean \pm SEM). Lines designate mean values.

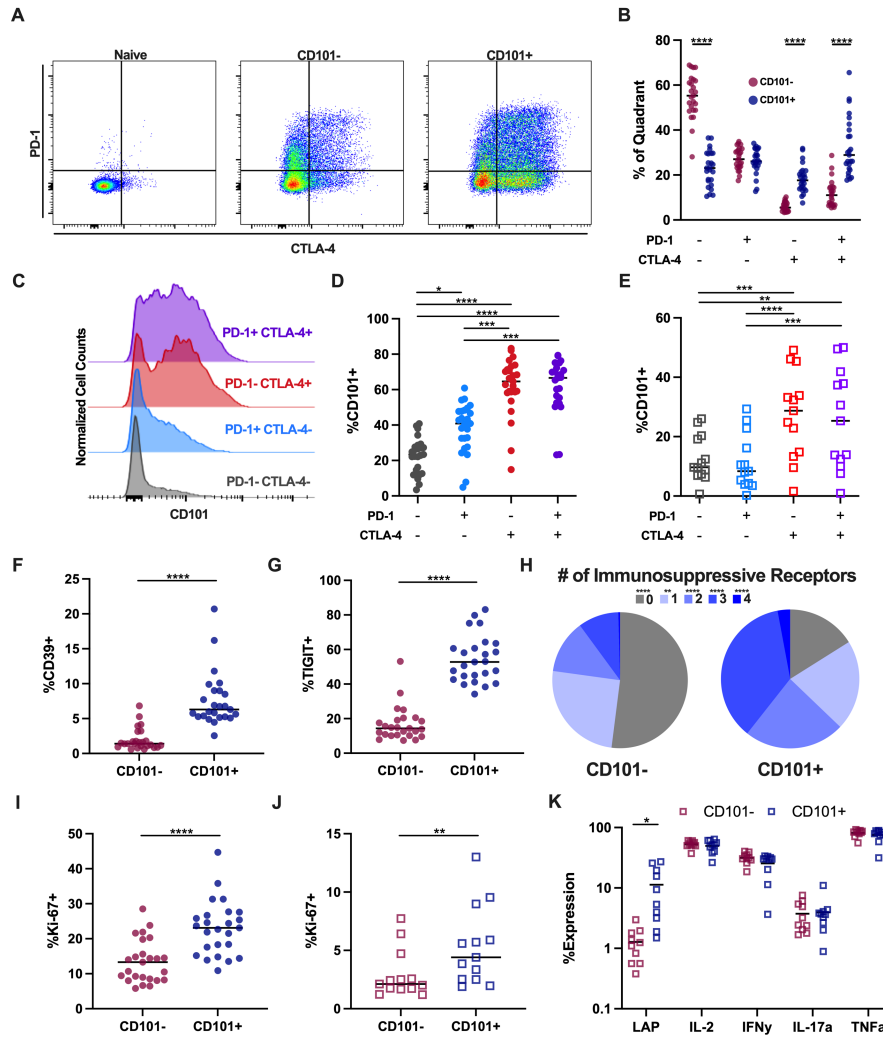


Figure 3.3 Phenotypic profile of CD101+ CD4 during long-term antiretroviral therapy A)

Representative staining of PD-1 and CTLA-4 within naïve, memory CD101⁻ and CD101⁺ CD4 T cells in lymph node (LN) from ART-suppressed SIV-infected RM. B) Quadrant distribution of PD-1 and CTLA-4 expression within CD101⁻ and CD101⁺ LN memory CD4 from ART-suppressed SIV-infected RM. C) Representative histogram of CD101 expression across PD-1 and CTLA-4 expression quadrants in LN memory CD4 from ART-suppressed SIV-infected RM. D) CD101 expression across PD-1 and CTLA-4 quadrants in LN memory CD4 from ART-suppressed SIV-infected RM. E) CD101 expression across PD-1 and CTLA-4 quadrants in PBMC memory CD4 from ART-suppressed HIV-infected individuals. F,G) Expression levels of

CD39 (F) and TIGIT (G) within CD101⁻ and CD101⁺ LN memory CD4. H) Pie chart representing the frequency of cells expressing PD-1 and/or CTLA-4 and/or CD39 and/or TIGIT within CD101⁻ and CD101⁺ LN memory CD4. I,J) Expression levels of Ki-67 within CD101⁻ and CD101⁺ memory CD4 from LN from ART-suppressed SIV-infected RM (I) and PBMC from ART-suppressed HIV-infected individuals (J). K) Cytokine expression levels in CD101⁻ and CD101⁺ memory CD4 after 3hr PMA/ionomycin stimulation of total PBMC from ART-suppressed PLWH. Lines designate mean values.

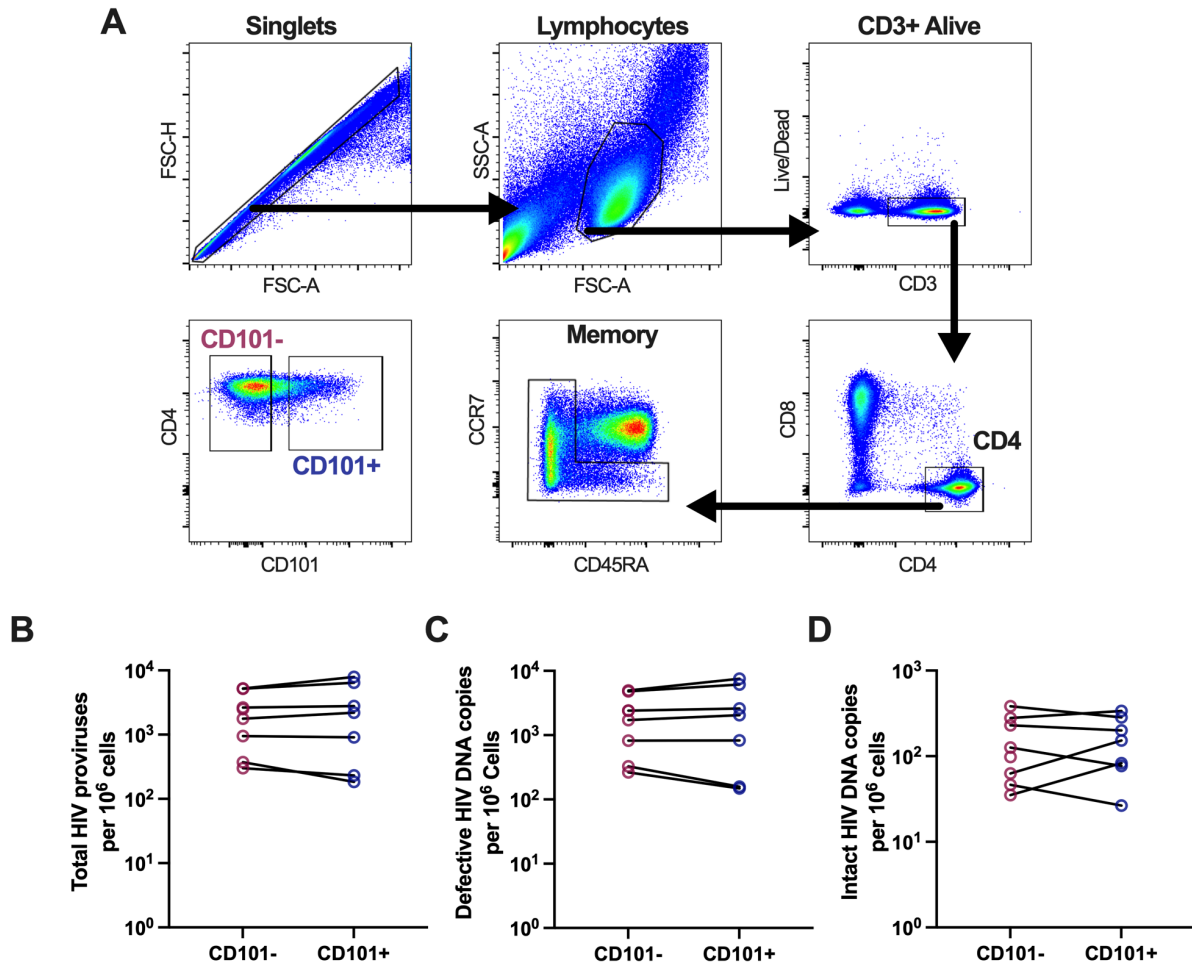


Figure 3.4. HIV DNA levels in sorted memory CD4 T cells A) Sorting strategy for memory CD101⁻ and CD101⁺ memory CD4 T cells. B-D) Total HIV proviruses (B), defective HIV DNA copies (C) and intact HIV DNA copies (D) measured by IPDA in sorted CD101⁻ and CD101⁺ memory CD4 T cells from PBMC from ART-suppressed individuals.

			Disease Progression (D14 p.i)			Disease Progression (D42 p.i)			Plasma Cytokine Levels (D42 p.i.)			
	Parameter	Spearman values	Plasma Viral Load	Memory CD4 HLA-DR+ CD38+	Memory CD8 HLA-DR+ CD38+	Plasma Viral Load	Memory CD4 HLA-DR+ CD38+	Memory CD8 HLA-DR+ CD38+	IL-6	IP-10	MIP-1a	TNF-a
D14 p.i.	%CD101+ Memory CD4	r	0.04	0.07	-0.01	-0.22	-0.02	0.04	0.05	-0.22	0.07	-0.16
		p	0.83	0.71	0.95	0.27	0.92	0.83	0.79	0.27	0.74	0.42
	CD101+ Memory CD4 Counts	r	0.20	0.24	0.22	-0.16	0.24	0.33	0.05	-0.19	0.25	-0.2
		p	0.30	0.23	0.26	0.41	0.22	0.09	0.79	0.34	0.21	0.32
	CD101+ Memory CD4 Loss	r	-0.05	-0.13	-0.13	0.01	0.03	0.14	0.29	0.02	-0.25	0
		p	0.79	0.52	0.51	0.95	0.1	0.48	0.89	0.92	0.21	0.99
	%CD101+ on CD4 Treg	r	-0.04	0.02	0.05	-0.08	-0.12	-0.09	0.03	-0.2	0.13	-0.19
		p	0.85	0.91	0.79	0.68	0.53	0.64	0.9	0.32	0.53	0.35
D42 p.i.	%CD101+ Memory CD4	r	-0.01	0.03	-0.1	-0.72	0.12	0.34	-0.05	-0.42	-0.38	-0.27
		p	0.97	0.9	0.61	0.0001	0.53	0.08	0.79	0.03	0.056	0.17
	CD101+ Memory CD4 Counts	r	0.03	0.21	0.13	-0.78	0.36	0.52	-0.09	-0.4	-0.27	-0.17
		p	0.87	0.29	0.51	0.0001	0.06	0.004	0.67	0.04	0.19	0.42
	CD101+ Memory CD4 Loss	r	0.03	-0.13	-0.002	0.79	-0.14	-0.41	0.25	0.23	0.43	0.02
		p	0.9	0.52	0.99	0.0001	0.48	0.03	0.23	0.27	0.03	0.92
	%CD101+ on CD4 Treg	r	-0.06	0.05	-0.04	-0.7	0.11	0.3	-0.22	-0.35	-0.39	-0.27
		p	0.75	0.81	0.84	0.0001	0.59	0.12	0.27	0.08	0.051	0.18

Table 3.1. Correlations of CD101 dynamics with plasma viral load, immune activation and plasma cytokine levels. Analyses were done as Spearman correlations with r and p value displayed. All values are from the D14 p.i. or D42 p.i for 28 SIV-infected RMs. CD4 loss was calculated based on absolute counts of CD101+ CD4 pre- and post-infection. Statistically significant findings are highlighted in yellow (n=28).

		SIV DNA RB D14 p.i.	SIV RNA RB D14 p.i.
%CD101+ Memory CD4 RB D14 p.i.	r	-0.13	0.32
	p	0.74	0.41
%Depletion of CD101+ CD4 RB D14 p.i.	r	-0.75	0.55
	p	0.03	0.13
%Depletion of CD101- CD4 RB D14 p.i.	r	0.52	0.53
	p	0.16	0.15

Table 3.S1. Association of CD101 gut depletion and mucosal viral burden. Analyses were done as Spearman correlations with r and p value displayed. %Remaining (amount of depletion) was calculated from baseline to d14 p.i. as % of live lymphocytes. Statistically significant findings are highlighted in yellow (n=9).

		D14 p.i.			D42 p.i.		
		FC Zonulin	FC sCD14	FC IFABp	FC Zonulin	FC sCD14	FC IFABp
%CD101+ Memory CD4 RB D14 p.i.	r	-0.2527	0.1758	0.2582	-0.5874	0.2198	0.3626
	p	0.4043	0.5659	0.3939	0.0489	0.4703	0.224
%CD101+ Memory CD4 RB D42 p.i.	r	-0.5385	0.01099	-0.3132	-0.5804	0.3297	0.2747
	p	0.0611	0.9782	0.2975	0.0521	0.2715	0.3633

Table 3.S2. Intestinal epithelial damage biomarker correlations. Analyses were done as Spearman correlations with r and p value displayed. Fold-change of biomarkers was assessed as change from pre-infection baseline to either d14 or d42 post-infection. Statistically significant findings are highlighted in yellow (n=13).

	Virus	Sex	Age at Infection (Months)	Mamu A*01	Acute Plasma Viral Load (copies/mL)	Pre-ART Plasma Viral Load (copies/mL)	ART Initiation (week post-infection)	Time on ART (weeks)	Figures
RF17	SIVmac239	M	44	+	1.23E+07	8.87E+05	6	60	1 D-E, 2 A-E, 3A-D, 3F-I
RVk17	SIVmac239	M	45	+	7.92E+06	8.02E+03	6	60	1 D-E, 2 A-E, 3A-D, 3F-I
RVz16	SIVmac239	M	47	+	6.02E+06	4.04E+05	6	60	1 D-E, 2 A-E, 3A-D, 3F-I
RYm17	SIVmac239	M	44	+	1.16E+07	1.28E+06	6	60	1 D-E, 2 A-E, 3A-D, 3F-I
RHm17	SIVmac239	M	44	-	9.68E+06	9.10E+06	6	60	1 D-E, 2 A-E, 3A-D, 3F-I
RNy16	SIVmac239	M	48	+	1.45E+07	2.33E+05	6	60	1 D-E, 2 A-E, 3A-D, 3F-I
RTd17	SIVmac239	M	46	+	2.16E+07	1.33E+06	6	60	1 D-E, 2 A-E, 3A-D, 3F-I
34897	SIVmac239	M	45	-	8.23E+06	1.15E+06	6	60	1 D-E, 2 A-E, 3A-D, 3F-I
RRh17	SIVmac239	M	45	-	8.98E+06	7.97E+04	6	60	1 D-E, 2 A-E, 3A-D, 3F-I
RFn17	SIVmac239	M	44	-	1.66E+07	4.11E+06	6	60	1 D-E, 2 A-E, 3A-D, 3F-I
RVm17	SIVmac239	M	44	-	5.81E+06	2.68E+05	6	60	1 D-E, 2 A-E, 3A-D, 3F-I
RBe17	SIVmac239	M	46	-	1.13E+07	6.92E+05	6	60	1 D-E, 2 A-E, 3A-D, 3F-I
RMI17	SIVmac239	M	44	+	1.90E+07	4.67E+06	6	60	1 D-E, 2 A-E, 3A-D, 3F-I
Rlb17	SIVmac239	M	47	-	4.26E+07	1.39E+07	6	60	1 D-E, 2 A-E, 3A-D, 3F-I
34918	SIVmac239	F	48	-	2.00E+07	1.25E+06	6	60	2G-H, 2J, 3A-D, 3F-I
RBf17	SIVmac239	M	50	-	2.88E+07	5.32E+06	6	60	2G-H, 2J, 3A-D, 3F-I
RBv17	SIVmac239	M	38	-	2.88E+07	2.28E+05	6	60	2G-H, 3A-D, 3F-I
REu17	SIVmac239	F	38	-	1.70E+07	2.32E+05	6	60	2G-H, 2J, 3A-D, 3F-I
RKq17	SIVmac239	M	39	-	3.04E+07	1.11E+06	6	60	2G-H, 3A-D, 3F-I
RVc17	SIVmac239	M	50	-	2.90E+07	6.11E+05	6	60	2G-H, 2J, 3A-D, 3F-I
RZg17	SIVmac239	M	49	-	1.92E+07	2.06E+05	6	60	2G-H, 3A-D, 3F-I
34920	SIVmac239	F	48	-	6.74E+07	4.68E+06	6	60	2G-H, 2J, 3A-D, 3F-I
34930	SIVmac239	M	48	-	3.50E+07	2.36E+06	6	60	2G-H, 3A-D, 3F-I
REq17	SIVmac239	M	39	-	2.92E+07	2.79E+05	6	60	2G-H, 2J, 3A-D, 3F-I
RGr17	SIVmac239	M	39	-	1.10E+07	1.05E+07	6	60	2G-H, 3A-D, 3F-I
RVi17	SIVmac239	M	49	+	2.42E+07	2.50E+07	6	60	2G-H, 2J, 3A-D, 3F-I
RWs17	SIVmac239	M	38	-	1.07E+07	5.60E+05	6	60	2G-H, 2J, 3A-D, 3F-I
RZp17	SIVmac239	M	39	-	4.73E+06	5.10E+04	6	60	2G-H, 2J, 3A-D, 3F-I
RAg16	SIVmac239	M	41	-	6.70E+07	3.60E+07	8	44	2K-L
Rgt16	SIVmac239	M	28	-	3.60E+07	2.60E+06	8	50	2K-L
RHk16	SIVmac239	M	30	-	1.50E+07	3.20E+04	8	33	2K-L
Rls16	SIVmac239	M	29	+	2.00E+07	1.70E+06	8	34	2K-L
RLw16	SIVmac239	M	29	-	1.60E+07	1.20E+07	8	41	2K-L
RNI16	SIVmac239	M	32	-	5.80E+07	3.10E+07	8	44	2K-L
RQj16	SIVmac239	M	31	-	2.20E+08	2.40E+07	8	46	2K-L
RWn16	SIVmac239	M	30	+	3.20E+07	3.50E+06	8	37	2K-L
Rla17	Uninfected			N/A	N/A		N/A	N/A	2I
RSd17	Uninfected			N/A	N/A		N/A	N/A	2I
RSk17	Uninfected			N/A	N/A		N/A	N/A	2I
RTb17	Uninfected			N/A	N/A		N/A	N/A	2I
RZe17	Uninfected			N/A	N/A		N/A	N/A	2I
RZn17	Uninfected			N/A	N/A		N/A	N/A	2I
93-11R	Uninfected			N/A	N/A		N/A	N/A	1A-C
97-11R	Uninfected			N/A	N/A		N/A	N/A	1A-C
103-11R	Uninfected			N/A	N/A		N/A	N/A	1A-C
112-11R	Uninfected			N/A	N/A		N/A	N/A	1A-C
131-11R	Uninfected			N/A	N/A		N/A	N/A	1A-C
131-11R	Uninfected			N/A	N/A		N/A	N/A	1A-C
176-11R	Uninfected			N/A	N/A		N/A	N/A	1A-C
187-11R	Uninfected			N/A	N/A		N/A	N/A	1A-C
189-11R	Uninfected			N/A	N/A		N/A	N/A	1A-C
202-11R	Uninfected			N/A	N/A		N/A	N/A	1A-C
315-11R	Uninfected			N/A	N/A		N/A	N/A	1A-C

Table 3.S3. Animal characteristics.

Figure 3.S1. CD101 in healthy RM. A) Representative gating strategy for CD4 subsets within LN samples from healthy rhesus macaques. B) CD101 expression on CD4 subsets in rectal biopsy samples from healthy rhesus macaques. Lines designate means.

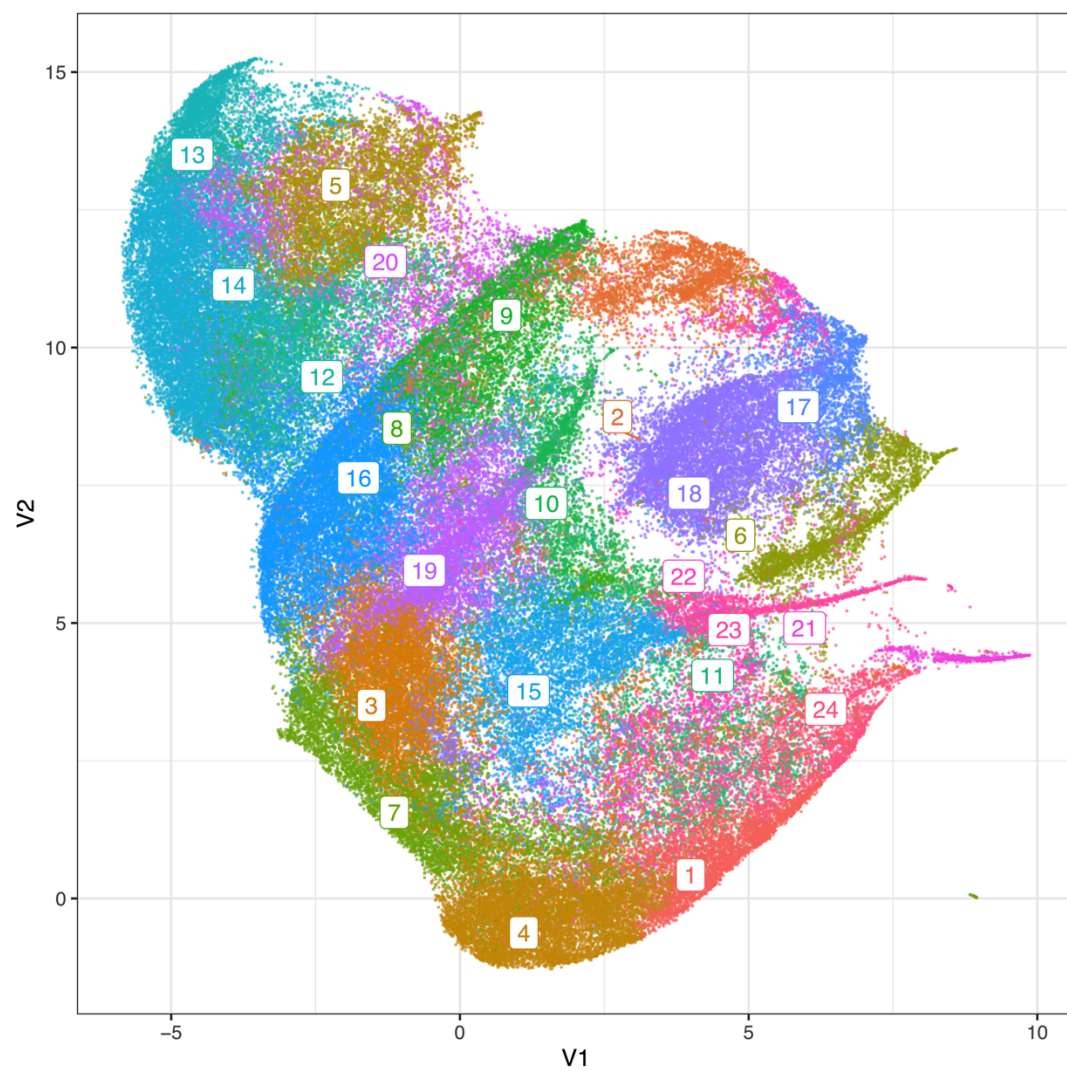


Figure 3.S2. UMAP with phenograph cluster locations

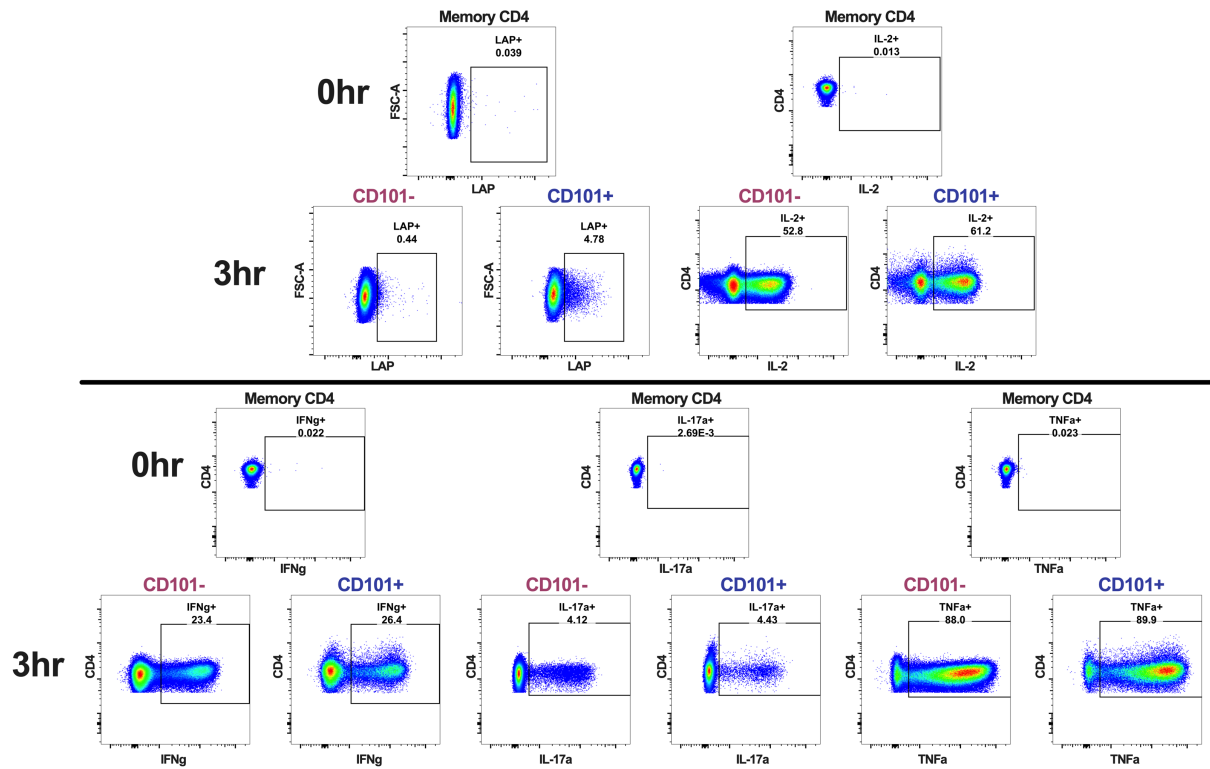


Figure 3.S3. Representative gating for cytokine expression after stimulation. Representative gates for cytokine levels within memory CD4 at 0hr post-stimulation and within CD101- and CD101+ memory CD4 at 3hr post-stimulation with PMA/ionomycin.

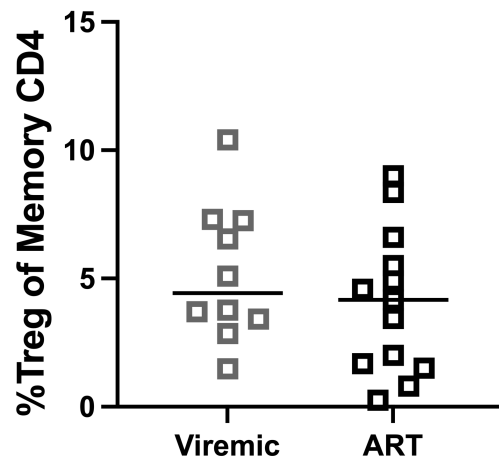


Figure 3.S4. Frequency of CD4 Tregs in HIV-infected individuals. The frequency of Tregs (CD25+ CD127- FoxP3+) within the memory pool of CD4 Tregs evaluated in PBMC from viremic and ART-suppressed individuals. Lines designate means.

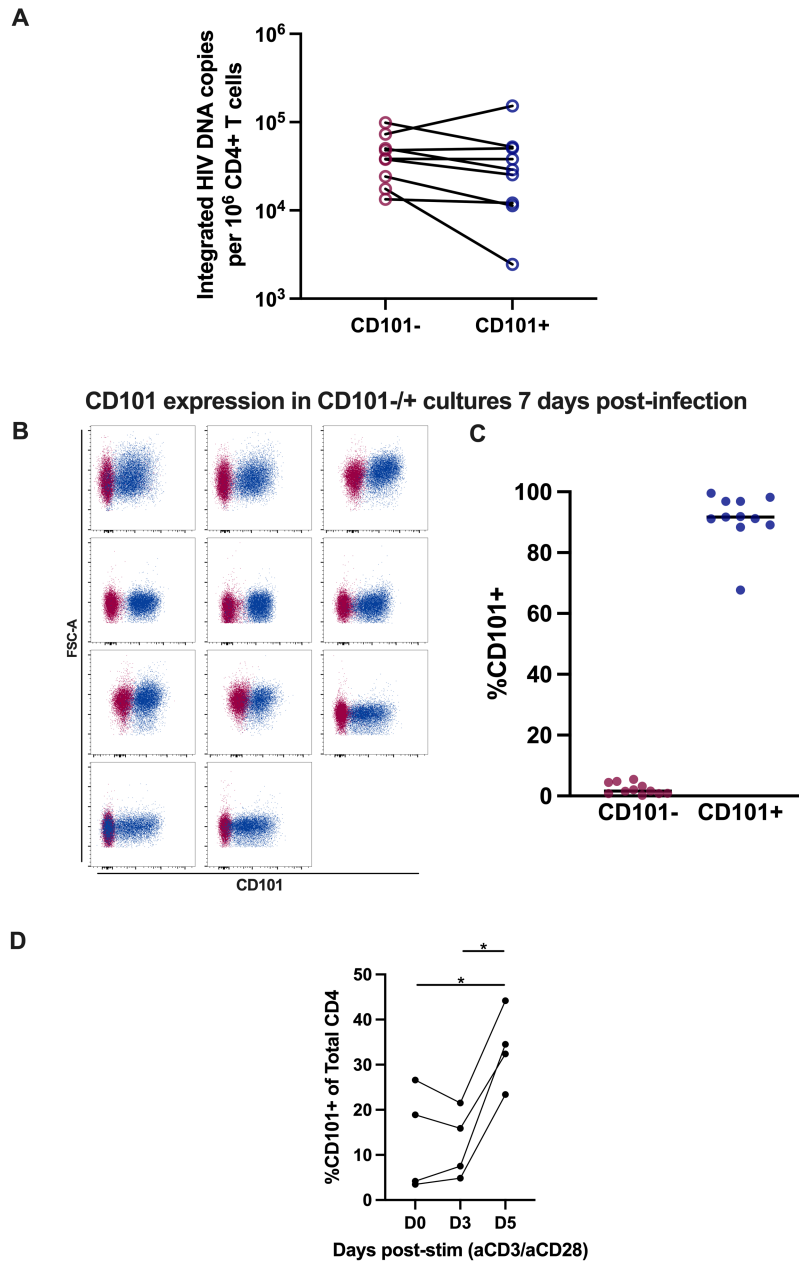
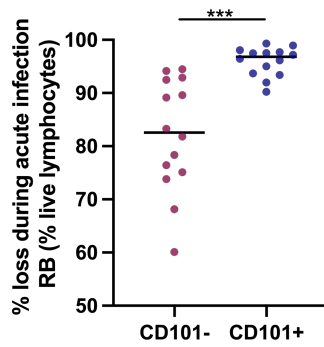


Figure 3.S5. *In vitro* infection of sorted CD4 T cells and exclusion of CD101

downregulation. A) Levels of integrated HIV DNA from CD101- or CD101-positive cell cultures 7 days after *in vitro* infection of sorted cells. B) Overlaid flow plot of expression of CD101 on CD4 T cells from CD101- (maroon) and CD101+ (blue) cultures 7 days after *in vitro*

infection of sorted cells. C) Gated expression levels of CD101 on CD4 T cells from CD101- and CD101+ cultures. D) CD101 expression levels on total CD4 T cells after aCD3/aCD28 stimulation of PBMC from healthy individuals.

A



B

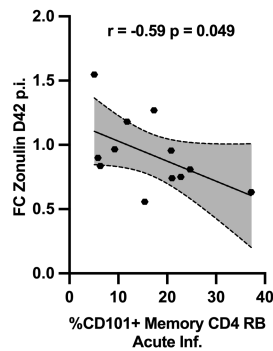


Figure 3.S6. Preferential depletion of CD101+ CD4 T cells in the gut. A) Loss of CD101- and CD101+ CD4 T cells in the gut during acute infection, calculated as %loss from baseline using the frequency of CD101- and CD101+ cells of total live lymphocytes. B) Association between levels of CD101-expressing CD4 T cells in the gut during acute infection and fold change of circulating zonulin in plasma at day 42 p.i. compared with pre-infection (spearman correlation with linear regression and 95% confidence interval).

Chapter Four: Distinct SIV-specific lymphoid tissue CD8 T cells simultaneously exhibit effector and stem-like profiles and associate with viral control and reduced reservoir size

Authors: Zachary Strongin¹, Claire Deleage², Timothy N Hoang^{1†}, Gregory K. Tharp¹, Kevin Nguyen¹, Maria Cardenas³, Laurence R. Marchand¹, Stacey Lapp¹, Andrew R. Rahmberg⁴, Guido Silvestri^{1,5,6}, Deanna Kulpa^{1,5,6}, Jason M. Brenchley⁴, Steven E. Bosinger^{1,5,6}, Haydn T Kissick^{3,6,7}, Mirko Paiardini^{1,5,6*}

Affiliations:

¹Division of Microbiology and Immunology, Emory National Primate Research Center, Emory University; Atlanta, Georgia, USA

²AIDS and Cancer Virus Program, Frederick National Laboratory for Cancer Research, National Cancer Institute, NCI; Frederick, Maryland, USA

³Department of Urology, Emory University School of Medicine; Atlanta, Georgia, USA

⁴Barrier Immunity Section, Laboratory of Viral Diseases, NIAID, NIH; Bethesda, Maryland, USA

⁵Department of Pathology and Laboratory Medicine, Emory University School of Medicine; Atlanta, Georgia, USA

⁶Emory Vaccine Center, Emory University; Atlanta, Georgia, USA

⁷Winship Cancer Institute of Emory University; Atlanta, Georgia, USA

Abstract

HIV cure efforts are increasingly focused on harnessing CD8 T-cell functions and better understanding the profile of CD8 T-cells promoting HIV control can critically inform novel therapeutic approaches. Here, we explored dynamics of TOX and TCF1 expression in CD8 T-cells after SIV infection in lymphoid tissue. CD8 T-cells upregulated TOX and differentiated into distinct subsets, including a novel TCF1+CD39+ subset expressing high levels of TOX and inhibitory receptors, but not expressing cytotoxic molecules despite responsiveness to antigen stimulation. Transcriptional analysis of SIV-specific CD8 revealed TCF1+CD39+ cells as an intermediate effector population retaining stem-like features. TOX+TCF1+CD39+ CD8 T-cells express higher levels of CXCR5 than terminally-differentiated cells and were found at higher frequency in follicular micro-environments. Importantly, their levels were strongly associated with viral control and lower reservoir size. Collectively, these data describe a unique population of lymphoid CD8 T-cells possessing both stem-like and effector properties that contribute to limiting SIV persistence.

Introduction

The persistence of an antigen, such as in cancer and chronic viral infections, is associated with a state of persistent activation of the immune system, which is unable to completely overcome the antigen load. Oftentimes, this failure is defined, at least in part, by CD8 T cell exhaustion, a state in which CD8 T cells have significantly reduced effector functions and increased expression of inhibitory receptors driven by large-scale transcriptional and epigenetic reprogramming³⁹².

While CD8 T cell exhaustion can be defined by a combination of markers and functional assessments, a distinct identifier of exhausted CD8 T cells is the recently described transcription factor thymocyte selection-associated high mobility group box protein (TOX)¹⁸⁹⁻¹⁹¹. TOX was shown to be the transcriptional driver of exhausted CD8 T cell differentiation and was responsible for the downstream phenotype and functional profile of these cells in both chronic LCMV and cancer models¹⁸⁸⁻¹⁹². Concurrently, TOX was also shown to be vital for the persistence and dampening of the CD8 response to chronic antigen, as loss of TOX leads to the collapse of stem-like CD8 T cell populations, driving responding cells towards a damaging effector state causing immunopathology¹⁸⁹⁻¹⁹². Additional work has demonstrated that Tox is not uniquely expressed in exhausted CD8 T cells, but also in polyfunctional effector memory CD8 T cells and can be expressed in conjunction with TCF1, a transcription factor expressed by stem-like CD8 T cells^{218, 393, 394}. TCF1+ stem-like CD8 T cells are responsible for maintaining the CD8 response to chronic antigen, providing the effective response to anti-PD-1 blockade and fueling the development of terminally differentiated effector/exhausted CD8 T cells, typically defined by expression of effector molecules and surface markers such as TIM-3, CD101 and CD39^{169, 348}.

These dynamics of CD8 T cell biology are highly relevant to current HIV research. CD8 T cells are vital for limiting viremia in HIV infection, and in rare individuals are capable of inducing complete viral control in absence of antiretroviral therapy (ART)²²⁹. However, in most individuals, CD8 T cells reach a state of exhaustion and markers of exhaustion have traditionally been linked to higher viral loads and worse disease progression^{206, 207, 209, 212-215, 229}. HIV cure efforts in recent years include a major focus on immunotherapies designed to restore functional CD8 T cell responses; as such, a better understanding of the stem-like, effector and exhausted CD8 T cell populations that emerge after HIV infection will substantially improve the ability to design targeted therapeutic strategies^{257, 395}. Recent work has indeed demonstrated that Tox expression is increased on CD8 T cells after HIV infection and that Tox and TCF-1 can be co-expressed in a fraction of HIV-specific CD8 T cells²¹⁸. These important findings were limited to the periphery, where HIV-specific CD8 T cells are primarily cytotoxic, and these mechanisms have not yet been investigated in lymphoid tissue. This is vital as CD8 T cells in lymphoid tissue, a primary site of viral replication, have been shown to be phenotypically and functionally distinct from peripheral CD8, including having the potential for limiting viremia through non-traditional cytolytic pathways⁸²⁻⁸⁴.

Given the unique nature of lymphoid CD8 T cells, we took advantage of the longitudinal tissue access afforded by the SIV model of HIV infection to investigate the dynamics of TOX and TCF-1 expressing CD8 T cells in lymph nodes after SIV infection. We found that TOX is upregulated on CD8 T cells after early chronic SIV infection and is highly expressed in SIV-specific CD8 T cells. Furthermore, we identified a unique subset of TCF1⁺ CD39⁺, distinct from

traditionally described stem-like and terminally differentiated CD8 T cell populations, that emerges after infection and is characterized by high expression of TOX, inhibitory receptors and Ki-67, but very low levels of granzyme B while maintaining functional responsiveness to SIV peptides. Transcriptional analysis confirms an intermediate profile of TCF1⁺ CD39⁺ CD8 T cells as a preliminary effector cell that maintains stem-like properties. Increased presence of both TOX⁺ and TCF1⁺ CD39⁺ CD8 T cells is strongly associated with viral control during early chronic infection and lower size of the intact reservoir on ART, potentially due to a higher frequency of these cells within lymph node B cell follicles. Together, our findings reveal a previously unrecognized subset of SIV-specific CD8 T cells that display phenotypic and transcriptional hallmarks of effector cells while still maintaining stem-like properties and contribute to the ability of lymphoid CD8 T cells to limit viremia without traditional cytolytic molecules.

Results

TOX is upregulated on LN CD8 T cells after SIV infection and associated with high inhibitory receptor expression

To assess the dynamics of LN CD8 T cells, we performed a cross-sectional phenotypic analysis of LN from uninfected Rhesus Macaques (RMs) at early chronic infection (D42 post-infection (p.i)) and RMs at late chronic infection (all >6 months p.i.; average 17 months p.i.) (Supp Table 1). Flow cytometry plots for Tox expression are shown in Fig 1A for a representative uninfected, early chronic, and late chronic RMs. TOX is significantly upregulated in total CD8 T cells following SIV infection and is further upregulated during the late chronic stage of infection (Fig 1B). In order to confirm this upregulation is directly in response to SIV infection, we evaluated

the frequency of memory and SIV-specific (CM9+) CD8 T cells expressing TOX at d42 p.i. in a subset of A*01+ animals (Fig 1C). While memory cells express TOX at levels significantly higher than naïve (mean 47% vs. 2%; $p=0.02$; Fig 1D), SIV-specific cells express significantly more (mean 61%; $p=0.02$; Fig 1D), indicating the upregulation of this transcription factor is occurring directly in response to antigen stimulation.

TOX is well described to be co-expressed with inhibitory receptors on CD8 T cells during LCMV infection and cancer. We found the same to be true following SIV infection of RMs, with significantly higher levels of PD-1, CD39, CD101 and TIGIT in TOX+ memory CD8 T cells as compared to TOX- cells at early chronic infection (Fig S1A). To understand the broad phenotypic profile of LN CD8 during early chronic infection, we utilized Uniform Manifold Approximation and Projection (UMAP) of our flow cytometry data and, in combination with Phenograph analysis, identified distinct clusters of LN memory CD8 T cells (Fig 1E, S1B-DD). Cells in clusters 7, 11, 6 and 15 comprised the population of traditional effector CD8 T cells, defined by high expression of granzyme B, low expression of TCF1 and high expression of CD39, and primarily expressing high levels of inhibitory receptors (Fig 1E-F). Notably, our analysis identified a group of cells, comprising clusters 2 and 9, expressing high levels of inhibitory/exhaustion markers, including TOX and CD39, while simultaneously maintaining high levels of TCF1. In contrast to the traditional effector population, these cells expressed low levels of granzyme B. CD39, often co-expressed with Tim-3, has been primarily described as a terminal differentiation marker, and its co-expression with TCF1 in CD8 T cells during chronic viral infection has not been shown to this point^{175, 212, 396, 397}. In all, we find that following SIV infection, TOX expression is increased on responding LN memory CD8 T cells and is expressed

in cells with high inhibitory receptor expression with a phenotypic profile resembling traditional effector cells, but is also expressed in a unique subset of TCF1⁺ CD39⁺ granzyme B⁻ cells.

Unique population of TCF1⁺ CD39⁺ CD8 T cells expand in LN after infection

Given the undescribed nature of this subset of TCF1⁺ CD39⁺ CD8 T cells, we explored our cross-sectional flow cytometry data to understand the emergence of these cells after SIV infection in LN. Flow cytometry plots for TCF1 vs CD39 staining are shown in Fig 2A for a representative uninfected, early chronic and late chronic RM. In uninfected RMs, the large majority (mean 87%) of LN memory CD8 T cells are TCF1⁺ CD39⁻, indicative of large pool of non-differentiated, resting CD8 T cell (Fig 2B). However, during early chronic SIV infection, the pool of TCF1⁺ CD39⁻ cells contracts significantly down to 60% of memory CD8 T cells, concurrent with a large expansion of the TCF1⁺ CD39⁺ cell subset (27% compared to 6% in uninfected; Fig 2B). In addition, TCF1⁻ CD39⁺ cells, the traditional effector population, also significantly expand during early chronic infection to an average of 8% of the memory CD8 T cell population. During late chronic infection, there is a further significant differentiation out of the TCF1⁺ CD39⁻ pool, with the majority of these cells shifting to the terminally differentiated effector pool (TCF1⁺ CD39⁻; Fig 2B).

To further understand the profile of these cells, we focused specifically on LN from early chronic infection and found that phenotypically, these 3 TCF1/CD39 LN CD8 T cell subsets are distinct populations. TCF1⁺ CD39⁺ cells are significantly higher in TOX expression than the other two subsets, and only slightly, but significantly, lower in expression of other inhibitory receptors compared to TCF1⁻ CD39⁺ cells (Fig 2C). Stem-like TCF1⁺ CD39⁻ cells are consistently low in inhibitory/exhaustion markers (Fig 2C). Ki-67, indicative of recent proliferation and cell

division, was highest in TCF1⁻ CD39⁺ cells, but was also expressed by 61% of the TCF1⁺ CD39⁺ cells (Fig 2D). This same phenotypic profile was observed in cells from late chronic infection (Fig S2).

The most striking difference between the TCF1/CD39 subsets was found in granzyme B expression, as TCF1⁻ CD39⁺ cells are the only subset expressing high levels of granzyme B (Fig 2E). While granzyme B is a well described CD8 T cell effector molecule that is known to be expressed by traditional cytolytic CD8 T cells, granzyme K has been shown to be expressed earlier in CD8 T cell differentiation and can mark distinct CD8 populations with different functional properties than GzmB⁺ cells ^{398, 399}. In assessing GzmB and GzmK expression, we found that the majority of TCF1⁺ CD39⁺ cells are GzmB⁻ GzmK⁺, significantly more so than both TCF1⁺ CD39⁻ and TCF1⁻ CD39⁺ cells, while TCF1⁻ CD39⁺ cells are primarily GzmB⁺ GzmK⁺ (Fig 2F-G). Finally, to assess the functional capacity of these CD8 subsets, we performed SIV-peptide stimulation of total LN cells from early chronic infection. While TCF1⁺ CD39⁺ and TCF1⁻ CD39⁺ CD8 T cells degranulated at similar rates in response to antigen, TCF1⁻ CD39⁺ cells produced significantly more IFN γ , potentially indicative of a more differentiated effector profile (Fig 2H). Collectively, these data suggest that an intermediate effector CD8 T cell population emerges in LN after SIV infection that is responsive to antigen despite lacking expression of traditional cytolytic molecules.

Transcriptional profile of SIV-specific LN CD8 T cells identifies intermediate effector cells maintaining stem-like properties

In order to further explore unique LN CD8 populations during SIV infection, we expanded our analyses to understand the transcriptional profile of SIV-specific CD8 T cells. We sorted Gag-

specific (CM9+) CD8 T cells from LN biopsies of 5 RMs during early chronic (D42 p.i.) SIV infection and performed single-cell RNAseq (Fig 3A, S3). SIV-specific LN CD8 T cells were distributed across 5 transcriptionally distinct clusters (Fig 3B, S4A, Supp File 1). Cluster 1 was characterized by high expression of traditional effector molecules including *GZMA*, *GZMB*, *GZMK*, *PRF1* and *IFNG* (FIG 3C). Additionally, while most of the SIV-specific cells expressed moderate levels of inhibitory receptors and traditional exhaustion markers, they were highest in cluster 1, including *PDCD1*, *TIGIT*, *LAG3*, and *CTLA4*. Cluster 2 was primarily characterized by high expression of *TCF7* and a number of other genes typically associated with stem-like CD8 T cell populations including *SELL*, *JUN*, *FOS* and *IL7R*. Clusters 3 and 4 were defined primarily by genes involved in cell cycling (*MKI67*, *BRCA1* etc.) and type 1 interferon signaling (*IRF7*, *MX1* etc.) respectively, while cluster 5 was differentiated primarily by non-annotated genes with little discernible pattern. Neither *TOX* nor *ENTPD1* were significantly enriched in any of the defined clusters. Given the gene expression patterns in these clusters, we used gene signature analyses to compare our single-cell data to previously defined CD8 T cell signatures from human cancer studies (S4B, Supp File 1)⁴⁰⁰. We found clear overlap with our defined clusters and human signatures of cell cycling, type 1 interferon signaling, stem-like CD8 and terminally differentiated CD8 T cell, reinforcing a definition of cluster 1 as effector cells and cluster 2 as stem-like cells. Overall, the effector cluster made up approximately 50% of the total SIV-specific LN CD8 T cell population, while the stem cluster accounted for 13% of these cells (Fig 3D). This distribution was consistent across all 5 animals, with the exception of RHm17, in which there was a major enrichment of cells in the proliferating cluster.

To specifically identify and characterize our TCF1+ CD39+ subset of interest within our scRNA-seq data, we defined expression thresholds for *TCF7* and *ENTPD1* and identified all SIV-specific

cells that were above these thresholds as *TCF7*⁺ *ENTPDI*⁺ (S4C). *TCF7*⁺ *ENTPDI*⁺ cells were distributed across all 5 clusters but were largely enriched in the stem cluster compared to the total SIV-specific CD8 T cell population (Fig 3E). To understand how these cells were transcriptionally unique, we examined differentially expressed genes between the *TCF7*⁺ *ENTPDI*⁺ cells and the stem and effector clusters. Compared to the stem cluster, *TCF7*⁺ *ENTPDI*⁺ cells displayed a more effector-like transcriptional profile, with higher expression of effector molecules and differentiation markers compared to higher traditional stem-like gene expression in the stem cluster (Fig 3F). However, compared to the effector cluster, *TCF7*⁺ *ENTPDI*⁺ cells were significantly more stem-like, with higher expression of stem-like genes such as *SELL* and *FOS*, while there was an enrichment of the effector genes within the effector cluster (Fig 3G). Overall, the transcriptional profile of *TCF7*⁺ *ENTPDI*⁺ cells is consistent with the phenotypic profile of an intermediate effector cell that maintains some stem-like properties.

TOX⁺ and TCF1⁺ CD39⁺ CD8 T cells strongly associate with viral control

Given the expansion of a previously unrecognized CD8 T cell population in response to SIV infection, and previous reports of relationships between inhibitory receptor expression on CD8 T cells and disease progression, we evaluated potential relationships between the LN CD8 T cell populations identified by flow cytometry and viral burden during early chronic infection.

Notably, we found that RMs with higher frequency of TOX⁺ LN CD8 T cells had lower plasma viral loads at day 42 p.i. ($r=-0.78$, $p<0.0001$) and this relationship held true when evaluating TOX expression only in SIV-specific LN CD8 T cells ($r=-0.76$, $p=0.04$) (Fig 4A-B).

In evaluating TCF1/CD39 memory CD8 subsets, we similarly found that animals with higher frequencies of TCF1⁺ CD39⁺ LN CD8 T cells had lower plasma viral loads during early chronic

infection ($r=-0.64$, $p=0.0003$) (Fig 4C). Conversely, animals with higher frequencies of TCF1+ CD39- cells had higher viral loads at this time point, potentially indicative of a failure of CD8 T cells to progress into the precursor effector state (Fig 4D). Surprisingly, despite being the most differentiated effector population and having high cytolytic potential, there was no relationship between frequencies of TCF1- CD39+ cells and plasma viral load (Fig 4E).

To understand whether the strong association of TOX+ and TCF1+/CD39+ LN CD8 T cells with better viral control was limited only to plasma viremia or extended to tissue viral burden, we evaluated levels of total SIV DNA and cell-associated RNA in memory CD4 T cells from the same LN biopsies from which we performed flow cytometry. In concordance with the plasma viral load relationship, we found that a higher frequency of both TOX+ and TCF1+ CD39+ cells was strongly associated with lower levels of both SIV DNA (Fig 4F-G) and CA-RNA (Fig S5A-B) in LN memory CD4 during early chronic infection. These data indicate that these cells are associated with immune responses limiting the overall viral burden and not simply reducing viral production from infected cells. Finally, this reduction of viral burden also resulted in limited overall disease progression, as RMs with higher frequencies of TOX+ LN CD8 T cells maintained higher memory CD4 T cell counts during early chronic infection, and a similar trend was observed with TCF1+ CD39+ CD8 T cells (Fig 4H-I). Together, these data demonstrate that the emergence of TOX+ and TCF1+ CD39+ LN CD8 T cells is associated with better viral control and limited disease progression.

TOX+ and TCF1+ CD39+ cells express higher levels of CXCR5 and are present at higher frequency within B cell follicles

Given the significant relationship between TOX⁺ and TCF1⁺ CD39⁺ CD8 T cells in LN with viral burden, it is important to understand the positioning of these cells within the LN environment, as cells with higher migratory potential or positioned in viral hotbeds may have a better chance to interact with infected cells. In particular, CXCR5, a chemokine receptor involved in lymphoid microenvironment migration, is upregulated on lymphoid CD8 T cells upon HIV infection and has been previously associated with lower viral burden ^{82, 84, 133, 401, 402}. During early chronic infection, we did not find a significant association between expression of CXCR5 within total memory CD8 T cells and viral burden (S6A-C). Within the TCF1/CD39 subsets, we found that both TCF1⁺ CD39⁻ and TCF1⁺ CD39⁺ cells expressed significantly higher levels of CXCR5 as compared to TCF1⁻ CD39⁺ cells (Fig 5A-B). Notably, higher expression of CXCR5 within both the TCF1⁺ CD39⁺ subset and TCF1⁻ CD39⁺ subset was strongly associated with better control of plasma viremia, while this relationship did not exist for CXCR5 expression within the TCF1⁺ CD39⁻ subset (Fig 5C-E). The expression of CXCR5 within these subsets was also significantly associated with lower cell-associated SIV DNA and SIV RNA levels in LN memory CD4 T cells (Fig 5F-H, S6 C-E). Additionally, we find that the highest level of CXCR5 is found in GzmK⁺ GzmB⁻ CD8, with significantly lower expression of CXCR5 in GzmB⁺ cells (S6G). Given the significant expression of CXCR5 on TCF1⁺ CD39⁺, we utilized immunofluorescence imaging to directly investigate the presence of these cells within the B cell follicle during early chronic infection. Due to high expression of CD39 by a myriad of cell types within LN, it is difficult to distinctly identify CD39⁺ CD8 T cells in conjunction with other markers (S7A). Therefore, we focused on TCF1⁺ TOX⁺ CD8 T cells in our IHC analysis, as more than 75% of TCF1⁺ CD39⁺ cells are TOX⁺ (Fig 2B). Importantly, TOX⁺ CD8 T cells also have significantly higher levels of CXCR5 expression than TOX⁻ cells (S7B). TCF1⁺

TOX⁺ CD8 T cells were found in both the T cell zone (TCZ) and B cell follicles (BCF) of LN at D42 post-infection (Fig 5F). Furthermore, TOX⁺ TCF1⁺ cells make up a larger proportion of the total CD8 T cell population in the B cell follicle than the T cell zone, while TOX⁺ TCF1⁻ and TOX⁻ TCF1⁺ CD8 populations do not differ significantly between the TCZ and BCF (Fig 5G). Overall, these data suggest that the intermediate effector population of TOX⁺ TCF1⁺ CD39⁺ CD8 T cells have increased presence within B cell follicles where there is high potential to have a major impact on viral burden.

TOX⁺ and TCF1⁺ CD39⁺ CD8 T cell populations are associated with reduced size of the intact SIV reservoir in lymphoid tissues during ART

To understand the dynamics of TOX expression and TCF1/CD39 subsets in LN memory CD8 T cells in the absence of antigen, we analyzed LN samples collected after more than 1 year of antiretroviral therapy (ART) from the same animals assessed during early chronic infection (ART was initiated at day 42 post-infection). We found a limited but significant decrease in TOX expression on memory CD8 T cells after long-term ART (Fig 6A-B). The lack of reduction in TOX expression despite over a year without antigen is consistent with previous reports of TOX as a major epigenetic regulator and a recent study showing the *TOX* gene locus remains open and active in CD8 T cells from HCV-infected individuals even after DAA therapy and clearance of chronic antigen^{189-191, 194}.

In contrast to TOX expression, the large majority (87%) of LN memory CD8 T cells return to the TCF1⁺ CD39⁻ subset during long-term ART, identical to the proportion observed in uninfected RM (Fig 6C-D). Simultaneously, there is a significant contraction of both the TCF1⁺ CD39⁺ and

TCF1⁺ CD39⁺ subset. While the frequencies of these subsets is reduced, they maintain a similar phenotype to that seen during early chronic infection (S8A). Considering there remained substantial heterogeneity across animals in the frequency of TCF1⁺ CD39⁺ within LN memory CD8 T cells (range 4.3%-13.5%), we performed the intact proviral DNA assay (IPDA) on the same LN biopsies from which the flow cytometry data was generated to assess whether the presence of these cells is associated with lower size of the viral reservoir during long-term ART³⁶⁸. Notably, we found that having higher frequencies of TCF1⁺ CD39⁺ CD8 T cells was associated with lower levels of intact SIV DNA in LN (Fig 6E). Collectively, these data suggest that despite an expected contraction of active, functional T cells in the absence of antigen during long-term ART, TCF1⁺ CD39⁺ CD8 T cell are consistently associated with reduced viral burden, including the size of the intact SIV reservoir in lymphoid tissues.

Discussion

In this study, we investigated the dynamics of TOX and TCF1 expressing CD8 T cells in lymphoid tissue in SIV-infected nonhuman primates. We found that following SIV infection, TOX is upregulated on SIV-specific CD8 T cells and is co-expressed with numerous inhibitory receptors. Importantly, we identified a unique subset of TOX⁺ CD8 T cells that are defined by co-expression of TCF1 and CD39. These cells are additionally high in inhibitory receptor expression and are responsive to SIV peptide stimulation, but do not express significant levels of granzyme B. Transcriptional analysis of LN SIV-specific CD8 T cells revealed distinct clusters of stem-like and terminally differentiated effector cells, with TCF1⁺ CD39⁺ cells being enriched in stem-like features while also showing evidence of preliminary effector differentiation. Remarkably, during early chronic infection, increased presence of both TOX⁺ and TCF1⁺

CD39⁺ CD8 T cells in LN was strongly associated with better viral control, including lower plasma viremia and cell-associated SIV-DNA and RNA in lymphoid tissues. Furthermore, the levels of both TOX⁺ and TCF1⁺ CD39⁺ LN CD8 T cells was also strongly associated with the size of the intact SIV-reservoir in LN after one year of ART, as determined by IPDA.

Mechanistically, these cells are found at higher frequencies within B cell follicles, which are known sites of high viral replication and persistence ⁴⁰³.

In chronic antigen settings, TCF1 is the critical transcription factor in stem-like and precursor exhausted CD8 T cells responsible for maintaining CD8 T cell responses by feeding the pool of terminally differentiated effector/exhausted CD8 T cells ^{169, 178, 183, 393, 400}. The transcription factor TOX is known to be a distinct driver of the exhaustion program ¹⁸⁸⁻¹⁹². Terminally differentiated effector/exhausted cells are typically identifiable by lack of TCF1, expression of TOX, expression of effector molecules and of various surface markers such as TIM-3, CD101 and CD39 ^{169, 348}. CD39 has been previously identified as a marker of terminal differentiation in LCMV, cancer and HIV ^{175, 396, 397}. While it has been demonstrated that TCF1 and TOX can be coexpressed in functional cells, there remains a clear distinction between cells expressing TCF1 and cells expressing CD39 or other markers of terminal differentiation ^{218, 393, 394}. In contrast, our data in chronic SIV infection and lymphoid tissues indicate that CD39 is not uniquely expressed on terminally differentiated cells, but is also expressed on TCF1⁺ cells that have maintained several stem-like properties. Notably, these TCF1⁺ and CD39⁺ cells are responsive to antigen stimulation and express granzyme K but not granzyme B, suggestive of a unique effector phenotype. Indeed, granzyme K expression has been shown to mark distinct functional subsets of antigen-specific cells in both AML and rheumatoid arthritis and granzyme K⁺ CD8 T cells have

been found in mucosal tissue from HIV infected individuals, despite lower levels of granzyme B^{398, 399, 404}. Given the strong association with viral control in plasma and tissues, TCF1+ CD39+ cells may serve as a preliminary effector population that fuels the SIV-specific response and assists in viral clearance. Previous reports have reported that increased TCF1 expression on peripheral CD8 T cells of SIV and HIV controllers is associated with better viral control, while acknowledging this may substantially differ in tissue^{219, 405}. Additionally, the authors acknowledge that promoting stem-like TCF1+ cells alone may not be sufficient for viral control, as these cells are not directly poised with effector capacity²¹⁹. Indeed, we show that having more TCF1+ CD39- cells in the canonical stem-like state is associated with worse viral control, potentially representing a failure of the SIV-specific CD8 T cells to differentiate to an effective state to limit antigen load. This highlights the notion that particular subsets of TCF1+ CD8 T cells, while all maintaining stem-like properties, likely serve differing roles in the CD8 response.

The unique nature and importance of TCF1+ CD39+ CD8 T cells may be directly linked to its existence within lymphoid tissue. Previous studies have demonstrated substantial differences in the effector profile of HIV-specific CD8 T cells in both lymphoid and mucosal tissue sites when compared to those in peripheral blood, specifically with lower cytotoxicity in tissue-derived CD8 T cells^{82-84, 404, 406, 407}. Additionally, elite controllers of HIV, individuals able to naturally (i.e. in absence of ART) control viral replication, have higher levels of lymphoid CD8 T cells with a unique profile and these cells exhibit increased ability to penetrate into the follicular environment⁸⁴. Our data highlight the emergence of TCF1+ CD39+ CD8 T cells in lymph node during early chronic SIV infection and expands on these findings to demonstrate a transcriptional profile consistent with a preliminary effector maintaining stem-like properties. Furthermore, our

finding that animals with higher expression of CXCR5 on TCF1⁺ CD39⁺ CD8 T cells have better control of viremia is consistent with previous findings that the frequency of CXCR5⁺ CD8 T cells is inversely associated with viral load, independent of cytolytic activity. However, we also found that increased CXCR5 expression on terminally differentiated effector TCF1⁻ CD39⁺ CD8 T cells was also associated with better viral control, despite much lower levels of CXCR5 on these cells. This suggests that, regardless of the cytolytic profile, follicular penetrance is a critical feature for SIV-specific CD8 T cells to limit viremia, but TCF1⁺ CD39⁺ cells are armed with a preferential ability to penetrate the B cell follicle and a stem-like profile that likely favors sustained responsiveness as compared to the terminally differentiated effector cells.

Due to their strong association with lower viral burden and their ability to penetrate the follicle, our findings support the conclusion that TCF1⁺ CD39⁺ CD8 T cells play a key role in promoting viral control in lymphoid tissue during early chronic SIV infection. Unfortunately, we are unable to demonstrate a direct mechanism by which these cells are acting on virally infected cells. Given the dependence on TCF1 for identifying stem-like CD8 T cells and the inability to sort live cells on transcription factors, including TOX, work in mice and humans often relies on sorting strategies involving GFP-tagged TCF1 or using CXCR5 as a surrogate for TCF1 expression^{169, 178, 400}. Unfortunately, CXCR5 does not serve as a good surrogate marker for TCF1 in non-human primates, and therefore sorts of TCF1/CD39 populations for functional assessments, differentiation assays and direct measurements of SIV-specific killing capacity were not possible. Although we cannot establish a direct causal link between increased presence of these cells and lower viral burden, it would be counterintuitive that lower viral loads would drive increased differentiation of CD8 T cells. The association of lower viral burden and the

presence of TCF1⁺ CD39⁺ cells expressing high levels of PD-1, TIGIT and CD101, traditional markers of CD8 T cell exhaustion, is in contrast to previous research demonstrating a link between CD8 T cell exhaustion and higher viral loads during chronic HIV infection^{206, 207, 209, 212-215}. Importantly, we are primarily focused on a time point 6 weeks post-infection, which is traditionally considered early chronic in the SIV infection model, but is likely not representative of CD8 T cell responses after months of antigen exposure. Studying how this population may change over time as CD8 control of viremia becomes less effective may give further insight into the dynamics of stem-like, effector and exhausted CD8 T cells in HIV infection and treatment.

Our investigations into the dynamics of lymphoid tissue CD8 T cells during early chronic SIV infection reveal the emergence of a unique subset of SIV-specific CD8 T cells that simultaneously exhibit stem-like and effector phenotypic and transcriptional profiles, penetrate B cell follicles and are associated with better viral control and reduced size of the intact reservoir in the absence of a traditional cytolytic profile. This data advances our understanding of the differentiation and function of stem-like and effector CD8 T cell populations in HIV infection and provide rationale for investigating immunotherapeutic strategies promoting the expansion of TOX⁺, TCF1⁺ and CD39⁺ CD8 T cells to potentially promote viral control and HIV cure.

Acknowledgements:

This manuscript is dedicated in loving memory of our colleague and friend Dr. Timothy Hoang. We would like to thank Sherrie Jean, Stephanie Ehnert, Chelsea Wallace and all veterinary and animal care staff at the Emory National Primate Research Center. We would like to thank Justin Harper for IACUC management. We also thank the Emory Flow Cytometry core (Kiran Gill) for flow cytometry support, the Emory National Primate Research Center Genomics Core for RNAseq support, the NIH Tetramer Core facility at Emory University for providing tetramer and Accelevir Diagnostics for intact proviral DNA measurements. Peptide pools of SIVmac239 Gag were provided by the HIV Reagent Program, which were contributed by the Division of AIDS (DAIDS) at NIAID.

Funding: This work was supported by UM1AI164562 (M.P.), co-funded by NIH/NHLBI/NIDDK/NINDS/NIDA/NIAID and by the NIAID, NIH under award number R37AI141258. Additional support was provided by: NIH OD, ORIP, P51 OD011132 and U42 OD011023; Division of Intramural Research, NIAID, P30AI050409; National Cancer Institute, National Institutes of Health, Contract No. 75N91019D00024; Divisions of Intramural Research of the National Institute of Allergy and Infectious Diseases, JMB received a funding award from the National Institute of Allergy and Infectious Diseases, NIH (number: 1ZIAAI001029). Sequencing data was acquired on an Illumina NovaSeq6000 funded by NIH S10 OD026799. The content of this publication does not necessarily reflect the views or policies of the Department of Health and Human Services, nor does mention of trade names, commercial products, or organizations imply endorsement by the U.S. Government. The funders had no role in study design, data collection and analysis, decision to publish, or preparation of the manuscript.

Author Contributions:

Conceptualization: ZS, MP

Investigation: ZS, CD, TNH, KN, SL, ARR, HTK

Formal Analysis: ZS, CD, GKT, MC, ARR, HTK

Visualization: ZS, CD, MC, HTK

Funding acquisition: CD, DAK, GS, SEB, MP

Supervision: MP

Writing – original draft: ZS, MP

Writing – review & editing: ZS, CD, MC, LRM, HTK, MP

Competing interests:

The authors have nothing to disclose.

Data Availability Statement

Source data supporting this work are available from the corresponding author upon reasonable request. RNA sequencing data will be deposited in the NCBI's Gene Expression Omnibus (GEO).

Materials and Methods

Animals, SIV infection, antiretroviral therapy and sample collection

48 total Indian rhesus macaques (RMs) were included in this study and animal details and infection information are listed in Supp Table 1. All animals that initiated ART started a daily subcutaneous antiretroviral therapy regimen of FTC (40 mg/kg), TDF (5.1 mg/kg) and DTG (2.5 mg/kg) during the early chronic phase of infection (D42 post-infection), reached levels of undetectable plasma viremia and were maintained on ART for 64 weeks prior to the late ART collection timepoint. Lymph node biopsy sample collections were performed and processed as previously described ¹³⁴.

Ethics Statement

All animal experimentation was conducted following guidelines set forth by the Animal Welfare Act and by the NIH's Guide for the Care and Use of Laboratory Animals, 8th edition. All studies were reviewed and approved by Emory's Institutional Animal Care and Use Committee (IACUC; permit number 201800047) and animal care facilities at Emory National Primate Research Center are accredited by the U.S. Department of Agriculture (USDA) and the Association for Assessment and Accreditation of Laboratory Animal Care (AAALAC) International. Proper steps were taken to minimize animal suffering and all procedures were conducted under anesthesia with follow-up pain management as needed. The National Institute of Allergy and Infectious Diseases (NIAID) animal care and use committee, as part of the National Institute of Health (NIH) intramural research program, approved all experimental procedures pertaining to the animals (protocol LVD 26E).

SIV plasma viral load and DNA measurements

SIV plasma viral loads were measured as previously described with a limit of detection of 15 copies/mL⁴⁰⁸. Total SIV DNA levels were measured in memory CD4 T cells sorted from total LN samples. Cells were sorted on live CD3⁺ CD4⁺ CD95⁺ cells. Levels of SIV DNA were then measured as previously described³⁹¹. For intact proviral DNA measurements, total cryopreserved LN samples were processed and analyzed by Accelevir Diagnostics as previously described³⁶⁸.

Flow Cytometry

Flow cytometric analyses for this study were performed on peripheral blood and LN cells according to previously optimized and standardized procedures with anti-human antibodies with confirmed cross-reactivity with RMs. The following antibodies were used at pre-optimized staining concentrations: anti-CD95-BV605 (clone DX2), anti-CD39-BV711 (clone A1), anti-PD-1-BV785 (clone EH12.2H7), anti-CD4-PE/Cy5 (clone OKT4), anti-CD101-PE/Cy7 (clone BB27) (all from Biolegend); anti-CTLA-4-BV421 (clone BNI3), anti-Ki-67-BV480 (clone B56), anti-CCR7-BV650 (clone 3D12), anti-CD3-BUV395 (clone SP34-2), anti-CD8-BUV496 (clone RPA-T8), anti-CD28-BUV737 (clone CD28.2), anti-GzmK-AF647 (clone G3H69), Fixable Viability Stain 700 (all from BD Biosciences); anti-TIGIT-PerCP-eFluor710 (clone MBSA43), anti-TOX-PE (clone TXRX10), anti-GzmB-PETR (clone GB11), anti-CXCR5-PE-Cy7 (clone MU5UBEE), anti-EOMES-APC-eF780 (clone WD1928) (all from Thermofisher Scientific); anti-TCF1-AF488 (clone C63D9) (from Cell Signaling Technology); anti-Gag-APC (CM9 tetramer) (from the NIH Tetramer Facility at Emory University). To detect intracellular expression of TCF1, cells were fixed and permeabilized with FoxP3/Transcription Factor

Staining Buffer Kit Fix/Perm (Tonbo) and subsequently stained for intracellular markers of interest. Acquisition of stained cells was performed on minimum of 100,000 live CD3⁺ cells on a FACSymphony (BD Biosciences) driven by FACSDiva software and analyzed using FlowJo software (version 10.8, Treestar). For early chronic samples, FCS files were imported into FlowJo, compensated electronically, gated on memory CD8 T cells (CD3⁺ CD8⁺ CD95⁺) and equivalent numbers of cells from each animal were input into UMAP analysis (Uniform Manifold Approximation and Projection for Dimension Reduction) for unbiased evaluation of the distribution of markers of interest and projection was visualized/plotted on a 2 dimensional UMAP (<https://arxiv.org/abs/1802.03426>, <https://github.com/lmcinnes/umap>) and clusters were identified using the Phenograph clustering approach (<https://github.com/jacoblevine/PhenoGraph>).

Peptide Stimulation

Cryopreserved LN samples from D42 post-infection were thawed, rested and resuspended in RPMI supplemented with 10% FBS in the presence of BFA and Monensin (BD Biosciences), anti-CD107a-BV711 (clone H4A3, Biolegend), anti-CD49D-pure (clone 9F10, BD Biosciences), and anti-CD28-BUV737 (clone CD28.2, BD Biosciences). PBMCs were left unstimulated or stimulated for 6 hours at 37°C with SIVmac₂₃₉ Gag peptide pool (ARP-12364, NIH HIV Reagent Program) at a concentration 2ug/mL. After stimulation, cells were washed and stained with the following antibodies: anti-CD95-BV605 (clone DX2), anti-CD39-APC/Cy7 (clone A1), anti-PD-1-BV785 (clone EH12.2H7), anti-CD4-PE/Cy5 (clone OKT4), anti-CD101-PE/Cy7 (clone BB27) (all from Biolegend); anti-Ki-67-BV480 (clone B56), anti-CD3-BUV395 (clone SP34-2), anti-CD8-BUV496 (clone RPA-T8), anti-IFN γ -BB700 (clone B27), Fixable Viability Stain 700

(all from BD Biosciences); anti-TOX-PE (clone TXRX10), anti-GzmB-PETR (clone GB11) (all from Thermofisher Scientific); anti-TCF1-AF488 (clone C63D9) (from Cell Signaling Technology). To detect intracellular expression of cytokines and TCF1, cells were fixed and permeabilized with FoxP3/Transcription Factor Staining Buffer Kit Fix/Perm (Tonbo) and subsequently stained for intracellular markers of interest. The frequency of SIV-specific memory CD8 responding to stimulation was determined after background subtraction of matching unstimulated controls.

SIV-specific CD8 T cell single-cell RNA sequencing

Cryopreserved LN samples from 5 A*01+ animals at day 42 post-infection were thawed and stained with the following antibodies: anti-CD8-FITC (clone RPA-T8, BD Biosciences), anti-CD4-BV650 (clone OKT4, Biolegend), anti-Gag-PE (CM9 tetramer, NIH Tetramer Facility at Emory University, anti-CD95-PE/Cy7 (clone DX2, BD Biosciences), anti-CD28-APC (clone CD28.2, BD Biosciences), anti-CD3-APC/Cy7 (clone SP34-2, BD Biosciences). A minimum of 10,000 SIV-specific CD8 from each animal was sorted using a FACS Aria II system (BD Biosciences) as shown in the gating strategy in S4A-B.

For single-cell RNA-Seq, single-cell suspensions of lymph node peripheral mononuclear cells targeting 10,000 cells were loaded onto 10X Chromium Controller. Single cells were partitioned into droplets (Gel Beads in Emulsion: GEMs) using Chromium NextGEM Single Cell 5' Library & Gel Bead kits on the 10X Chromium Controller. The resulting cDNA was amplified and libraries were prepared for transcriptomic analysis as described previously⁴⁰⁹. Gene expression libraries were sequenced as paired-end 26x91 reads on an Illumina NovaSeq6000 targeting a depth of 50,000 reads per cell in the Yerkes Genomics Core

Laboratory(http://www.yerkes.emory.edu/nhp_genomics_core/). Cell Ranger software was used to perform demultiplexing of cellular transcript data, and mapping and annotation of UMIs and transcripts for downstream data analysis.

Single-cell RNA-Seq Bioinformatic Analysis

Sorted LN samples from five Rhesus macaques were run on 2 Nova Seq 1000 lanes and the resultant bcl files were converted to counts matrices using Cell Ranger v3.1 (10X Genomics). Alignment, filtering, barcode counting, and unique molecular identifier counting were performed using Cell Ranger v3.1 using the Mmul10 from Ensembl release 100 as a reference genome of *Macaca mulatta*. Data were further analyzed using Seurat v.3.0⁴¹⁰. Briefly, cells with a percentage of mitochondrial genes below 0.05% were included. Cells with more than 2500 or less than 500 detected genes were considered as outliers and excluded from the downstream analyses. Raw unique molecular identifier counts were normalized to unique molecular identifier count per million total counts and log-transformed. Variable genes were selected based on average expression and dispersion. Principal component analysis was performed using variable genes. Clusters and t-SNE plots were generated based on selected principal component analysis dimensions. Marker genes were identified by the Seurat function FindAllMarkers. Scaled expression data of these marker genes were used for creating the heatmaps. Normalized data are shown in the form of feature plots or violin plots. Gene set scoring was performed using the VISION R package v.1.1.0. The scoring algorithm is described here⁴¹¹. Briefly, expression of signature genes is weighted based on predicted dropout probability calculated from nearest neighbors, and the normalized expression summed for all genes in the gene set. Gene sets were

derived from significantly upregulated genes of CXCR5⁺ stem-like CD8 versus TIM3⁺ CD8 T cells from individuals with human papillomavirus-positive head and neck cancer⁴⁰⁰.

Immunofluorescence and quantitative image analysis

Immunofluorescent staining assay (IFA) and quantification were performed as previously described¹³⁴. In brief, IFA was performed on 5- μ m tissue sections, which were dewaxed and rehydrated. IFA multistaining of CD8 (HPA037756; SIGMA) + TCF1 (AF5596; R&D) + Tox1 (ab237009; Abcam) was performed on two distinct tissue section 20 μ m apart, to quantify the different subtypes of CD8T cells in all animals.

High magnification confocal images were collected from regions of interests (T cell zone and all B cell follicles) using an Olympus FV10i confocal microscope using a 60x phase contrast oil-immersion objective (NA 1.35) imaging using sequential mode to separately capture the fluorescence from the different fluorochromes at an image resolution of 1024x1024 pixels. Each subset of single, dual, or triple positive cells were quantified using Fiji/ image J2.

Statistical analysis

Analyses were performed using R studio or GraphPad Prism 9. P values ≤ 0.05 were considered statistically significant with the following definitions: $*P < 0.05$, $**P < 0.01$, $***P < 0.001$, $****P < 0.0001$. All specific analyses are designated in the relevant figure legend. Differences in matched data were evaluated using Wilcoxon matched-pairs signed rank test. For analyses with multiple comparisons, Kruskal-Wallis one-way ANOVA or two-way ANOVA were employed with relevant corrections for multiple comparisons using Dunn's, Tukey or Sidak corrections. Correlations were calculated using nonparametric Spearman analysis.

Chapter Four Figures

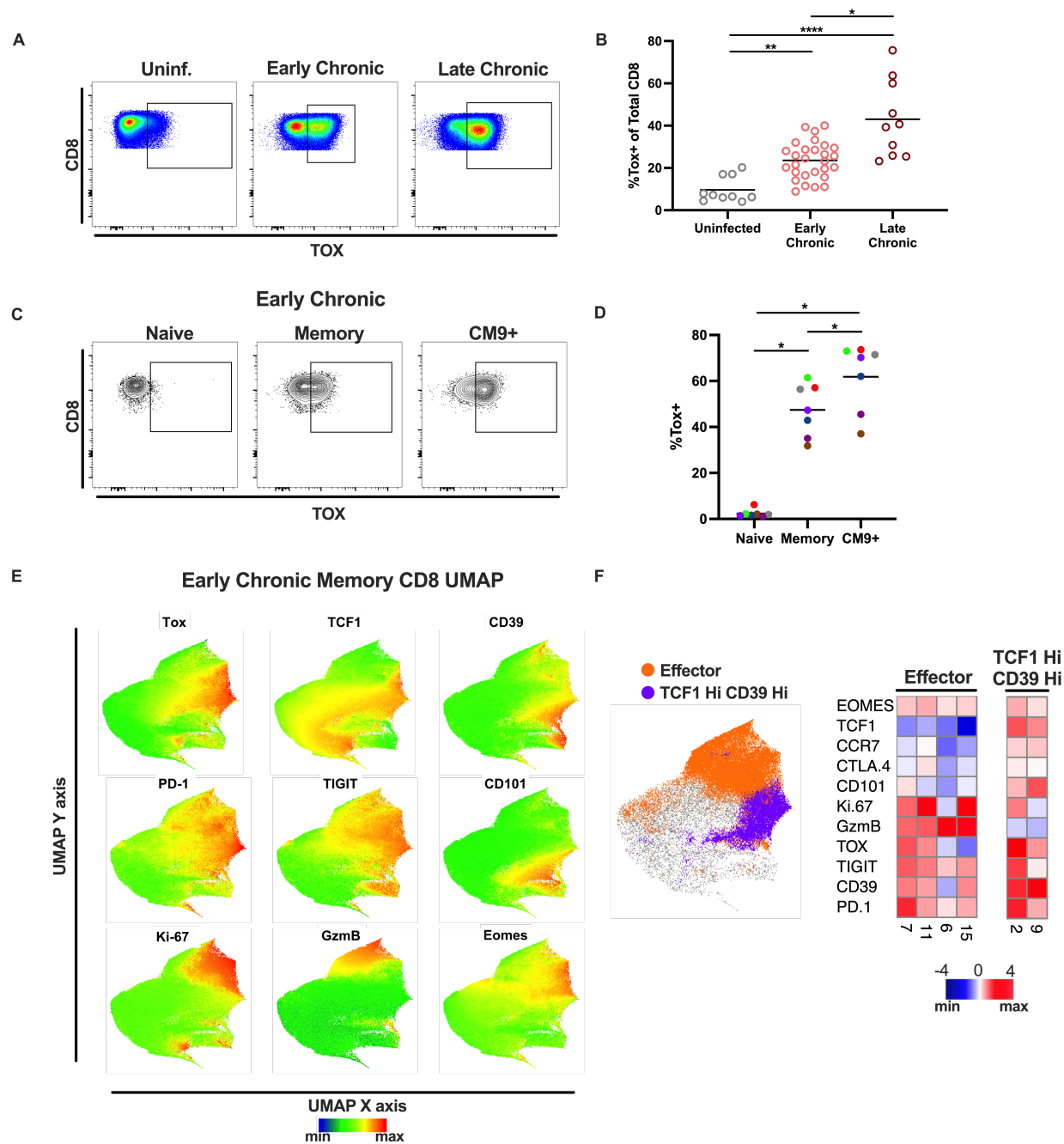


Figure 4.1. TOX expression and CD8 phenotype during SIV infection. A) Representative staining of TOX in LN total CD8 T cells in animals at various infection stages. B) TOX expression in LN total CD8 T cells in uninfected RMs (n=10), during early chronic infection (n=28) (D42 p.i.) and late chronic infection (n=10) (>6 months p.i.). C) Representative staining

of TOX in Naïve, Memory and SIV-specific (Gag-specific) CD8 T cells. D) TOX expression within LN CD8 T cell subsets of A*01+ RMs (n=7) at early chronic infection. E) UMAP plot of flow cytometry data showing expression patterns of markers of interest. F) Heatmap of expression measured of markers of interest within a subset of clusters identified through Phenograph analysis of flow cytometry data that represent traditional effector cells and TCF1 Hi CD39 Hi cell clusters. P values determined using Kruskal-Wallis one way-ANOVA with Dunn's multiple comparisons. $*P < 0.05$, $**P < 0.01$, $***P < 0.001$, $****P < 0.0001$.

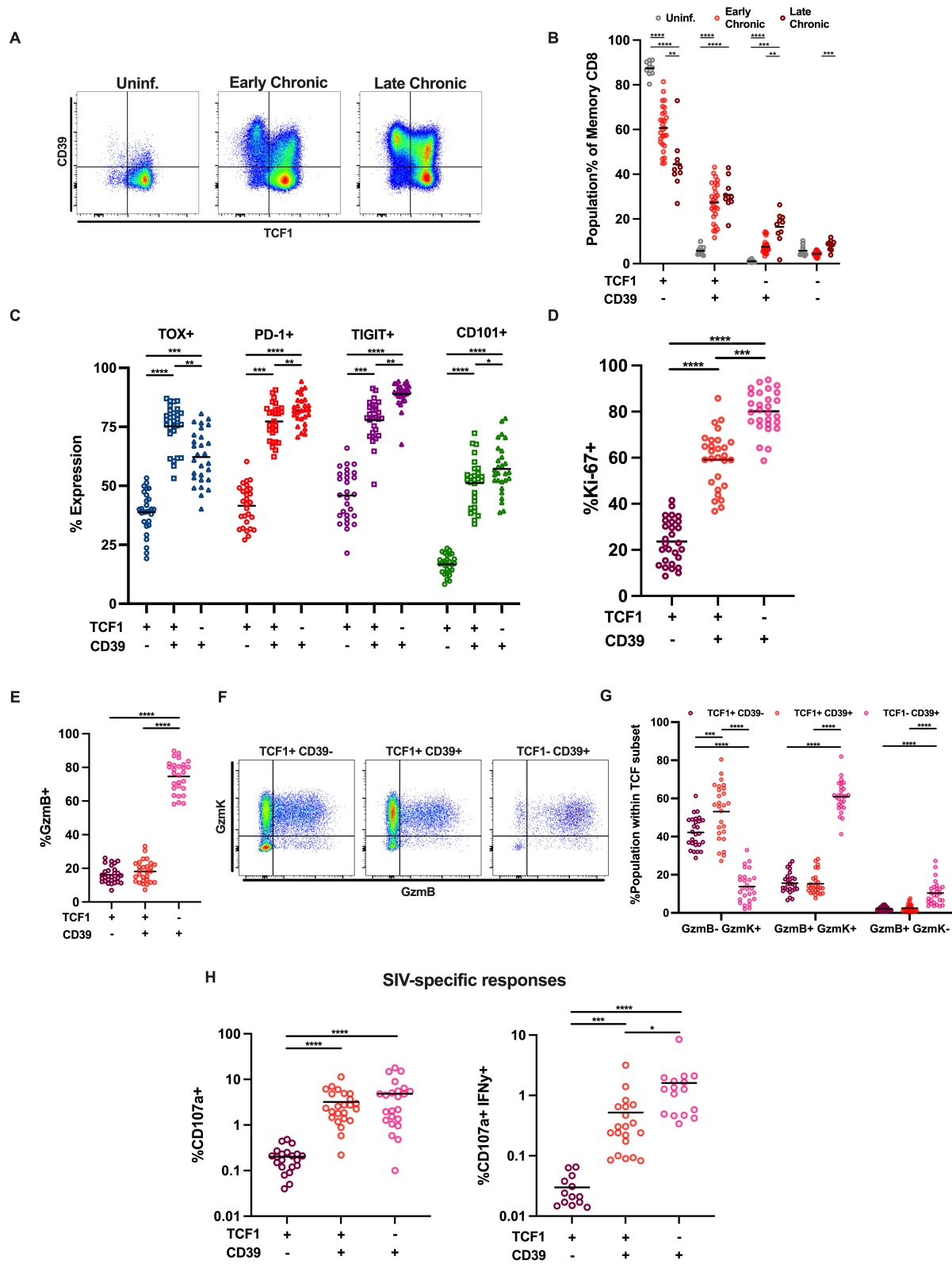


Figure 4.2. TCF1+ CD39+ CD8 T cells expand after SIV infection and are a unique phenotypic population. A-B) Representative staining of TCF1 and CD39 and (B) proportion of LN memory CD8 T cells falling within TCF1/CD39 subsets in uninfected RMs (n=10), during early chronic infection (n=28) (D42 p.i.) and late chronic infection (n=10) (>6 months p.i.). C-E) Expression of (C) traditional inhibitory markers, (D) Ki-67 and (E) Granzyme B within TCF1/CD39 subsets of LN memory CD8 during early chronic infection (n=28). F-G) Representative staining of granzyme B and granzyme K and (G) proportion of cells within each TCF1/CD39 subset expressing one or both of GzmB and GzmK within LN memory CD8 T cells during early chronic infection (n=28). H) Proportion of cells within each TCF1/CD39 subset expressing CD107a and CD107a in combination with production of IFN γ . Only animals exhibiting significant responses (>0.01% of cells responding) are shown. P values determined using two-way ANOVA with Tukey's multiple comparisons test (B) and Kruskal-Wallis one way-ANOVA with Dunn's multiple comparisons (C-H). * $P < 0.05$, ** $P < 0.01$, *** $P < 0.001$, **** $P < 0.0001$.

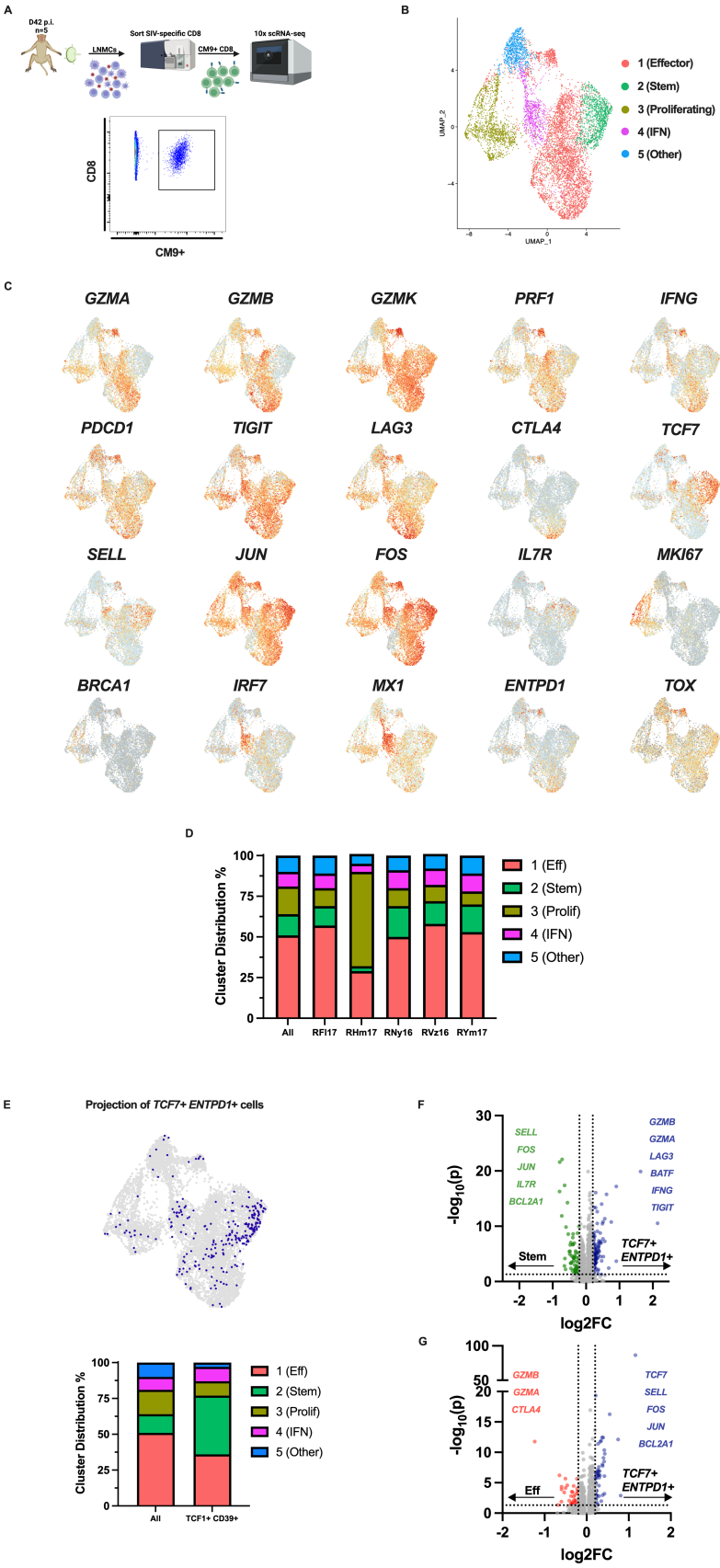


Figure 4.3. scRNA-seq of SIV-specific LN CD8 reveals distinct transcriptional clusters. A)

Study schematic depicting sorting of SIV-specific LN CD8 T cells and downstream scRNA-seq.

Representative stain of SIV-specific cells is shown. B) UMAP analyses of SIV-specific LN CD8

T cells from 5 RMs at early chronic infection were combined to identify 5 distinct clusters. C)

UMAP plots showing expression of genes of interest. D) Distribution of SIV-specific CD8 T

cells across the identified clusters within the total cell population and for each animal. E)

Projection of cells expressing both *TCF7* and *ENTPD1* onto UMAP plot and distribution of these

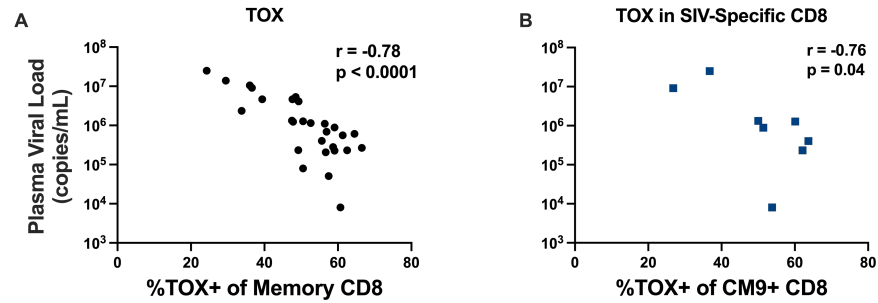
cells across the 5 clusters. F-G) Violin plot displaying differentially expressed genes between f)

Stem (3) cluster and *TCF7*⁺ *ENTPD1*⁺ cells and g) Effector (1) cluster and *TCF7*⁺ *ENTPD1*⁺

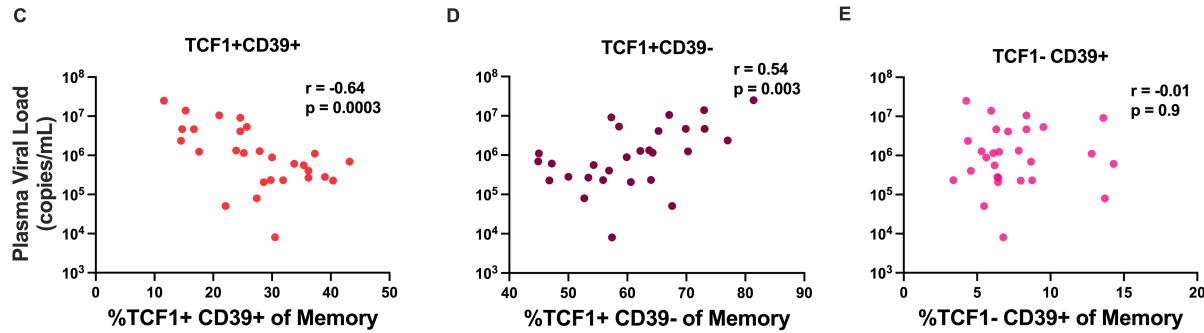
cells. Selected genes with significantly different expression are listed. * $P < 0.05$, ** $P < 0.01$,

*** $P < 0.001$, **** $P < 0.0001$.

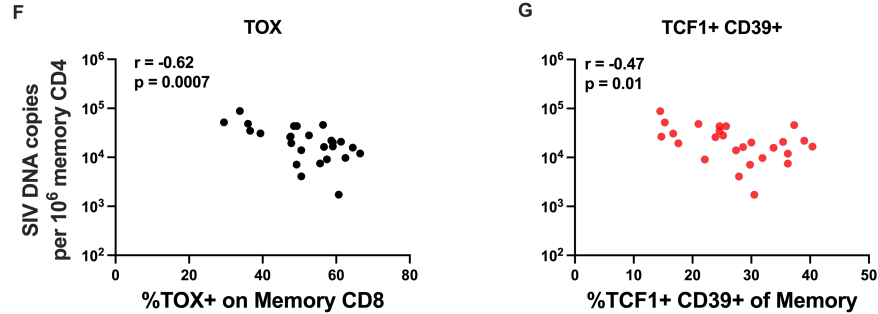
Viral Load vs TOX



Viral Load vs TCF subsets



SIV DNA



CD4 preservation

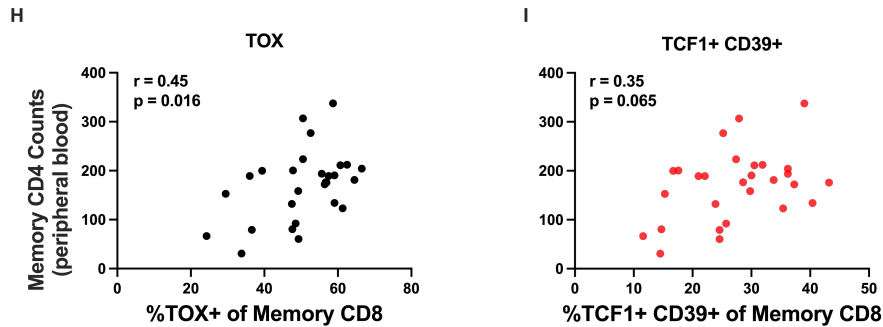


Figure 4.4. Association between TOX⁺ and TCF1⁺ CD39⁺ LN CD8 frequencies and viral burden. A) Association of frequency of TOX⁺ cells within LN memory CD8 and plasma viral load (n=28). B) Association between expression of TOX by SIV-specific LN CD8 and plasma viral load (n=8). C-E) Association of frequency of TCF1/CD39 subsets within LN memory CD8 and plasma viral load (n=28). F-G) Association of frequency of f) TOX⁺ or g) TCF1⁺ CD39⁺ cells within LN memory CD8 and total SIV DNA within LN memory CD4 (n=26). H-I) Association of frequency of f) TOX⁺ or g) TCF1⁺ CD39⁺ cells LN memory CD8 and memory CD4 T cell counts in peripheral blood (n=28). All measurements are from early chronic infection (D42 p.i.). All correlations determined using Spearman analysis.

Figure 4.5. TCF1+ CD39+ CD8 T cells penetrate follicular environment. A-B)

Representative staining and quantification (B) of CXCR5 expression within TCF1/CD39 memory CD8 T cell subsets in LN during early chronic infection (n=27). C-E) Association of CXCR5 expression within TCF1/CD39 subsets and plasma viral load during early chronic infection (n=27). F-G) Association of CXCR5 expression within TCF1/CD39 subsets and SIV DNA levels in LN memory CD4 (n=25). I) Representative image of immunofluorescence analysis identifying TCF1+ and TOX+ CD8 T cells in LN. Arrows designate examples of TCF1+ TOX+ CD8+ cells. J) Quantification of proportion of CD8 T cells expressing TOX and TCF1 within B cell follicles and T cell zone during early chronic infection (n=8). Differences in CXCR5 expression were determined using Kruskal-Wallis one way-ANOVA with Dunn's multiple comparisons. Correlations were determined using Spearman analysis. Differences in BCF and TCZ CD8 populations were determined by 2-way ANOVA with Sidaks multiple comparison test. * $P < 0.05$, ** $P < 0.01$, *** $P < 0.001$, **** $P < 0.0001$.

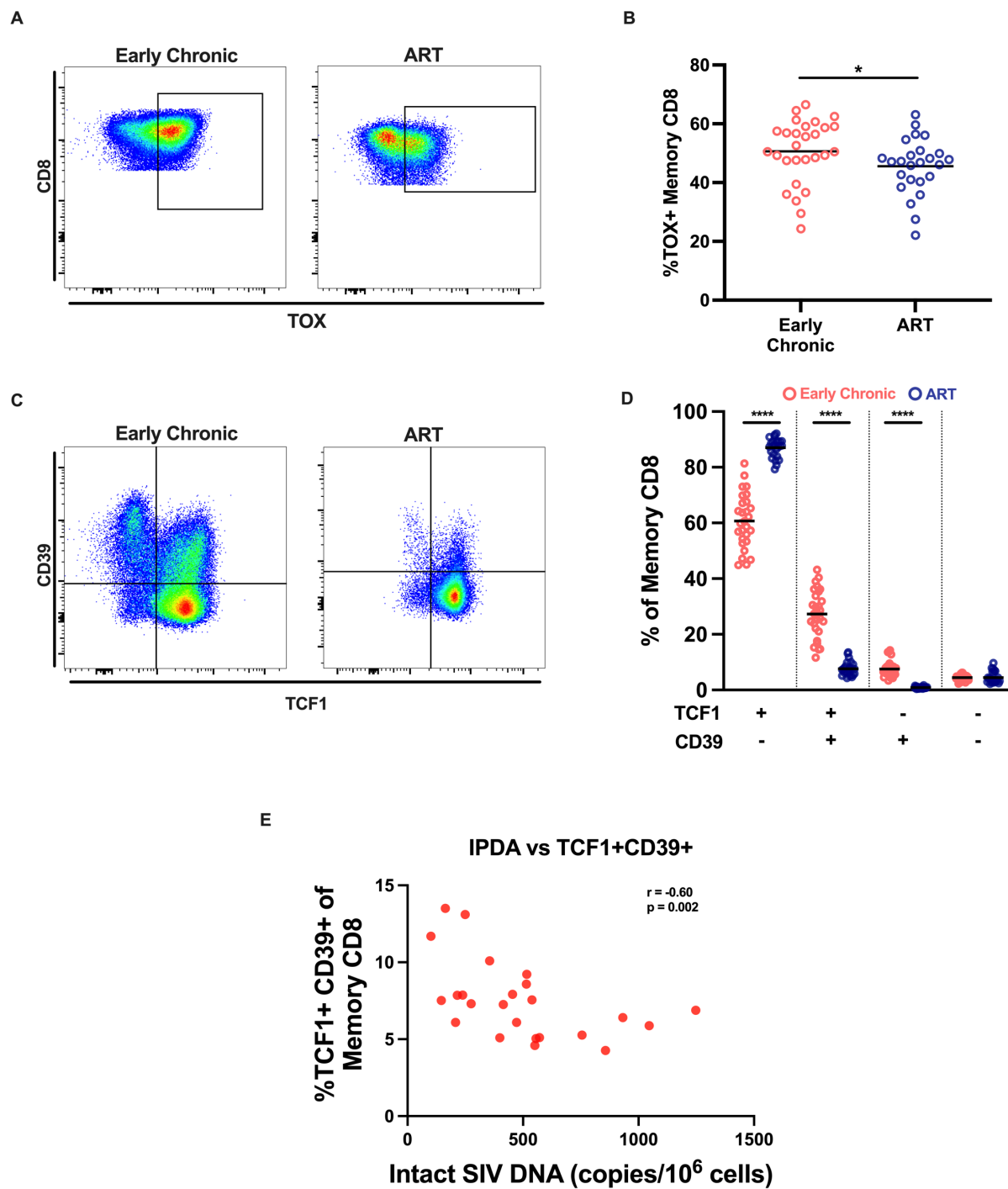


Figure 4.6. TCF1+ CD39+ CD8 T cells contract during long-term ART but remain associated with viral burden. A-B) Representative staining and quantification (B) of TOX expression within LN memory CD8 in 25 longitudinally matched RMs during early chronic

infection and long-term ART (>1 yr). C-D) Representative staining and quantification (D) of TCF1/CD39 subsets within LN memory CD8 in 25 longitudinally matched RMs during early chronic infection long-term ART. C) Association between frequency of TCF1+ CD39+ LN CD8 T cells during ART and levels of intact SIV DNA in total LN cells during ART (Spearman correlation, n=24). Differences between early chronic and ART marker expression were determined using Wilcoxon matched-pairs signed rank test. * $P < 0.05$, ** $P < 0.01$, *** $P < 0.001$, **** $P < 0.0001$.

Animal Code	Virus	Infection Dose	Infection Status	Days Post-Infection	Plasma Viral Load (copies/mL)
495	-	-	Uninfected	-	-
595	-	-	Uninfected	-	-
DBM6	-	-	Uninfected	-	-
769	-	-	Uninfected	-	-
485	-	-	Uninfected	-	-
DBV1	-	-	Uninfected	-	-
DGGB	-	-	Uninfected	-	-
DFNJ	-	-	Uninfected	-	-
DFZC	-	-	Uninfected	-	-
DGMH	-	-	Uninfected	-	-
34897	SIVmac239	300 TCID50	Early Chronic/ART	42	1.15E+06
RRh17	SIVmac239	300 TCID50	Early Chronic/ART	42	7.97E+04
RFn17	SIVmac239	300 TCID50	Early Chronic/ART	42	4.11E+06
RVm17	SIVmac239	300 TCID50	Early Chronic/ART	42	2.68E+05
RBe17	SIVmac239	300 TCID50	Early Chronic/ART	42	6.92E+05
RMI17	SIVmac239	300 TCID50	Early Chronic/ART	42	4.67E+06
RIb17	SIVmac239	300 TCID50	Early Chronic/ART	42	1.39E+07
34918	SIVmac239	300 TCID50	Early Chronic/ART	42	1.25E+06
RBf17	SIVmac239	300 TCID50	Early Chronic/ART	42	5.32E+06
RBv17	SIVmac239	300 TCID50	Early Chronic/ART	42	2.28E+05
REu17	SIVmac239	300 TCID50	Early Chronic/ART	42	2.32E+05
RKq17	SIVmac239	300 TCID50	Early Chronic/ART	42	1.11E+06
RVc17	SIVmac239	300 TCID50	Early Chronic/ART	42	6.11E+05
RZg17	SIVmac239	300 TCID50	Early Chronic/ART	42	2.06E+05
RFI17	SIVmac239	300 TCID50	Early Chronic/ART	42	8.87E+05
RYk17	SIVmac239	300 TCID50	Early Chronic/ART	42	8.02E+03
RVz16	SIVmac239	300 TCID50	Early Chronic/ART	42	4.04E+05
RYm17	SIVmac239	300 TCID50	Early Chronic/ART	42	1.28E+06
RHm17	SIVmac239	300 TCID50	Early Chronic/ART	42	9.10E+06
RNy16	SIVmac239	300 TCID50	Early Chronic/ART	42	2.33E+05
RTd17	SIVmac239	300 TCID50	Early Chronic/ART	42	1.33E+06
34920	SIVmac239	300 TCID50	Early Chronic/ART	42	4.68E+06
34930	SIVmac239	300 TCID50	Early Chronic/ART	42	2.36E+06
REq17	SIVmac239	300 TCID50	Early Chronic/ART	42	2.79E+05
RGr17	SIVmac239	300 TCID50	Early Chronic/ART	42	1.05E+07
RVi17	SIVmac239	300 TCID50	Early Chronic/ART	42	2.50E+07
RWs17	SIVmac239	300 TCID50	Early Chronic/ART	42	5.60E+05
RZp17	SIVmac239	300 TCID50	Early Chronic/ART	42	5.10E+04
DA8K	SIVmac239	3000 TCID50	Late Chronic	370	2.30E+04
CF5T	SIVmac239	3000 TCID50	Late Chronic	651	8.00E+05
A3P013	SIVmac239	3000 TCID50	Late Chronic	264	1.00E+07
DCVF	SIVmac239	3000 TCID50	Late Chronic	274	1.30E+06
ZG24	SIVmac239	3000 TCID50	Late Chronic	957	5.50E+05
DCKj	SIVmac239	3000 TCID50	Late Chronic	239	9.50E+05
DB17	SIVmac239	3000 TCID50	Late Chronic	683	9.20E+04
DE2W	SIVmac239	3000 TCID50	Late Chronic	205	2.70E+05
ZA52	SIVmac239	3000 TCID50	Late Chronic	929	1.30E+06
DE1a	SIVmac239	3000 TCID50	Late Chronic	471	4.90E+05

Table 4.1. Rhesus macaque characteristics.

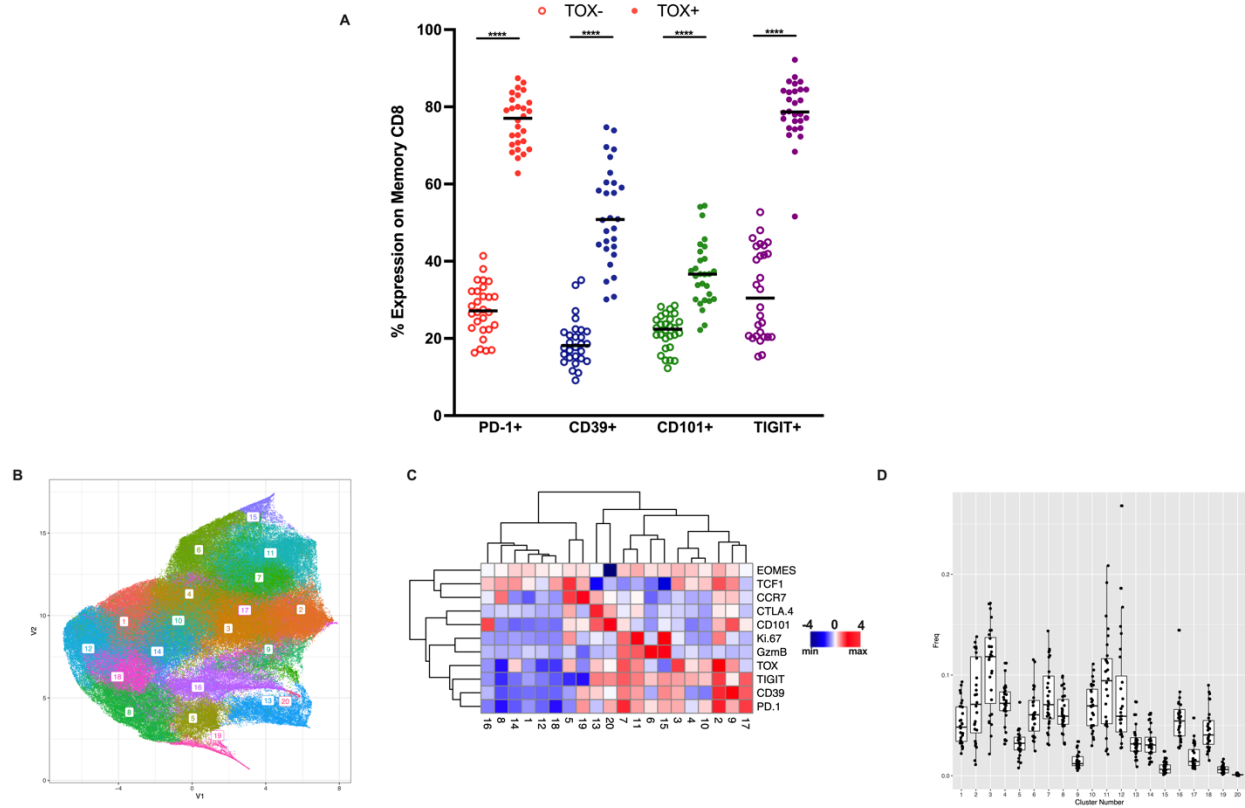


Figure 4.S1. Dynamics of TOX-expressing LN CD8 T cells during early chronic SIV infection. A) Expression of inhibitory receptors on Tox+ and Tox- LN memory CD8 T cells during early chronic infection. Significance determined by Wilcoxon matched-pairs signed rank test. B) UMAP visualization of Phenograph clusters. C) Heatmap of expression of markers of interest across all Phenograph clusters. D) Proportion of total memory CD8 T cell population made up by individual Phenograph clusters across all 28 RMs. * $P < 0.05$, ** $P < 0.01$, *** $P < 0.001$, **** $P < 0.0001$.

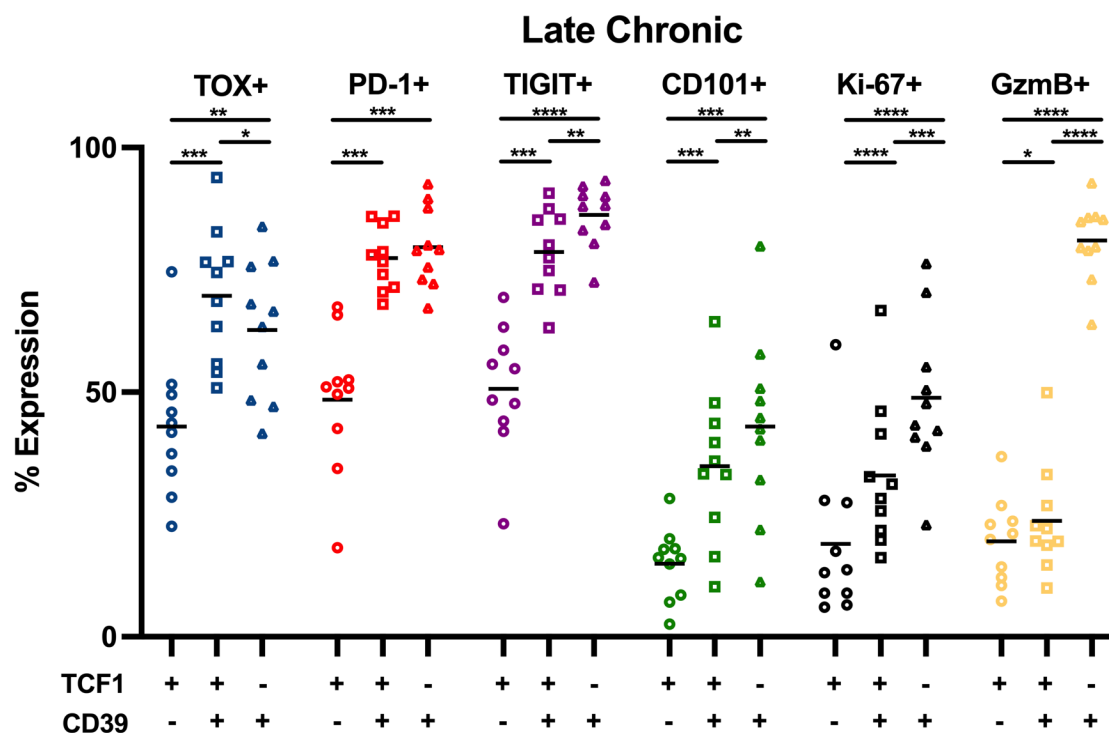
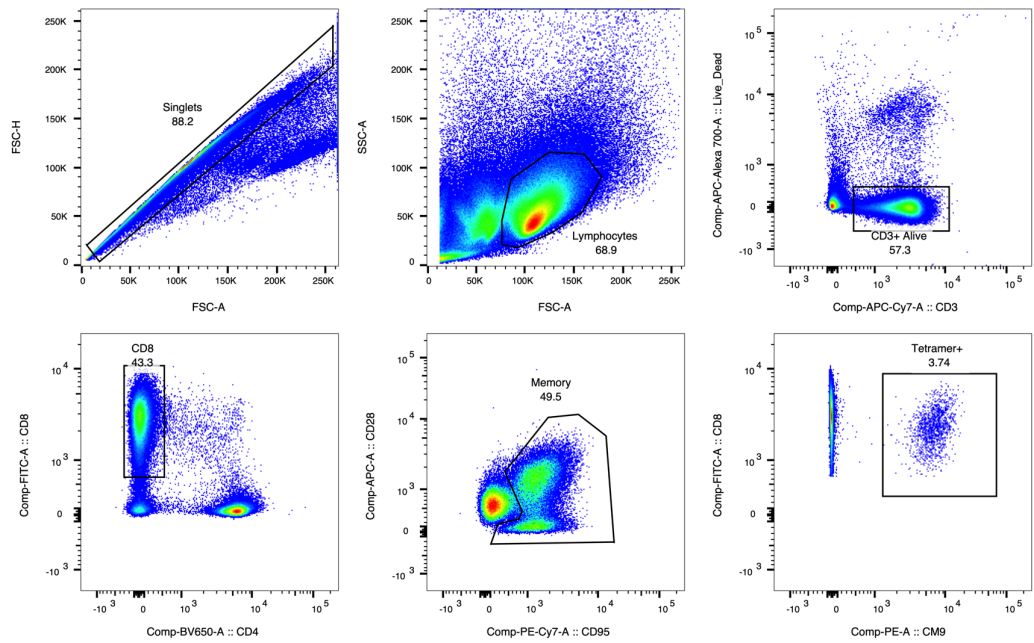


Figure 4.S2. Phenotype of TCF1/CD39 LN CD8 subsets during late chronic SIV infection.

Expression of markers of interest within TCF1/CD39 subsets of LN memory CD8 during late chronic infection (n=10). Differences within each marker determined by Kruskal-Wallis one way-ANOVA with Dunn's multiple comparisons. * $P < 0.05$, ** $P < 0.01$, *** $P < 0.001$, **** $P < 0.0001$.

A



B

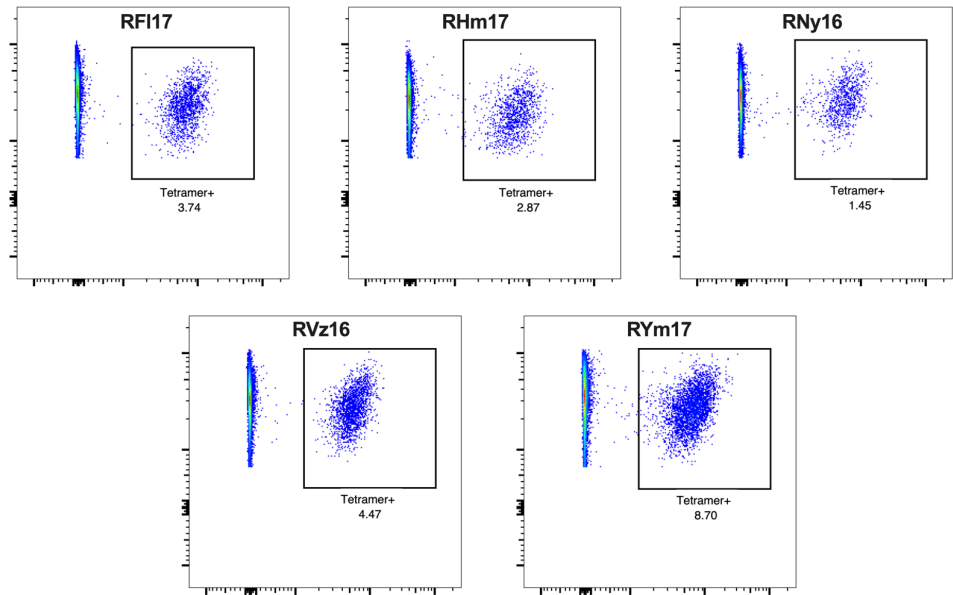


Figure 4.S3. Sorting of SIV-specific LN CD8 T cells. A) Sorting strategy for SIV-specific (CM9+) CD8 T cells for downstream scRNA-seq. B) Plots of sorted SIV-specific CD8 T cells for all 5 RMs.

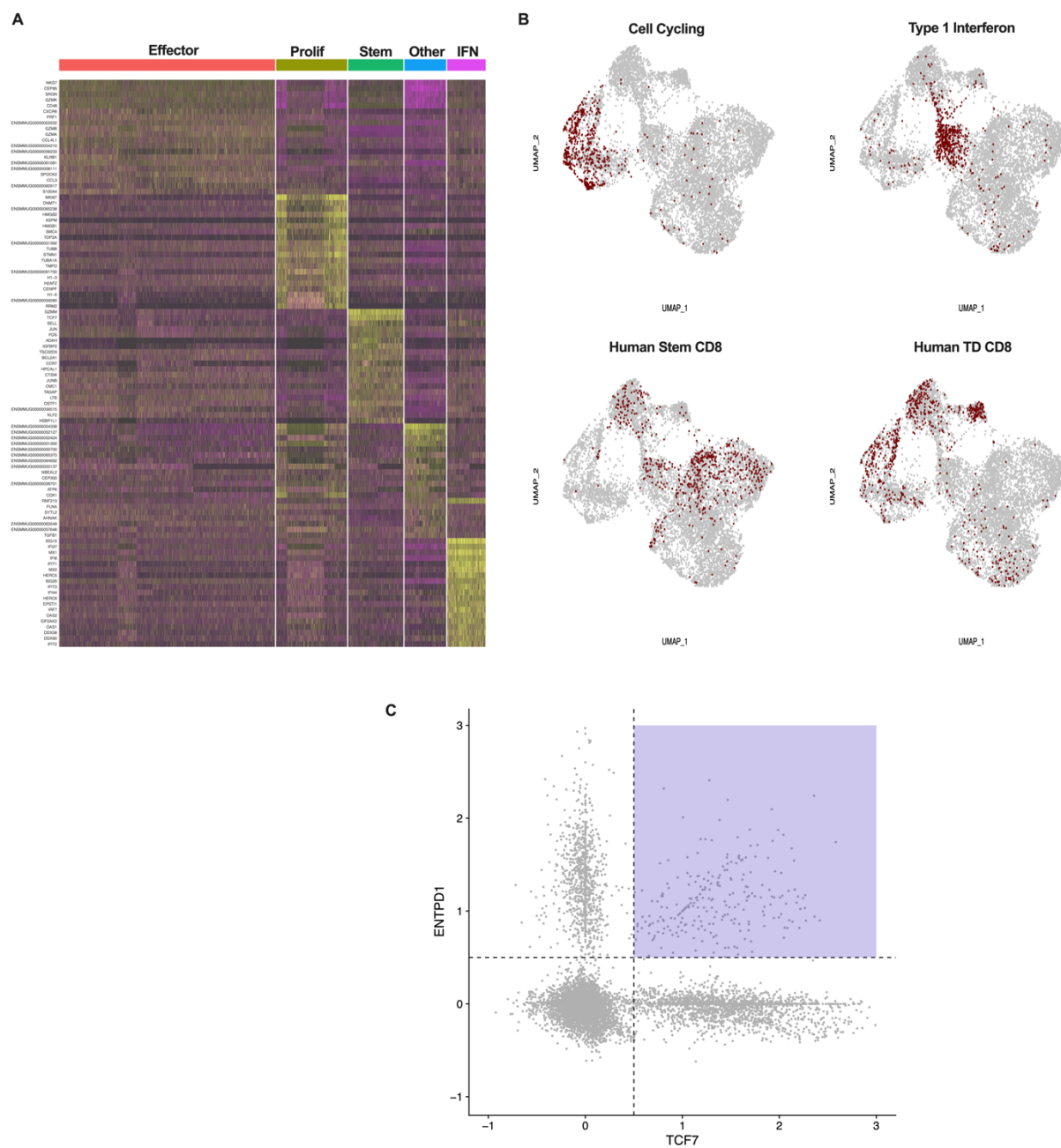


Figure 4.S4. scRNA-seq of SIV-specific LN CD8 T cells. A) Heatmap of top 20 differentially expressed genes across the 5 identified clusters. B) UMAP projection of cells expressing defined human CD8 T cell signatures. C) Expression thresholds chosen for identified *TCF7*⁺ *ENTPD1*⁺ cells.

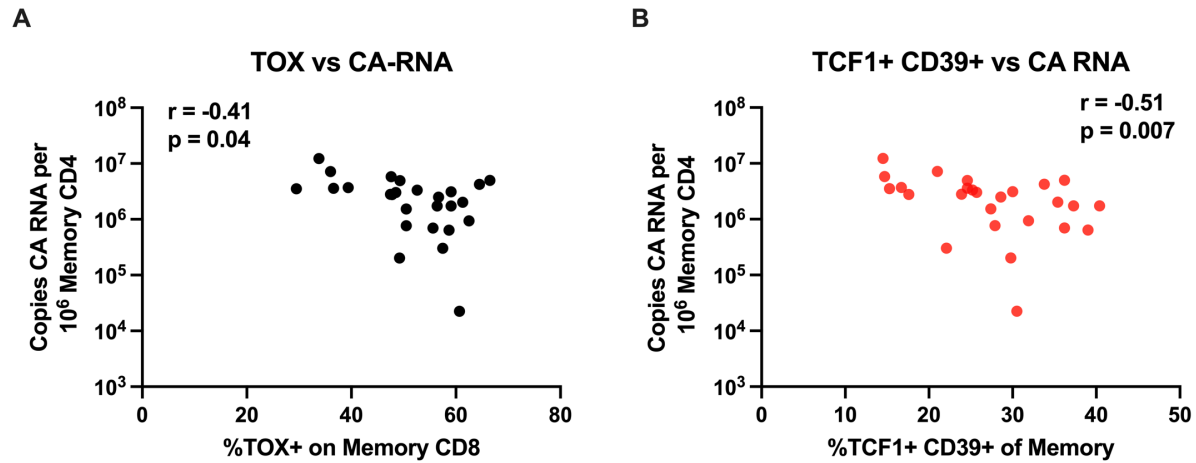


Figure 4.S5. Association of LN CD8 T cells with cell-associated SIV RNA. A-B) Association of frequency of (a) Tox+ and (b) TCF1+ CD39+ cells with levels of cell-associated SIV RNA in LN memory CD4 T cells during early chronic infection (Spearman correlation, n=26).

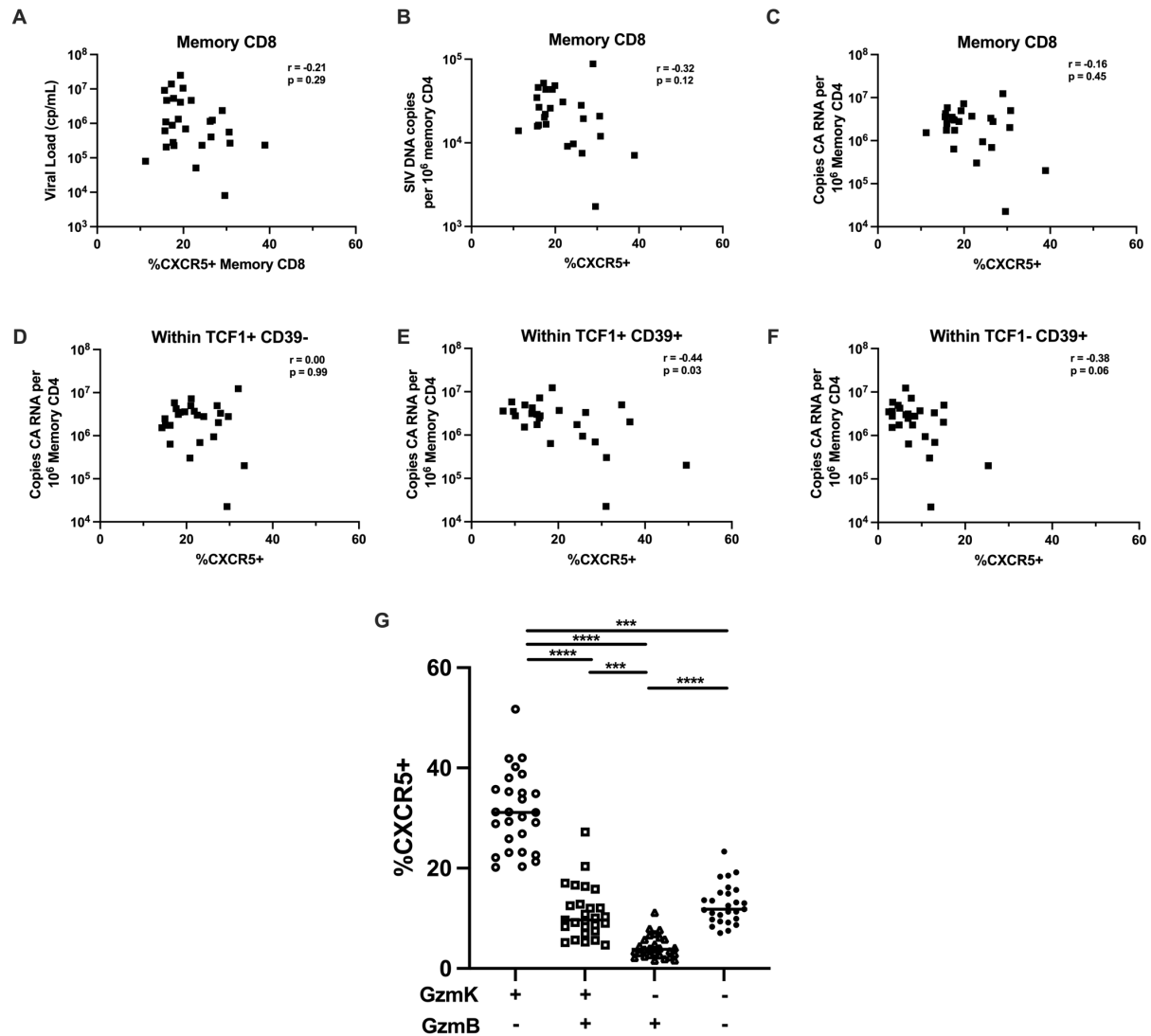
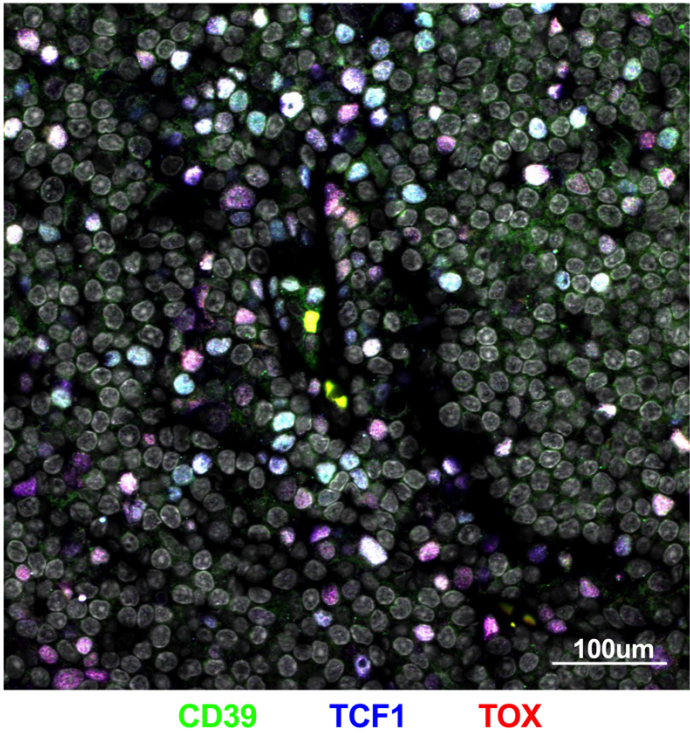


Figure 4.S6. CXCR5 within LN CD8 T cells during early chronic SIV infection. A-C) Association of CXCR5 expression within memory CD8 with measurements of viral burden (A $n=27$, B-C $n=25$). D-F) Association of CXCR5 expression within TCF1/CD39 subsets of memory CD8 with cell-associated SIV RNA levels in sorted LN memory CD4 T cells ($n=25$). G) Expression of CXCR5 across granzyme K/granzyme B-expressing memory CD8 T cells ($n=27$). Correlations represent

Spearman analysis. Differences across granzyme subsets were determined using Friedman test with Dunn's multiple comparison test. $*P < 0.05$, $**P < 0.01$, $***P < 0.001$, $****P < 0.0001$.

A



B

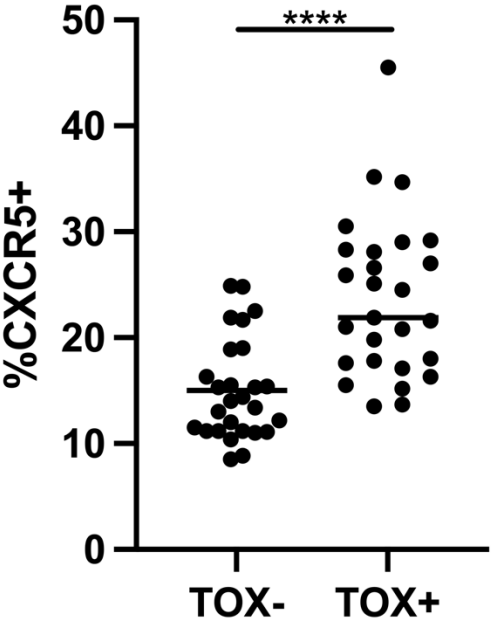


Figure 4.S7. Imaging and dynamics of LN CD8 T cells. A) Representative image of immunofluorescence staining of CD39 (green) TCF1 (blue) and TOX (red) showing the difficulty of imaging with high CD39 background signal on non-CD8 T cells. B) Expression of CXCR5 on TOX⁻ and TOX⁺ memory CD8 T cells during early chronic infection. Wilcoxon matched-pairs ranked test; * $P < 0.05$, ** $P < 0.01$, *** $P < 0.001$, **** $P < 0.0001$.

Chapter Five: Discussion

Since its discovery in 1984, HIV has posed one of the largest public health problems worldwide. HIV is immensely difficult to eradicate given persistence as a chronic infection in individuals, taking advantage of immense mutational capacity that allows for evasion of innate, humoral and cellular immune responses, as well as a distinct ability to persist latently in infected cells. The advent of ART has greatly reduced HIV transmission, morbidity and mortality, but is unable to eradicate the latent viral reservoir and lifelong therapy is required ²²⁰. Unfortunately, to date, there have been no successful vaccines to prevent HIV spread and no therapeutics effective in achieving HIV cure. Hence, there is much work to be done in our understanding of how HIV targets the immune system and how to best counteract this virus. In this work, we utilized the SIV model of HIV infection in rhesus macaques to interrogate specific mechanisms by which HIV induces pathogenesis and persists as the viral reservoir, as well as virology immunologic mechanisms that contribute to the ability to control viremia. These findings further our understanding of specific pathways and cell types to be targeted in our attempts to curb HIV pathogenesis and induce complete viral remission.

Natural control of HIV occurs in a rare population of HIV-infected individuals, defined by two distinct subpopulations: elite controllers (ECs), representing less than 1% of all infected individuals who possess unique MHC haplotypes and CD8 T cell functionality resulting in control of infection in the absence of ART, and post-treatment controllers (PTCs), representing 5-10% of the infected population who initiate ART to stop disease progression and suppress viral loads but are able to interrupt ART without resulting viral rebound and CD4 T cell loss ²⁶⁶. Studies of the viral and immune dynamics in these individuals has yielded critical insights into the potential of CD8 T cells and limited reservoir size to lead to HIV remission. However, given limitations with human sampling, these analyses are frequently restricted to peripheral blood.

The HIV reservoir is largely present in lymphoid tissue and studies have demonstrated unique HIV-specific T cell populations in these tissues, highlighting the importance of expanding our understanding of peripheral viral and immune dynamics to the tissues⁸²⁻⁸⁴. We identified 7 SIV-infected rhesus macaques (RMs) that mirrored the definitions of HIV-infected PTCs and took advantage of the macaque model to explore the virologic and immunologic dynamics in blood, lymph node and mucosal tissues and determine distinguishing factors between PTCs and non-controllers (NCs).

Following ART interruption, RM PTCs maintained viral loads significantly lower than NCs and experienced decreased pathogenesis, with higher CD4 T cell counts and lower T cell activation. Additionally, we found lower levels of SIV DNA in PTCs compared to NCs at all timepoints post-infection, including prior to ART initiation and at ART interruption. Importantly, levels of SIV DNA were lower in both peripheral blood and lymphoid tissue and across a variety of CD4 T cell subsets. This data is compatible with data in clinical studies of HIV-infected PTCs, where it has been shown that HIV DNA levels are lower in PTCs than NCs^{47, 262, 300, 314, 315}. In addition to lower reservoir sizes, we found limited immune activation and immune damage in these animals. In particular, while both NCs and PTCs experienced significant mucosal CD4 T cell depletion prior to ART initiation, PTCs selectively maintained higher levels of Th17 CD4 T cells, a phenotype similar to that observed in nonpathogenic SIV infection of sooty mangabeys³²¹. Collectively, combined with our understanding of HIV-infected PTCs, these data reaffirm the importance of limiting immune activation and damage and restricting the size of the reservoir early in HIV/SIV infection. Importantly, these characteristics have been shown to be achievable via early ART initiation in SIV and HIV-infected individuals treated during the acute stages of infection^{103, 105, 106, 322}. Individuals with smaller reservoirs and lower

immune activation may be most likely to achieve viral control, and may be best suited for early stages of trials of new therapeutic approaches. These data also reaffirm the desire for therapeutic options capable of reducing the reservoir size prior to ART interruption for the greatest chance at remission in the absence of ART.

As demonstrated in controllers of HIV infection, it is critical to understand and limit the pathogenesis and persistence of the virus. In order to advance our knowledge of CD4 T cell populations that contribute to these mechanisms, we focused on the dynamics of CD4 T cells expressing CD101 in HIV/SIV infection. CD101 is a cell surface glycoprotein that is upregulated upon cell activation, acts to inhibit T cell activation and proliferation, has been shown to play a critical role in CD4 Treg function and is highly expressed in the gut mucosa where it acts in an anti-inflammatory manner³³⁹⁻³⁴⁶. We found that CD101+ CD4 T cells are preferentially depleted following HIV/SIV infection, with a severe depletion within the Treg compartment and in the gut mucosa, and that preferential depletion is associated with increased gut viral burden, plasma viral load and inflammatory cytokine levels. In concordance with their increased depletion in gut mucosa and increased expression on $\alpha 4\beta 7$ cells, we additionally found that depletion of mucosal CD101+ CD4 T cells was associated with increased levels of zonulin during early chronic infection, suggestive of destruction of intestinal epithelial integrity^{358, 359}.

While these CD101+ CD4 T cells are restored during long-term ART, they demonstrate significant potential to contribute to the persistence of the viral reservoir. While they were not directly enriched for HIV compared to CD101- cells, CD101+ CD4 T cells exhibited high levels of expression of PD-1, CTLA-4 and TIGIT and demonstrated significant immunosuppressive potential with enriched production of TGF β . These features are suggestive that CD101+ CD4 T cells persist in an immunosuppressive environment, where reactivation of latency and CD8 T cell

killing are less likely to occur. Additionally, CD101⁺ Tregs express high levels of *LGALS3*, suggestive of a potential mechanism to restrict CD8-mediated clearance of these cells ³⁵².

Overall, these investigations revealed an important role of CD101⁺ CD4 T cells in both HIV/SIV pathogenesis and persistence, and additional studies assessing the modulation of CD101 to impact viral pathogenesis and latent reservoir dynamics could reveal additional strategies for HIV therapeutics.

While the PTC population suggests promise for HIV cure in the area of reduced inflammation and viral persistence, ECs demonstrate significant potential for CD8 T cells to mediate HIV remission. As previously mentioned, studies of ECs have also elucidated that HIV-specific CD8 T cells in lymphoid tissue are remarkably distinct from those in the periphery and therefore additional understanding of lymphoid tissue CD8 T cells could reveal distinct mechanisms by which HIV can be controlled in tissues that serve as viral hotbeds ^{82, 84}.

To that end, we examined lymphoid tissue CD8 T cell dynamics after SIV infection with a particular focus on TOX and TCF1-expressing CD8 T cells, two transcription factors that are vital in CD8 differentiation and function during chronic infection and exhaustion. Similar to reports in other chronic diseases, we find that lymphoid CD8 T cells upregulated TOX after SIV infection and these TOX⁺ cells co-express numerous inhibitory receptors. We further identified a novel subset of CD8 T cells defined by co-expression of TCF1 and CD39, which have been previously shown to be exclusively expressed in stem-like and terminally differentiated, exhausted cells, respectively. These unique TCF1⁺ CD39⁺ express high levels of TOX and other inhibitory receptors, but low levels of traditional cytotoxic molecules despite demonstrated ability to express effector function in response to antigen stimulation. Transcriptional analysis reveals these cells to be an intermediate population with properties of terminally differentiated

effector cells while maintaining stem-like properties. Importantly, the levels TOX⁺ and TCF1⁺ CD39⁺ CD8 T cells in lymph nodes was strongly associated with better viral control, with reduced plasma viremia and viral DNA/RNA in tissues in animals with more of these cells. We demonstrate that these cells express CXCR5 and are found at significantly higher frequencies in B cell follicles than other CD8 populations, suggestive of an ability to penetrate sites of high viral replication and persistence that could lead to increased potential for viremic control. The stem-like nature of TCF1⁺ CD39⁺ cells likely favors the persistence of these cells in an important anatomical location compared to a traditional terminally differentiated effector population. These data are congruent with studies showing unique effector profiles of HIV-specific CD8 T cells in both lymphoid and mucosal tissue sites, particularly with lower cytotoxicity compared to peripheral CD8 T cells ^{82-84, 404, 406, 407}. Collectively, it is clear that persistence of functional HIV/SIV-specific CD8 T cell responses within lymphoid tissue are an important element of viral control, and that follicular penetrance in particular may be a critical feature.

Cumulatively, these data highlight both the hope and need for an HIV cure. In the majority SIV-infected animals and HIV-infected individuals, the failure to mount a sufficient immune response leads to immense pathogenesis and disease. However, ongoing work continues to reveal important mechanisms and correlates of viral control when it does occur. In our studies, we highlight some of the most significant dynamics of HIV persistence involving T cell reservoirs and responses, including the impact of the size, anatomical and cellular location of the viral reservoir in CD4 T cells, as well as the ability of CD8 T cells to control infection of these cells. We demonstrate the critical role of limiting reservoir establishment and viral pathogenesis in the development of post-treatment control, while also highlighting potential reservoirs of viral

persistence such as CD101+ CD4 T cells. Additionally, we highlight the importance of lymphoid CD8 T cell responses and the potential for highly functional CD8 T cells to contribute to HIV remission.

Given the complexity of the HIV reservoir and the virus's capacity for immune escape, any successful cure approach will likely require a combinatorial approach that reduces the size of the viral reservoir and promotes enhanced clearance of infected cells. Ultimately, any intervention should be safe, effective and scalable, as the worldwide population of HIV-infected individuals mostly reside in resource poor areas. Future studies also must focus on interventions that do not carry significant toxicities, as longer-acting ART regimens significantly alter the risk-reward balance of an immune-based intervention that may not provide 100% effectiveness. The incremental progress made over the past 40 years of HIV research should provide hope to those infected with HIV, and continued investment should be made in our understanding of the disease with the goal of a safe and scalable approach to induce HIV remission.

References

1. Centers for Disease C. Kaposi's sarcoma and Pneumocystis pneumonia among homosexual men--New York City and California. *MMWR Morb Mortal Wkly Rep*. 1981;30(25):305-8. PubMed PMID: 6789108.
2. Centers for Disease C. Possible transfusion-associated acquired immune deficiency syndrome (AIDS) - California. *MMWR Morb Mortal Wkly Rep*. 1982;31(48):652-4. PubMed PMID: 6819440.
3. Barre-Sinoussi F, Chermann JC, Rey F, Nugeyre MT, Chamaret S, Gruest J, Dauguet C, Axler-Blin C, Vezinet-Brun F, Rouzioux C, Rozenbaum W, Montagnier L. Isolation of a T-lymphotropic retrovirus from a patient at risk for acquired immune deficiency syndrome (AIDS). *Science*. 1983;220(4599):868-71. doi: 10.1126/science.6189183. PubMed PMID: 6189183.
4. Shaw GM, Hunter E. HIV transmission. *Cold Spring Harb Perspect Med*. 2012;2(11). Epub 20121101. doi: 10.1101/cshperspect.a006965. PubMed PMID: 23043157; PMCID: PMC3543106.
5. Robb ML, Eller LA, Kibuuka H, Rono K, Maganga L, Nitayaphan S, Kroon E, Sawe FK, Sinei S, Sriplienchan S, Jagodzinski LL, Malia J, Manak M, de Souza MS, Tovanabutra S, Sanders-Buell E, Rolland M, Dorsey-Spitz J, Eller MA, Milazzo M, Li Q, Lewandowski A, Wu H, Swann E, O'Connell RJ, Peel S, Dawson P, Kim JH, Michael NL, Team RVS. Prospective Study of Acute HIV-1 Infection in Adults in East Africa and Thailand. *N Engl J Med*. 2016;374(22):2120-30. Epub 20160518. doi: 10.1056/NEJMoa1508952. PubMed PMID: 27192360; PMCID: PMC5111628.
6. Henn A, Flateau C, Gallien S. Primary HIV Infection: Clinical Presentation, Testing, and Treatment. *Curr Infect Dis Rep*. 2017;19(10):37. Epub 20170907. doi: 10.1007/s11908-017-0588-3. PubMed PMID: 28884279.
7. Frankel AD, Young JA. HIV-1: fifteen proteins and an RNA. *Annu Rev Biochem*. 1998;67:1-25. doi: 10.1146/annurev.biochem.67.1.1. PubMed PMID: 9759480.
8. Dalgleish AG, Beverley PC, Clapham PR, Crawford DH, Greaves MF, Weiss RA. The CD4 (T4) antigen is an essential component of the receptor for the AIDS retrovirus. *Nature*. 1984;312(5996):763-7. doi: 10.1038/312763a0. PubMed PMID: 6096719.
9. Rizzuto CD, Wyatt R, Hernandez-Ramos N, Sun Y, Kwong PD, Hendrickson WA, Sodroski J. A conserved HIV gp120 glycoprotein structure involved in chemokine receptor binding. *Science*. 1998;280(5371):1949-53. doi: 10.1126/science.280.5371.1949. PubMed PMID: 9632396.
10. Kwong PD, Wyatt R, Robinson J, Sweet RW, Sodroski J, Hendrickson WA. Structure of an HIV gp120 envelope glycoprotein in complex with the CD4 receptor and a neutralizing human antibody. *Nature*. 1998;393(6686):648-59. doi: 10.1038/31405. PubMed PMID: 9641677; PMCID: PMC5629912.
11. Buzon V, Natrajan G, Schibli D, Campelo F, Kozlov MM, Weissenhorn W. Crystal structure of HIV-1 gp41 including both fusion peptide and membrane proximal external regions. *PLoS Pathog*. 2010;6(5):e1000880. Epub 20100506. doi: 10.1371/journal.ppat.1000880. PubMed PMID: 20463810; PMCID: PMC2865522.

12. Weissenhorn W, Dessen A, Harrison SC, Skehel JJ, Wiley DC. Atomic structure of the ectodomain from HIV-1 gp41. *Nature*. 1997;387(6631):426-30. doi: 10.1038/387426a0. PubMed PMID: 9163431.
13. Hu WS, Hughes SH. HIV-1 reverse transcription. *Cold Spring Harb Perspect Med*. 2012;2(10). Epub 20121001. doi: 10.1101/cshperspect.a006882. PubMed PMID: 23028129; PMCID: PMC3475395.
14. Miller CJ, Li Q, Abel K, Kim EY, Ma ZM, Wietgreffe S, La Franco-Scheuch L, Compton L, Duan L, Shore MD, Zupancic M, Busch M, Carlis J, Wolinsky S, Haase AT. Propagation and dissemination of infection after vaginal transmission of simian immunodeficiency virus. *J Virol*. 2005;79(14):9217-27. doi: 10.1128/JVI.79.14.9217-9227.2005. PubMed PMID: 15994816; PMCID: PMC1168785.
15. Zhang Z, Schuler T, Zupancic M, Wietgreffe S, Staskus KA, Reimann KA, Reinhart TA, Rogan M, Cavert W, Miller CJ, Veazey RS, Notermans D, Little S, Danner SA, Richman DD, Havlir D, Wong J, Jordan HL, Schacker TW, Racz P, Tenner-Racz K, Letvin NL, Wolinsky S, Haase AT. Sexual transmission and propagation of SIV and HIV in resting and activated CD4+ T cells. *Science*. 1999;286(5443):1353-7. doi: 10.1126/science.286.5443.1353. PubMed PMID: 10558989.
16. Spira AI, Marx PA, Patterson BK, Mahoney J, Koup RA, Wolinsky SM, Ho DD. Cellular targets of infection and route of viral dissemination after an intravaginal inoculation of simian immunodeficiency virus into rhesus macaques. *J Exp Med*. 1996;183(1):215-25. doi: 10.1084/jem.183.1.215. PubMed PMID: 8551225; PMCID: PMC2192425.
17. Kelley CF, Barbour JD, Hecht FM. The relation between symptoms, viral load, and viral load set point in primary HIV infection. *J Acquir Immune Defic Syndr*. 2007;45(4):445-8. doi: 10.1097/QAI.0b013e318074ef6e. PubMed PMID: 17514014.
18. Fiebig EW, Wright DJ, Rawal BD, Garrett PE, Schumacher RT, Peddada L, Heldebrandt C, Smith R, Conrad A, Kleinman SH, Busch MP. Dynamics of HIV viremia and antibody seroconversion in plasma donors: implications for diagnosis and staging of primary HIV infection. *AIDS*. 2003;17(13):1871-9. doi: 10.1097/00002030-200309050-00005. PubMed PMID: 12960819.
19. Mattapallil JJ, Douek DC, Hill B, Nishimura Y, Martin M, Roederer M. Massive infection and loss of memory CD4+ T cells in multiple tissues during acute SIV infection. *Nature*. 2005;434(7037):1093-7. doi: 10.1038/nature03501. PubMed PMID: 15793563.
20. Brenchley JM, Schacker TW, Ruff LE, Price DA, Taylor JH, Beilman GJ, Nguyen PL, Khoruts A, Larson M, Haase AT, Douek DC. CD4+ T cell depletion during all stages of HIV disease occurs predominantly in the gastrointestinal tract. *J Exp Med*. 2004;200(6):749-59. Epub 20040913. doi: 10.1084/jem.20040874. PubMed PMID: 15365096; PMCID: PMC2211962.
21. Dong C, Janas AM, Wang JH, Olson WJ, Wu L. Characterization of human immunodeficiency virus type 1 replication in immature and mature dendritic cells reveals dissociable cis- and trans-infection. *J Virol*. 2007;81(20):11352-62. Epub 20070808. doi: 10.1128/JVI.01081-07. PubMed PMID: 17686876; PMCID: PMC2045571.
22. Bakri Y, Schiffer C, Zennou V, Charneau P, Kahn E, Benjouad A, Gluckman JC, Canque B. The maturation of dendritic cells results in postintegration inhibition of HIV-1 replication. *J Immunol*. 2001;166(6):3780-8. doi: 10.4049/jimmunol.166.6.3780. PubMed PMID: 11238620.

23. Meltzer MS, Gendelman HE. Mononuclear phagocytes as targets, tissue reservoirs, and immunoregulatory cells in human immunodeficiency virus disease. *Curr Top Microbiol Immunol.* 1992;181:239-63. doi: 10.1007/978-3-642-77377-8_9. PubMed PMID: 1424782.
24. Joseph SB, Swanstrom R, Kashuba AD, Cohen MS. Bottlenecks in HIV-1 transmission: insights from the study of founder viruses. *Nat Rev Microbiol.* 2015;13(7):414-25. Epub 20150608. doi: 10.1038/nrmicro3471. PubMed PMID: 26052661; PMCID: PMC4793885.
25. Derdeyn CA, Decker JM, Bibollet-Ruche F, Mokili JL, Muldoon M, Denham SA, Heil ML, Kasolo F, Musonda R, Hahn BH, Shaw GM, Korber BT, Allen S, Hunter E. Envelope-constrained neutralization-sensitive HIV-1 after heterosexual transmission. *Science.* 2004;303(5666):2019-22. doi: 10.1126/science.1093137. PubMed PMID: 15044802.
26. Liu R, Paxton WA, Choe S, Ceradini D, Martin SR, Horuk R, MacDonald ME, Stuhlmann H, Koup RA, Landau NR. Homozygous defect in HIV-1 coreceptor accounts for resistance of some multiply-exposed individuals to HIV-1 infection. *Cell.* 1996;86(3):367-77. doi: 10.1016/s0092-8674(00)80110-5. PubMed PMID: 8756719.
27. Goh WC, Markee J, Akridge RE, Meldorf M, Musey L, Karchmer T, Krone M, Collier A, Corey L, Emerman M, McElrath MJ. Protection against human immunodeficiency virus type 1 infection in persons with repeated exposure: evidence for T cell immunity in the absence of inherited CCR5 coreceptor defects. *J Infect Dis.* 1999;179(3):548-57. doi: 10.1086/314632. PubMed PMID: 9952360.
28. Veazey RS, DeMaria M, Chalifoux LV, Shvetz DE, Pauley DR, Knight HL, Rosenzweig M, Johnson RP, Desrosiers RC, Lackner AA. Gastrointestinal tract as a major site of CD4+ T cell depletion and viral replication in SIV infection. *Science.* 1998;280(5362):427-31. doi: 10.1126/science.280.5362.427. PubMed PMID: 9545219.
29. Mehandru S, Poles MA, Tenner-Racz K, Horowitz A, Hurley A, Hogan C, Boden D, Racz P, Markowitz M. Primary HIV-1 infection is associated with preferential depletion of CD4+ T lymphocytes from effector sites in the gastrointestinal tract. *J Exp Med.* 2004;200(6):761-70. Epub 20040913. doi: 10.1084/jem.20041196. PubMed PMID: 15365095; PMCID: PMC2211967.
30. Moir S, Chun TW, Fauci AS. Pathogenic mechanisms of HIV disease. *Annu Rev Pathol.* 2011;6:223-48. doi: 10.1146/annurev-pathol-011110-130254. PubMed PMID: 21034222.
31. Koup RA, Safrit JT, Cao Y, Andrews CA, McLeod G, Borkowsky W, Farthing C, Ho DD. Temporal association of cellular immune responses with the initial control of viremia in primary human immunodeficiency virus type 1 syndrome. *J Virol.* 1994;68(7):4650-5. doi: 10.1128/JVI.68.7.4650-4655.1994. PubMed PMID: 8207839; PMCID: PMC236393.
32. Beignon AS, McKenna K, Skoberne M, Manches O, DaSilva I, Kavanagh DG, Larsson M, Gorelick RJ, Lifson JD, Bhardwaj N. Endocytosis of HIV-1 activates plasmacytoid dendritic cells via Toll-like receptor-viral RNA interactions. *J Clin Invest.* 2005;115(11):3265-75. Epub 20051013. doi: 10.1172/JCI26032. PubMed PMID: 16224540; PMCID: PMC1253628.
33. Heil F, Hemmi H, Hochrein H, Ampenberger F, Kirschning C, Akira S, Lipford G, Wagner H, Bauer S. Species-specific recognition of single-stranded RNA via toll-like receptor 7 and 8. *Science.* 2004;303(5663):1526-9. Epub 20040219. doi: 10.1126/science.1093620. PubMed PMID: 14976262.
34. Diebold SS, Kaisho T, Hemmi H, Akira S, Reis e Sousa C. Innate antiviral responses by means of TLR7-mediated recognition of single-stranded RNA. *Science.* 2004;303(5663):1529-31. Epub 20040219. doi: 10.1126/science.1093616. PubMed PMID: 14976261.

35. Stacey AR, Norris PJ, Qin L, Haygreen EA, Taylor E, Heitman J, Lebedeva M, DeCamp A, Li D, Grove D, Self SG, Borrow P. Induction of a striking systemic cytokine cascade prior to peak viremia in acute human immunodeficiency virus type 1 infection, in contrast to more modest and delayed responses in acute hepatitis B and C virus infections. *J Virol*. 2009;83(8):3719-33. Epub 20090128. doi: 10.1128/JVI.01844-08. PubMed PMID: 19176632; PMCID: PMC2663284.
36. Lane HC, Kovacs JA, Feinberg J, Herpin B, Davey V, Walker R, Deyton L, Metcalf JA, Baseler M, Salzman N, et al. Anti-retroviral effects of interferon-alpha in AIDS-associated Kaposi's sarcoma. *Lancet*. 1988;2(8622):1218-22. doi: 10.1016/s0140-6736(88)90811-2. PubMed PMID: 2903954.
37. de Wit R, Schattenkerk JK, Boucher CA, Bakker PJ, Veenhof KH, Danner SA. Clinical and virological effects of high-dose recombinant interferon-alpha in disseminated AIDS-related Kaposi's sarcoma. *Lancet*. 1988;2(8622):1214-7. doi: 10.1016/s0140-6736(88)90810-0. PubMed PMID: 2903953.
38. Brook MG, Gor D, Forster SM, Harris W, Jeffries DJ, Thomas HC. Suppression of HIV p24 antigen and induction of HIV anti-p24 antibody by alpha interferon in patients with chronic hepatitis B. *AIDS*. 1988;2(5):391-3. PubMed PMID: 3146270.
39. Bosinger SE, Utay NS. Type I interferon: understanding its role in HIV pathogenesis and therapy. *Curr HIV/AIDS Rep*. 2015;12(1):41-53. doi: 10.1007/s11904-014-0244-6. PubMed PMID: 25662992.
40. Sandler NG, Bosinger SE, Estes JD, Zhu RT, Tharp GK, Boritz E, Levin D, Wijeyesinghe S, Makamdop KN, del Prete GQ, Hill BJ, Timmer JK, Reiss E, Yarden G, Darko S, Contijoch E, Todd JP, Silvestri G, Nason M, Norgren RB, Jr., Keele BF, Rao S, Langer JA, Lifson JD, Schreiber G, Douek DC. Type I interferon responses in rhesus macaques prevent SIV infection and slow disease progression. *Nature*. 2014;511(7511):601-5. Epub 20140709. doi: 10.1038/nature13554. PubMed PMID: 25043006; PMCID: PMC4418221.
41. Hardy GA, Sieg S, Rodriguez B, Anthony D, Asaad R, Jiang W, Mudd J, Schacker T, Funderburg NT, Pilch-Cooper HA, Debernardo R, Rabin RL, Lederman MM, Harding CV. Interferon-alpha is the primary plasma type-I IFN in HIV-1 infection and correlates with immune activation and disease markers. *PLoS One*. 2013;8(2):e56527. Epub 20130220. doi: 10.1371/journal.pone.0056527. PubMed PMID: 23437155; PMCID: PMC3577907.
42. Stoddart CA, Keir ME, McCune JM. IFN-alpha-induced upregulation of CCR5 leads to expanded HIV tropism in vivo. *PLoS Pathog*. 2010;6(2):e1000766. Epub 20100219. doi: 10.1371/journal.ppat.1000766. PubMed PMID: 20174557; PMCID: PMC2824759.
43. Fernandez S, Tanaskovic S, Helbig K, Rajasuriar R, Kramski M, Murray JM, Beard M, Purcell D, Lewin SR, Price P, French MA. CD4+ T-cell deficiency in HIV patients responding to antiretroviral therapy is associated with increased expression of interferon-stimulated genes in CD4+ T cells. *J Infect Dis*. 2011;204(12):1927-35. Epub 20111017. doi: 10.1093/infdis/jir659. PubMed PMID: 22006994.
44. Bogerd HP, Cullen BR. Single-stranded RNA facilitates nucleocapsid: APOBEC3G complex formation. *RNA*. 2008;14(6):1228-36. Epub 20080502. doi: 10.1261/rna.964708. PubMed PMID: 18456846; PMCID: PMC2390788.
45. Sheehy AM, Gaddis NC, Choi JD, Malim MH. Isolation of a human gene that inhibits HIV-1 infection and is suppressed by the viral Vif protein. *Nature*. 2002;418(6898):646-50. Epub 20020714. doi: 10.1038/nature00939. PubMed PMID: 12167863.

46. Yu X, Yu Y, Liu B, Luo K, Kong W, Mao P, Yu XF. Induction of APOBEC3G ubiquitination and degradation by an HIV-1 Vif-Cul5-SCF complex. *Science*. 2003;302(5647):1056-60. Epub 20031016. doi: 10.1126/science.1089591. PubMed PMID: 14564014.
47. Sharaf R, Lee GQ, Sun X, Etemad B, Aboukhater LM, Hu Z, Brumme ZL, Aga E, Bosch RJ, Wen Y, Namazi G, Gao C, Acosta EP, Gandhi RT, Jacobson JM, Skiest D, Margolis DM, Mitsuyasu R, Volberding P, Connick E, Kuritzkes DR, Lederman MM, Yu XG, Lichterfeld M, Li JZ. HIV-1 proviral landscapes distinguish posttreatment controllers from noncontrollers. *J Clin Invest*. 2018;128(9):4074-85. Epub 20180820. doi: 10.1172/JCI120549. PubMed PMID: 30024859; PMCID: PMC6118642.
48. Grutter MG, Luban J. TRIM5 structure, HIV-1 capsid recognition, and innate immune signaling. *Curr Opin Virol*. 2012;2(2):142-50. Epub 20120305. doi: 10.1016/j.coviro.2012.02.003. PubMed PMID: 22482711; PMCID: PMC3322363.
49. Stremlau M, Owens CM, Perron MJ, Kiessling M, Autissier P, Sodroski J. The cytoplasmic body component TRIM5alpha restricts HIV-1 infection in Old World monkeys. *Nature*. 2004;427(6977):848-53. doi: 10.1038/nature02343. PubMed PMID: 14985764.
50. Van Damme N, Goff D, Katsura C, Jorgenson RL, Mitchell R, Johnson MC, Stephens EB, Guatelli J. The interferon-induced protein BST-2 restricts HIV-1 release and is downregulated from the cell surface by the viral Vpu protein. *Cell Host Microbe*. 2008;3(4):245-52. Epub 20080313. doi: 10.1016/j.chom.2008.03.001. PubMed PMID: 18342597; PMCID: PMC2474773.
51. Neil SJ, Zang T, Bieniasz PD. Tetherin inhibits retrovirus release and is antagonized by HIV-1 Vpu. *Nature*. 2008;451(7177):425-30. Epub 20080116. doi: 10.1038/nature06553. PubMed PMID: 18200009.
52. Rosenberg ES, Billingsley JM, Caliendo AM, Boswell SL, Sax PE, Kalams SA, Walker BD. Vigorous HIV-1-specific CD4+ T cell responses associated with control of viremia. *Science*. 1997;278(5342):1447-50. doi: 10.1126/science.278.5342.1447. PubMed PMID: 9367954.
53. Soghoian DZ, Jessen H, Flanders M, Sierra-Davidson K, Cutler S, Pertel T, Ranasinghe S, Lindqvist M, Davis I, Lane K, Rychert J, Rosenberg ES, Piechocka-Trocha A, Brass AL, Brenchley JM, Walker BD, Streeck H. HIV-specific cytolytic CD4 T cell responses during acute HIV infection predict disease outcome. *Sci Transl Med*. 2012;4(123):123ra25. doi: 10.1126/scitranslmed.3003165. PubMed PMID: 22378925; PMCID: PMC3918726.
54. Douek DC, Brenchley JM, Betts MR, Ambrozak DR, Hill BJ, Okamoto Y, Casazza JP, Kuruppu J, Kunstman K, Wolinsky S, Grossman Z, Dybul M, Oxenius A, Price DA, Connors M, Koup RA. HIV preferentially infects HIV-specific CD4+ T cells. *Nature*. 2002;417(6884):95-8. doi: 10.1038/417095a. PubMed PMID: 11986671.
55. Younes SA, Yassine-Diab B, Dumont AR, Boulassel MR, Grossman Z, Routy JP, Sekaly RP. HIV-1 viremia prevents the establishment of interleukin 2-producing HIV-specific memory CD4+ T cells endowed with proliferative capacity. *J Exp Med*. 2003;198(12):1909-22. doi: 10.1084/jem.20031598. PubMed PMID: 14676302; PMCID: PMC2194146.
56. Palmer BE, Boritz E, Wilson CC. Effects of sustained HIV-1 plasma viremia on HIV-1 Gag-specific CD4+ T cell maturation and function. *J Immunol*. 2004;172(5):3337-47. doi: 10.4049/jimmunol.172.5.3337. PubMed PMID: 14978142.
57. Steinman L. A brief history of T(H)17, the first major revision in the T(H)1/T(H)2 hypothesis of T cell-mediated tissue damage. *Nat Med*. 2007;13(2):139-45. doi: 10.1038/nm1551. PubMed PMID: 17290272.

58. Brenchley JM, Paiardini M, Knox KS, Asher AI, Cervasi B, Asher TE, Scheinberg P, Price DA, Hage CA, Kholi LM, Khoruts A, Frank I, Else J, Schacker T, Silvestri G, Douek DC. Differential Th17 CD4 T-cell depletion in pathogenic and nonpathogenic lentiviral infections. *Blood*. 2008;112(7):2826-35. Epub 20080729. doi: 10.1182/blood-2008-05-159301. PubMed PMID: 18664624; PMCID: PMC2556618.
59. Brenchley JM, Price DA, Schacker TW, Asher TE, Silvestri G, Rao S, Kazzaz Z, Bornstein E, Lambotte O, Altmann D, Blazar BR, Rodriguez B, Teixeira-Johnson L, Landay A, Martin JN, Hecht FM, Picker LJ, Lederman MM, Deeks SG, Douek DC. Microbial translocation is a cause of systemic immune activation in chronic HIV infection. *Nat Med*. 2006;12(12):1365-71. Epub 20061119. doi: 10.1038/nm1511. PubMed PMID: 17115046.
60. Micci L, Ryan ES, Fromentin R, Bosinger SE, Harper JL, He T, Paganini S, Easley KA, Chahroudi A, Benne C, Gumber S, McGary CS, Rogers KA, Deleage C, Lucero C, Byraredy SN, Apetrei C, Estes JD, Lifson JD, Piatak M, Jr., Chomont N, Villinger F, Silvestri G, Brenchley JM, Paiardini M. Interleukin-21 combined with ART reduces inflammation and viral reservoir in SIV-infected macaques. *J Clin Invest*. 2015;125(12):4497-513. Epub 20151109. doi: 10.1172/JCI81400. PubMed PMID: 26551680; PMCID: PMC4665780.
61. Ryan ES, Micci L, Fromentin R, Paganini S, McGary CS, Easley K, Chomont N, Paiardini M. Loss of Function of Intestinal IL-17 and IL-22 Producing Cells Contributes to Inflammation and Viral Persistence in SIV-Infected Rhesus Macaques. *PLoS Pathog*. 2016;12(2):e1005412. Epub 20160201. doi: 10.1371/journal.ppat.1005412. PubMed PMID: 26829644; PMCID: PMC4735119.
62. Tomaras GD, Yates NL, Liu P, Qin L, Fouda GG, Chavez LL, Decamp AC, Parks RJ, Ashley VC, Lucas JT, Cohen M, Eron J, Hicks CB, Liao HX, Self SG, Landucci G, Forthal DN, Weinhold KJ, Keele BF, Hahn BH, Greenberg ML, Morris L, Karim SS, Blattner WA, Montefiori DC, Shaw GM, Perelson AS, Haynes BF. Initial B-cell responses to transmitted human immunodeficiency virus type 1: virion-binding immunoglobulin M (IgM) and IgG antibodies followed by plasma anti-gp41 antibodies with ineffective control of initial viremia. *J Virol*. 2008;82(24):12449-63. Epub 20081008. doi: 10.1128/JVI.01708-08. PubMed PMID: 18842730; PMCID: PMC2593361.
63. Moir S, Fauci AS. B-cell responses to HIV infection. *Immunol Rev*. 2017;275(1):33-48. doi: 10.1111/imr.12502. PubMed PMID: 28133792; PMCID: PMC5300048.
64. Cubas R, Perreau M. The dysfunction of T follicular helper cells. *Curr Opin HIV AIDS*. 2014;9(5):485-91. doi: 10.1097/COH.0000000000000095. PubMed PMID: 25023620; PMCID: PMC4176897.
65. Klein F, Mouquet H, Dosenovic P, Scheid JF, Scharf L, Nussenzweig MC. Antibodies in HIV-1 vaccine development and therapy. *Science*. 2013;341(6151):1199-204. doi: 10.1126/science.1241144. PubMed PMID: 24031012; PMCID: PMC3970325.
66. Haynes BF, Burton DR, Mascola JR. Multiple roles for HIV broadly neutralizing antibodies. *Sci Transl Med*. 2019;11(516). doi: 10.1126/scitranslmed.aaz2686. PubMed PMID: 31666399; PMCID: PMC7171597.
67. Mayr LM, Su B, Moog C. Non-Neutralizing Antibodies Directed against HIV and Their Functions. *Front Immunol*. 2017;8:1590. Epub 20171120. doi: 10.3389/fimmu.2017.01590. PubMed PMID: 29209323; PMCID: PMC5701973.
68. Haynes BF, Gilbert PB, McElrath MJ, Zolla-Pazner S, Tomaras GD, Alam SM, Evans DT, Montefiori DC, Karnasuta C, Sutthent R, Liao HX, DeVico AL, Lewis GK, Williams C, Pinter A, Fong

- Y, Janes H, DeCamp A, Huang Y, Rao M, Billings E, Karasavvas N, Robb ML, Ngaury V, de Souza MS, Paris R, Ferrari G, Bailer RT, Soderberg KA, Andrews C, Berman PW, Frahm N, De Rosa SC, Alpert MD, Yates NL, Shen X, Koup RA, Pitisuttithum P, Kaewkungwal J, Nitayaphan S, Rerks-Ngarm S, Michael NL, Kim JH. Immune-correlates analysis of an HIV-1 vaccine efficacy trial. *N Engl J Med*. 2012;366(14):1275-86. doi: 10.1056/NEJMoa1113425. PubMed PMID: 22475592; PMCID: PMC3371689.
69. Ndhlovu ZM, Kamya P, Mewalal N, Klooverpris HN, Nkosi T, Pretorius K, Laher F, Ogunshola F, Chopera D, Shekhar K, Ghebremichael M, Ismail N, Moodley A, Malik A, Leslie A, Goulder PJ, Buus S, Chakraborty A, Dong K, Ndung'u T, Walker BD. Magnitude and Kinetics of CD8+ T Cell Activation during Hyperacute HIV Infection Impact Viral Set Point. *Immunity*. 2015;43(3):591-604. Epub 20150908. doi: 10.1016/j.immuni.2015.08.012. PubMed PMID: 26362266; PMCID: PMC4575777.
70. Borrow P, Lewicki H, Hahn BH, Shaw GM, Oldstone MB. Virus-specific CD8+ cytotoxic T-lymphocyte activity associated with control of viremia in primary human immunodeficiency virus type 1 infection. *J Virol*. 1994;68(9):6103-10. doi: 10.1128/JVI.68.9.6103-6110.1994. PubMed PMID: 8057491; PMCID: PMC237022.
71. Goonetilleke N, Liu MK, Salazar-Gonzalez JF, Ferrari G, Giorgi E, Ghanusov VV, Keele BF, Learn GH, Turnbull EL, Salazar MG, Weinhold KJ, Moore S, B CCC, Letvin N, Haynes BF, Cohen MS, Hraber P, Bhattacharya T, Borrow P, Perelson AS, Hahn BH, Shaw GM, Korber BT, McMichael AJ. The first T cell response to transmitted/founder virus contributes to the control of acute viremia in HIV-1 infection. *J Exp Med*. 2009;206(6):1253-72. Epub 20090601. doi: 10.1084/jem.20090365. PubMed PMID: 19487423; PMCID: PMC2715063.
72. Statzu M, Jin W, Fray EJ, Wong AKH, Kumar MR, Ferrer E, Docken SS, Pinkevych M, McBrien JB, Fennessey CM, Keele BF, Liang S, Harper JL, Mutascio S, Franchitti L, Wang H, Cicetti D, Bosinger SE, Carnathan DG, Vanderford TH, Margolis DM, Garcia-Martinez JV, Chahroudi A, Paiardini M, Siliciano J, Davenport MP, Kulpa DA, Siliciano RS, Silvestri G. CD8(+) lymphocytes do not impact SIV reservoir establishment under ART. *Nat Microbiol*. 2023;8(2):299-308. Epub 20230123. doi: 10.1038/s41564-022-01311-9. PubMed PMID: 36690860; PMCID: PMC9894752.
73. Schmitz JE, Kuroda MJ, Santra S, Sasseville VG, Simon MA, Lifton MA, Racz P, Tenner-Racz K, Dalesandro M, Scallan BJ, Ghayeb J, Forman MA, Montefiori DC, Rieber EP, Letvin NL, Reimann KA. Control of viremia in simian immunodeficiency virus infection by CD8+ lymphocytes. *Science*. 1999;283(5403):857-60. doi: 10.1126/science.283.5403.857. PubMed PMID: 9933172.
74. Jin X, Bauer DE, Tuttleton SE, Lewin S, Gettie A, Blanchard J, Irwin CE, Safrit JT, Mittler J, Weinberger L, Kostrikis LG, Zhang L, Perelson AS, Ho DD. Dramatic rise in plasma viremia after CD8(+) T cell depletion in simian immunodeficiency virus-infected macaques. *J Exp Med*. 1999;189(6):991-8. doi: 10.1084/jem.189.6.991. PubMed PMID: 10075982; PMCID: PMC2193038.
75. Arcia D, Acevedo-Saenz L, Rugeles MT, Velilla PA. Role of CD8(+) T Cells in the Selection of HIV-1 Immune Escape Mutations. *Viral Immunol*. 2017;30(1):3-12. Epub 20161102. doi: 10.1089/vim.2016.0095. PubMed PMID: 27805477.

76. Walker B, McMichael A. The T-cell response to HIV. *Cold Spring Harb Perspect Med*. 2012;2(11). Epub 20121101. doi: 10.1101/cshperspect.a007054. PubMed PMID: 23002014; PMCID: PMC3543107.
77. Pereyra F, Addo MM, Kaufmann DE, Liu Y, Miura T, Rathod A, Baker B, Trocha A, Rosenberg R, Mackey E, Ueda P, Lu Z, Cohen D, Wrin T, Petropoulos CJ, Rosenberg ES, Walker BD. Genetic and immunologic heterogeneity among persons who control HIV infection in the absence of therapy. *J Infect Dis*. 2008;197(4):563-71. doi: 10.1086/526786. PubMed PMID: 18275276.
78. Betts MR, Ambrozak DR, Douek DC, Bonhoeffer S, Brenchley JM, Casazza JP, Koup RA, Picker LJ. Analysis of total human immunodeficiency virus (HIV)-specific CD4(+) and CD8(+) T-cell responses: relationship to viral load in untreated HIV infection. *J Virol*. 2001;75(24):11983-91. doi: 10.1128/JVI.75.24.11983-11991.2001. PubMed PMID: 11711588; PMCID: PMC116093.
79. Gea-Banacloche JC, Migueles SA, Martino L, Shupert WL, McNeil AC, Sabbaghian MS, Ehler L, Prussin C, Stevens R, Lambert L, Altman J, Hallahan CW, de Quiros JC, Connors M. Maintenance of large numbers of virus-specific CD8+ T cells in HIV-infected progressors and long-term nonprogressors. *J Immunol*. 2000;165(2):1082-92. doi: 10.4049/jimmunol.165.2.1082. PubMed PMID: 10878387.
80. Westermann J, Pabst R. Distribution of lymphocyte subsets and natural killer cells in the human body. *Clin Investig*. 1992;70(7):539-44. doi: 10.1007/BF00184787. PubMed PMID: 1392422.
81. Estes JD. Pathobiology of HIV/SIV-associated changes in secondary lymphoid tissues. *Immunol Rev*. 2013;254(1):65-77. doi: 10.1111/imr.12070. PubMed PMID: 23772615; PMCID: PMC6066369.
82. Reuter MA, Del Rio Estrada PM, Buggert M, Petrovas C, Ferrando-Martinez S, Nguyen S, Sada Japp A, Ablanedo-Terrazas Y, Rivero-Arrieta A, Kuri-Cervantes L, Gunzelman HM, Gostick E, Price DA, Koup RA, Naji A, Canaday DH, Reyes-Teran G, Betts MR. HIV-Specific CD8(+) T Cells Exhibit Reduced and Differentially Regulated Cytolytic Activity in Lymphoid Tissue. *Cell Rep*. 2017;21(12):3458-70. doi: 10.1016/j.celrep.2017.11.075. PubMed PMID: 29262326; PMCID: PMC5764192.
83. Buggert M, Nguyen S, Salgado-Montes de Oca G, Bengsch B, Darko S, Ransier A, Roberts ER, Del Alcazar D, Brody IB, Vella LA, Beura L, Wijeyesinghe S, Herati RS, Del Rio Estrada PM, Ablanedo-Terrazas Y, Kuri-Cervantes L, Sada Japp A, Manne S, Vartanian S, Huffman A, Sandberg JK, Gostick E, Nadolski G, Silvestri G, Canaday DH, Price DA, Petrovas C, Su LF, Vahedi G, Dori Y, Frank I, Itkin MG, Wherry EJ, Deeks SG, Naji A, Reyes-Teran G, Masopust D, Douek DC, Betts MR. Identification and characterization of HIV-specific resident memory CD8(+) T cells in human lymphoid tissue. *Sci Immunol*. 2018;3(24). doi: 10.1126/sciimmunol.aar4526. PubMed PMID: 29858286; PMCID: PMC6357781.
84. Nguyen S, Deleage C, Darko S, Ransier A, Truong DP, Agarwal D, Japp AS, Wu VH, Kuri-Cervantes L, Abdel-Mohsen M, Del Rio Estrada PM, Ablanedo-Terrazas Y, Gostick E, Hoxie JA, Zhang NR, Naji A, Reyes-Teran G, Estes JD, Price DA, Douek DC, Deeks SG, Buggert M, Betts MR. Elite control of HIV is associated with distinct functional and transcriptional signatures in lymphoid tissue CD8(+) T cells. *Sci Transl Med*. 2019;11(523). Epub 2019/12/20. doi: 10.1126/scitranslmed.aax4077. PubMed PMID: 31852798.

85. Fauci AS. HIV and AIDS: 20 years of science. *Nat Med*. 2003;9(7):839-43. doi: 10.1038/nm0703-839. PubMed PMID: 12835701.
86. Arts EJ, Hazuda DJ. HIV-1 antiretroviral drug therapy. *Cold Spring Harb Perspect Med*. 2012;2(4):a007161. doi: 10.1101/cshperspect.a007161. PubMed PMID: 22474613; PMCID: PMC3312400.
87. Staszewski S, Miller V, Rehmet S, Stark T, De Cree J, De Brabander M, Peeters M, Andries K, Moeremans M, De Raeymaeker M, Pearce G, Van den Broeck R, Verbiest W, Stoffels P. Virological and immunological analysis of a triple combination pilot study with loviride, lamivudine and zidovudine in HIV-1-infected patients. *AIDS*. 1996;10(5):F1-7. doi: 10.1097/00002030-199605000-00001. PubMed PMID: 8724034.
88. D'Aquila RT, Hughes MD, Johnson VA, Fischl MA, Sommadossi JP, Liou SH, Timpone J, Myers M, Basgoz N, Niu M, Hirsch MS. Nevirapine, zidovudine, and didanosine compared with zidovudine and didanosine in patients with HIV-1 infection. A randomized, double-blind, placebo-controlled trial. National Institute of Allergy and Infectious Diseases AIDS Clinical Trials Group Protocol 241 Investigators. *Ann Intern Med*. 1996;124(12):1019-30. doi: 10.7326/0003-4819-124-12-199606150-00001. PubMed PMID: 8633815.
89. Collier AC, Coombs RW, Schoenfeld DA, Bassett RL, Timpone J, Baruch A, Jones M, Facey K, Whitacre C, McAuliffe VJ, Friedman HM, Merigan TC, Reichman RC, Hooper C, Corey L. Treatment of human immunodeficiency virus infection with saquinavir, zidovudine, and zalcitabine. AIDS Clinical Trials Group. *N Engl J Med*. 1996;334(16):1011-7. doi: 10.1056/NEJM199604183341602. PubMed PMID: 8598838.
90. Smith SJ, Zhao XZ, Passos DO, Lyumkis D, Burke TR, Jr., Hughes SH. Integrase Strand Transfer Inhibitors Are Effective Anti-HIV Drugs. *Viruses*. 2021;13(2). Epub 20210129. doi: 10.3390/v13020205. PubMed PMID: 33572956; PMCID: PMC7912079.
91. Menendez-Arias L, Delgado R. Update and latest advances in antiretroviral therapy. *Trends Pharmacol Sci*. 2022;43(1):16-29. Epub 20211103. doi: 10.1016/j.tips.2021.10.004. PubMed PMID: 34742581.
92. Venkatesan P. Long-acting injectable ART for HIV: a (cautious) step forward. *Lancet Microbe*. 2022;3(2):e94. Epub 20220202. doi: 10.1016/S2666-5247(22)00009-X. PubMed PMID: 35544049.
93. Wong JK, Hezareh M, Gunthard HF, Havlir DV, Ignacio CC, Spina CA, Richman DD. Recovery of replication-competent HIV despite prolonged suppression of plasma viremia. *Science*. 1997;278(5341):1291-5. Epub 1997/11/21. doi: 10.1126/science.278.5341.1291. PubMed PMID: 9360926.
94. Chun TW, Stuyver L, Mizell SB, Ehler LA, Mican JA, Baseler M, Lloyd AL, Nowak MA, Fauci AS. Presence of an inducible HIV-1 latent reservoir during highly active antiretroviral therapy. *Proc Natl Acad Sci U S A*. 1997;94(24):13193-7. doi: 10.1073/pnas.94.24.13193. PubMed PMID: 9371822; PMCID: PMC24285.
95. Finzi D, Blankson J, Siliciano JD, Margolick JB, Chadwick K, Pierson T, Smith K, Lisiewicz J, Lori F, Flexner C, Quinn TC, Chaisson RE, Rosenberg E, Walker B, Gange S, Gallant J, Siliciano RF. Latent infection of CD4+ T cells provides a mechanism for lifelong persistence of HIV-1, even in patients on effective combination therapy. *Nat Med*. 1999;5(5):512-7. Epub 1999/05/06. doi: 10.1038/8394. PubMed PMID: 10229227.

96. Cohn LB, Chomont N, Deeks SG. The Biology of the HIV-1 Latent Reservoir and Implications for Cure Strategies. *Cell Host Microbe*. 2020;27(4):519-30. doi: 10.1016/j.chom.2020.03.014. PubMed PMID: 32272077; PMCID: PMC7219958.
97. Mouton JP, Cohen K, Maartens G. Key toxicity issues with the WHO-recommended first-line antiretroviral therapy regimen. *Expert Rev Clin Pharmacol*. 2016;9(11):1493-503. Epub 20160822. doi: 10.1080/17512433.2016.1221760. PubMed PMID: 27498720.
98. Deeks SG, Tracy R, Douek DC. Systemic effects of inflammation on health during chronic HIV infection. *Immunity*. 2013;39(4):633-45. doi: 10.1016/j.immuni.2013.10.001. PubMed PMID: 24138880; PMCID: PMC4012895.
99. Chun TW, Davey RT, Jr., Engel D, Lane HC, Fauci AS. Re-emergence of HIV after stopping therapy. *Nature*. 1999;401(6756):874-5. doi: 10.1038/44755. PubMed PMID: 10553903.
100. Strain MC, Gunthard HF, Havlir DV, Ignacio CC, Smith DM, Leigh-Brown AJ, Macaranas TR, Lam RY, Daly OA, Fischer M, Opravil M, Levine H, Bacheler L, Spina CA, Richman DD, Wong JK. Heterogeneous clearance rates of long-lived lymphocytes infected with HIV: intrinsic stability predicts lifelong persistence. *Proc Natl Acad Sci U S A*. 2003;100(8):4819-24. Epub 20030408. doi: 10.1073/pnas.0736332100. PubMed PMID: 12684537; PMCID: PMC153639.
101. Siliciano JD, Kajdas J, Finzi D, Quinn TC, Chadwick K, Margolick JB, Kovacs C, Gange SJ, Siliciano RF. Long-term follow-up studies confirm the stability of the latent reservoir for HIV-1 in resting CD4+ T cells. *Nat Med*. 2003;9(6):727-8. Epub 20030518. doi: 10.1038/nm880. PubMed PMID: 12754504.
102. Crooks AM, Bateson R, Cope AB, Dahl NP, Griggs MK, Kuruc JD, Gay CL, Eron JJ, Margolis DM, Bosch RJ, Archin NM. Precise Quantitation of the Latent HIV-1 Reservoir: Implications for Eradication Strategies. *J Infect Dis*. 2015;212(9):1361-5. Epub 20150415. doi: 10.1093/infdis/jiv218. PubMed PMID: 25877550; PMCID: PMC4601910.
103. Okoye AA, Hansen SG, Vaidya M, Fukazawa Y, Park H, Duell DM, Lum R, Hughes CM, Ventura AB, Ainslie E, Ford JC, Morrow D, Gilbride RM, Legasse AW, Hesselgesser J, Geleziunas R, Li Y, Oswald K, Shoemaker R, Fast R, Bosche WJ, Borate BR, Edlefsen PT, Axthelm MK, Picker LJ, Lifson JD. Early antiretroviral therapy limits SIV reservoir establishment to delay or prevent post-treatment viral rebound. *Nat Med*. 2018;24(9):1430-40. Epub 20180806. doi: 10.1038/s41591-018-0130-7. PubMed PMID: 30082858; PMCID: PMC6389357.
104. Henrich TJ, Hatano H, Bacon O, Hogan LE, Rutishauser R, Hill A, Kearney MF, Anderson EM, Buchbinder SP, Cohen SE, Abdel-Mohsen M, Pohlmeier CW, Fromentin R, Hoh R, Liu AY, McCune JM, Spindler J, Metcalf-Pate K, Hobbs KS, Thanh C, Gibson EA, Kuritzkes DR, Siliciano RF, Price RW, Richman DD, Chomont N, Siliciano JD, Mellors JW, Yukl SA, Blankson JN, Liegler T, Deeks SG. HIV-1 persistence following extremely early initiation of antiretroviral therapy (ART) during acute HIV-1 infection: An observational study. *PLoS Med*. 2017;14(11):e1002417. Epub 20171107. doi: 10.1371/journal.pmed.1002417. PubMed PMID: 29112956; PMCID: PMC5675377.
105. Colby DJ, Trautmann L, Pinyakorn S, Leyre L, Pagliuzza A, Kroon E, Rolland M, Takata H, Buranapraditkun S, Intasan J, Chomchey N, Muir R, Haddad EK, Tovanabuttra S, Ubolyam S, Bolton DL, Fullmer BA, Gorelick RJ, Fox L, Crowell TA, Trichavaroj R, O'Connell R, Chomont N, Kim JH, Michael NL, Robb ML, Phanuphak N, Ananworanich J, group RVs. Rapid HIV RNA rebound after antiretroviral treatment interruption in persons durably suppressed in Fiebig I

- acute HIV infection. *Nat Med*. 2018;24(7):923-6. Epub 20180611. doi: 10.1038/s41591-018-0026-6. PubMed PMID: 29892063; PMCID: PMC6092240.
106. Ananworanich J, Chomont N, Eller LA, Kroon E, Tovanabutra S, Bose M, Nau M, Fletcher JLK, Tipsuk S, Vandergeeten C, O'Connell RJ, Pinyakorn S, Michael N, Phanuphak N, Robb ML, Rv, groups RSs. HIV DNA Set Point is Rapidly Established in Acute HIV Infection and Dramatically Reduced by Early ART. *EBioMedicine*. 2016;11:68-72. Epub 20160720. doi: 10.1016/j.ebiom.2016.07.024. PubMed PMID: 27460436; PMCID: PMC5049918.
 107. Macallan DC, Asquith B, Irvine AJ, Wallace DL, Worth A, Ghattas H, Zhang Y, Griffin GE, Tough DF, Beverley PC. Measurement and modeling of human T cell kinetics. *Eur J Immunol*. 2003;33(8):2316-26. doi: 10.1002/eji.200323763. PubMed PMID: 12884307.
 108. Farber DL, Yudanin NA, Restifo NP. Human memory T cells: generation, compartmentalization and homeostasis. *Nat Rev Immunol*. 2014;14(1):24-35. Epub 20131213. doi: 10.1038/nri3567. PubMed PMID: 24336101; PMCID: PMC4032067.
 109. De Boer RJ, Perelson AS. Quantifying T lymphocyte turnover. *J Theor Biol*. 2013;327:45-87. Epub 20130109. doi: 10.1016/j.jtbi.2012.12.025. PubMed PMID: 23313150; PMCID: PMC3640348.
 110. Vandergeeten C, Fromentin R, DaFonseca S, Lawani MB, Sereti I, Lederman MM, Ramgopal M, Routy JP, Sekaly RP, Chomont N. Interleukin-7 promotes HIV persistence during antiretroviral therapy. *Blood*. 2013;121(21):4321-9. Epub 20130415. doi: 10.1182/blood-2012-11-465625. PubMed PMID: 23589672; PMCID: PMC3663425.
 111. Bosque A, Famiglietti M, Weyrich AS, Goulston C, Planelles V. Homeostatic proliferation fails to efficiently reactivate HIV-1 latently infected central memory CD4+ T cells. *PLoS Pathog*. 2011;7(10):e1002288. Epub 20111006. doi: 10.1371/journal.ppat.1002288. PubMed PMID: 21998586; PMCID: PMC3188522.
 112. Chomont N, El-Far M, Ancuta P, Trautmann L, Procopio FA, Yassine-Diab B, Boucher G, Boulassel MR, Ghattas G, Brenchley JM, Schacker TW, Hill BJ, Douek DC, Routy JP, Haddad EK, Sekaly RP. HIV reservoir size and persistence are driven by T cell survival and homeostatic proliferation. *Nat Med*. 2009;15(8):893-900. Epub 20090621. doi: 10.1038/nm.1972. PubMed PMID: 19543283; PMCID: PMC2859814.
 113. Wagner TA, McLaughlin S, Garg K, Cheung CY, Larsen BB, Styrchak S, Huang HC, Edlefsen PT, Mullins JI, Frenkel LM. HIV latency. Proliferation of cells with HIV integrated into cancer genes contributes to persistent infection. *Science*. 2014;345(6196):570-3. Epub 20140710. doi: 10.1126/science.1256304. PubMed PMID: 25011556; PMCID: PMC4230336.
 114. Simonetti FR, Sobolewski MD, Fyne E, Shao W, Spindler J, Hattori J, Anderson EM, Watters SA, Hill S, Wu X, Wells D, Su L, Luke BT, Halvas EK, Besson G, Penrose KJ, Yang Z, Kwan RW, Van Waes C, Uldrick T, Citrin DE, Kovacs J, Polis MA, Rehm CA, Gorelick R, Piatak M, Keele BF, Kearney MF, Coffin JM, Hughes SH, Mellors JW, Maldarelli F. Clonally expanded CD4+ T cells can produce infectious HIV-1 in vivo. *Proc Natl Acad Sci U S A*. 2016;113(7):1883-8. Epub 20160208. doi: 10.1073/pnas.1522675113. PubMed PMID: 26858442; PMCID: PMC4763755.
 115. Maldarelli F, Wu X, Su L, Simonetti FR, Shao W, Hill S, Spindler J, Ferris AL, Mellors JW, Kearney MF, Coffin JM, Hughes SH. HIV latency. Specific HIV integration sites are linked to clonal expansion and persistence of infected cells. *Science*. 2014;345(6193):179-83. Epub 20140626. doi: 10.1126/science.1254194. PubMed PMID: 24968937; PMCID: PMC4262401.

116. Cohn LB, Silva IT, Oliveira TY, Rosales RA, Parrish EH, Learn GH, Hahn BH, Czartoski JL, McElrath MJ, Lehmann C, Klein F, Caskey M, Walker BD, Siliciano JD, Siliciano RF, Jankovic M, Nussenzweig MC. HIV-1 integration landscape during latent and active infection. *Cell*. 2015;160(3):420-32. doi: 10.1016/j.cell.2015.01.020. PubMed PMID: 25635456; PMCID: PMC4371550.
117. Cohn LB, da Silva IT, Valieris R, Huang AS, Lorenzi JCC, Cohen YZ, Pai JA, Butler AL, Caskey M, Jankovic M, Nussenzweig MC. Clonal CD4(+) T cells in the HIV-1 latent reservoir display a distinct gene profile upon reactivation. *Nat Med*. 2018;24(5):604-9. Epub 20180423. doi: 10.1038/s41591-018-0017-7. PubMed PMID: 29686423; PMCID: PMC5972543.
118. Bui JK, Sobolewski MD, Keele BF, Spindler J, Musick A, Wiegand A, Luke BT, Shao W, Hughes SH, Coffin JM, Kearney MF, Mellors JW. Proviruses with identical sequences comprise a large fraction of the replication-competent HIV reservoir. *PLoS Pathog*. 2017;13(3):e1006283. Epub 20170322. doi: 10.1371/journal.ppat.1006283. PubMed PMID: 28328934; PMCID: PMC5378418.
119. Halvas EK, Joseph KW, Brandt LD, Guo S, Sobolewski MD, Jacobs JL, Tumiotto C, Bui JK, Cyktor JC, Keele BF, Morse GD, Bale MJ, Shao W, Kearney MF, Coffin JM, Rausch JW, Wu X, Hughes SH, Mellors JW. HIV-1 viremia not suppressible by antiretroviral therapy can originate from large T cell clones producing infectious virus. *J Clin Invest*. 2020;130(11):5847-57. doi: 10.1172/JCI138099. PubMed PMID: 33016926; PMCID: PMC7598056.
120. Jacobs JL, Halvas EK, Tosiano MA, Mellors JW. Persistent HIV-1 Viremia on Antiretroviral Therapy: Measurement and Mechanisms. *Front Microbiol*. 2019;10:2383. Epub 20191015. doi: 10.3389/fmicb.2019.02383. PubMed PMID: 31681237; PMCID: PMC6804636.
121. Wang Z, Gurule EE, Brennan TP, Gerold JM, Kwon KJ, Hosmane NN, Kumar MR, Beg SA, Capoferri AA, Ray SC, Ho YC, Hill AL, Siliciano JD, Siliciano RF. Expanded cellular clones carrying replication-competent HIV-1 persist, wax, and wane. *Proc Natl Acad Sci U S A*. 2018;115(11):E2575-E84. Epub 20180226. doi: 10.1073/pnas.1720665115. PubMed PMID: 29483265; PMCID: PMC5856552.
122. Mendoza P, Jackson JR, Oliveira TY, Gaebler C, Ramos V, Caskey M, Jankovic M, Nussenzweig MC, Cohn LB. Antigen-responsive CD4+ T cell clones contribute to the HIV-1 latent reservoir. *J Exp Med*. 2020;217(7). doi: 10.1084/jem.20200051. PubMed PMID: 32311008; PMCID: PMC7336300.
123. Venanzi Rullo E, Pinzone MR, Cannon L, Weissman S, Ceccarelli M, Zurakowski R, Nunnari G, O'Doherty U. Persistence of an intact HIV reservoir in phenotypically naive T cells. *JCI Insight*. 2020;5(20). Epub 20201015. doi: 10.1172/jci.insight.133157. PubMed PMID: 33055422; PMCID: PMC7605525.
124. Roche M, Tumpach C, Symons J, Gartner M, Anderson JL, Khoury G, Cashin K, Cameron PU, Churchill MJ, Deeks SG, Gorry PR, Lewin SR. CXCR4-Using HIV Strains Predominate in Naive and Central Memory CD4(+) T Cells in People Living with HIV on Antiretroviral Therapy: Implications for How Latency Is Established and Maintained. *J Virol*. 2020;94(6). Epub 20200228. doi: 10.1128/JVI.01736-19. PubMed PMID: 31852784; PMCID: PMC7158712.
125. Venanzi Rullo E, Cannon L, Pinzone MR, Ceccarelli M, Nunnari G, O'Doherty U. Genetic Evidence That Naive T Cells Can Contribute Significantly to the Human Immunodeficiency Virus Intact Reservoir: Time to Re-evaluate Their Role. *Clin Infect Dis*. 2019;69(12):2236-7. doi: 10.1093/cid/ciz378. PubMed PMID: 31063189; PMCID: PMC6880327.

126. Honeycutt JB, Thayer WO, Baker CE, Ribeiro RM, Lada SM, Cao Y, Cleary RA, Hudgens MG, Richman DD, Garcia JV. HIV persistence in tissue macrophages of humanized myeloid-only mice during antiretroviral therapy. *Nat Med.* 2017;23(5):638-43. Epub 20170417. doi: 10.1038/nm.4319. PubMed PMID: 28414330; PMCID: PMC5419854.
127. Abreu C, Shirk EN, Queen SE, Beck SE, Mangus LM, Pate KAM, Mankowski JL, Gama L, Clements JE. Brain macrophages harbor latent, infectious simian immunodeficiency virus. *AIDS.* 2019;33 Suppl 2(Suppl 2):S181-S8. doi: 10.1097/QAD.0000000000002269. PubMed PMID: 31789817; PMCID: PMC7058191.
128. Kwon KJ, Timmons AE, Sengupta S, Simonetti FR, Zhang H, Hoh R, Deeks SG, Siliciano JD, Siliciano RF. Different human resting memory CD4(+) T cell subsets show similar low inducibility of latent HIV-1 proviruses. *Sci Transl Med.* 2020;12(528). doi: 10.1126/scitranslmed.aax6795. PubMed PMID: 31996465; PMCID: PMC7875249.
129. Kulpa DA, Talla A, Brehm JH, Ribeiro SP, Yuan S, Bebin-Blackwell AG, Miller M, Barnard R, Deeks SG, Hazuda D, Chomont N, Sekaly RP. Differentiation into an Effector Memory Phenotype Potentiates HIV-1 Latency Reversal in CD4(+) T Cells. *J Virol.* 2019;93(24). Epub 20191126. doi: 10.1128/JVI.00969-19. PubMed PMID: 31578289; PMCID: PMC6880164.
130. Jaafoura S, de Goer de Herve MG, Hernandez-Vargas EA, Hendel-Chavez H, Abdoh M, Mateo MC, Krzysiek R, Merad M, Seng R, Tardieu M, Delfraissy JF, Goujard C, Taoufik Y. Progressive contraction of the latent HIV reservoir around a core of less-differentiated CD4(+) memory T Cells. *Nat Commun.* 2014;5:5407. Epub 20141110. doi: 10.1038/ncomms6407. PubMed PMID: 25382623; PMCID: PMC4241984.
131. Buzon MJ, Sun H, Li C, Shaw A, Seiss K, Ouyang Z, Martin-Gayo E, Leng J, Henrich TJ, Li JZ, Pereyra F, Zurakowski R, Walker BD, Rosenberg ES, Yu XG, Lichterfeld M. HIV-1 persistence in CD4+ T cells with stem cell-like properties. *Nat Med.* 2014;20(2):139-42. Epub 20140112. doi: 10.1038/nm.3445. PubMed PMID: 24412925; PMCID: PMC3959167.
132. Pantaleo G, Graziosi C, Butini L, Pizzo PA, Schnittman SM, Kotler DP, Fauci AS. Lymphoid organs function as major reservoirs for human immunodeficiency virus. *Proc Natl Acad Sci U S A.* 1991;88(21):9838-42. doi: 10.1073/pnas.88.21.9838. PubMed PMID: 1682922; PMCID: PMC52816.
133. Petrovas C, Ferrando-Martinez S, Gerner MY, Casazza JP, Pegu A, Deleage C, Cooper A, Hataye J, Andrews S, Ambrozak D, Del Rio Estrada PM, Boritz E, Paris R, Moysi E, Boswell KL, Ruiz-Mateos E, Vagios I, Leal M, Ablanado-Terrazas Y, Rivero A, Gonzalez-Hernandez LA, McDermott AB, Moir S, Reyes-Teran G, Docobo F, Pantaleo G, Douek DC, Betts MR, Estes JD, Germain RN, Mascola JR, Koup RA. Follicular CD8 T cells accumulate in HIV infection and can kill infected cells in vitro via bispecific antibodies. *Sci Transl Med.* 2017;9(373). doi: 10.1126/scitranslmed.aag2285. PubMed PMID: 28100833; PMCID: PMC5497679.
134. McGary CS, Deleage C, Harper J, Micci L, Ribeiro SP, Paganini S, Kuri-Cervantes L, Benne C, Ryan ES, Balderas R, Jean S, Easley K, Marconi V, Silvestri G, Estes JD, Sekaly RP, Paiardini M. CTLA-4(+)PD-1(-) Memory CD4(+) T Cells Critically Contribute to Viral Persistence in Antiretroviral Therapy-Suppressed, SIV-Infected Rhesus Macaques. *Immunity.* 2017;47(4):776-88 e5. doi: 10.1016/j.immuni.2017.09.018. PubMed PMID: 29045906; PMCID: PMC5679306.
135. Banga R, Procopio FA, Ruggiero A, Noto A, Ohmiti K, Cavassini M, Corpataux JM, Paxton WA, Pollakis G, Perreau M. Blood CXCR3(+) CD4 T Cells Are Enriched in Inducible Replication Competent HIV in Aviremic Antiretroviral Therapy-Treated Individuals. *Front Immunol.*

- 2018;9:144. Epub 20180205. doi: 10.3389/fimmu.2018.00144. PubMed PMID: 29459864; PMCID: PMC5807378.
136. Perreau M, Savoye AL, De Crignis E, Corpataux JM, Cubas R, Haddad EK, De Leval L, Graziosi C, Pantaleo G. Follicular helper T cells serve as the major CD4 T cell compartment for HIV-1 infection, replication, and production. *J Exp Med*. 2013;210(1):143-56. Epub 20121217. doi: 10.1084/jem.20121932. PubMed PMID: 23254284; PMCID: PMC3549706.
137. Banga R, Procopio FA, Noto A, Pollakis G, Cavassini M, Ohmiti K, Corpataux JM, de Leval L, Pantaleo G, Perreau M. PD-1(+) and follicular helper T cells are responsible for persistent HIV-1 transcription in treated aviremic individuals. *Nat Med*. 2016;22(7):754-61. Epub 20160530. doi: 10.1038/nm.4113. PubMed PMID: 27239760.
138. Chomont N. Silence, escape and survival drive the persistence of HIV. *Nature*. 2023;614(7947):236-7. doi: 10.1038/d41586-022-04492-9. PubMed PMID: 36599993.
139. Sun W, Gao C, Hartana CA, Osborn MR, Einkauf KB, Lian X, Bone B, Bonheur N, Chun TW, Rosenberg ES, Walker BD, Yu XG, Lichterfeld M. Phenotypic signatures of immune selection in HIV-1 reservoir cells. *Nature*. 2023;614(7947):309-17. Epub 20230104. doi: 10.1038/s41586-022-05538-8. PubMed PMID: 36599977; PMCID: PMC9908552.
140. Clark IC, Mudvari P, Thaploo S, Smith S, Abu-Laban M, Hamouda M, Theberge M, Shah S, Ko SH, Perez L, Bunis DG, Lee JS, Kilam D, Zakaria S, Choi S, Darko S, Henry AR, Wheeler MA, Hoh R, Butrus S, Deeks SG, Quintana FJ, Douek DC, Abate AR, Boritz EA. HIV silencing and cell survival signatures in infected T cell reservoirs. *Nature*. 2023;614(7947):318-25. Epub 20230104. doi: 10.1038/s41586-022-05556-6. PubMed PMID: 36599978; PMCID: PMC9908556.
141. Wu VH, Nordin JML, Nguyen S, Joy J, Mampe F, Del Rio Estrada PM, Torres-Ruiz F, Gonzalez-Navarro M, Luna-Villalobos YA, Avila-Rios S, Reyes-Teran G, Tebas P, Montaner LJ, Bar KJ, Vella LA, Betts MR. Profound phenotypic and epigenetic heterogeneity of the HIV-1-infected CD4(+) T cell reservoir. *Nat Immunol*. 2023;24(2):359-70. Epub 20221219. doi: 10.1038/s41590-022-01371-3. PubMed PMID: 36536105; PMCID: PMC9892009.
142. Cantero-Perez J, Grau-Exposito J, Serra-Peinado C, Rosero DA, Luque-Ballesteros L, Astorga-Gamaza A, Castellvi J, Sanhueza T, Tapia G, Lloveras B, Fernandez MA, Prado JG, Sole-Sedeno JM, Tarrats A, Lecumberri C, Manalich-Barrachina L, Centeno-Mediavilla C, Falco V, Buzon MJ, Genesca M. Resident memory T cells are a cellular reservoir for HIV in the cervical mucosa. *Nat Commun*. 2019;10(1):4739. Epub 20191018. doi: 10.1038/s41467-019-12732-2. PubMed PMID: 31628331; PMCID: PMC6802119.
143. Tran TA, de Goer de Herve MG, Hendel-Chavez H, Dembele B, Le Nevot E, Abbed K, Pallier C, Goujard C, Gasnault J, Delfraissy JF, Balazuc AM, Taoufik Y. Resting regulatory CD4 T cells: a site of HIV persistence in patients on long-term effective antiretroviral therapy. *PLoS One*. 2008;3(10):e3305. Epub 20081001. doi: 10.1371/journal.pone.0003305. PubMed PMID: 18827929; PMCID: PMC2551739.
144. Lee E, Bacchetti P, Milush J, Shao W, Boritz E, Douek D, Fromentin R, Liegler T, Hoh R, Deeks SG, Hecht FM, Chomont N, Palmer S. Memory CD4 + T-Cells Expressing HLA-DR Contribute to HIV Persistence During Prolonged Antiretroviral Therapy. *Front Microbiol*. 2019;10:2214. Epub 20190926. doi: 10.3389/fmicb.2019.02214. PubMed PMID: 31611857; PMCID: PMC6775493.
145. Horsburgh BA, Lee E, Hiener B, Eden JS, Schlub TE, von Stockenstrom S, Odevall L, Milush JM, Liegler T, Sinclair E, Hoh R, Boritz EA, Douek DC, Fromentin R, Chomont N, Deeks SG,

- Hecht FM, Palmer S. High levels of genetically intact HIV in HLA-DR+ memory T cells indicates their value for reservoir studies. *AIDS*. 2020;34(5):659-68. doi: 10.1097/QAD.0000000000002465. PubMed PMID: 31913161; PMCID: PMC7071960.
146. Strongin Z, Hoang TN, Tharp GK, Rahmberg AR, Harper JL, Nguyen K, Franchitti L, Cervasi B, Lee M, Zhang Z, Boritz EA, Silvestri G, Marconi VC, Bosinger SE, Brenchley JM, Kulpa DA, Paiardini M. The role of CD101-expressing CD4 T cells in HIV/SIV pathogenesis and persistence. *PLoS Pathog*. 2022;18(7):e1010723. Epub 20220722. doi: 10.1371/journal.ppat.1010723. PubMed PMID: 35867722; PMCID: PMC9348691.
147. Fromentin R, Bakeman W, Lawani MB, Khoury G, Hartogensis W, DaFonseca S, Killian M, Epling L, Hoh R, Sinclair E, Hecht FM, Bacchetti P, Deeks SG, Lewin SR, Sekaly RP, Chomont N. CD4+ T Cells Expressing PD-1, TIGIT and LAG-3 Contribute to HIV Persistence during ART. *PLoS Pathog*. 2016;12(7):e1005761. Epub 20160714. doi: 10.1371/journal.ppat.1005761. PubMed PMID: 27415008; PMCID: PMC4944956.
148. Pardons M, Baxter AE, Massanella M, Pagliuzza A, Fromentin R, Dufour C, Leyre L, Routy JP, Kaufmann DE, Chomont N. Single-cell characterization and quantification of translation-competent viral reservoirs in treated and untreated HIV infection. *PLoS Pathog*. 2019;15(2):e1007619. Epub 20190227. doi: 10.1371/journal.ppat.1007619. PubMed PMID: 30811499; PMCID: PMC6411230.
149. Gallimore A, Glithero A, Godkin A, Tissot AC, Plückthun A, Elliott T, Hengartner H, Zinkernagel R. Induction and exhaustion of lymphocytic choriomeningitis virus-specific cytotoxic T lymphocytes visualized using soluble tetrameric major histocompatibility complex class I-peptide complexes. *J Exp Med*. 1998;187(9):1383-93. doi: 10.1084/jem.187.9.1383. PubMed PMID: 9565631; PMCID: PMC2212278.
150. Zajac AJ, Blattman JN, Murali-Krishna K, Sourdiv DJ, Suresh M, Altman JD, Ahmed R. Viral immune evasion due to persistence of activated T cells without effector function. *J Exp Med*. 1998;188(12):2205-13. doi: 10.1084/jem.188.12.2205. PubMed PMID: 9858507; PMCID: PMC2212420.
151. Kaech SM, Ahmed R. Memory CD8+ T cell differentiation: initial antigen encounter triggers a developmental program in naïve cells. *Nat Immunol*. 2001;2(5):415-22. doi: 10.1038/87720. PubMed PMID: 11323695; PMCID: PMC3760150.
152. Cui W, Kaech SM. Generation of effector CD8+ T cells and their conversion to memory T cells. *Immunol Rev*. 2010;236:151-66. doi: 10.1111/j.1600-065X.2010.00926.x. PubMed PMID: 20636815; PMCID: PMC4380273.
153. McLane LM, Abdel-Hakeem MS, Wherry EJ. CD8 T Cell Exhaustion During Chronic Viral Infection and Cancer. *Annu Rev Immunol*. 2019;37:457-95. Epub 20190124. doi: 10.1146/annurev-immunol-041015-055318. PubMed PMID: 30676822.
154. Fenwick C, Joo V, Jacquier P, Noto A, Banga R, Perreau M, Pantaleo G. T-cell exhaustion in HIV infection. *Immunol Rev*. 2019;292(1):149-63. doi: 10.1111/imr.12823. PubMed PMID: 31883174; PMCID: PMC7003858.
155. Wherry EJ, Blattman JN, Murali-Krishna K, van der Most R, Ahmed R. Viral persistence alters CD8 T-cell immunodominance and tissue distribution and results in distinct stages of functional impairment. *J Virol*. 2003;77(8):4911-27. doi: 10.1128/jvi.77.8.4911-4927.2003. PubMed PMID: 12663797; PMCID: PMC152117.

156. Fuller MJ, Zajac AJ. Ablation of CD8 and CD4 T cell responses by high viral loads. *J Immunol.* 2003;170(1):477-86. doi: 10.4049/jimmunol.170.1.477. PubMed PMID: 12496434.
157. Agnellini P, Wolint P, Rehr M, Cahenzli J, Karrer U, Oxenius A. Impaired NFAT nuclear translocation results in split exhaustion of virus-specific CD8+ T cell functions during chronic viral infection. *Proc Natl Acad Sci U S A.* 2007;104(11):4565-70. Epub 20070307. doi: 10.1073/pnas.0610335104. PubMed PMID: 17360564; PMCID: PMC1815473.
158. Fuller MJ, Khanolkar A, Tebo AE, Zajac AJ. Maintenance, loss, and resurgence of T cell responses during acute, protracted, and chronic viral infections. *J Immunol.* 2004;172(7):4204-14. doi: 10.4049/jimmunol.172.7.4204. PubMed PMID: 15034033.
159. Mackerness KJ, Cox MA, Lilly LM, Weaver CT, Harrington LE, Zajac AJ. Pronounced virus-dependent activation drives exhaustion but sustains IFN- γ transcript levels. *J Immunol.* 2010;185(6):3643-51. Epub 20100818. doi: 10.4049/jimmunol.1000841. PubMed PMID: 20720198; PMCID: PMC2933304.
160. Kao C, Oestreich KJ, Paley MA, Crawford A, Angelosanto JM, Ali MA, Intlekofer AM, Boss JM, Reiner SL, Weinmann AS, Wherry EJ. Transcription factor T-bet represses expression of the inhibitory receptor PD-1 and sustains virus-specific CD8+ T cell responses during chronic infection. *Nat Immunol.* 2011;12(7):663-71. Epub 20110529. doi: 10.1038/ni.2046. PubMed PMID: 21623380; PMCID: PMC3306165.
161. Wherry EJ, Ha SJ, Kaech SM, Haining WN, Sarkar S, Kalia V, Subramaniam S, Blattman JN, Barber DL, Ahmed R. Molecular signature of CD8+ T cell exhaustion during chronic viral infection. *Immunity.* 2007;27(4):670-84. Epub 20071018. doi: 10.1016/j.immuni.2007.09.006. PubMed PMID: 17950003.
162. Beltra JC, Bourbonnais S, Bédard N, Charpentier T, Boulangé M, Michaud E, Boufaied I, Bruneau J, Shoukry NH, Lamarre A, Decaluwe H. IL2R β -dependent signals drive terminal exhaustion and suppress memory development during chronic viral infection. *Proc Natl Acad Sci U S A.* 2016;113(37):E5444-53. Epub 20160829. doi: 10.1073/pnas.1604256113. PubMed PMID: 27573835; PMCID: PMC5027416.
163. Wherry EJ, Teichgräber V, Becker TC, Masopust D, Kaech SM, Antia R, von Andrian UH, Ahmed R. Lineage relationship and protective immunity of memory CD8 T cell subsets. *Nat Immunol.* 2003;4(3):225-34. Epub 20030203. doi: 10.1038/ni889. PubMed PMID: 12563257.
164. Wherry EJ, Barber DL, Kaech SM, Blattman JN, Ahmed R. Antigen-independent memory CD8 T cells do not develop during chronic viral infection. *Proc Natl Acad Sci U S A.* 2004;101(45):16004-9. Epub 20041025. doi: 10.1073/pnas.0407192101. PubMed PMID: 15505208; PMCID: PMC524220.
165. Paley MA, Kroy DC, Odorizzi PM, Johnnidis JB, Dolfi DV, Barnett BE, Bikoff EK, Robertson EJ, Lauer GM, Reiner SL, Wherry EJ. Progenitor and terminal subsets of CD8+ T cells cooperate to contain chronic viral infection. *Science.* 2012;338(6111):1220-5. doi: 10.1126/science.1229620. PubMed PMID: 23197535; PMCID: PMC3653769.
166. Shin H, Blackburn SD, Blattman JN, Wherry EJ. Viral antigen and extensive division maintain virus-specific CD8 T cells during chronic infection. *J Exp Med.* 2007;204(4):941-9. Epub 20070409. doi: 10.1084/jem.20061937. PubMed PMID: 17420267; PMCID: PMC2118542.
167. Odorizzi PM, Wherry EJ. Inhibitory receptors on lymphocytes: insights from infections. *J Immunol.* 2012;188(7):2957-65. doi: 10.4049/jimmunol.1100038. PubMed PMID: 22442493; PMCID: PMC3320038.

168. Barber DL, Wherry EJ, Masopust D, Zhu B, Allison JP, Sharpe AH, Freeman GJ, Ahmed R. Restoring function in exhausted CD8 T cells during chronic viral infection. *Nature*. 2006;439(7077):682-7. Epub 20051228. doi: 10.1038/nature04444. PubMed PMID: 16382236.
169. Im SJ, Hashimoto M, Gerner MY, Lee J, Kissick HT, Burger MC, Shan Q, Hale JS, Lee J, Nasti TH, Sharpe AH, Freeman GJ, Germain RN, Nakaya HI, Xue HH, Ahmed R. Defining CD8+ T cells that provide the proliferative burst after PD-1 therapy. *Nature*. 2016;537(7620):417-21. Epub 20160802. doi: 10.1038/nature19330. PubMed PMID: 27501248; PMCID: PMC5297183.
170. Jin HT, Anderson AC, Tan WG, West EE, Ha SJ, Araki K, Freeman GJ, Kuchroo VK, Ahmed R. Cooperation of Tim-3 and PD-1 in CD8 T-cell exhaustion during chronic viral infection. *Proc Natl Acad Sci U S A*. 2010;107(33):14733-8. Epub 20100802. doi: 10.1073/pnas.1009731107. PubMed PMID: 20679213; PMCID: PMC2930455.
171. Richter K, Agnellini P, Oxenius A. On the role of the inhibitory receptor LAG-3 in acute and chronic LCMV infection. *Int Immunol*. 2010;22(1):13-23. Epub 20091030. doi: 10.1093/intimm/dxp107. PubMed PMID: 19880580.
172. Blackburn SD, Shin H, Haining WN, Zou T, Workman CJ, Polley A, Betts MR, Freeman GJ, Vignali DA, Wherry EJ. Coregulation of CD8+ T cell exhaustion by multiple inhibitory receptors during chronic viral infection. *Nat Immunol*. 2009;10(1):29-37. Epub 20081130. doi: 10.1038/ni.1679. PubMed PMID: 19043418; PMCID: PMC2605166.
173. Johnston RJ, Comps-Agrar L, Hackney J, Yu X, Huseni M, Yang Y, Park S, Javinal V, Chiu H, Irving B, Eaton DL, Grogan JL. The immunoreceptor TIGIT regulates antitumor and antiviral CD8(+) T cell effector function. *Cancer Cell*. 2014;26(6):923-37. Epub 20141126. doi: 10.1016/j.ccell.2014.10.018. PubMed PMID: 25465800.
174. Philip M, Fairchild L, Sun L, Horste EL, Camara S, Shakiba M, Scott AC, Viale A, Lauer P, Merghoub T, Hellmann MD, Wolchok JD, Leslie CS, Schietinger A. Chromatin states define tumour-specific T cell dysfunction and reprogramming. *Nature*. 2017;545(7655):452-6. Epub 20170517. doi: 10.1038/nature22367. PubMed PMID: 28514453; PMCID: PMC5693219.
175. Gupta PK, Godec J, Wolski D, Adland E, Yates K, Pauken KE, Cosgrove C, Ledderose C, Junger WG, Robson SC, Wherry EJ, Alter G, Goulder PJ, Klenerman P, Sharpe AH, Lauer GM, Haining WN. CD39 Expression Identifies Terminally Exhausted CD8+ T Cells. *PLoS Pathog*. 2015;11(10):e1005177. Epub 20151020. doi: 10.1371/journal.ppat.1005177. PubMed PMID: 26485519; PMCID: PMC4618999.
176. Chung HK, McDonald B, Kaech SM. The architectural design of CD8+ T cell responses in acute and chronic infection: Parallel structures with divergent fates. *J Exp Med*. 2021;218(4). doi: 10.1084/jem.20201730. PubMed PMID: 33755719; PMCID: PMC7992501.
177. Giles JR, Ngiow SF, Manne S, Baxter AE, Khan O, Wang P, Staupe R, Abdel-Hakeem MS, Huang H, Mathew D, Painter MM, Wu JE, Huang YJ, Goel RR, Yan PK, Karakousis GC, Xu X, Mitchell TC, Huang AC, Wherry EJ. Shared and distinct biological circuits in effector, memory and exhausted CD8(+) T cells revealed by temporal single-cell transcriptomics and epigenetics. *Nat Immunol*. 2022;23(11):1600-13. Epub 20221021. doi: 10.1038/s41590-022-01338-4. PubMed PMID: 36271148.
178. Utzschneider DT, Charmoy M, Chennupati V, Pousse L, Ferreira DP, Calderon-Copete S, Danilo M, Alfei F, Hofmann M, Wieland D, Pradervand S, Thimme R, Zehn D, Held W. T Cell Factor 1-Expressing Memory-like CD8(+) T Cells Sustain the Immune Response to Chronic Viral

- Infections. Immunity. 2016;45(2):415-27. Epub 2016/08/18. doi: 10.1016/j.immuni.2016.07.021. PubMed PMID: 27533016.
179. Jansen CS, Prokhnevskaya N, Master VA, Sanda MG, Carlisle JW, Bilen MA, Cardenas M, Wilkinson S, Lake R, Sowalsky AG, Valanparambil RM, Hudson WH, McGuire D, Melnick K, Khan AI, Kim K, Chang YM, Kim A, Filson CP, Alemozaffar M, Osunkoya AO, Mullane P, Ellis C, Akondy R, Im SJ, Kamphorst AO, Reyes A, Liu Y, Kissick H. An intra-tumoral niche maintains and differentiates stem-like CD8 T cells. *Nature*. 2019;576(7787):465-70. Epub 20191211. doi: 10.1038/s41586-019-1836-5. PubMed PMID: 31827286; PMCID: PMC7108171.
180. Yan Y, Cao S, Liu X, Harrington SM, Bindeman WE, Adjei AA, Jang JS, Jen J, Li Y, Chanana P, Mansfield AS, Park SS, Markovic SN, Dronca RS, Dong H. CX3CR1 identifies PD-1 therapy-responsive CD8+ T cells that withstand chemotherapy during cancer chemoimmunotherapy. *JCI Insight*. 2018;3(8). Epub 20180419. doi: 10.1172/jci.insight.97828. PubMed PMID: 29669928; PMCID: PMC5931117.
181. Zander R, Schauder D, Xin G, Nguyen C, Wu X, Zajac A, Cui W. CD4(+) T Cell Help Is Required for the Formation of a Cytolytic CD8(+) T Cell Subset that Protects against Chronic Infection and Cancer. *Immunity*. 2019;51(6):1028-42.e4. Epub 20191203. doi: 10.1016/j.immuni.2019.10.009. PubMed PMID: 31810883; PMCID: PMC6929322.
182. Hudson WH, Gensheimer J, Hashimoto M, Wieland A, Valanparambil RM, Li P, Lin JX, Konieczny BT, Im SJ, Freeman GJ, Leonard WJ, Kissick HT, Ahmed R. Proliferating Transitory T Cells with an Effector-like Transcriptional Signature Emerge from PD-1(+) Stem-like CD8(+) T Cells during Chronic Infection. *Immunity*. 2019;51(6):1043-58.e4. Epub 20191203. doi: 10.1016/j.immuni.2019.11.002. PubMed PMID: 31810882; PMCID: PMC6920571.
183. Wu T, Ji Y, Moseman EA, Xu HC, Manglani M, Kirby M, Anderson SM, Handon R, Kenyon E, Elkahoul A, Wu W, Lang PA, Gattinoni L, McGavern DB, Schwartzberg PL. The TCF1-Bcl6 axis counteracts type I interferon to repress exhaustion and maintain T cell stemness. *Sci Immunol*. 2016;1(6). Epub 20161209. doi: 10.1126/sciimmunol.aai8593. PubMed PMID: 28018990; PMCID: PMC5179228.
184. Im SJ, Konieczny BT, Hudson WH, Masopust D, Ahmed R. PD-1+ stemlike CD8 T cells are resident in lymphoid tissues during persistent LCMV infection. *Proc Natl Acad Sci U S A*. 2020;117(8):4292-9. Epub 20200207. doi: 10.1073/pnas.1917298117. PubMed PMID: 32034098; PMCID: PMC7049149.
185. Beltra JC, Manne S, Abdel-Hakeem MS, Kurachi M, Giles JR, Chen Z, Casella V, Ngiow SF, Khan O, Huang YJ, Yan P, Nzingha K, Xu W, Amaravadi RK, Xu X, Karakousis GC, Mitchell TC, Schuchter LM, Huang AC, Wherry EJ. Developmental Relationships of Four Exhausted CD8(+) T Cell Subsets Reveals Underlying Transcriptional and Epigenetic Landscape Control Mechanisms. *Immunity*. 2020;52(5):825-41.e8. Epub 20200511. doi: 10.1016/j.immuni.2020.04.014. PubMed PMID: 32396847; PMCID: PMC8360766.
186. Leong YA, Chen Y, Ong HS, Wu D, Man K, Deleage C, Minnich M, Meckiff BJ, Wei Y, Hou Z, Zotos D, Fenix KA, Atnerkar A, Preston S, Chipman JG, Beilman GJ, Allison CC, Sun L, Wang P, Xu J, Toe JG, Lu HK, Tao Y, Palendira U, Dent AL, Landay AL, Pellegrini M, Comerford I, McColl SR, Schacker TW, Long HM, Estes JD, Busslinger M, Belz GT, Lewin SR, Kallies A, Yu D. CXCR5(+) follicular cytotoxic T cells control viral infection in B cell follicles. *Nat Immunol*. 2016;17(10):1187-96. Epub 20160803. doi: 10.1038/ni.3543. PubMed PMID: 27487330.

187. Miller BC, Sen DR, Al Abosy R, Bi K, Virkud YV, LaFleur MW, Yates KB, Lako A, Felt K, Naik GS, Manos M, Gjini E, Kuchroo JR, Ishizuka JJ, Collier JL, Griffin GK, Maleri S, Comstock DE, Weiss SA, Brown FD, Panda A, Zimmer MD, Manguso RT, Hodi FS, Rodig SJ, Sharpe AH, Haining WN. Subsets of exhausted CD8(+) T cells differentially mediate tumor control and respond to checkpoint blockade. *Nat Immunol.* 2019;20(3):326-36. Epub 20190218. doi: 10.1038/s41590-019-0312-6. PubMed PMID: 30778252; PMCID: PMC6673650.
188. Seo H, Chen J, Gonzalez-Avalos E, Samaniego-Castruita D, Das A, Wang YH, Lopez-Moyado IF, Georges RO, Zhang W, Onodera A, Wu CJ, Lu LF, Hogan PG, Bhandoola A, Rao A. TOX and TOX2 transcription factors cooperate with NR4A transcription factors to impose CD8(+) T cell exhaustion. *Proc Natl Acad Sci U S A.* 2019;116(25):12410-5. Epub 2019/06/04. doi: 10.1073/pnas.1905675116. PubMed PMID: 31152140; PMCID: PMC6589758.
189. Scott AC, Dundar F, Zumbo P, Chandran SS, Klebanoff CA, Shakiba M, Trivedi P, Menocal L, Appleby H, Camara S, Zamarin D, Walther T, Snyder A, Femia MR, Comen EA, Wen HY, Hellmann MD, Anandasabapathy N, Liu Y, Altorki NK, Lauer P, Levy O, Glickman MS, Kaye J, Betel D, Philip M, Schietinger A. TOX is a critical regulator of tumour-specific T cell differentiation. *Nature.* 2019;571(7764):270-4. Epub 2019/06/18. doi: 10.1038/s41586-019-1324-y. PubMed PMID: 31207604.
190. Khan O, Giles JR, McDonald S, Manne S, Ngiew SF, Patel KP, Werner MT, Huang AC, Alexander KA, Wu JE, Attanasio J, Yan P, George SM, Bengsch B, Staupe RP, Donahue G, Xu W, Amaravadi RK, Xu X, Karakousis GC, Mitchell TC, Schuchter LM, Kaye J, Berger SL, Wherry EJ. TOX transcriptionally and epigenetically programs CD8(+) T cell exhaustion. *Nature.* 2019;571(7764):211-8. Epub 2019/06/18. doi: 10.1038/s41586-019-1325-x. PubMed PMID: 31207603; PMCID: PMC6713202.
191. Alfei F, Kanev K, Hofmann M, Wu M, Ghoneim HE, Roelli P, Utzschneider DT, von Hoesslin M, Cullen JG, Fan Y, Eisenberg V, Wohlleber D, Steiger K, Merkler D, Delorenzi M, Knolle PA, Cohen CJ, Thimme R, Youngblood B, Zehn D. TOX reinforces the phenotype and longevity of exhausted T cells in chronic viral infection. *Nature.* 2019;571(7764):265-9. Epub 2019/06/18. doi: 10.1038/s41586-019-1326-9. PubMed PMID: 31207605.
192. Yao C, Sun HW, Lacey NE, Ji Y, Moseman EA, Shih HY, Heuston EF, Kirby M, Anderson S, Cheng J, Khan O, Handon R, Reilley J, Fioravanti J, Hu J, Gossa S, Wherry EJ, Gattinoni L, McGavern DB, O'Shea JJ, Schwartzberg PL, Wu T. Single-cell RNA-seq reveals TOX as a key regulator of CD8(+) T cell persistence in chronic infection. *Nat Immunol.* 2019;20(7):890-901. Epub 2019/06/19. doi: 10.1038/s41590-019-0403-4. PubMed PMID: 31209400; PMCID: PMC6588409.
193. Mann TH, Kaech SM. Tick-TOX, it's time for T cell exhaustion. *Nat Immunol.* 2019;20(9):1092-4. doi: 10.1038/s41590-019-0478-y. PubMed PMID: 31427776.
194. Yates KB, Tonnerre P, Martin GE, Gerdemann U, Al Abosy R, Comstock DE, Weiss SA, Wolski D, Tully DC, Chung RT, Allen TM, Kim AY, Fidler S, Fox J, Frater J, Lauer GM, Haining WN, Sen DR. Epigenetic scars of CD8(+) T cell exhaustion persist after cure of chronic infection in humans. *Nat Immunol.* 2021;22(8):1020-9. Epub 20210726. doi: 10.1038/s41590-021-00979-1. PubMed PMID: 34312547; PMCID: PMC8600539.
195. Guo L, Li X, Liu R, Chen Y, Ren C, Du S. TOX correlates with prognosis, immune infiltration, and T cells exhaustion in lung adenocarcinoma. *Cancer Med.* 2020;9(18):6694-709. Epub 20200723. doi: 10.1002/cam4.3324. PubMed PMID: 32700817; PMCID: PMC7520261.

196. Zhang H, Fan F, Yu Y, Wang Z, Liu F, Dai Z, Zhang L, Liu Z, Cheng Q. Clinical characterization, genetic profiling, and immune infiltration of TOX in diffuse gliomas. *J Transl Med.* 2020;18(1):305. Epub 20200806. doi: 10.1186/s12967-020-02460-3. PubMed PMID: 32762688; PMCID: PMC7409670.
197. Page N, Lemeille S, Vincenti I, Klimek B, Mariotte A, Wagner I, Di Liberto G, Kaye J, Merkler D. Persistence of self-reactive CD8+ T cells in the CNS requires TOX-dependent chromatin remodeling. *Nat Commun.* 2021;12(1):1009. Epub 20210212. doi: 10.1038/s41467-021-21109-3. PubMed PMID: 33579927; PMCID: PMC7881115.
198. Heim K, Binder B, Sagar, Wieland D, Hensel N, Llewellyn-Lacey S, Gostick E, Price DA, Emmerich F, Vingerhoet H, Kraft ARM, Cornberg M, Boettler T, Neumann-Haefelin C, Zehn D, Bengsch B, Hofmann M, Thimme R. TOX defines the degree of CD8+ T cell dysfunction in distinct phases of chronic HBV infection. *Gut.* 2020;70(8):1550-60. Epub 20201023. doi: 10.1136/gutjnl-2020-322404. PubMed PMID: 33097558; PMCID: PMC8292571.
199. Huang S, Liang C, Zhao Y, Deng T, Tan J, Lu Y, Liu S, Li Y, Chen S. Increased TOX expression concurrent with PD-1, Tim-3, and CD244 in T cells from patients with non-Hodgkin lymphoma. *Asia Pac J Clin Oncol.* 2022;18(1):143-9. Epub 20210219. doi: 10.1111/ajco.13545. PubMed PMID: 33608984.
200. Sekine T, Perez-Potti A, Nguyen S, Gorin JB, Wu VH, Gostick E, Llewellyn-Lacey S, Hammer Q, Falck-Jones S, Vangeti S, Yu M, Smed-Sørensen A, Gaballa A, Uhlin M, Sandberg JK, Brander C, Nowak P, Goepfert PA, Price DA, Betts MR, Buggert M. TOX is expressed by exhausted and polyfunctional human effector memory CD8(+) T cells. *Sci Immunol.* 2020;5(49). doi: 10.1126/sciimmunol.aba7918. PubMed PMID: 32620560.
201. Han HS, Jeong S, Kim H, Kim HD, Kim AR, Kwon M, Park SH, Woo CG, Kim HK, Lee KH, Seo SP, Kang HW, Kim WT, Kim WJ, Yun SJ, Shin EC. TOX-expressing terminally exhausted tumor-infiltrating CD8(+) T cells are reinvigorated by co-blockade of PD-1 and TIGIT in bladder cancer. *Cancer Lett.* 2021;499:137-47. Epub 20201127. doi: 10.1016/j.canlet.2020.11.035. PubMed PMID: 33249194.
202. Wang X, He Q, Shen H, Xia A, Tian W, Yu W, Sun B. TOX promotes the exhaustion of antitumor CD8(+) T cells by preventing PD1 degradation in hepatocellular carcinoma. *J Hepatol.* 2019;71(4):731-41. Epub 20190605. doi: 10.1016/j.jhep.2019.05.015. PubMed PMID: 31173813.
203. Papagno L, Spina CA, Marchant A, Salio M, Rufer N, Little S, Dong T, Chesney G, Waters A, Easterbrook P, Dunbar PR, Shepherd D, Cerundolo V, Emery V, Griffiths P, Conlon C, McMichael AJ, Richman DD, Rowland-Jones SL, Appay V. Immune activation and CD8+ T-cell differentiation towards senescence in HIV-1 infection. *PLoS Biol.* 2004;2(2):E20. Epub 20040217. doi: 10.1371/journal.pbio.0020020. PubMed PMID: 14966528; PMCID: PMC340937.
204. Kostense S, Vandenbergh K, Joling J, Van Baarle D, Nanlohy N, Manting E, Miedema F. Persistent numbers of tetramer+ CD8(+) T cells, but loss of interferon-gamma+ HIV-specific T cells during progression to AIDS. *Blood.* 2002;99(7):2505-11. doi: 10.1182/blood.v99.7.2505. PubMed PMID: 11895786.
205. Appay V, Nixon DF, Donahoe SM, Gillespie GM, Dong T, King A, Ogg GS, Spiegel HM, Conlon C, Spina CA, Havlir DV, Richman DD, Waters A, Easterbrook P, McMichael AJ, Rowland-Jones SL. HIV-specific CD8(+) T cells produce antiviral cytokines but are impaired in cytolytic

- function. *J Exp Med*. 2000;192(1):63-75. doi: 10.1084/jem.192.1.63. PubMed PMID: 10880527; PMCID: PMC1887711.
206. Trautmann L, Janbazian L, Chomont N, Said EA, Gimmig S, Bessette B, Boulassel MR, Delwart E, Sepulveda H, Balderas RS, Routy JP, Haddad EK, Sekaly RP. Upregulation of PD-1 expression on HIV-specific CD8+ T cells leads to reversible immune dysfunction. *Nat Med*. 2006;12(10):1198-202. Epub 2006/08/19. doi: 10.1038/nm1482. PubMed PMID: 16917489.
207. Petrovas C, Casazza JP, Brenchley JM, Price DA, Gostick E, Adams WC, Precopio ML, Schacker T, Roederer M, Douek DC, Koup RA. PD-1 is a regulator of virus-specific CD8+ T cell survival in HIV infection. *J Exp Med*. 2006;203(10):2281-92. Epub 2006/09/07. doi: 10.1084/jem.20061496. PubMed PMID: 16954372; PMCID: PMC2118095.
208. Roberts ER, Carnathan DG, Li H, Shaw GM, Silvestri G, Betts MR. Collapse of Cytolytic Potential in SIV-Specific CD8+ T Cells Following Acute SIV Infection in Rhesus Macaques. *PLoS Pathog*. 2016;12(12):e1006135. Epub 2016/12/31. doi: 10.1371/journal.ppat.1006135. PubMed PMID: 28036372; PMCID: PMC5231392.
209. Day CL, Kaufmann DE, Kiepiela P, Brown JA, Moodley ES, Reddy S, Mackey EW, Miller JD, Leslie AJ, DePierres C, Mncube Z, Duraiswamy J, Zhu B, Eichbaum Q, Altfeld M, Wherry EJ, Coovadia HM, Goulder PJ, Klenerman P, Ahmed R, Freeman GJ, Walker BD. PD-1 expression on HIV-specific T cells is associated with T-cell exhaustion and disease progression. *Nature*. 2006;443(7109):350-4. Epub 2006/08/22. doi: 10.1038/nature05115. PubMed PMID: 16921384.
210. Velu V, Titanji K, Zhu B, Husain S, Pladevega A, Lai L, Vanderford TH, Chennareddi L, Silvestri G, Freeman GJ, Ahmed R, Amara RR. Enhancing SIV-specific immunity in vivo by PD-1 blockade. *Nature*. 2009;458(7235):206-10. Epub 2008/12/10. doi: 10.1038/nature07662. PubMed PMID: 19078956; PMCID: PMC2753387.
211. Seung E, Dudek TE, Allen TM, Freeman GJ, Luster AD, Tager AM. PD-1 blockade in chronically HIV-1-infected humanized mice suppresses viral loads. *PLoS One*. 2013;8(10):e77780. Epub 2013/10/21. doi: 10.1371/journal.pone.0077780. PubMed PMID: 24204962; PMCID: PMC3804573.
212. Hoffmann M, Pantazis N, Martin GE, Hickling S, Hurst J, Meyerowitz J, Willberg CB, Robinson N, Brown H, Fisher M, Kinloch S, Babiker A, Weber J, Nwokolo N, Fox J, Fidler S, Phillips R, Frater J, Spartac, Investigators C. Exhaustion of Activated CD8 T Cells Predicts Disease Progression in Primary HIV-1 Infection. *PLoS Pathog*. 2016;12(7):e1005661. Epub 2016/07/14. doi: 10.1371/journal.ppat.1005661. PubMed PMID: 27415828; PMCID: PMC4945085.
213. Bengsch B, Ohtani T, Khan O, Setty M, Manne S, O'Brien S, Gherardini PF, Herati RS, Huang AC, Chang KM, Newell EW, Bovenschen N, Pe'er D, Albelda SM, Wherry EJ. Epigenomic-Guided Mass Cytometry Profiling Reveals Disease-Specific Features of Exhausted CD8 T Cells. *Immunity*. 2018;48(5):1029-45 e5. Epub 2018/05/17. doi: 10.1016/j.immuni.2018.04.026. PubMed PMID: 29768164; PMCID: PMC6010198.
214. Collins DR, Urbach JM, Racenet ZJ, Arshad U, Power KA, Newman RM, Mylvaganam GH, Ly NL, Lian X, Rull A, Rassadkina Y, Yanez AG, Peluso MJ, Deeks SG, Vidal F, Lichtenfeld M, Yu XG, Gaiha GD, Allen TM, Walker BD. Functional impairment of HIV-specific CD8(+) T cells precedes aborted spontaneous control of viremia. *Immunity*. 2021;54(10):2372-84 e7. Epub 2021/09/07. doi: 10.1016/j.immuni.2021.08.007. PubMed PMID: 34496223; PMCID: PMC8516715.

215. Chew GM, Fujita T, Webb GM, Burwitz BJ, Wu HL, Reed JS, Hammond KB, Clayton KL, Ishii N, Abdel-Mohsen M, Liegler T, Mitchell BI, Hecht FM, Ostrowski M, Shikuma CM, Hansen SG, Maurer M, Korman AJ, Deeks SG, Sacha JB, Ndhlovu LC. TIGIT Marks Exhausted T Cells, Correlates with Disease Progression, and Serves as a Target for Immune Restoration in HIV and SIV Infection. *PLoS Pathog.* 2016;12(1):e1005349. Epub 20160107. doi: 10.1371/journal.ppat.1005349. PubMed PMID: 26741490; PMCID: PMC4704737.
216. Brooks DG, Ha SJ, Elsaesser H, Sharpe AH, Freeman GJ, Oldstone MB. IL-10 and PD-L1 operate through distinct pathways to suppress T-cell activity during persistent viral infection. *Proc Natl Acad Sci U S A.* 2008;105(51):20428-33. Epub 20081215. doi: 10.1073/pnas.0811139106. PubMed PMID: 19075244; PMCID: PMC2629263.
217. Harper J, Ribeiro SP, Chan CN, Aid M, Deleage C, Micci L, Pino M, Cervasi B, Raghunathan G, Rimmer E, Ayanoglu G, Wu G, Shenvi N, Barnard RJ, Del Prete GQ, Busman-Sahay K, Silvestri G, Kulpa DA, Bosinger SE, Easley KA, Howell BJ, Gorman D, Hazuda DJ, Estes JD, Sekaly RP, Paiardini M. Interleukin-10 contributes to reservoir establishment and persistence in SIV-infected macaques treated with antiretroviral therapy. *J Clin Invest.* 2022;132(8). doi: 10.1172/JCI155251. PubMed PMID: 35230978; PMCID: PMC9012284.
218. Sekine T, Perez-Potti A, Nguyen S, Gorin JB, Wu VH, Gostick E, Llewellyn-Lacey S, Hammer Q, Falck-Jones S, Vangeti S, Yu M, Smed-Sorensen A, Gaballa A, Uhlin M, Sandberg JK, Brander C, Nowak P, Goepfert PA, Price DA, Betts MR, Buggert M. TOX is expressed by exhausted and polyfunctional human effector memory CD8(+) T cells. *Sci Immunol.* 2020;5(49). doi: 10.1126/sciimmunol.aba7918. PubMed PMID: 32620560.
219. Rutishauser RL, Deguit CDT, Hiatt J, Blaeschke F, Roth TL, Wang L, Raymond KA, Starke CE, Mudd JC, Chen W, Smullin C, Matus-Nicodemos R, Hoh R, Krone M, Hecht FM, Pilcher CD, Martin JN, Koup RA, Douek DC, Brenchley JM, Sekaly RP, Pillai SK, Marson A, Deeks SG, McCune JM, Hunt PW. TCF-1 regulates HIV-specific CD8+ T cell expansion capacity. *JCI Insight.* 2021;6(3). Epub 20210208. doi: 10.1172/jci.insight.136648. PubMed PMID: 33351785; PMCID: PMC7934879.
220. Ndung'u T, McCune JM, Deeks SG. Why and where an HIV cure is needed and how it might be achieved. *Nature.* 2019;576(7787):397-405. Epub 20191218. doi: 10.1038/s41586-019-1841-8. PubMed PMID: 31853080; PMCID: PMC8052635.
221. Persaud D, Gay H, Ziemniak C, Chen YH, Piatak M, Jr., Chun TW, Strain M, Richman D, Luzuriaga K. Absence of detectable HIV-1 viremia after treatment cessation in an infant. *N Engl J Med.* 2013;369(19):1828-35. Epub 20131023. doi: 10.1056/NEJMoa1302976. PubMed PMID: 24152233; PMCID: PMC3954754.
222. Henrich TJ, Hanhauser E, Marty FM, Sirignano MN, Keating S, Lee TH, Robles YP, Davis BT, Li JZ, Heisey A, Hill AL, Busch MP, Armand P, Soiffer RJ, Altfeld M, Kuritzkes DR. Antiretroviral-free HIV-1 remission and viral rebound after allogeneic stem cell transplantation: report of 2 cases. *Ann Intern Med.* 2014;161(5):319-27. doi: 10.7326/M14-1027. PubMed PMID: 25047577; PMCID: PMC4236912.
223. Dickter J, et al. The "City of Hope" Patient: prolonged HIV-1 remission without antiretrovirals (ART) after allogeneic hematopoietic stem cell transplantation (aHCT) of CCR5-Δ32/Δ32 donor cells for acute myelogenous leukemia (AML). *AIDS* 20222022.
224. JingMei Hsu KVB, Marshall J. Glesby, Anne Coletti, Savita G. Pahwa, Meredith Warshaw, Amanda Golner, Frederic Bone, Nicole Tobin, Marcie Riches, John W. Mellors, Renee Browning,

Deborah Persaud, Yvonne Bryson. HIV-1 REMISSION WITH CCR5 Δ 32 Δ 32 HAPLO-CORD TRANSPLANT IN A US WOMAN: IMPAACT P1107. CROI 20222022.

225. Jensen BO, Knops E, Cords L, Lubke N, Salgado M, Busman-Sahay K, Estes JD, Huyveneers LEP, Perdomo-Celis F, Wittner M, Galvez C, Mummert C, Passaes C, Eberhard JM, Munk C, Hauber I, Hauber J, Heger E, De Clercq J, Vandekerckhove L, Bergmann S, Dunay GA, Klein F, Haussinger D, Fischer JC, Nachtkamp K, Timm J, Kaiser R, Harrer T, Luedde T, Nijhuis M, Saez-Cirion A, Schulze Zur Wiesch J, Wensing AMJ, Martinez-Picado J, Kobbe G. In-depth virological and immunological characterization of HIV-1 cure after CCR5Delta32/Delta32 allogeneic hematopoietic stem cell transplantation. *Nat Med*. 2023. Epub 20230220. doi: 10.1038/s41591-023-02213-x. PubMed PMID: 36807684.

226. Hutter G, Nowak D, Mossner M, Ganepola S, Mussig A, Allers K, Schneider T, Hofmann J, Kucherer C, Blau O, Blau IW, Hofmann WK, Thiel E. Long-term control of HIV by CCR5 Delta32/Delta32 stem-cell transplantation. *N Engl J Med*. 2009;360(7):692-8. doi: 10.1056/NEJMoa0802905. PubMed PMID: 19213682.

227. Gupta RK, Abdul-Jawad S, McCoy LE, Mok HP, Peppas D, Salgado M, Martinez-Picado J, Nijhuis M, Wensing AMJ, Lee H, Grant P, Nastouli E, Lambert J, Pace M, Salasc F, Monit C, Innes AJ, Muir L, Waters L, Frater J, Lever AML, Edwards SG, Gabriel IH, Olavarria E. HIV-1 remission following CCR5Delta32/Delta32 haematopoietic stem-cell transplantation. *Nature*. 2019;568(7751):244-8. Epub 20190305. doi: 10.1038/s41586-019-1027-4. PubMed PMID: 30836379; PMCID: PMC7275870.

228. Verheyen J, Thielen A, Lubke N, Dirks M, Widera M, Dittmer U, Kordelas L, Daumer M, de Jong DCM, Wensing AMJ, Kaiser R, Nijhuis M, Esser S. Rapid Rebound of a Preexisting CXCR4-tropic Human Immunodeficiency Virus Variant After Allogeneic Transplantation With CCR5 Delta32 Homozygous Stem Cells. *Clin Infect Dis*. 2019;68(4):684-7. doi: 10.1093/cid/ciy565. PubMed PMID: 30020413.

229. Collins DR, Gaiha GD, Walker BD. CD8(+) T cells in HIV control, cure and prevention. *Nat Rev Immunol*. 2020;20(8):471-82. Epub 20200212. doi: 10.1038/s41577-020-0274-9. PubMed PMID: 32051540; PMCID: PMC7222980.

230. Limou S, Le Clerc S, Coulonges C, Carpentier W, Dina C, Delaneau O, Labib T, Taing L, Sladek R, Deveau C, Ratsimandresy R, Montes M, Spadoni JL, Lelievre JD, Levy Y, Therwath A, Schachter F, Matsuda F, Gut I, Froguel P, Delfraissy JF, Hercberg S, Zagury JF, Group AG. Genomewide association study of an AIDS-nonprogression cohort emphasizes the role played by HLA genes (ANRS Genomewide Association Study 02). *J Infect Dis*. 2009;199(3):419-26. doi: 10.1086/596067. PubMed PMID: 19115949.

231. McLaren PJ, Pulit SL, Gurdasani D, Bartha I, Shea PR, Pomilla C, Gupta N, Gkrania-Klotsas E, Young EH, Bannert N, Del Amo J, Gill MJ, Gilmour J, Kellam P, Kelleher AD, Sonnerborg A, Zangerle R, Post FA, Fisher M, Haas DW, Walker BD, Porter K, Goldstein DB, Sandhu MS, de Bakker PIW, Fellay J. Evaluating the Impact of Functional Genetic Variation on HIV-1 Control. *J Infect Dis*. 2017;216(9):1063-9. doi: 10.1093/infdis/jix470. PubMed PMID: 28968755; PMCID: PMC5853944.

232. Fellay J, Shianna KV, Ge D, Colombo S, Ledergerber B, Weale M, Zhang K, Gumbs C, Castagna A, Cossarizza A, Cozzi-Lepri A, De Luca A, Easterbrook P, Francioli P, Mallal S, Martinez-Picado J, Miro JM, Obel N, Smith JP, Wyniger J, Descombes P, Antonarakis SE, Letvin NL, McMichael AJ, Haynes BF, Telenti A, Goldstein DB. A whole-genome association study of

major determinants for host control of HIV-1. *Science*. 2007;317(5840):944-7. Epub 20070719. doi: 10.1126/science.1143767. PubMed PMID: 17641165; PMCID: PMC1991296.

233. International HIVCS, Pereyra F, Jia X, McLaren PJ, Telenti A, de Bakker PI, Walker BD, Ripke S, Brumme CJ, Pulit SL, Carrington M, Kadie CM, Carlson JM, Heckerman D, Graham RR, Plenge RM, Deeks SG, Gianniny L, Crawford G, Sullivan J, Gonzalez E, Davies L, Camargo A, Moore JM, Beattie N, Gupta S, Crenshaw A, Burt NP, Guiducci C, Gupta N, Gao X, Qi Y, Yuki Y, Piechocka-Trocha A, Cutrell E, Rosenberg R, Moss KL, Lemay P, O'Leary J, Schaefer T, Verma P, Toth I, Block B, Baker B, Rothchild A, Lian J, Proudfoot J, Alvino DM, Vine S, Addo MM, Allen TM, Altfeld M, Henn MR, Le Gall S, Streeck H, Haas DW, Kuritzkes DR, Robbins GK, Shafer RW, Gulick RM, Shikuma CM, Haubrich R, Riddler S, Sax PE, Daar ES, Ribaud HJ, Agan B, Agarwal S, Ahern RL, Allen BL, Altidor S, Altschuler EL, Ambardar S, Anastos K, Anderson B, Anderson V, Andraday U, Antoniskis D, Bangsberg D, Barbaro D, Barrie W, Bartczak J, Barton S, Basden P, Basgoz N, Bazner S, Bellos NC, Benson AM, Berger J, Bernard NF, Bernard AM, Birch C, Bodner SJ, Bolan RK, Boudreaux ET, Bradley M, Braun JF, Brndjar JE, Brown SJ, Brown K, Brown ST, Burack J, Bush LM, Cafaro V, Campbell O, Campbell J, Carlson RH, Carmichael JK, Casey KK, Cavacuiti C, Celestin G, Chambers ST, Chez N, Chirch LM, Cimoch PJ, Cohen D, Cohn LE, Conway B, Cooper DA, Cornelson B, Cox DT, Cristofano MV, Cuchural G, Jr., Czartoski JL, Dahman JM, Daly JS, Davis BT, Davis K, Davod SM, DeJesus E, Dietz CA, Dunham E, Dunn ME, Ellerlin TB, Eron JJ, Fangman JJ, Farel CE, Ferlazzo H, Fidler S, Fleenor-Ford A, Frankel R, Freedberg KA, French NK, Fuchs JD, Fuller JD, Gaberman J, Gallant JE, Gandhi RT, Garcia E, Garmon D, Gathe JC, Jr., Gaultier CR, Gebre W, Gilman FD, Gilson I, Goepfert PA, Gottlieb MS, Goulston C, Groger RK, Gurley TD, Haber S, Hardwicke R, Hardy WD, Harrigan PR, Hawkins TN, Heath S, Hecht FM, Henry WK, Hladek M, Hoffman RP, Horton JM, Hsu RK, Huhn GD, Hunt P, Hupert MJ, Illeman ML, Jaeger H, Jellinger RM, John M, Johnson JA, Johnson KL, Johnson H, Johnson K, Joly J, Jordan WC, Kauffman CA, Khanlou H, Killian RK, Kim AY, Kim DD, Kinder CA, Kirchner JT, Kogelman L, Kojic EM, Korthuis PT, Kurisu W, Kwon DS, LaMar M, Lampiris H, Lanzafame M, Lederman MM, Lee DM, Lee JM, Lee MJ, Lee ET, Lemoine J, Levy JA, Llibre JM, Liguori MA, Little SJ, Liu AY, Lopez AJ, Loutfy MR, Loy D, Mohammed DY, Man A, Mansour MK, Marconi VC, Markowitz M, Marques R, Martin JN, Martin HL, Jr., Mayer KH, McElrath MJ, McGhee TA, McGovern BH, McGowan K, McIntyre D, McLeod GX, Menezes P, Mesa G, Metroka CE, Meyer-Olson D, Miller AO, Montgomery K, Mounzer KC, Nagami EH, Nagin I, Nahass RG, Nelson MO, Nielsen C, Norene DL, O'Connor DH, Ojikutu BO, Okulicz J, Oladehin OO, Oldfield EC, 3rd, Olender SA, Ostrowski M, Owen WF, Jr., Pae E, Parsonnet J, Pavlatos AM, Perlmutter AM, Pierce MN, Pincus JM, Pisani L, Price LJ, Proia L, Prokesch RC, Pujet HC, Ramgopal M, Rathod A, Rausch M, Ravishankar J, Rhame FS, Richards CS, Richman DD, Rodes B, Rodriguez M, Rose RC, 3rd, Rosenberg ES, Rosenthal D, Ross PE, Rubin DS, Rumbaugh E, Saenz L, Salvaggio MR, Sanchez WC, Sanjana VM, Santiago S, Schmidt W, Schuitemaker H, Sestak PM, Shalit P, Shay W, Shirvani VN, Silebi VI, Sizemore JM, Jr., Skolnik PR, Sokol-Anderson M, Sosman JM, Stabile P, Stapleton JT, Starrett S, Stein F, Stellbrink HJ, Sterman FL, Stone VE, Stone DR, Tambussi G, Taplitz RA, Tedaldi EM, Telenti A, Theisen W, Torres R, Tosiello L, Tremblay C, Tribble MA, Trinh PD, Tsao A, Ueda P, Vaccaro A, Valadas E, Vanig TJ, Vecino I, Vega VM, Veikley W, Wade BH, Walworth C, Wanidworanun C, Ward DJ, Warner DA, Weber RD, Webster D, Weis S, Wheeler DA, White DJ, Wilkins E, Winston A, Wlodaver CG, van't Wout A, Wright DP, Yang OO, Yuridin DL, Zabukovic BW, Zachary KC, Zeeman B, Zhao M. The major genetic determinants of HIV-1 control affect

- HLA class I peptide presentation. *Science*. 2010;330(6010):1551-7. Epub 20101104. doi: 10.1126/science.1195271. PubMed PMID: 21051598; PMCID: PMC3235490.
234. Migueles SA, Sabbaghian MS, Shupert WL, Bettinotti MP, Marincola FM, Martino L, Hallahan CW, Selig SM, Schwartz D, Sullivan J, Connors M. HLA B*5701 is highly associated with restriction of virus replication in a subgroup of HIV-infected long term nonprogressors. *Proc Natl Acad Sci U S A*. 2000;97(6):2709-14. doi: 10.1073/pnas.050567397. PubMed PMID: 10694578; PMCID: PMC15994.
235. Ndhlovu ZM, Stampouloglou E, Cesa K, Mavrothalassitis O, Alvino DM, Li JZ, Wilton S, Karel D, Piechocka-Trocha A, Chen H, Pereyra F, Walker BD. The Breadth of Expandable Memory CD8+ T Cells Inversely Correlates with Residual Viral Loads in HIV Elite Controllers. *J Virol*. 2015;89(21):10735-47. Epub 20150812. doi: 10.1128/JVI.01527-15. PubMed PMID: 26269189; PMCID: PMC4621138.
236. Migueles SA, Osborne CM, Royce C, Compton AA, Joshi RP, Weeks KA, Rood JE, Berkley AM, Sacha JB, Cogliano-Shutta NA, Lloyd M, Roby G, Kwan R, McLaughlin M, Stallings S, Rehm C, O'Shea MA, Mican J, Packard BZ, Komoriya A, Palmer S, Wiegand AP, Maldarelli F, Coffin JM, Mellors JW, Hallahan CW, Follman DA, Connors M. Lytic granule loading of CD8+ T cells is required for HIV-infected cell elimination associated with immune control. *Immunity*. 2008;29(6):1009-21. Epub 20081208. doi: 10.1016/j.immuni.2008.10.010. PubMed PMID: 19062316; PMCID: PMC2622434.
237. Migueles SA, Laborico AC, Shupert WL, Sabbaghian MS, Rabin R, Hallahan CW, Van Baarle D, Kostense S, Miedema F, McLaughlin M, Ehler L, Metcalf J, Liu S, Connors M. HIV-specific CD8+ T cell proliferation is coupled to perforin expression and is maintained in nonprogressors. *Nat Immunol*. 2002;3(11):1061-8. Epub 20021007. doi: 10.1038/ni845. PubMed PMID: 12368910.
238. Saez-Cirion A, Lacabartz C, Lambotte O, Versmisse P, Urrutia A, Boufassa F, Barre-Sinoussi F, Delfraissy JF, Sinet M, Pancino G, Venet A, Agence Nationale de Recherches sur le Sida EPHIVCSG. HIV controllers exhibit potent CD8 T cell capacity to suppress HIV infection ex vivo and peculiar cytotoxic T lymphocyte activation phenotype. *Proc Natl Acad Sci U S A*. 2007;104(16):6776-81. Epub 20070411. doi: 10.1073/pnas.0611244104. PubMed PMID: 17428922; PMCID: PMC1851664.
239. Betts MR, Nason MC, West SM, De Rosa SC, Migueles SA, Abraham J, Lederman MM, Benito JM, Goepfert PA, Connors M, Roederer M, Koup RA. HIV nonprogressors preferentially maintain highly functional HIV-specific CD8+ T cells. *Blood*. 2006;107(12):4781-9. Epub 20060207. doi: 10.1182/blood-2005-12-4818. PubMed PMID: 16467198; PMCID: PMC1895811.
240. Hersperger AR, Pereyra F, Nason M, Demers K, Sheth P, Shin LY, Kovacs CM, Rodriguez B, Sieg SF, Teixeira-Johnson L, Gudonis D, Goepfert PA, Lederman MM, Frank I, Makedonas G, Kaul R, Walker BD, Betts MR. Perforin expression directly ex vivo by HIV-specific CD8 T-cells is a correlate of HIV elite control. *PLoS Pathog*. 2010;6(5):e1000917. Epub 20100527. doi: 10.1371/journal.ppat.1000917. PubMed PMID: 20523897; PMCID: PMC2877741.
241. Pereyra F, Heckerman D, Carlson JM, Kadie C, Soghoian DZ, Karel D, Goldenthal A, Davis OB, DeZiel CE, Lin T, Peng J, Piechocka A, Carrington M, Walker BD. HIV control is mediated in part by CD8+ T-cell targeting of specific epitopes. *J Virol*. 2014;88(22):12937-48. Epub 20140827. doi: 10.1128/JVI.01004-14. PubMed PMID: 25165115; PMCID: PMC4249072.

242. Macatangay BJ, Riddler SA, Wheeler ND, Spindler J, Lawani M, Hong F, Buffo MJ, Whiteside TL, Kearney MF, Mellors JW, Rinaldo CR. Therapeutic Vaccination With Dendritic Cells Loaded With Autologous HIV Type 1-Infected Apoptotic Cells. *J Infect Dis*. 2016;213(9):1400-9. Epub 20151208. doi: 10.1093/infdis/jiv582. PubMed PMID: 26647281; PMCID: PMC4813736.
243. Levy Y, Thiebaut R, Montes M, Lacabartz C, Sloan L, King B, Perusat S, Harrod C, Cobb A, Roberts LK, Surenaud M, Boucherie C, Zurawski S, Delaugerre C, Richert L, Chene G, Banchereau J, Palucka K. Dendritic cell-based therapeutic vaccine elicits polyfunctional HIV-specific T-cell immunity associated with control of viral load. *Eur J Immunol*. 2014;44(9):2802-10. doi: 10.1002/eji.201344433. PubMed PMID: 25042008.
244. Garcia F, Climent N, Guardo AC, Gil C, Leon A, Autran B, Lifson JD, Martinez-Picado J, Dalmau J, Clotet B, Gatell JM, Plana M, Gallart T, Group DMOS. A dendritic cell-based vaccine elicits T cell responses associated with control of HIV-1 replication. *Sci Transl Med*. 2013;5(166):166ra2. doi: 10.1126/scitranslmed.3004682. PubMed PMID: 23283367.
245. Lu W, Arraes LC, Ferreira WT, Andrieu JM. Therapeutic dendritic-cell vaccine for chronic HIV-1 infection. *Nat Med*. 2004;10(12):1359-65. Epub 20041128. doi: 10.1038/nm1147. PubMed PMID: 15568033.
246. Kloverpris H, Karlsson I, Bonde J, Thorn M, Vinner L, Pedersen AE, Hentze JL, Andresen BS, Svane IM, Gerstoft J, Kronborg G, Fomsgaard A. Induction of novel CD8+ T-cell responses during chronic untreated HIV-1 infection by immunization with subdominant cytotoxic T-lymphocyte epitopes. *AIDS*. 2009;23(11):1329-40. doi: 10.1097/QAD.0b013e32832d9b00. PubMed PMID: 19528789.
247. Ondondo B, Murakoshi H, Clutton G, Abdul-Jawad S, Wee EG, Gatanaga H, Oka S, McMichael AJ, Takiguchi M, Korber B, Hanke T. Novel Conserved-region T-cell Mosaic Vaccine With High Global HIV-1 Coverage Is Recognized by Protective Responses in Untreated Infection. *Mol Ther*. 2016;24(4):832-42. Epub 20160108. doi: 10.1038/mt.2016.3. PubMed PMID: 26743582; PMCID: PMC4886941.
248. Barouch DH, O'Brien KL, Simmons NL, King SL, Abbink P, Maxfield LF, Sun YH, La Porte A, Riggs AM, Lynch DM, Clark SL, Backus K, Perry JR, Seaman MS, Carville A, Mansfield KG, Szinger JJ, Fischer W, Muldoon M, Korber B. Mosaic HIV-1 vaccines expand the breadth and depth of cellular immune responses in rhesus monkeys. *Nat Med*. 2010;16(3):319-23. Epub 20100221. doi: 10.1038/nm.2089. PubMed PMID: 20173752; PMCID: PMC2834868.
249. Barouch DH, Tomaka FL, Wegmann F, Stieh DJ, Alter G, Robb ML, Michael NL, Peter L, Nkolola JP, Borducchi EN, Chandrashekar A, Jetton D, Stephenson KE, Li W, Korber B, Tomaras GD, Montefiori DC, Gray G, Frahm N, McElrath MJ, Baden L, Johnson J, Hutter J, Swann E, Karita E, Kibuuka H, Mpendo J, Garrett N, Mngadi K, Chinyenze K, Priddy F, Lazarus E, Laher F, Nitayapan S, Pitisuttithum P, Bart S, Campbell T, Feldman R, Lucksinger G, Borremans C, Callewaert K, Roten R, Sadoff J, Scheppler L, Weijtens M, Feddes-de Boer K, van Manen D, Vreugdenhil J, Zahn R, Lavreys L, Nijs S, Tolboom J, Hendriks J, Euler Z, Pau MG, Schuitemaker H. Evaluation of a mosaic HIV-1 vaccine in a multicentre, randomised, double-blind, placebo-controlled, phase 1/2a clinical trial (APPROACH) and in rhesus monkeys (NHP 13-19). *Lancet*. 2018;392(10143):232-43. Epub 20180706. doi: 10.1016/S0140-6736(18)31364-3. PubMed PMID: 30047376; PMCID: PMC6192527.

250. Colby DJ, Sarnecki M, Barouch DH, Tipsuk S, Stieh DJ, Kroon E, Schuetz A, Intasan J, Sacdalan C, Pinyakorn S, Grandin P, Song H, Tovanabutra S, Shubin Z, Kim D, Paquin-Proulx D, Eller MA, Thomas R, de Souza M, Wieczorek L, Polonis VR, Pagliuzza A, Chomont N, Peter L, Nkolola JP, Vingerhoets J, Truysers C, Pau MG, Schuitemaker H, Phanuphak N, Michael N, Robb ML, Tomaka FL, Ananworanich J. Safety and immunogenicity of Ad26 and MVA vaccines in acutely treated HIV and effect on viral rebound after antiretroviral therapy interruption. *Nat Med*. 2020;26(4):498-501. Epub 20200323. doi: 10.1038/s41591-020-0774-y. PubMed PMID: 32235883.
251. Borducchi EN, Cabral C, Stephenson KE, Liu J, Abbink P, Ng'ang'a D, Nkolola JP, Brinkman AL, Peter L, Lee BC, Jimenez J, Jetton D, Mondesir J, Mojta S, Chandrashekar A, Molloy K, Alter G, Gerold JM, Hill AL, Lewis MG, Pau MG, Schuitemaker H, Hesselgesser J, Geleziunas R, Kim JH, Robb ML, Michael NL, Barouch DH. Ad26/MVA therapeutic vaccination with TLR7 stimulation in SIV-infected rhesus monkeys. *Nature*. 2016;540(7632):284-7. Epub 20161109. doi: 10.1038/nature20583. PubMed PMID: 27841870; PMCID: PMC5145754.
252. Bekerman E, Hesselgesser J, Carr B, Nagel M, Hung M, Wang A, Stapleton L, von Gegerfelt A, Elyard HA, Lifson JD, Geleziunas R. PD-1 Blockade and TLR7 Activation Lack Therapeutic Benefit in Chronic Simian Immunodeficiency Virus-Infected Macaques on Antiretroviral Therapy. *Antimicrob Agents Chemother*. 2019;63(11). Epub 20191022. doi: 10.1128/AAC.01163-19. PubMed PMID: 31501143; PMCID: PMC6811450.
253. Harper J, Gordon S, Chan CN, Wang H, Lindemuth E, Galardi C, Falcinelli SD, Raines SLM, Read JL, Nguyen K, McGary CS, Nekorchuk M, Busman-Sahay K, Schawalder J, King C, Pino M, Micci L, Cervasi B, Jean S, Sanderson A, Johns B, Koblansky AA, Amrine-Madsen H, Lifson J, Margolis DM, Silvestri G, Bar KJ, Favre D, Estes JD, Paiardini M. CTLA-4 and PD-1 dual blockade induces SIV reactivation without control of rebound after antiretroviral therapy interruption. *Nat Med*. 2020;26(4):519-28. Epub 20200316. doi: 10.1038/s41591-020-0782-y. PubMed PMID: 32284611; PMCID: PMC7790171.
254. Rasmussen TA, Rajdev L, Rhodes A, Dantanarayana A, Tennakoon S, Chea S, Spelman T, Lensing S, Rutishauser R, Bakkour S, Busch M, Siliciano JD, Siliciano RF, Einstein MH, Dittmer DP, Chiao E, Deeks SG, Durand C, Lewin SR. Impact of Anti-PD-1 and Anti-CTLA-4 on the Human Immunodeficiency Virus (HIV) Reservoir in People Living With HIV With Cancer on Antiretroviral Therapy: The AIDS Malignancy Consortium 095 Study. *Clin Infect Dis*. 2021;73(7):e1973-e81. doi: 10.1093/cid/ciaa1530. PubMed PMID: 33677480; PMCID: PMC8492152.
255. Mylvaganam GH, Chea LS, Tharp GK, Hicks S, Velu V, Iyer SS, Deleage C, Estes JD, Bosinger SE, Freeman GJ, Ahmed R, Amara RR. Combination anti-PD-1 and antiretroviral therapy provides therapeutic benefit against SIV. *JCI Insight*. 2018;3(18). Epub 20180920. doi: 10.1172/jci.insight.122940. PubMed PMID: 30232277; PMCID: PMC6237231.
256. Rahman SA, Yagnik B, Bally AP, Morrow KN, Wang S, Vanderford TH, Freeman GJ, Ahmed R, Amara RR. PD-1 blockade and vaccination provide therapeutic benefit against SIV by inducing broad and functional CD8(+) T cells in lymphoid tissue. *Sci Immunol*. 2021;6(63):eabh3034. Epub 20210903. doi: 10.1126/sciimmunol.abh3034. PubMed PMID: 34516743; PMCID: PMC8500359.
257. Ward AR, Mota TM, Jones RB. Immunological approaches to HIV cure. *Semin Immunol*. 2021;51:101412. Epub 20200924. doi: 10.1016/j.smim.2020.101412. PubMed PMID: 32981836.

258. Webb GM, Li S, Mwakalundwa G, Folkvord JM, Greene JM, Reed JS, Stanton JJ, Legasse AW, Hobbs T, Martin LD, Park BS, Whitney JB, Jeng EK, Wong HC, Nixon DF, Jones RB, Connick E, Skinner PJ, Sacha JB. The human IL-15 superagonist ALT-803 directs SIV-specific CD8(+) T cells into B-cell follicles. *Blood Adv.* 2018;2(2):76-84. doi: 10.1182/bloodadvances.2017012971. PubMed PMID: 29365313; PMCID: PMC5787870.
259. Watson DC, Moysi E, Valentin A, Bergamaschi C, Devasundaram S, Fortis SP, Bear J, Chertova E, Bess J, Jr., Sowder R, Venzon DJ, Deleage C, Estes JD, Lifson JD, Petrovas C, Felber BK, Pavlakis GN. Treatment with native heterodimeric IL-15 increases cytotoxic lymphocytes and reduces SHIV RNA in lymph nodes. *PLoS Pathog.* 2018;14(2):e1006902. Epub 20180223. doi: 10.1371/journal.ppat.1006902. PubMed PMID: 29474450; PMCID: PMC5825155.
260. Namazi G, Fajnzylber JM, Aga E, Bosch RJ, Acosta EP, Sharaf R, Hartogensis W, Jacobson JM, Connick E, Volberding P, Skiest D, Margolis D, Sneller MC, Little SJ, Gianella S, Smith DM, Kuritzkes DR, Gulick RM, Mellors JW, Mehraj V, Gandhi RT, Mitsuyasu R, Schooley RT, Henry K, Tebas P, Deeks SG, Chun TW, Collier AC, Routy JP, Hecht FM, Walker BD, Li JZ. The Control of HIV After Antiretroviral Medication Pause (CHAMP) Study: Posttreatment Controllers Identified From 14 Clinical Studies. *J Infect Dis.* 2018;218(12):1954-63. doi: 10.1093/infdis/jiy479. PubMed PMID: 30085241; PMCID: PMC6217727.
261. Investigators ST, Fidler S, Porter K, Ewings F, Frater J, Ramjee G, Cooper D, Rees H, Fisher M, Schechter M, Kaleebu P, Tambussi G, Kinloch S, Miro JM, Kelleher A, McClure M, Kaye S, Gabriel M, Phillips R, Weber J, Babiker A. Short-course antiretroviral therapy in primary HIV infection. *N Engl J Med.* 2013;368(3):207-17. doi: 10.1056/NEJMoa1110039. PubMed PMID: 23323897; PMCID: PMC4131004.
262. Martin GE, Gossez M, Williams JP, Stohr W, Meyerowitz J, Leitman EM, Goulder P, Porter K, Fidler S, Frater J, the STI. Post-treatment control or treated controllers? Viral remission in treated and untreated primary HIV infection. *AIDS.* 2017;31(4):477-84. doi: 10.1097/QAD.0000000000001382. PubMed PMID: 28060012; PMCID: PMC5278888.
263. Lodi S, Meyer L, Kelleher AD, Rosinska M, Ghosn J, Sannes M, Porter K. Immunovirologic control 24 months after interruption of antiretroviral therapy initiated close to HIV seroconversion. *Arch Intern Med.* 2012;172(16):1252-5. doi: 10.1001/archinternmed.2012.2719. PubMed PMID: 22826124.
264. Saez-Cirion A, Bacchus C, Hocqueloux L, Avettand-Fenoel V, Girault I, Lecuroux C, Potard V, Versmisse P, Melard A, Prazuck T, Descours B, Guernon J, Viard JP, Boufassa F, Lambotte O, Goujard C, Meyer L, Costagliola D, Venet A, Pancino G, Autran B, Rouzioux C, Group AVS. Post-treatment HIV-1 controllers with a long-term virological remission after the interruption of early initiated antiretroviral therapy ANRS VISCONTI Study. *PLoS Pathog.* 2013;9(3):e1003211. Epub 20130314. doi: 10.1371/journal.ppat.1003211. PubMed PMID: 23516360; PMCID: PMC3597518.
265. Etemad B, Esmaeilzadeh E, Li JZ. Learning From the Exceptions: HIV Remission in Post-treatment Controllers. *Front Immunol.* 2019;10:1749. Epub 20190724. doi: 10.3389/fimmu.2019.01749. PubMed PMID: 31396237; PMCID: PMC6668499.
266. Mastrangelo A, Banga R, Perreau M. Elite and posttreatment controllers, two facets of HIV control. *Curr Opin HIV AIDS.* 2022;17(5):325-32. Epub 20220725. doi: 10.1097/COH.0000000000000751. PubMed PMID: 35938466.

267. Krebs SJ, Ananworanich J. Immune activation during acute HIV infection and the impact of early antiretroviral therapy. *Curr Opin HIV AIDS*. 2016;11(2):163-72. doi: 10.1097/COH.0000000000000228. PubMed PMID: 26599167.
268. Takata H, Kakazu JC, Mitchell JL, Kroon E, Colby DJ, Sacdalan C, Bai H, Ehrenberg PK, Geretz A, Buranapraditkun S, Pinyakorn S, Intasan J, Tipsuk S, Suttichom D, Prueksakaew P, Chalermchai T, Chomchey N, Phanuphak N, de Souza M, Michael NL, Robb ML, Haddad EK, Crowell TA, Vasan S, Valcour VG, Douek DC, Thomas R, Rolland M, Chomont N, Ananworanich J, Trautmann L, Rv254/Search RS, groups Ss. Long-term antiretroviral therapy initiated in acute HIV infection prevents residual dysfunction of HIV-specific CD8(+) T cells. *EBioMedicine*. 2022;84:104253. Epub 20220908. doi: 10.1016/j.ebiom.2022.104253. PubMed PMID: 36088683; PMCID: PMC9471490.
269. Pitman MC, Lau JSY, McMahon JH, Lewin SR. Barriers and strategies to achieve a cure for HIV. *Lancet HIV*. 2018;5(6):e317-e28. doi: 10.1016/S2352-3018(18)30039-0. PubMed PMID: 29893245; PMCID: PMC6559798.
270. Hany L, Turmel MO, Barat C, Ouellet M, Tremblay MJ. Bryostatin-1 Decreases HIV-1 Infection and Viral Production in Human Primary Macrophages. *J Virol*. 2022;96(4):e0195321. Epub 20211208. doi: 10.1128/JVI.01953-21. PubMed PMID: 34878918; PMCID: PMC8865430.
271. Rasmussen TA, Tolstrup M, Brinkmann CR, Olesen R, Erikstrup C, Solomon A, Winkelmann A, Palmer S, Dinarello C, Buzon M, Lichterfeld M, Lewin SR, Ostergaard L, Sogaard OS. Panobinostat, a histone deacetylase inhibitor, for latent-virus reactivation in HIV-infected patients on suppressive antiretroviral therapy: a phase 1/2, single group, clinical trial. *Lancet HIV*. 2014;1(1):e13-21. Epub 20140915. doi: 10.1016/S2352-3018(14)70014-1. PubMed PMID: 26423811.
272. Elliott JH, Wightman F, Solomon A, Ghneim K, Ahlers J, Cameron MJ, Smith MZ, Spelman T, McMahon J, Velayudham P, Brown G, Roney J, Watson J, Prince MH, Hoy JF, Chomont N, Fromentin R, Procopio FA, Zeidan J, Palmer S, Odevall L, Johnstone RW, Martin BP, Sinclair E, Deeks SG, Hazuda DJ, Cameron PU, Sekaly RP, Lewin SR. Activation of HIV transcription with short-course vorinostat in HIV-infected patients on suppressive antiretroviral therapy. *PLoS Pathog*. 2014;10(10):e1004473. Epub 20141113. doi: 10.1371/journal.ppat.1004473. PubMed PMID: 25393648; PMCID: PMC4231123.
273. Riddler SA, Para M, Benson CA, Mills A, Ramgopal M, DeJesus E, Brinson C, Cyktor J, Jacobs J, Koontz D, Mellors JW, Laird GM, Wrin T, Patel H, Guo S, Wallin J, Boice J, Zhang L, Humeniuk R, Begley R, German P, Graham H, Geleziunas R, Brainard DM, SenGupta D. Vesatolimod, a Toll-like Receptor 7 Agonist, Induces Immune Activation in Virally Suppressed Adults Living With Human Immunodeficiency Virus-1. *Clin Infect Dis*. 2021;72(11):e815-e24. doi: 10.1093/cid/ciaa1534. PubMed PMID: 33043969.
274. Lim SY, Osuna CE, Hraber PT, Hesselgesser J, Gerold JM, Barnes TL, Sanisetty S, Seaman MS, Lewis MG, Geleziunas R, Miller MD, Cihlar T, Lee WA, Hill AL, Whitney JB. TLR7 agonists induce transient viremia and reduce the viral reservoir in SIV-infected rhesus macaques on antiretroviral therapy. *Sci Transl Med*. 2018;10(439). doi: 10.1126/scitranslmed.aao4521. PubMed PMID: 29720451; PMCID: PMC5973480.
275. McBrien JB, Mavigner M, Franchitti L, Smith SA, White E, Tharp GK, Walum H, Busman-Sahay K, Aguilera-Sandoval CR, Thayer WO, Spagnuolo RA, Kovarova M, Wahl A, Cervasi B, Margolis DM, Vanderford TH, Carnathan DG, Paiardini M, Lifson JD, Lee JH, Safrit JT, Bosinger

- SE, Estes JD, Derdeyn CA, Garcia JV, Kulpa DA, Chahroudi A, Silvestri G. Robust and persistent reactivation of SIV and HIV by N-803 and depletion of CD8(+) cells. *Nature*. 2020;578(7793):154-9. Epub 20200122. doi: 10.1038/s41586-020-1946-0. PubMed PMID: 31969705; PMCID: PMC7580846.
276. Cartwright EK, Spicer L, Smith SA, Lee D, Fast R, Paganini S, Lawson BO, Nega M, Easley K, Schmitz JE, Bosinger SE, Paiardini M, Chahroudi A, Vanderford TH, Estes JD, Lifson JD, Derdeyn CA, Silvestri G. CD8(+) Lymphocytes Are Required for Maintaining Viral Suppression in SIV-Infected Macaques Treated with Short-Term Antiretroviral Therapy. *Immunity*. 2016;45(3):656-68. doi: 10.1016/j.immuni.2016.08.018. PubMed PMID: 27653601; PMCID: PMC5087330.
277. Nixon CC, Mavigner M, Sampey GC, Brooks AD, Spagnuolo RA, Irlbeck DM, Mattingly C, Ho PT, Schoof N, Cammon CG, Tharp GK, Kanke M, Wang Z, Cleary RA, Upadhyay AA, De C, Wills SR, Falcinelli SD, Galardi C, Walum H, Schramm NJ, Deutsch J, Lifson JD, Fennessey CM, Keele BF, Jean S, Maguire S, Liao B, Browne EP, Ferris RG, Brehm JH, Favre D, Vanderford TH, Bosinger SE, Jones CD, Routy JP, Archin NM, Margolis DM, Wahl A, Dunham RM, Silvestri G, Chahroudi A, Garcia JV. Systemic HIV and SIV latency reversal via non-canonical NF-kappaB signalling in vivo. *Nature*. 2020;578(7793):160-5. Epub 20200122. doi: 10.1038/s41586-020-1951-3. PubMed PMID: 31969707; PMCID: PMC7111210.
278. Mavigner M, Liao LE, Brooks AD, Ke R, Mattingly C, Schoof N, McBrien J, Carnathan D, Liang S, Vanderford TH, Paiardini M, Kulpa D, Lifson JD, Dunham RM, Easley KA, Margolis DM, Perelson AS, Silvestri G, Chahroudi A. CD8 lymphocyte depletion enhances the latency reversal activity of the SMAC mimetic AZD5582 in ART-suppressed SIV-infected rhesus macaques. *J Virol*. 2021;95(8). Epub 20210210. doi: 10.1128/JVI.01429-20. PubMed PMID: 33568515; PMCID: PMC8103677.
279. Uldrick TS, Adams SV, Fromentin R, Roche M, Fling SP, Goncalves PH, Lurain K, Ramaswami R, Wang CJ, Gorelick RJ, Welker JL, O'Donoghue L, Choudhary H, Lifson JD, Rasmussen TA, Rhodes A, Tumpach C, Yarchoan R, Maldarelli F, Cheever MA, Sekaly R, Chomont N, Deeks SG, Lewin SR. Pembrolizumab induces HIV latency reversal in people living with HIV and cancer on antiretroviral therapy. *Sci Transl Med*. 2022;14(629):eabl3836. Epub 20220126. doi: 10.1126/scitranslmed.abl3836. PubMed PMID: 35080914; PMCID: PMC9014398.
280. Fromentin R, DaFonseca S, Costiniuk CT, El-Far M, Procopio FA, Hecht FM, Hoh R, Deeks SG, Hazuda DJ, Lewin SR, Routy JP, Sekaly RP, Chomont N. PD-1 blockade potentiates HIV latency reversal ex vivo in CD4(+) T cells from ART-suppressed individuals. *Nat Commun*. 2019;10(1):814. Epub 20190218. doi: 10.1038/s41467-019-08798-7. PubMed PMID: 30778080; PMCID: PMC6379401.
281. Bui JK, Cyktor JC, Fyne E, Campellone S, Mason SW, Mellors JW. Blockade of the PD-1 axis alone is not sufficient to activate HIV-1 virion production from CD4+ T cells of individuals on suppressive ART. *PLoS One*. 2019;14(1):e0211112. Epub 20190125. doi: 10.1371/journal.pone.0211112. PubMed PMID: 30682108; PMCID: PMC6347234.
282. Etienne L, Nerrienet E, LeBreton M, Bibila GT, Foupouapouognigni Y, Rousset D, Nana A, Djoko CF, Tamoufe U, Aghokeng AF, Mpoudi-Ngole E, Delaporte E, Peeters M, Wolfe ND, Ayoub A. Characterization of a new simian immunodeficiency virus strain in a naturally infected Pan troglodytes troglodytes chimpanzee with AIDS related symptoms. *Retrovirology*.

- 2011;8:4. Epub 20110113. doi: 10.1186/1742-4690-8-4. PubMed PMID: 21232091; PMCID: PMC3034674.
283. Keele BF, Jones JH, Terio KA, Estes JD, Rudicell RS, Wilson ML, Li Y, Learn GH, Beasley TM, Schumacher-Stankey J, Wroblewski E, Mosser A, Raphael J, Kamenya S, Lonsdorf EV, Travis DA, Mlengeya T, Kinsel MJ, Else JG, Silvestri G, Goodall J, Sharp PM, Shaw GM, Pusey AE, Hahn BH. Increased mortality and AIDS-like immunopathology in wild chimpanzees infected with SIVcpz. *Nature*. 2009;460(7254):515-9. doi: 10.1038/nature08200. PubMed PMID: 19626114; PMCID: PMC2872475.
284. Novembre FJ, Saucier M, Anderson DC, Klumpp SA, O'Neil SP, Brown CR, 2nd, Hart CE, Guenther PC, Swenson RB, McClure HM. Development of AIDS in a chimpanzee infected with human immunodeficiency virus type 1. *J Virol*. 1997;71(5):4086-91. doi: 10.1128/JVI.71.5.4086-4091.1997. PubMed PMID: 9094687; PMCID: PMC191562.
285. Kumar N, Chahroudi A, Silvestri G. Animal models to achieve an HIV cure. *Curr Opin HIV AIDS*. 2016;11(4):432-41. doi: 10.1097/COH.0000000000000290. PubMed PMID: 27152962; PMCID: PMC4922307.
286. Hatzioannou T, Evans DT. Animal models for HIV/AIDS research. *Nat Rev Microbiol*. 2012;10(12):852-67. doi: 10.1038/nrmicro2911. PubMed PMID: 23154262; PMCID: PMC4334372.
287. Strongin Z, Micci L, Fromentin R, Harper J, McBrien J, Ryan E, Shenvi N, Easley K, Chomont N, Silvestri G, Paiardini M. Virologic and Immunologic Features of Simian Immunodeficiency Virus Control Post-ART Interruption in Rhesus Macaques. *J Virol*. 2020;94(14). Epub 20200701. doi: 10.1128/JVI.00338-20. PubMed PMID: 32350073; PMCID: PMC7343203.
288. Immonen TT, Camus C, Reid C, Fennessey CM, Del Prete GQ, Davenport MP, Lifson JD, Keele BF. Genetically barcoded SIV reveals the emergence of escape mutations in multiple viral lineages during immune escape. *Proc Natl Acad Sci U S A*. 2020;117(1):494-502. Epub 20191216. doi: 10.1073/pnas.1914967117. PubMed PMID: 31843933; PMCID: PMC6955354.
289. Williams K, Lackner A, Mallard J. Non-human primate models of SIV infection and CNS neuropathology. *Curr Opin Virol*. 2016;19:92-8. Epub 20160818. doi: 10.1016/j.coviro.2016.07.012. PubMed PMID: 27544476; PMCID: PMC5021597.
290. Bar KJ, Coronado E, Hensley-McBain T, O'Connor MA, Osborn JM, Miller C, Gott TM, Wangari S, Iwayama N, Ahrens CY, Smedley J, Moats C, Lynch RM, Haddad EK, Haigwood NL, Fuller DH, Shaw GM, Klatt NR, Manuzak JA. Simian-Human Immunodeficiency Virus SHIV.CH505 Infection of Rhesus Macaques Results in Persistent Viral Replication and Induces Intestinal Immunopathology. *J Virol*. 2019;93(18). Epub 20190828. doi: 10.1128/JVI.00372-19. PubMed PMID: 31217249; PMCID: PMC6714786.
291. Li J, Lord CI, Haseltine W, Letvin NL, Sodroski J. Infection of cynomolgus monkeys with a chimeric HIV-1/SIVmac virus that expresses the HIV-1 envelope glycoproteins. *J Acquir Immune Defic Syndr (1988)*. 1992;5(7):639-46. PubMed PMID: 1613662.
292. Huot N, Jacquelin B, Garcia-Tellez T, Rasclé P, Ploquin MJ, Madec Y, Reeves RK, Derreudre-Bosquet N, Muller-Trutwin M. Natural killer cells migrate into and control simian immunodeficiency virus replication in lymph node follicles in African green monkeys. *Nat Med*. 2017;23(11):1277-86. Epub 20171016. doi: 10.1038/nm.4421. PubMed PMID: 29035370; PMCID: PMC6362838.

293. Bosinger SE, Li Q, Gordon SN, Klatt NR, Duan L, Xu L, Francella N, Sidahmed A, Smith AJ, Cramer EM, Zeng M, Masopust D, Carlis JV, Ran L, Vanderford TH, Paiardini M, Isett RB, Baldwin DA, Else JG, Staprans SI, Silvestri G, Haase AT, Kelvin DJ. Global genomic analysis reveals rapid control of a robust innate response in SIV-infected sooty mangabeys. *J Clin Invest.* 2009;119(12):3556-72. doi: 10.1172/JCI40115. PubMed PMID: 19959874; PMCID: PMC2786806.
294. Jacquelin B, Mayau V, Targat B, Liovat AS, Kunkel D, Petitjean G, Dillies MA, Roques P, Butor C, Silvestri G, Giavedoni LD, Lebon P, Barre-Sinoussi F, Benecke A, Muller-Trutwin MC. Nonpathogenic SIV infection of African green monkeys induces a strong but rapidly controlled type I IFN response. *J Clin Invest.* 2009;119(12):3544-55. doi: 10.1172/JCI40093. PubMed PMID: 19959873; PMCID: PMC2786805.
295. Marsden MD. Benefits and limitations of humanized mice in HIV persistence studies. *Retrovirology.* 2020;17(1):7. Epub 20200406. doi: 10.1186/s12977-020-00516-2. PubMed PMID: 32252791; PMCID: PMC7137310.
296. Global HIV & AIDS statistics — Fact sheet: UNAIDS. Available from: <https://www.unaids.org/en/resources/fact-sheet>.
297. Teeraananchai S, Kerr SJ, Amin J, Ruxrungtham K, Law MG. Life expectancy of HIV-positive people after starting combination antiretroviral therapy: a meta-analysis. *HIV Med.* 2017;18(4):256-66. Epub 20160831. doi: 10.1111/hiv.12421. PubMed PMID: 27578404.
298. Bhaskaran K, Hamouda O, Sannes M, Boufassa F, Johnson AM, Lambert PC, Porter K, Collaboration C. Changes in the risk of death after HIV seroconversion compared with mortality in the general population. *JAMA.* 2008;300(1):51-9. doi: 10.1001/jama.300.1.51. PubMed PMID: 18594040.
299. Calin R, Hamimi C, Lambert-Niclot S, Carcelain G, Bellet J, Assoumou L, Tubiana R, Calvez V, Dudoit Y, Costagliola D, Autran B, Katlama C, Group US. Treatment interruption in chronically HIV-infected patients with an ultralow HIV reservoir. *AIDS.* 2016;30(5):761-9. doi: 10.1097/QAD.0000000000000987. PubMed PMID: 26730568.
300. Van Gulck E, Bracke L, Heyndrickx L, Coppens S, Atkinson D, Merlin C, Pasternak A, Florence E, Vanham G. Immune and viral correlates of "secondary viral control" after treatment interruption in chronically HIV-1 infected patients. *PLoS One.* 2012;7(5):e37792. Epub 20120530. doi: 10.1371/journal.pone.0037792. PubMed PMID: 22666392; PMCID: PMC3364270.
301. Fidler S, Olson AD, Bucher HC, Fox J, Thornhill J, Morrison C, Muga R, Phillips A, Frater J, Porter K. Virological Blips and Predictors of Post Treatment Viral Control After Stopping ART Started in Primary HIV Infection. *J Acquir Immune Defic Syndr.* 2017;74(2):126-33. doi: 10.1097/QAI.0000000000001220. PubMed PMID: 27846036; PMCID: PMC5228612.
302. Sneller MC, Justement JS, Gittens KR, Petrone ME, Clarridge KE, Proschan MA, Kwan R, Shi V, Blazkova J, Refsland EW, Morris DE, Cohen KW, McElrath MJ, Xu R, Egan MA, Eldridge JH, Benko E, Kovacs C, Moir S, Chun TW, Fauci AS. A randomized controlled safety/efficacy trial of therapeutic vaccination in HIV-infected individuals who initiated antiretroviral therapy early in infection. *Sci Transl Med.* 2017;9(419). doi: 10.1126/scitranslmed.aan8848. PubMed PMID: 29212716.
303. Samri A, Bacchus-Souffan C, Hocqueloux L, Avettand-Fenoel V, Descours B, Theodorou I, Larsen M, Saez-Cirion A, Rouzioux C, Autran B, group AVs. Polyfunctional HIV-specific T cells in

- Post-Treatment Controllers. *AIDS*. 2016;30(15):2299-302. doi: 10.1097/QAD.0000000000001195. PubMed PMID: 27428742.
304. Migueles SA, Connors M. Long-term nonprogressive disease among untreated HIV-infected individuals: clinical implications of understanding immune control of HIV. *JAMA*. 2010;304(2):194-201. doi: 10.1001/jama.2010.925. PubMed PMID: 20628133.
305. Assoumou L, Weiss L, Piketty C, Burgard M, Melard A, Girard PM, Rouzioux C, Costagliola D, group ASs. A low HIV-DNA level in peripheral blood mononuclear cells at antiretroviral treatment interruption predicts a higher probability of maintaining viral control. *AIDS*. 2015;29(15):2003-7. doi: 10.1097/QAD.0000000000000734. PubMed PMID: 26355572.
306. Yant LJ, Friedrich TC, Johnson RC, May GE, Maness NJ, Enz AM, Lifson JD, O'Connor DH, Carrington M, Watkins DI. The high-frequency major histocompatibility complex class I allele Mamu-B*17 is associated with control of simian immunodeficiency virus SIVmac239 replication. *J Virol*. 2006;80(10):5074-7. doi: 10.1128/JVI.80.10.5074-5077.2006. PubMed PMID: 16641299; PMCID: PMC1472056.
307. Loffredo JT, Friedrich TC, Leon EJ, Stephany JJ, Rodrigues DS, Spencer SP, Bean AT, Beal DR, Burwitz BJ, Rudersdorf RA, Wallace LT, Piaskowski SM, May GE, Sidney J, Gostick E, Wilson NA, Price DA, Kallas EG, Piontkivska H, Hughes AL, Sette A, Watkins DI. CD8+ T cells from SIV elite controller macaques recognize Mamu-B*08-bound epitopes and select for widespread viral variation. *PLoS One*. 2007;2(11):e1152. Epub 20071114. doi: 10.1371/journal.pone.0001152. PubMed PMID: 18000532; PMCID: PMC2062500.
308. Pino M, Paganini S, Deleage C, Padhan K, Harper JL, King CT, Micci L, Cervasi B, Mudd JC, Gill KP, Jean SM, Easley K, Silvestri G, Estes JD, Petrovas C, Lederman MM, Paiardini M. Fingolimod retains cytolytic T cells and limits T follicular helper cell infection in lymphoid sites of SIV persistence. *PLoS Pathog*. 2019;15(10):e1008081. Epub 20191018. doi: 10.1371/journal.ppat.1008081. PubMed PMID: 31626660; PMCID: PMC6834281.
309. Cecchinato V, Trindade CJ, Laurence A, Heraud JM, Brenchley JM, Ferrari MG, Zaffiri L, Trynieszewska E, Tsai WP, Vaccari M, Parks RW, Venzon D, Douek DC, O'Shea JJ, Franchini G. Altered balance between Th17 and Th1 cells at mucosal sites predicts AIDS progression in simian immunodeficiency virus-infected macaques. *Mucosal Immunol*. 2008;1(4):279-88. Epub 20080507. doi: 10.1038/mi.2008.14. PubMed PMID: 19079189; PMCID: PMC2997489.
310. Micci L, Cervasi B, Ende ZS, Iriele RI, Reyes-Aviles E, Vinton C, Else J, Silvestri G, Ansari AA, Villinger F, Pahwa S, Estes JD, Brenchley JM, Paiardini M. Paucity of IL-21-producing CD4(+) T cells is associated with Th17 cell depletion in SIV infection of rhesus macaques. *Blood*. 2012;120(19):3925-35. Epub 20120918. doi: 10.1182/blood-2012-04-420240. PubMed PMID: 22990011; PMCID: PMC3496953.
311. Pallikkuth S, Micci L, Ende ZS, Iriele RI, Cervasi B, Lawson B, McGary CS, Rogers KA, Else JG, Silvestri G, Easley K, Estes JD, Villinger F, Pahwa S, Paiardini M. Maintenance of intestinal Th17 cells and reduced microbial translocation in SIV-infected rhesus macaques treated with interleukin (IL)-21. *PLoS Pathog*. 2013;9(7):e1003471. Epub 20130704. doi: 10.1371/journal.ppat.1003471. PubMed PMID: 23853592; PMCID: PMC3701718.
312. Klatt NR, Estes JD, Sun X, Ortiz AM, Barber JS, Harris LD, Cervasi B, Yokomizo LK, Pan L, Vinton CL, Tabb B, Canary LA, Dang Q, Hirsch VM, Alter G, Belkaid Y, Lifson JD, Silvestri G, Milner JD, Paiardini M, Haddad EK, Brenchley JM. Loss of mucosal CD103+ DCs and IL-17+ and IL-22+ lymphocytes is associated with mucosal damage in SIV infection. *Mucosal Immunol*.

2012;5(6):646-57. Epub 20120530. doi: 10.1038/mi.2012.38. PubMed PMID: 22643849; PMCID: PMC3443541.

313. Del Prete GQ, Shoemaker R, Oswald K, Lara A, Trubey CM, Fast R, Schneider DK, Kiser R, Coalter V, Wiles A, Wiles R, Freemire B, Keele BF, Estes JD, Quinones OA, Smedley J, Macallister R, Sanchez RI, Wai JS, Tan CM, Alvord WG, Hazuda DJ, Piatak M, Jr., Lifson JD. Effect of suberoylanilide hydroxamic acid (SAHA) administration on the residual virus pool in a model of combination antiretroviral therapy-mediated suppression in SIVmac239-infected indian rhesus macaques. *Antimicrob Agents Chemother.* 2014;58(11):6790-806. Epub 20140902. doi: 10.1128/AAC.03746-14. PubMed PMID: 25182644; PMCID: PMC4249371.

314. Goujard C, Girault I, Rouzioux C, Lecuroux C, Deveau C, Chaix ML, Jacomet C, Talamali A, Delfraissy JF, Venet A, Meyer L, Sinet M, Group ACPS. HIV-1 control after transient antiretroviral treatment initiated in primary infection: role of patient characteristics and effect of therapy. *Antivir Ther.* 2012;17(6):1001-9. Epub 20120806. doi: 10.3851/IMP2273. PubMed PMID: 22865544.

315. Williams JP, Hurst J, Stohr W, Robinson N, Brown H, Fisher M, Kinloch S, Cooper D, Schechter M, Tambussi G, Fidler S, Carrington M, Babiker A, Weber J, Koelsch KK, Kelleher AD, Phillips RE, Frater J, Investigators SP. HIV-1 DNA predicts disease progression and post-treatment virological control. *Elife.* 2014;3:e03821. Epub 20140912. doi: 10.7554/eLife.03821. PubMed PMID: 25217531; PMCID: PMC4199415.

316. Khoury G, Anderson JL, Fromentin R, Hartogenesis W, Smith MZ, Bacchetti P, Hecht FM, Chomont N, Cameron PU, Deeks SG, Lewin SR. Persistence of integrated HIV DNA in CXCR3 + CCR6 + memory CD4+ T cells in HIV-infected individuals on antiretroviral therapy. *AIDS.* 2016;30(10):1511-20. doi: 10.1097/QAD.0000000000001029. PubMed PMID: 26807971; PMCID: PMC4889535.

317. Gosselin A, Wiche Salinas TR, Planas D, Wacleche VS, Zhang Y, Fromentin R, Chomont N, Cohen EA, Shacklett B, Mehraj V, Ghali MP, Routy JP, Ancuta P. HIV persists in CCR6+CD4+ T cells from colon and blood during antiretroviral therapy. *AIDS.* 2017;31(1):35-48. doi: 10.1097/QAD.0000000000001309. PubMed PMID: 27835617; PMCID: PMC5131694.

318. Wacleche VS, Goulet JP, Gosselin A, Monteiro P, Soudeyns H, Fromentin R, Jenabian MA, Vartanian S, Deeks SG, Chomont N, Routy JP, Ancuta P. New insights into the heterogeneity of Th17 subsets contributing to HIV-1 persistence during antiretroviral therapy. *Retrovirology.* 2016;13(1):59. Epub 20160824. doi: 10.1186/s12977-016-0293-6. PubMed PMID: 27553844; PMCID: PMC4995622.

319. Stieh DJ, Matias E, Xu H, Fought AJ, Blanchard JL, Marx PA, Veazey RS, Hope TJ. Th17 Cells Are Preferentially Infected Very Early after Vaginal Transmission of SIV in Macaques. *Cell Host Microbe.* 2016;19(4):529-40. doi: 10.1016/j.chom.2016.03.005. PubMed PMID: 27078070; PMCID: PMC4841252.

320. Macal M, Sankaran S, Chun TW, Reay E, Flamm J, Prindiville TJ, Dandekar S. Effective CD4+ T-cell restoration in gut-associated lymphoid tissue of HIV-infected patients is associated with enhanced Th17 cells and polyfunctional HIV-specific T-cell responses. *Mucosal Immunol.* 2008;1(6):475-88. Epub 20080910. doi: 10.1038/mi.2008.35. PubMed PMID: 19079215.

321. Gordon SN, Klatt NR, Bosinger SE, Brenchley JM, Milush JM, Engram JC, Dunham RM, Paiardini M, Klucking S, Danesh A, Strobert EA, Apetrei C, Pandrea IV, Kelvin D, Douek DC, Staprans SI, Sodora DL, Silvestri G. Severe depletion of mucosal CD4+ T cells in AIDS-free simian

- immunodeficiency virus-infected sooty mangabeys. *J Immunol*. 2007;179(5):3026-34. doi: 10.4049/jimmunol.179.5.3026. PubMed PMID: 17709517; PMCID: PMC2365740.
322. Schuetz A, Deleage C, Sereti I, Rerknimitr R, Phanuphak N, Phuang-Ngern Y, Estes JD, Sandler NG, Sukhumvittaya S, Marovich M, Jongrakthaitae S, Akapirat S, Fletscher JL, Kroon E, Dewar R, Trichavaroj R, Chomchey N, Douek DC, RJ OC, Ngauy V, Robb ML, Phanuphak P, Michael NL, Excler JL, Kim JH, de Souza MS, Ananworanich J, Rv254/Search, Groups RSS. Initiation of ART during early acute HIV infection preserves mucosal Th17 function and reverses HIV-related immune activation. *PLoS Pathog*. 2014;10(12):e1004543. Epub 20141211. doi: 10.1371/journal.ppat.1004543. PubMed PMID: 25503054; PMCID: PMC4263756.
323. Kok A, Hocqueloux L, Hocini H, Carriere M, Lefrou L, Guguin A, Tisserand P, Bonnabau H, Avettand-Fenoel V, Prazuck T, Katsahian S, Gaulard P, Thiebaut R, Levy Y, Hue S. Early initiation of combined antiretroviral therapy preserves immune function in the gut of HIV-infected patients. *Mucosal Immunol*. 2015;8(1):127-40. Epub 20140702. doi: 10.1038/mi.2014.50. PubMed PMID: 24985081.
324. Frange P, Faye A, Avettand-Fenoel V, Bellaton E, Descamps D, Angin M, David A, Caillat-Zucman S, Peytavin G, Dollfus C, Le Chenadec J, Warszawski J, Rouzioux C, Saez-Cirion A, Cohort AE-CP, the AEPVsg. HIV-1 virological remission lasting more than 12 years after interruption of early antiretroviral therapy in a perinatally infected teenager enrolled in the French ANRS EPF-CO10 paediatric cohort: a case report. *Lancet HIV*. 2016;3(1):e49-54. Epub 20151209. doi: 10.1016/S2352-3018(15)00232-5. PubMed PMID: 26762993.
325. Salgado M, Rabi SA, O'Connell KA, Buckheit RW, 3rd, Bailey JR, Chaudhry AA, Breaud AR, Marzinke MA, Clarke W, Margolick JB, Siliciano RF, Blankson JN. Prolonged control of replication-competent dual- tropic human immunodeficiency virus-1 following cessation of highly active antiretroviral therapy. *Retrovirology*. 2011;8:97. Epub 20111205. doi: 10.1186/1742-4690-8-97. PubMed PMID: 22141397; PMCID: PMC3293762.
326. Hofmann-Lehmann R, Swenerton RK, Liska V, Leutenegger CM, Lutz H, McClure HM, Ruprecht RM. Sensitive and robust one-tube real-time reverse transcriptase-polymerase chain reaction to quantify SIV RNA load: comparison of one- versus two-enzyme systems. *AIDS Res Hum Retroviruses*. 2000;16(13):1247-57. doi: 10.1089/08892220050117014. PubMed PMID: 10957722.
327. Myers LE, McQuay LJ, Hollinger FB. Dilution assay statistics. *J Clin Microbiol*. 1994;32(3):732-9. doi: 10.1128/jcm.32.3.732-739.1994. PubMed PMID: 8195386; PMCID: PMC263116.
328. Antiretroviral Therapy Cohort C. Life expectancy of individuals on combination antiretroviral therapy in high-income countries: a collaborative analysis of 14 cohort studies. *Lancet*. 2008;372(9635):293-9. Epub 2008/07/29. doi: 10.1016/S0140-6736(08)61113-7. PubMed PMID: 18657708; PMCID: PMC3130543.
329. Hiener B, Horsburgh BA, Eden JS, Barton K, Schlub TE, Lee E, von Stockenstrom S, Odevall L, Milush JM, Liegler T, Sinclair E, Hoh R, Boritz EA, Douek D, Fromentin R, Chomont N, Deeks SG, Hecht FM, Palmer S. Identification of Genetically Intact HIV-1 Proviruses in Specific CD4(+) T Cells from Effectively Treated Participants. *Cell Rep*. 2017;21(3):813-22. doi: 10.1016/j.celrep.2017.09.081. PubMed PMID: 29045846; PMCID: PMC5960642.
330. Gosselin A, Monteiro P, Chomont N, Diaz-Griffero F, Said EA, Fonseca S, Wacleche V, El-Far M, Boulassel MR, Routy JP, Sekaly RP, Ancuta P. Peripheral blood CCR4+CCR6+ and

- CXCR3+CCR6+CD4+ T cells are highly permissive to HIV-1 infection. *J Immunol.* 2010;184(3):1604-16. Epub 20091230. doi: 10.4049/jimmunol.0903058. PubMed PMID: 20042588; PMCID: PMC4321756.
331. Duette G, Hiener B, Morgan H, Mazur FG, Mathivanan V, Horsburgh BA, Fisher K, Tong O, Lee E, Ahn H, Shaik A, Fromentin R, Hoh R, Bacchus-Souffan C, Nasr N, Cunningham A, Hunt PW, Chomont N, Turville SG, Deeks SG, Kelleher AD, Schlub TE, Palmer S. The HIV-1 proviral landscape reveals Nef contributes to HIV-1 persistence in effector memory CD4+ T-cells. *J Clin Invest.* 2022. Epub 20220208. doi: 10.1172/JCI154422. PubMed PMID: 35133986.
332. Soriano-Sarabia N, Bateson RE, Dahl NP, Crooks AM, Kuruc JD, Margolis DM, Archin NM. Quantitation of replication-competent HIV-1 in populations of resting CD4+ T cells. *J Virol.* 2014;88(24):14070-7. Epub 20140924. doi: 10.1128/JVI.01900-14. PubMed PMID: 25253353; PMCID: PMC4249150.
333. Pino M, Pereira Ribeiro S, Pagliuzza A, Ghneim K, Khan A, Ryan E, Harper JL, King CT, Welbourn S, Micci L, Aldrete S, Delman KA, Stuart T, Lowe M, Brenchley JM, Derdeyn CA, Easley K, Sekaly RP, Chomont N, Paiardini M, Marconi VC. Increased homeostatic cytokines and stability of HIV-infected memory CD4 T-cells identify individuals with suboptimal CD4 T-cell recovery on-ART. *PLoS Pathog.* 2021;17(8):e1009825. Epub 20210827. doi: 10.1371/journal.ppat.1009825. PubMed PMID: 34449812; PMCID: PMC8397407.
334. Baxter AE, Niessl J, Fromentin R, Richard J, Porichis F, Charlebois R, Massanella M, Brassard N, Alsahafi N, Delgado GG, Routy JP, Walker BD, Finzi A, Chomont N, Kaufmann DE. Single-Cell Characterization of Viral Translation-Competent Reservoirs in HIV-Infected Individuals. *Cell Host Microbe.* 2016;20(3):368-80. Epub 20160818. doi: 10.1016/j.chom.2016.07.015. PubMed PMID: 27545045; PMCID: PMC5025389.
335. Oswald-Richter K, Grill SM, Shariat N, Leelawong M, Sundrud MS, Haas DW, Unutmaz D. HIV infection of naturally occurring and genetically reprogrammed human regulatory T-cells. *PLoS Biol.* 2004;2(7):E198. Epub 20040713. doi: 10.1371/journal.pbio.0020198. PubMed PMID: 15252446; PMCID: PMC449855.
336. Abrahams MR, Joseph SB, Garrett N, Tyers L, Moeser M, Archin N, Council OD, Matten D, Zhou S, Doolabh D, Anthony C, Goonetilleke N, Karim SA, Margolis DM, Pond SK, Williamson C, Swanstrom R. The replication-competent HIV-1 latent reservoir is primarily established near the time of therapy initiation. *Sci Transl Med.* 2019;11(513). Epub 2019/10/11. doi: 10.1126/scitranslmed.aaw5589. PubMed PMID: 31597754; PMCID: PMC7233356.
337. Brodin J, Zanini F, Thebo L, Lanz C, Bratt G, Neher RA, Albert J. Establishment and stability of the latent HIV-1 DNA reservoir. *Elife.* 2016;5. Epub 2016/11/18. doi: 10.7554/eLife.18889. PubMed PMID: 27855060; PMCID: PMC5201419.
338. Sereti I, Krebs SJ, Phanuphak N, Fletcher JL, Slike B, Pinyakorn S, O'Connell RJ, Rupert A, Chomont N, Valcour V, Kim JH, Robb ML, Michael NL, Douek DC, Ananworanich J, Utay NS, Rv254/Search RS, teams Sp. Persistent, Albeit Reduced, Chronic Inflammation in Persons Starting Antiretroviral Therapy in Acute HIV Infection. *Clin Infect Dis.* 2017;64(2):124-31. Epub 2016/10/16. doi: 10.1093/cid/ciw683. PubMed PMID: 27737952; PMCID: PMC5215214.
339. Rivas A, Ruegg CL, Zeitung J, Laus R, Warnke R, Benike C, Engleman EG. V7, a novel leukocyte surface protein that participates in T cell activation. I. Tissue distribution and functional studies. *J Immunol.* 1995;154(9):4423-33. PubMed PMID: 7722299.

340. Ruegg CL, Rivas A, Madani ND, Zeitung J, Laus R, Engleman EG. V7, a novel leukocyte surface protein that participates in T cell activation. II. Molecular cloning and characterization of the V7 gene. *J Immunol.* 1995;154(9):4434-43. PubMed PMID: 7722300.
341. Soares LR, Tsavaler L, Rivas A, Engleman EG. V7 (CD101) ligation inhibits TCR/CD3-induced IL-2 production by blocking Ca²⁺ flux and nuclear factor of activated T cell nuclear translocation. *J Immunol.* 1998;161(1):209-17. PubMed PMID: 9647226.
342. Fernandez I, Zeiser R, Karsunky H, Kambham N, Beilhack A, Soderstrom K, Negrin RS, Engleman E. CD101 surface expression discriminates potency among murine FoxP3⁺ regulatory T cells. *J Immunol.* 2007;179(5):2808-14. doi: 10.4049/jimmunol.179.5.2808. PubMed PMID: 17709494.
343. Rainbow DB, Moule C, Fraser HI, Clark J, Howlett SK, Burren O, Christensen M, Moody V, Steward CA, Mohammed JP, Fusakio ME, Masteller EL, Finger EB, Houchins JP, Naf D, Koentgen F, Ridgway WM, Todd JA, Bluestone JA, Peterson LB, Mattner J, Wicker LS. Evidence that Cd101 is an autoimmune diabetes gene in nonobese diabetic mice. *J Immunol.* 2011;187(1):325-36. Epub 20110525. doi: 10.4049/jimmunol.1003523. PubMed PMID: 21613616; PMCID: PMC3128927.
344. Schey R, Dornhoff H, Baier JL, Purtak M, Opoka R, Koller AK, Atreya R, Rau TT, Daniel C, Amann K, Bogdan C, Mattner J. CD101 inhibits the expansion of colitogenic T cells. *Mucosal Immunol.* 2016;9(5):1205-17. Epub 20160127. doi: 10.1038/mi.2015.139. PubMed PMID: 26813346; PMCID: PMC4963314.
345. Kumar BV, Ma W, Miron M, Granot T, Guyer RS, Carpenter DJ, Senda T, Sun X, Ho SH, Lerner H, Friedman AL, Shen Y, Farber DL. Human Tissue-Resident Memory T Cells Are Defined by Core Transcriptional and Functional Signatures in Lymphoid and Mucosal Sites. *Cell Rep.* 2017;20(12):2921-34. doi: 10.1016/j.celrep.2017.08.078. PubMed PMID: 28930685; PMCID: PMC5646692.
346. Snyder ME, Finlayson MO, Connors TJ, Dogra P, Senda T, Bush E, Carpenter D, Marboe C, Benvenuto L, Shah L, Robbins H, Hook JL, Sykes M, D'Ovidio F, Bacchetta M, Sonett JR, Lederer DJ, Arcasoy S, Sims PA, Farber DL. Generation and persistence of human tissue-resident memory T cells in lung transplantation. *Sci Immunol.* 2019;4(33). doi: 10.1126/sciimmunol.aav5581. PubMed PMID: 30850393; PMCID: PMC6435356.
347. Zander R, Schauder D, Xin G, Nguyen C, Wu X, Zajac A, Cui W. CD4(+) T Cell Help Is Required for the Formation of a Cytolytic CD8(+) T Cell Subset that Protects against Chronic Infection and Cancer. *Immunity.* 2019;51(6):1028-42 e4. Epub 20191203. doi: 10.1016/j.immuni.2019.10.009. PubMed PMID: 31810883; PMCID: PMC6929322.
348. Hudson WH, Gensheimer J, Hashimoto M, Wieland A, Valanparambil RM, Li P, Lin JX, Konieczny BT, Im SJ, Freeman GJ, Leonard WJ, Kissick HT, Ahmed R. Proliferating Transitory T Cells with an Effector-like Transcriptional Signature Emerge from PD-1(+) Stem-like CD8(+) T Cells during Chronic Infection. *Immunity.* 2019;51(6):1043-58 e4. Epub 2019/12/08. doi: 10.1016/j.immuni.2019.11.002. PubMed PMID: 31810882; PMCID: PMC6920571.
349. Beyer M, Thabet Y, Muller RU, Sadlon T, Classen S, Lahl K, Basu S, Zhou X, Bailey-Bucktrout SL, Krebs W, Schonfeld EA, Bottcher J, Golovina T, Mayer CT, Hofmann A, Sommer D, Debey-Pascher S, Endl E, Limmer A, Hippen KL, Blazar BR, Balderas R, Quast T, Waha A, Mayer G, Famulok M, Knolle PA, Wickenhauser C, Kolanus W, Schermer B, Bluestone JA, Barry SC, Sparwasser T, Riley JL, Schultze JL. Repression of the genome organizer SATB1 in regulatory T

cells is required for suppressive function and inhibition of effector differentiation. *Nat Immunol.* 2011;12(9):898-907. Epub 20110814. doi: 10.1038/ni.2084. PubMed PMID: 21841785; PMCID: PMC3669688.

350. Amoozgar Z, Kloepper J, Ren J, Tay RE, Kazer SW, Kiner E, Krishnan S, Posada JM, Ghosh M, Mamessier E, Wong C, Ferraro GB, Batista A, Wang N, Badeaux M, Roberge S, Xu L, Huang P, Shalek AK, Fukumura D, Kim HJ, Jain RK. Targeting Treg cells with GITR activation alleviates resistance to immunotherapy in murine glioblastomas. *Nat Commun.* 2021;12(1):2582. Epub 20210511. doi: 10.1038/s41467-021-22885-8. PubMed PMID: 33976133; PMCID: PMC8113440.

351. Schaer DA, Murphy JT, Wolchok JD. Modulation of GITR for cancer immunotherapy. *Curr Opin Immunol.* 2012;24(2):217-24. Epub 20120112. doi: 10.1016/j.coi.2011.12.011. PubMed PMID: 22245556; PMCID: PMC3413251.

352. Smith LK, Boukhaled GM, Condotta SA, Mazouz S, Guthmiller JJ, Vijay R, Butler NS, Bruneau J, Shoukry NH, Krawczyk CM, Richer MJ. Interleukin-10 Directly Inhibits CD8(+) T Cell Function by Enhancing N-Glycan Branching to Decrease Antigen Sensitivity. *Immunity.* 2018;48(2):299-312 e5. Epub 2018/02/06. doi: 10.1016/j.immuni.2018.01.006. PubMed PMID: 29396160; PMCID: PMC5935130.

353. Stockis J, Colau D, Coulie PG, Lucas S. Membrane protein GARP is a receptor for latent TGF-beta on the surface of activated human Treg. *Eur J Immunol.* 2009;39(12):3315-22. doi: 10.1002/eji.200939684. PubMed PMID: 19750484.

354. Tran DQ, Andersson J, Wang R, Ramsey H, Unutmaz D, Shevach EM. GARP (LRRC32) is essential for the surface expression of latent TGF-beta on platelets and activated FOXP3+ regulatory T cells. *Proc Natl Acad Sci U S A.* 2009;106(32):13445-50. Epub 20090727. doi: 10.1073/pnas.0901944106. PubMed PMID: 19651619; PMCID: PMC2726354.

355. Kim KK, Sheppard D, Chapman HA. TGF-beta1 Signaling and Tissue Fibrosis. *Cold Spring Harb Perspect Biol.* 2018;10(4). Epub 20180402. doi: 10.1101/cshperspect.a022293. PubMed PMID: 28432134; PMCID: PMC5880172.

356. Brenchley JM, Douek DC. The mucosal barrier and immune activation in HIV pathogenesis. *Curr Opin HIV AIDS.* 2008;3(3):356-61. doi: 10.1097/COH.0b013e3282f9ae9c. PubMed PMID: 19372990; PMCID: PMC2789390.

357. Hao XP, Lucero CM, Turkbey B, Bernardo ML, Morcock DR, Deleage C, Trubey CM, Smedley J, Klatt NR, Giavedoni LD, Kristoff J, Xu A, Del Prete GQ, Keele BF, Rao SS, Alvord WG, Choyke PL, Lifson JD, Brenchley JM, Apetrei C, Pandrea I, Estes JD. Experimental colitis in SIV-uninfected rhesus macaques recapitulates important features of pathogenic SIV infection. *Nat Commun.* 2015;6:8020. Epub 20150818. doi: 10.1038/ncomms9020. PubMed PMID: 26282376; PMCID: PMC4544774.

358. Siro A, Schuetz A, Sheward D, Joag V, Yegorov S, Liebenberg LJ, Yende-Zuma N, Stalker A, Mwatelah RS, Selhorst P, Garrett N, Samsunder N, Balgobin A, Nawaz F, Cicala C, Arthos J, Fauci AS, Anzala AO, Kimani J, Bagaya BS, Kiwanuka N, Williamson C, Kaul R, Passmore JS, Phanuphak N, Ananworanich J, Ansari A, Abdool Karim Q, Abdool Karim SS, McKinnon LR, Caprisona, groups RVs. Integrin alpha4beta7 expression on peripheral blood CD4(+) T cells predicts HIV acquisition and disease progression outcomes. *Sci Transl Med.* 2018;10(425). doi: 10.1126/scitranslmed.aam6354. PubMed PMID: 29367348; PMCID: PMC6820005.

359. Hunt PW, Sinclair E, Rodriguez B, Shive C, Clagett B, Funderburg N, Robinson J, Huang Y, Epling L, Martin JN, Deeks SG, Meinert CL, Van Natta ML, Jabs DA, Lederman MM. Gut epithelial

- barrier dysfunction and innate immune activation predict mortality in treated HIV infection. *J Infect Dis.* 2014;210(8):1228-38. Epub 2014/04/24. doi: 10.1093/infdis/jiu238. PubMed PMID: 24755434; PMCID: PMC4192038.
360. Borsellino G, Kleinewietfeld M, Di Mitri D, Sternjak A, Diamantini A, Giometto R, Hopner S, Centonze D, Bernardi G, Dell'Acqua ML, Rossini PM, Battistini L, Rotzschke O, Falk K. Expression of ectonucleotidase CD39 by Foxp3⁺ Treg cells: hydrolysis of extracellular ATP and immune suppression. *Blood.* 2007;110(4):1225-32. Epub 20070420. doi: 10.1182/blood-2006-12-064527. PubMed PMID: 17449799.
361. Joller N, Lozano E, Burkett PR, Patel B, Xiao S, Zhu C, Xia J, Tan TG, Sefik E, Yajnik V, Sharpe AH, Quintana FJ, Mathis D, Benoist C, Hafler DA, Kuchroo VK. Treg cells expressing the coinhibitory molecule TIGIT selectively inhibit proinflammatory Th1 and Th17 cell responses. *Immunity.* 2014;40(4):569-81. doi: 10.1016/j.immuni.2014.02.012. PubMed PMID: 24745333; PMCID: PMC4070748.
362. Kurtulus S, Sakuishi K, Ngiow SF, Joller N, Tan DJ, Teng MW, Smyth MJ, Kuchroo VK, Anderson AC. TIGIT predominantly regulates the immune response via regulatory T cells. *J Clin Invest.* 2015;125(11):4053-62. Epub 20150928. doi: 10.1172/JCI81187. PubMed PMID: 26413872; PMCID: PMC4639980.
363. Simonetti FR, Zhang H, Soroosh GP, Duan J, Rhodehouse K, Hill AL, Beg SA, McCormick K, Raymond HE, Nobles CL, Everett JK, Kwon KJ, White JA, Lai J, Margolick JB, Hoh R, Deeks SG, Bushman FD, Siliciano JD, Siliciano RF. Antigen-driven clonal selection shapes the persistence of HIV-1-infected CD4⁺ T cells in vivo. *J Clin Invest.* 2021;131(3). doi: 10.1172/JCI145254. PubMed PMID: 33301425; PMCID: PMC7843227.
364. Osuji FN, Onyenekwe CC, Ahaneku JE, Ukibe NR. The effects of highly active antiretroviral therapy on the serum levels of pro-inflammatory and anti-inflammatory cytokines in HIV infected subjects. *J Biomed Sci.* 2018;25(1):88. Epub 20181203. doi: 10.1186/s12929-018-0490-9. PubMed PMID: 30501642; PMCID: PMC6276218.
365. Bergstresser S, Kulpa DA. TGF-beta Signaling Supports HIV Latency in a Memory CD4⁺ T Cell Based In Vitro Model. *Methods Mol Biol.* 2022;2407:69-79. doi: 10.1007/978-1-0716-1871-4_6. PubMed PMID: 34985658.
366. Cheung KW, Wu T, Ho SF, Wong YC, Liu L, Wang H, Chen Z. alpha4beta7(+) CD4(+) Effector/Effector Memory T Cells Differentiate into Productively and Latently Infected Central Memory T Cells by Transforming Growth Factor beta1 during HIV-1 Infection. *J Virol.* 2018;92(8). Epub 20180328. doi: 10.1128/JVI.01510-17. PubMed PMID: 29386290; PMCID: PMC5874435.
367. Chinnapaiyan S, Dutta RK, Nair M, Chand HS, Rahman I, Unwalla HJ. TGF-beta1 increases viral burden and promotes HIV-1 latency in primary differentiated human bronchial epithelial cells. *Sci Rep.* 2019;9(1):12552. Epub 20190829. doi: 10.1038/s41598-019-49056-6. PubMed PMID: 31467373; PMCID: PMC6715689.
368. Bruner KM, Wang Z, Simonetti FR, Bender AM, Kwon KJ, Sengupta S, Fray EJ, Beg SA, Antar AAR, Jenike KM, Bertagnolli LN, Capoferri AA, Kufera JT, Timmons A, Nobles C, Gregg J, Wada N, Ho YC, Zhang H, Margolick JB, Blankson JN, Deeks SG, Bushman FD, Siliciano JD, Laird GM, Siliciano RF. A quantitative approach for measuring the reservoir of latent HIV-1 proviruses. *Nature.* 2019;566(7742):120-5. Epub 20190130. doi: 10.1038/s41586-019-0898-8. PubMed PMID: 30700913; PMCID: PMC6447073.

369. Andersson J, Boasso A, Nilsson J, Zhang R, Shire NJ, Lindback S, Shearer GM, Chougnet CA. The prevalence of regulatory T cells in lymphoid tissue is correlated with viral load in HIV-infected patients. *J Immunol.* 2005;174(6):3143-7. doi: 10.4049/jimmunol.174.6.3143. PubMed PMID: 15749840.
370. Angin M, Kwon DS, Streeck H, Wen F, King M, Rezai A, Law K, Hongo TC, Pyo A, Piechocka-Trocha A, Toth I, Pereyra F, Ghebremichael M, Rodig SJ, Milner DA, Jr., Richter JM, Altfeld M, Kaufmann DE, Walker BD, Addo MM. Preserved function of regulatory T cells in chronic HIV-1 infection despite decreased numbers in blood and tissue. *J Infect Dis.* 2012;205(10):1495-500. Epub 20120315. doi: 10.1093/infdis/jis236. PubMed PMID: 22427677; PMCID: PMC3415814.
371. Eggena MP, Barugahare B, Jones N, Okello M, Mutalya S, Kityo C, Mugenyi P, Cao H. Depletion of regulatory T cells in HIV infection is associated with immune activation. *J Immunol.* 2005;174(7):4407-14. doi: 10.4049/jimmunol.174.7.4407. PubMed PMID: 15778406.
372. Epple HJ, Loddenkemper C, Kunkel D, Troger H, Maul J, Moos V, Berg E, Ullrich R, Schulzke JD, Stein H, Duchmann R, Zeitz M, Schneider T. Mucosal but not peripheral FOXP3+ regulatory T cells are highly increased in untreated HIV infection and normalize after suppressive HAART. *Blood.* 2006;108(9):3072-8. Epub 20060525. doi: 10.1182/blood-2006-04-016923. PubMed PMID: 16728694.
373. Kleinman AJ, Sivanandham R, Pandrea I, Chougnet CA, Apetrei C. Regulatory T Cells As Potential Targets for HIV Cure Research. *Front Immunol.* 2018;9:734. Epub 20180413. doi: 10.3389/fimmu.2018.00734. PubMed PMID: 29706961; PMCID: PMC5908895.
374. Simonetta F, Lecroux C, Girault I, Goujard C, Sinet M, Lambotte O, Venet A, Bourgeois C. Early and long-lasting alteration of effector CD45RA(-)Foxp3(high) regulatory T-cell homeostasis during HIV infection. *J Infect Dis.* 2012;205(10):1510-9. Epub 20120328. doi: 10.1093/infdis/jis235. PubMed PMID: 22457280; PMCID: PMC3989210.
375. Yero A, Shi T, Farnos O, Routy JP, Tremblay C, Durand M, Tsoukas C, Costiniuk CT, Jenabian MA. Dynamics and epigenetic signature of regulatory T-cells following antiretroviral therapy initiation in acute HIV infection. *EBioMedicine.* 2021;71:103570. Epub 20210906. doi: 10.1016/j.ebiom.2021.103570. PubMed PMID: 34500304; PMCID: PMC8429924.
376. Mudd JC, Brenchley JM. Gut Mucosal Barrier Dysfunction, Microbial Dysbiosis, and Their Role in HIV-1 Disease Progression. *J Infect Dis.* 2016;214 Suppl 2:S58-66. doi: 10.1093/infdis/jiw258. PubMed PMID: 27625432; PMCID: PMC5021240.
377. Estes JD, Harris LD, Klatt NR, Tabb B, Pittaluga S, Paiardini M, Barclay GR, Smedley J, Pung R, Oliveira KM, Hirsch VM, Silvestri G, Douek DC, Miller CJ, Haase AT, Lifson J, Brenchley JM. Damaged intestinal epithelial integrity linked to microbial translocation in pathogenic simian immunodeficiency virus infections. *PLoS Pathog.* 2010;6(8):e1001052. Epub 20100819. doi: 10.1371/journal.ppat.1001052. PubMed PMID: 20808901; PMCID: PMC2924359.
378. Guadalupe M, Sankaran S, George MD, Reay E, Verhoeven D, Shacklett BL, Flamm J, Wegelin J, Prindiville T, Dandekar S. Viral suppression and immune restoration in the gastrointestinal mucosa of human immunodeficiency virus type 1-infected patients initiating therapy during primary or chronic infection. *J Virol.* 2006;80(16):8236-47. doi: 10.1128/JVI.00120-06. PubMed PMID: 16873279; PMCID: PMC1563811.
379. Kader M, Wang X, Piatak M, Lifson J, Roederer M, Veazey R, Mattapallil JJ. Alpha4(+)beta7(hi)CD4(+) memory T cells harbor most Th-17 cells and are preferentially

- infected during acute SIV infection. *Mucosal Immunol.* 2009;2(5):439-49. Epub 20090701. doi: 10.1038/mi.2009.90. PubMed PMID: 19571800; PMCID: PMC2763371.
380. Martinelli E, Veglia F, Goode D, Guerra-Perez N, Aravantinou M, Arthos J, Piatak M, Jr., Lifson JD, Blanchard J, Gettie A, Robbani M. The frequency of alpha(4)beta(7)(high) memory CD4(+) T cells correlates with susceptibility to rectal simian immunodeficiency virus infection. *J Acquir Immune Defic Syndr.* 2013;64(4):325-31. doi: 10.1097/QAI.0b013e31829f6e1a. PubMed PMID: 23797688; PMCID: PMC3815485.
381. Evans VA, van der Sluis RM, Solomon A, Dantanarayana A, McNeil C, Garsia R, Palmer S, Fromentin R, Chomont N, Sekaly RP, Cameron PU, Lewin SR. Programmed cell death-1 contributes to the establishment and maintenance of HIV-1 latency. *AIDS.* 2018;32(11):1491-7. doi: 10.1097/QAD.0000000000001849. PubMed PMID: 29746296; PMCID: PMC6026054.
382. Ghneim K, Sharma AA, Ribeiro SP, Fourati S, Ahlers J, Kulpa D, Xu X, Brehm J, Talla A, Arumugam S, Darko S, Rodriguez B, Shive C, Cristescu R, Loboda A, Balderas R, Wang I-M, Hunt P, Lamarre D, Douek D, Hazuda D, Lederman MM, Deeks S, Sekaly R-P. Microbiome and Metabolome driven differentiation of TGF- β producing Tregs leads to Senescence and HIV latency. *bioRxiv.* 2020:2020.12.15.422949. doi: 10.1101/2020.12.15.422949.
383. Samer S, Thomas Y, Araínga M, Carter C, Shirreff L, Arif M, Avita J, Frank I, McRaven M, Thuruthiyil C, Heybeli V, Anderson M, Owen B, Gaisin A, Bose D, Simons L, Hultquist J, Arthos J, Cicala C, Sereti I, Santangelo P, Lorenzo-Redondo R, Hope T, Villinger F, Martinelli E. Blockade of TGF- β signaling reactivates HIV-1/SIV reservoirs and immune responses *in vivo*. *bioRxiv.* 2022:2022.05.13.489595. doi: 10.1101/2022.05.13.489595.
384. Mackelprang RD, Bamshad MJ, Chong JX, Hou X, Buckingham KJ, Shively K, deBruyn G, Mugo NR, Mullins JI, McElrath MJ, Baeten JM, Celum C, Emond MJ, Lingappa JR, Partners in Prevention HSVHIVTS, the Partners Pr EPST. Whole genome sequencing of extreme phenotypes identifies variants in CD101 and UBE2V1 associated with increased risk of sexually acquired HIV-1. *PLoS Pathog.* 2017;13(11):e1006703. Epub 20171106. doi: 10.1371/journal.ppat.1006703. PubMed PMID: 29108000; PMCID: PMC5690691.
385. Richert-Spuhler LE, Mar CM, Shinde P, Wu F, Hong T, Greene E, Hou S, Thomas K, Gottardo R, Mugo N, de Bruyn G, Celum C, Baeten JM, Lingappa JR, Lund JM, Partners in Prevention HSVHIVTS, and the Partners Pr EPST. CD101 genetic variants modify regulatory and conventional T cell phenotypes and functions. *Cell Rep Med.* 2021;2(6):100322. Epub 20210615. doi: 10.1016/j.xcrm.2021.100322. PubMed PMID: 34195685; PMCID: PMC8233694.
386. Amara RR, Villinger F, Altman JD, Lydy SL, O'Neil SP, Staprans SI, Montefiori DC, Xu Y, Herndon JG, Wyatt LS, Candido MA, Kozyr NL, Earl PL, Smith JM, Ma HL, Grimm BD, Hulsey ML, Miller J, McClure HM, McNicholl JM, Moss B, Robinson HL. Control of a mucosal challenge and prevention of AIDS by a multiprotein DNA/MVA vaccine. *Science.* 2001;292(5514):69-74. doi: 10.1126/science.1058915. PubMed PMID: 11393868.
387. Trombetta JJ, Gennert D, Lu D, Satija R, Shalek AK, Regev A. Preparation of Single-Cell RNA-Seq Libraries for Next Generation Sequencing. *Curr Protoc Mol Biol.* 2014;107:4 22 1-17. Epub 2014/07/06. doi: 10.1002/0471142727.mb0422s107. PubMed PMID: 24984854; PMCID: PMC4338574.
388. Dobin A, Davis CA, Schlesinger F, Drenkow J, Zaleski C, Jha S, Batut P, Chaisson M, Gingeras TR. STAR: ultrafast universal RNA-seq aligner. *Bioinformatics.* 2013;29(1):15-21. Epub

2012/10/30. doi: 10.1093/bioinformatics/bts635. PubMed PMID: 23104886; PMCID: PMC3530905.

389. Anders S, Pyl PT, Huber W. HTSeq--a Python framework to work with high-throughput sequencing data. *Bioinformatics*. 2015;31(2):166-9. Epub 2014/09/28. doi: 10.1093/bioinformatics/btu638. PubMed PMID: 25260700; PMCID: PMC4287950.

390. Vandergeeten C, Fromentin R, Merlini E, Lawani MB, DaFonseca S, Bakeman W, McNulty A, Ramgopal M, Michael N, Kim JH, Ananworanich J, Chomont N. Cross-clade ultrasensitive PCR-based assays to measure HIV persistence in large-cohort studies. *J Virol*. 2014;88(21):12385-96. Epub 20140813. doi: 10.1128/JVI.00609-14. PubMed PMID: 25122785; PMCID: PMC4248919.

391. Langner CA, Brenchley JM. FRugally Optimized DNA Octomer (FRODO) qPCR Measurement of HIV and SIV in Human and Nonhuman Primate Samples. *Curr Protoc*. 2021;1(4):e93. doi: 10.1002/cpz1.93. PubMed PMID: 33861500; PMCID: PMC8054980.

392. Blank CU, Haining WN, Held W, Hogan PG, Kallies A, Lugli E, Lynn RC, Philip M, Rao A, Restifo NP, Schietinger A, Schumacher TN, Schwartzberg PL, Sharpe AH, Speiser DE, Wherry EJ, Youngblood BA, Zehn D. Defining 'T cell exhaustion'. *Nat Rev Immunol*. 2019;19(11):665-74. Epub 20190930. doi: 10.1038/s41577-019-0221-9. PubMed PMID: 31570879; PMCID: PMC7286441.

393. Beltra JC, Manne S, Abdel-Hakeem MS, Kurachi M, Giles JR, Chen Z, Casella V, Ngiow SF, Khan O, Huang YJ, Yan P, Nzingha K, Xu W, Amaravadi RK, Xu X, Karakousis GC, Mitchell TC, Schuchter LM, Huang AC, Wherry EJ. Developmental Relationships of Four Exhausted CD8(+) T Cell Subsets Reveals Underlying Transcriptional and Epigenetic Landscape Control Mechanisms. *Immunity*. 2020;52(5):825-41 e8. Epub 20200511. doi: 10.1016/j.immuni.2020.04.014. PubMed PMID: 32396847; PMCID: PMC8360766.

394. Heim K, Binder B, Sagar, Wieland D, Hensel N, Llewellyn-Lacey S, Gostick E, Price DA, Emmerich F, Vingerhoet H, Kraft ARM, Cornberg M, Boettler T, Neumann-Haefelin C, Zehn D, Bengsch B, Hofmann M, Thimme R. TOX defines the degree of CD8+ T cell dysfunction in distinct phases of chronic HBV infection. *Gut*. 2020. Epub 20201023. doi: 10.1136/gutjnl-2020-322404. PubMed PMID: 33097558; PMCID: PMC8292571.

395. Deeks SG, Archin N, Cannon P, Collins S, Jones RB, de Jong M, Lambotte O, Lamplough R, Ndung'u T, Sugarman J, Tiemessen CT, Vandekerckhove L, Lewin SR, International ASGSSwg. Research priorities for an HIV cure: International AIDS Society Global Scientific Strategy 2021. *Nat Med*. 2021;27(12):2085-98. Epub 20211201. doi: 10.1038/s41591-021-01590-5. PubMed PMID: 34848888.

396. Sade-Feldman M, Yizhak K, Bjorgaard SL, Ray JP, de Boer CG, Jenkins RW, Lieb DJ, Chen JH, Frederick DT, Barzily-Rokni M, Freeman SS, Reuben A, Hoover PJ, Villani AC, Ivanova E, Portell A, Lizotte PH, Aref AR, Eliane JP, Hammond MR, Vitzthum H, Blackmon SM, Li B, Gopalakrishnan V, Reddy SM, Cooper ZA, Paweletz CP, Barbie DA, Stemmer-Rachamimov A, Flaherty KT, Wargo JA, Boland GM, Sullivan RJ, Getz G, Hacohen N. Defining T Cell States Associated with Response to Checkpoint Immunotherapy in Melanoma. *Cell*. 2018;175(4):998-1013 e20. doi: 10.1016/j.cell.2018.10.038. PubMed PMID: 30388456; PMCID: PMC6641984.

397. Canale FP, Ramello MC, Nunez N, Araujo Furlan CL, Bossio SN, Gorosito Serran M, Tosello Boari J, Del Castillo A, Ledesma M, Sedlik C, Piaggio E, Gruppi A, Acosta Rodriguez EA, Montes CL. CD39 Expression Defines Cell Exhaustion in Tumor-Infiltrating CD8(+) T Cells. *Cancer*

Res. 2018;78(1):115-28. Epub 20171024. doi: 10.1158/0008-5472.CAN-16-2684. PubMed PMID: 29066514.

398. Abbas HA, Hao D, Tomczak K, Barrodia P, Im JS, Reville PK, Alaniz Z, Wang W, Wang R, Wang F, Al-Atrash G, Takahashi K, Ning J, Ding M, Beird HC, Mathews JT, Little L, Zhang J, Basu S, Konopleva M, Marques-Piubelli ML, Solis LM, Parra ER, Lu W, Tamegnon A, Garcia-Manero G, Green MR, Sharma P, Allison JP, Kornblau SM, Rai K, Wang L, Daver N, Futreal A. Single cell T cell landscape and T cell receptor repertoire profiling of AML in context of PD-1 blockade therapy. *Nat Commun.* 2021;12(1):6071. Epub 20211018. doi: 10.1038/s41467-021-26282-z. PubMed PMID: 34663807; PMCID: PMC8524723.

399. Jonsson AH, Zhang F, Dunlap G, Gomez-Rivas E, Watts GFM, Faust HJ, Rupani KV, Mears JR, Meednu N, Wang R, Keras G, Coblyn JS, Massarotti EM, Todd DJ, Anolik JH, McDavid A, Accelerating Medicines Partnership RASLEN, Wei K, Rao DA, Raychaudhuri S, Brenner MB. Granzyme K(+) CD8 T cells form a core population in inflamed human tissue. *Sci Transl Med.* 2022;14(649):eabo0686. Epub 20220615. doi: 10.1126/scitranslmed.abo0686. PubMed PMID: 35704599.

400. Eberhardt CS, Kissick HT, Patel MR, Cardenas MA, Prokhnevskaya N, Obeng RC, Nasti TH, Griffith CC, Im SJ, Wang X, Shin DM, Carrington M, Chen ZG, Sidney J, Sette A, Saba NF, Wieland A, Ahmed R. Functional HPV-specific PD-1(+) stem-like CD8 T cells in head and neck cancer. *Nature.* 2021;597(7875):279-84. Epub 20210901. doi: 10.1038/s41586-021-03862-z. PubMed PMID: 34471285.

401. Mylvaganam GH, Rios D, Abdelaal HM, Iyer S, Tharp G, Mavigner M, Hicks S, Chahroudi A, Ahmed R, Bosinger SE, Williams IR, Skinner PJ, Velu V, Amara RR. Dynamics of SIV-specific CXCR5+ CD8 T cells during chronic SIV infection. *Proc Natl Acad Sci U S A.* 2017;114(8):1976-81. Epub 20170203. doi: 10.1073/pnas.1621418114. PubMed PMID: 28159893; PMCID: PMC5338410.

402. Starke CE, Vinton CL, Ladell K, McLaren JE, Ortiz AM, Mudd JC, Flynn JK, Lai SH, Wu F, Hirsch VM, Darko S, Douek DC, Price DA, Brenchley JM. SIV-specific CD8+ T cells are clonotypically distinct across lymphoid and mucosal tissues. *J Clin Invest.* 2020;130(2):789-98. doi: 10.1172/JCI129161. PubMed PMID: 31661461; PMCID: PMC6994127.

403. Banga R, Munoz O, Perreau M. HIV persistence in lymph nodes. *Curr Opin HIV AIDS.* 2021;16(4):209-14. doi: 10.1097/COH.0000000000000686. PubMed PMID: 34059608.

404. Kiniry BE, Hunt PW, Hecht FM, Somsouk M, Deeks SG, Shacklett BL. Differential Expression of CD8(+) T Cell Cytotoxic Effector Molecules in Blood and Gastrointestinal Mucosa in HIV-1 Infection. *J Immunol.* 2018;200(5):1876-88. Epub 20180119. doi: 10.4049/jimmunol.1701532. PubMed PMID: 29352005; PMCID: PMC5821568.

405. Passaes C, Millet A, Madelain V, Monceaux V, David A, Versmisse P, Sylla N, Gostick E, Llewellyn-Lacey S, Price DA, Blancher A, Dereuddre-Bosquet N, Desjardins D, Pancino G, Le Grand R, Lambotte O, Muller-Trutwin M, Rouzioux C, Guedj J, Avettand-Fenoel V, Vaslin B, Saez-Cirion A. Optimal Maturation of the SIV-Specific CD8(+) T Cell Response after Primary Infection Is Associated with Natural Control of SIV: ANRS SIC Study. *Cell Rep.* 2020;32(12):108174. doi: 10.1016/j.celrep.2020.108174. PubMed PMID: 32966788.

406. Mvaya L, Khaba T, Lakudzala AE, Nkosi T, Jambo N, Kadwala I, Kankwatira A, Patel PD, Gordon MA, Nyirenda TS, Jambo KC, Ndhlovu ZM. Differential localization and limited cytotoxic

potential of duodenal CD8⁺ T cells. *JCI Insight*. 2022;7(3). Epub 20220208. doi: 10.1172/jci.insight.154195. PubMed PMID: 35132966; PMCID: PMC8855799.

407. Fardoos R, Nyquist SK, Asowata OE, Kazer SW, Singh A, Ngoepe A, Giandhari J, Mthabela N, Ramjit D, Singh S, Karim F, Buus S, Anderson F, Porterfield JZ, Sibiya AL, Bipath R, Moodley K, Kuhn W, Berger B, Nguyen S, de Oliveira T, Ndung'u T, Goulder P, Shalek AK, Leslie A, Kloverpris HN. HIV specific CD8⁺ T_{RM}-like cells in tonsils express exhaustive signatures in the absence of natural HIV control. *Front Immunol*. 2022;13:912038. Epub 20221018. doi: 10.3389/fimmu.2022.912038. PubMed PMID: 36330531; PMCID: PMC9623418.

408. Li H, Wang S, Kong R, Ding W, Lee FH, Parker Z, Kim E, Learn GH, Hahn P, Policicchio B, Brocca-Cofano E, Deleage C, Hao X, Chuang GY, Gorman J, Gardner M, Lewis MG, Hatzioannou T, Santra S, Apetrei C, Pandrea I, Alam SM, Liao HX, Shen X, Tomaras GD, Farzan M, Chertova E, Keele BF, Estes JD, Lifson JD, Doms RW, Montefiori DC, Haynes BF, Sodroski JG, Kwong PD, Hahn BH, Shaw GM. Envelope residue 375 substitutions in simian-human immunodeficiency viruses enhance CD4 binding and replication in rhesus macaques. *Proc Natl Acad Sci U S A*. 2016;113(24):E3413-22. Epub 20160531. doi: 10.1073/pnas.1606636113. PubMed PMID: 27247400; PMCID: PMC4914158.

409. Hoang TN, Pino M, Boddapati AK, Viox EG, Starke CE, Upadhyay AA, Gumber S, Nekorchuk M, Busman-Sahay K, Strongin Z, Harper JL, Tharp GK, Pellegrini KL, Kirejczyk S, Zandi K, Tao S, Horton TR, Beagle EN, Mahar EA, Lee MYH, Cohen J, Jean SM, Wood JS, Connor-Stroud F, Stammen RL, Delmas OM, Wang S, Cooney KA, Sayegh MN, Wang L, Filev PD, Weiskopf D, Silvestri G, Waggoner J, Piantadosi A, Kasturi SP, Al-Shakhshir H, Ribeiro SP, Sekaly RP, Levit RD, Estes JD, Vanderford TH, Schinazi RF, Bosinger SE, Paiardini M. Baricitinib treatment resolves lower-airway macrophage inflammation and neutrophil recruitment in SARS-CoV-2-infected rhesus macaques. *Cell*. 2021;184(2):460-75.e21. Epub 20201110. doi: 10.1016/j.cell.2020.11.007. PubMed PMID: 33278358; PMCID: PMC7654323.

410. Satija R, Farrell JA, Gennert D, Schier AF, Regev A. Spatial reconstruction of single-cell gene expression data. *Nat Biotechnol*. 2015;33(5):495-502. Epub 20150413. doi: 10.1038/nbt.3192. PubMed PMID: 25867923; PMCID: PMC4430369.

411. DeTomaso D, Yosef N. FastProject: a tool for low-dimensional analysis of single-cell RNA-Seq data. *BMC Bioinformatics*. 2016;17(1):315. Epub 20160823. doi: 10.1186/s12859-016-1176-5. PubMed PMID: 27553427; PMCID: PMC4995760.